Analysis of critical quality attributes in monoclonal antibodies for upstream process development

by

Sheun Oshinbolu

Advanced Centre for Biochemical Engineering

University College London

This thesis is submitted for the degree of

Engineering Doctorate (EngD)

June 2019

Declaration

I, Sheun Oshinbolu confirm that the work presented in this thesis is my own. Where information has been derived from other sources, I confirm that this has been indicated in the thesis.

Sheun Oshinbolu

June 2019

Acknowledgements

Firstly, I would like to acknowledge my supervisors, Prof. Daniel G Bracewell and Rachana Shah for their experience, extensive knowledge and guidance they have provided me throughout the EngD. I am also grateful for their support and encouragement in applying for the Industrial Fellowship and publishing papers. I would also like to acknowledge Mike Molloy, Mark Uden and Gary Finka for their support in approving publications and providing advice. In addition, I would like to acknowledge the staff in the Department of Biochemical Engineering, particularly: Derrick Abraham for aiding with expenses reimbursement and Gary Lye for providing references. Furthermore, I would also like to give thanks to the Royal Commission for the Exhibition of 1851 for awarding me with the Industrial Fellowship, which provided extra funding for materials and attending conferences.

Secondly, I would like to acknowledge certain individuals at GSK that have helped me: Marisa Bertolotti, Alan Lewis, Richard Upton, Claus Spitzfaden and Chun-wa Chung. In addition, I would also like to thank GSK BPR and BPMD departments for being warm and welcoming. I would like to extend a thank you to the whole BPR Analytical Team for helping me find my way around the lab and being incredibly approachable.

Finally, I would like to thank my family for their continued support throughout the EngD. My caring parents, and my sister who is generally the funniest person I know, all provided comfort and a great environment to come home to. I would also like to thank my Level 3 office friends- Darryl, Michael and Charnett for all the peer advice and much needed coffee breaks. In addition, I would like to thank my amazing and talented dance friends, Zuzana, Hanee, Anya and Patrick, for being there for me and for all the irreplaceable memories both on and off stage. Finally, my fresher dancers: Evita, Tan, Emma and Sara- thank you for continual support and encouragement till the end.

Abstract

In process development, there is an increasing demand to screen and select cell lines based on a more detailed understanding of the manufacturability and product quality of the candidate molecules. There is also an increasing need to have this detailed understanding available earlier in the process, in order to make better informed decisions as early as possible. One product quality attribute of interest in industry has been the aggregation of monoclonal antibodies (mAb). Thus, this thesis describes the development of an analytical assay to measure monoclonal antibody aggregates using three approaches.

The first approach utilised two types of fluorescent dyes: hydrophobic dyes (Bis-ANS and SYPRO Orange) and molecular rotors (Thioflavin T and ProteoStat). The fluorescent dyes measured aggregates on purified mAb down to 5% mAb aggregates, but they were found not to be specific to mAb aggregates in cell culture medium. A second approach used an affinity peptide (shown to be specific to mAb aggregates) conjugated to molecular rotors (Thioflavin T and CCVJ), bright dyes (Tide Fluor 2 and Fluorescein) and biotin for detection. However, the conjugates did not provide enhanced specificity towards mAb aggregates compared to the dyes on their own. Hence, further investigation would be needed to understand the binding site and mechanism of the affinity peptide.

In the third approach, a fluorescence resonance energy transfer (FRET) assay was designed. Experimental evidence showed weak energy transfer was due to aggregated mAbs placing the donor and acceptor outside the distance required to achieve FRET. Energy transfer improved when distances were reduced by using smaller proteins (lectin (38 kDa) and dAb (25 kDa)). The FRET assay was able to quantify 5-30% lectin aggregates (R^2>0.9) in both purified and CHO media/host cell protein background. Overall, this thesis showed the strengths and weaknesses of using fluorescent dyes in different formats to measure protein aggregates. Although further work is needed for both the FRET and affinity peptide assay, the thesis has explored some of the challenges of using FRET with proteins, donor and acceptor free in solution, which could be applied in designing and understanding other FRET assays. As well as highlighting the next steps required to fully develop and understand the labelled-affinity peptide assay system.

Impact Statement

As an EngD project, this project was designed to have impact to address and solve an industry relevant problem. Half of the top 10 best-selling drugs are monoclonal antibodies (mAbs). Biopharmaceutical companies are constantly developing new biologics to treat disease. To do so requires a toolbox of analytical techniques in order to measure different physicochemical properties of the product and ensure desired product quality.

Cell line development and upstream processing play a key role in the selection and production of stable cell lines and molecules. In terms of product quality, there has been a significant progress with upstream processing to maximise titres, cell counts and viability. However, there is little understanding to how changes in the upstream conditions impact product profile in the bioreactor. Currently, analytical techniques require samples to be purified prior to measurement. Although purification is possible, the main issue is that key components (e.g. large aggregates) may be removed as a result, ultimately providing data that may not be a true representation of the cell culture. In addition, purification is also time-consuming and costly.

Hence, there is a need to develop assays/tools that can help characterise aggregate levels in complex multi-component environment earlier in research and development. This can eventually lead to better decision-making for selecting cell lines and candidate molecules. These assays/tools would also be applicable to academia as this problem exists within the bioprocess development scientific community. In addition, there is also a need for fast, high-throughput analytical assays that can cope with measuring 100s of samples in a short period of time. These assays will need minimal sample preparation to cope with the demand and provide accurate results that are a true representation of the sample.

The FRET assay developed in this thesis was not able to measure mAb aggregates. However, it was able to characterise soluble protein aggregates of molecules smaller in size (lectin (38kDa)) down to 5% aggregation with strong linearity. This can be of use in measuring aggregates of small molecule products produced by biopharmaceutical companies such as certain domain antibodies (dAbs) and fragment antibodies (Fab). In terms of throughput, the assay was adapted to a 384 well-plate

format which would allow 100 samples to run in 2.5 hrs - 20X faster than a 30 min size exclusion chromatography method. Although, the assay was only tested with purified lectin, it did not require additional sample preparation.

The impact of the research has been disseminated through publications and presented at an international conference. The conclusions and learning about mAb aggregates used with fluorescent dyes in cell culture medium were published in the Journal of Chemical Technology and Biotechnology in 2018. In addition, the learnings from the development of the FRET assay were presented at the American Chemical Society conference in March 2018.

Table of Contents

List of figures

List of tables

Nomenclature

ΦD – Quantum yield of the donor chromophore

κ^2 – Orientation of the donor and acceptor transition dipoles

A – Acceptor

AC-SINS – Affinity Capture-Self Interaction Nanoparticles Spectroscopy

AP – Affinity peptide

AF350 – Alexa Fluor 350

AUC / SV-AUC – (Sedimentation velocity) analytical ultra-centrifugation

BSA – Bovine serum albumin

CD – Circular dichroism

CoD – Cost of dose

CoG – Cost of goods

CHO – Chinese hamster ovary

CMC – Critical micelle concentration

CPP – Critical process parameter

CQA – Critical quality attribute

Cryo-EM – Electron cryo-microscopy

D – Donor

dAb – Domain antibody

DLS – Dynamic light scattering

E – Energy Transfer

EC – Extinction Coefficient

E_{PR} – Proximity ratio

ELISA – Enzyme linked immunosorbent assay

Fab – Fragment antibody

FC – Flow Cell

FDA – Food and Drug Administration

FRET – Fluorescence Resonance Energy Transfer

FL – Fluorescein

FTIR – Fourier-transform Infrared

HCP – Host cell protein

HDX – Hydrogen deuterium exchange

HMW – High molecular weight

ICH – International Council for Harmonisation

IgG – Immunoglobulin G

J – Overlap integral of the donor emission and acceptor excitation spectrum

KB – Kinetics Buffer

K_d – Equilibrium dissociation constant

LMW – Low molecular weight

mAb – Monoclonal antibody

MD – Molecular dynamics

MS / MS-MS / LC-MS / HDX-MS – Mass spectrometry / Tandem mass spec / Liquid chromatography with mass spec / Hydrogen-deuterium exchange mass spec

n – Refractive index of the medium

NMR – Nuclear magnetic resonance

NTA – Nanoparticle tracking analysis

PCA – Principal component analysis

PLS – Partial least squares

ppm – parts per million

PrA – Protein A

PTM – Post-translational modifications

QbD – Quality by design

QC – Quality control

R_0 – Forster radius

r_h – Hydrodynamic radius

RFU – Relative fluorescence units

SAXS – Small-angle X-ray scattering

SA – Streptavidin

SEC – Size exclusion chromatography

SPR – Surface Plasmon Resonance

TEM - Transmission electron microscopy

ThT – Thioflavin T

TF2 – Tide Fluor 2

UPLC – Ultra performance liquid chromatography

UV – Ultra violet (light)

WGA – Wheat germ agglutinin

1 Literature review

1.1. Chapter Aims

In this chapter, the current literature on monoclonal antibodies was reviewed. The review covers the monoclonal antibodies market, manufacturing process and critical quality attributes. The aims of this chapter are as follows:

1. Provide a summary of the monoclonal antibody market and manufacturing process.

2. Outline what critical quality attributes are, how to control them and their importance from a regulatory perspective.

3. Discuss aggregation as a critical quality attribute and the role that analytics play in measuring aggregation in drug development.

4. Discuss factors which influence aggregation formation and highlight techniques currently used for both size quantification and structural analysis of aggregates.

1.2. Background and market of monoclonal antibodies

Recombinant therapeutic antibodies are present in many pharmaceutical company's portfolios and contribute a significant amount to the pharmaceutical industry revenue. Biopharmaceuticals represent 24% of the global drug market and antibody derived drugs, with sales reaching $82 billion in 2016 (Hall. M et al., 2017). Half of the top 10 best-selling drugs are monoclonal antibodies (mAbs) (Hall. M et al., 2017), and they are mostly used to treat cancer and autoimmune diseases. Therapeutic antibodies can be categorised as either monoclonal or polyclonal. Monoclonal antibodies (mAbs) are produced from the same parent cell and can only detect one epitope/binding site on an antigen. Whereas polyclonal antibodies are a heterogeneous mixture produced from different parent cells, and as a result can bind to many different epitopes on an antigen. Most licensed recombinant mAbs are of the IgG type which consist of a constant region (Fc) which is similar in antibodies of the same class, and a variable region (Fab) which serves as the antigen-binding site.

Some of the most notable therapeutic antibodies are: Humira (AbbVie, rheumatoid arthritis), Remicade (Johnson and Johnson, Crohn's disease) and Herceptin (Roche/Genentech, breast cancer). All of these drugs achieved 'blockbuster' status, reaching annual sales greater than $1bn (Lawrence, 2007). However, not all drugs are able to achieve this status and in reality, fewer than 10% of therapeutic candidate molecules in research and development actually make it to market (Zurdo, 2013).

The attrition funnel diagram in Figure 1-1 (commonly termed as the "valley of death") shows the high costs and long timelines required to develop a successful candidate. Therefore, to increase the likelihood of success, companies are adopting a 'fail early, fail cheap' mentality to reduce the impact (cost and time) of candidates that do not meet the selection criteria (e.g. efficacy, quality, safety, manufacturability). Regulatory agencies such as the Food and Drug Administration (FDA) in USA and European Medicines Agency (EMA) in Europe review and approve drugs and medical appliances that can be sold on their respective continents. To obtain this approval, biopharmaceutical companies must be able to show that candidate

molecules are safe by providing data on certain quality attributes which will be further discussed Chapter 1.4.

To develop a full understanding of the molecule being produced, analytical methods are required from discovery and process development, through to clinical trials. As such, analytics play a vital role in taking recombinant therapeutics from bench-to-market as it underlies all decision making.

The manufacture of therapeutic antibodies consists of various steps (See section 1.3) before the product is put in a form for use e.g. subcutaneous injection. It is important to understand not only how the manufacturing process produces the product (therapeutic antibodies), but also how it affects product stability and quality. This is because the process will influence the product that is created. This will be discussed in Chapter 1.2.

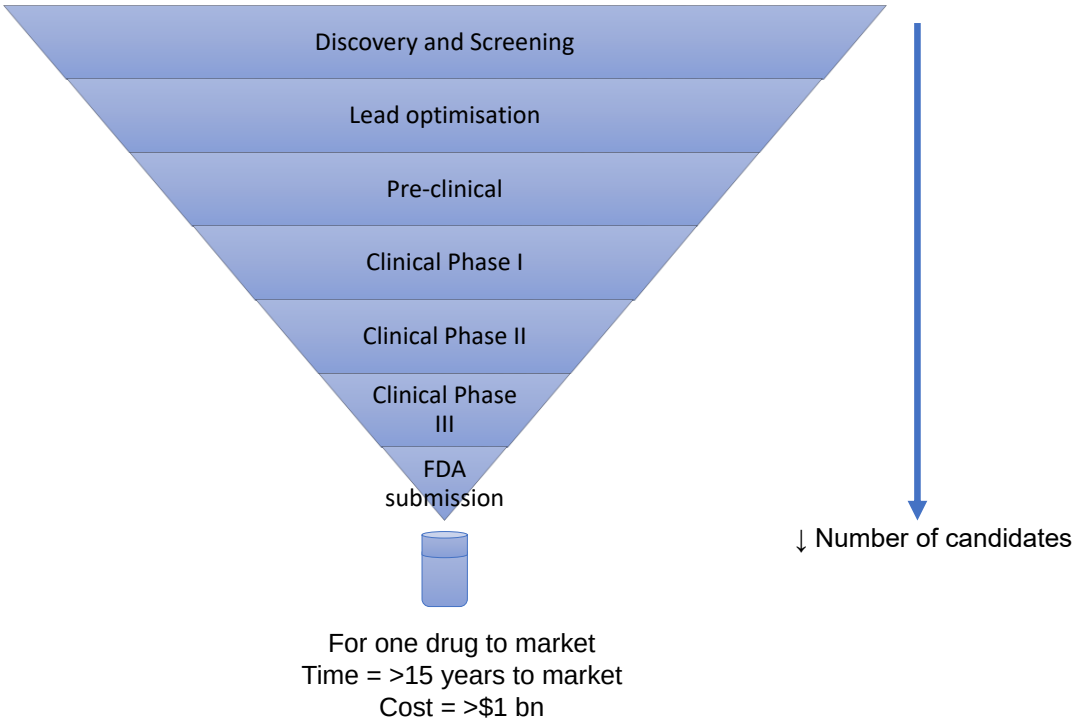

Figure 1-1: Attrition Funnel diagram which shows the investment required to bring a drug to market.
Over time the number of candidates in the pipeline decreases such that only one candidate molecule makes it to market. The whole process is costly (>$2bn (Mullard, 2014)) and time consuming (>15 years).

1.3. Manufacturing process

Recombinant therapeutics are produced in cells which have had the plasmid for the product of interest inserted into the DNA. The choice of cell/expression system is important and dependent on the capabilities required to produce the protein. Mammalian cells are the dominant expression system for mAbs as they can produce desired complex glycosylated proteins, whereas microbial expression systems cannot. Even still, microbial systems such as *E. coli* and yeast have been used to produce recombinant human insulin. Chinese Hamster Ovary (CHO) cells are the most commonly used mammalian cell line, although murine myeloma lymphoid cells (N20), human embryonic kidney cells and baby hamster kidney cells are also used. Plants and insects have also been used as an alternative expression system with FDA approving the first biopharmaceutical produced in a plant-based system (Walsh 2014).

A manufacturing process as shown in Figure 1-2 is used to produce the mAbs in large quantities. The process is generally split into two streams: upstream and downstream processing.

1.3.1. Upstream processing

After establishing an expression system (cell line) in cell line development, the cell line is handed to upstream to produce the product. The main priority at this stage is to produce high product titres, cell counts and viability. Cell counts are important as more cells present allow for more product to be formed. At low viabilities, apoptosis can cause the release of degradative enzymes which can damage the product (Pan, 2018). Titres have increased from 1-100 mg/L (Huang et al. 2010) to and exceeding 5 g/L (Birch and Racher 2006) which is a result of optimised media components, operating conditions and cell engineering to inhibit apoptosis. The increased titres and productivity in upstream have shifted the downstream to be the bottleneck due to limited capacities. To harvest the product, the supernatant is retained using centrifugation or (depth) filtration as mAbs are usually expressed extracellularly.

1.3.2. Downstream processing

The aim of downstream processing is to remove impurities and contaminants. Purification is usually carried out using a set of chromatography and filtration steps. Protein A is typically the main capture step whereby protein A resins bind with high affinity to the Fc portion of the mAb. This is often followed by at least one ion exchange polishing step to remove remaining impurities e.g. host cell proteins (HCP), DNA, endotoxins, viruses and leached protein A resin. Positively charged resins used in anion exchange chromatography are usually used to bind impurities whereas, negatively charged resins used in cation exchange chromatography bind the product. For therapeutic proteins produced with a mammalian expression system, viruses are an important contaminant to remove, requiring at least two clearance steps (inactivation and filtration). Finally, ultrafiltration/diafiltration concentrates and dialyses the product in to the final formulation buffer. The final yield depends on the number of processing steps but can range from 60-80% (Birch 2006).

Although the production of mAbs is a well-established process, it has benefits and drawbacks. One of these drawbacks are components that enter the process need to be removed (see Figure 1-2). Some of the components are added into the process are a necessity such as cells, however some are created by the process. These components can be categorised as critical quality attributes which is discussed in the next section.

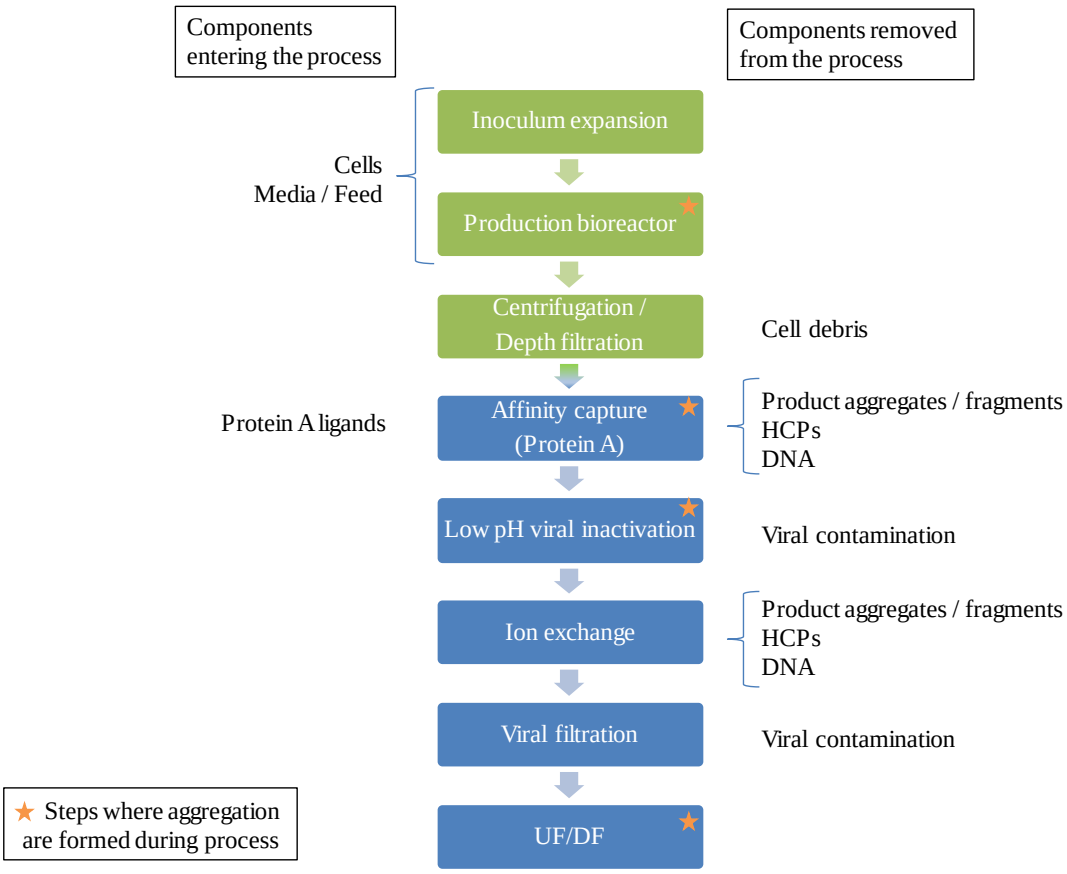

Figure 1-2: Bioprocess flow diagram.
Shows the stages during upstream (green) and downstream (blue) processing along with components that are entered and removed from the process. Star indicates where aggregates are formed in the process

1.4. Quality-by-Design and critical quality attributes

1.4.1. Defining Quality-by-Design

The development process of mAbs is highly regulated due to the 10^8 possible molecular variants (Kozlowski and Swann, 2006). To ensure high quality drugs are consistently produced, biopharmaceutical companies are becoming more risk adverse, and focusing on improving consistency in production and characterising product quality earlier in development. One approach, “Quality-by-Design” (QbD), enables confidence and predictability to be built into a process from the beginning of development.

The ICH have guidelines on pharmaceutical development using QbD (ICH Q8 (R2)). The first step QbD is to define a Quality Target Product Profile (QTPP) which is a summary of the quality characteristics (e.g. dosage, route of administration, purity) that will be achieved to ensure a desired quality is met which is safe and efficacious (ICH, 2009). The second step is to identify critical quality attributes which will be further discussed in section 1.4.2. Subsequent steps include creating a design space (to identify operating boundaries which will achieve the required product quality) and a control strategy to ensure that the required product quality is achieved consistently.

QbD is becoming a globally accepted strategy within the industry with the goal of enhancing pharmaceutical manufacture through design and control of processes (Finkler and Krummen, 2016). The strategy systematically establishes critical quality attributes (CQA) of a drug product and critical process parameters (CPP) which are parameters with significant impact to CQAs (Ohage et al., 2016).

1.4.2. Defining critical quality attributes

A CQA as outlined in ICH Q8 (R2) is a "physical, chemical, biological or microbiological property or characteristic that should be within an appropriate limit, range, or distribution to ensure the desired product quality" (ICH, 2009). Figure 1-3 outlines the key steps towards controlling CQAs based on the ICH specification Q6B. The first steps involve identifying the attributes which are critical and setting acceptable ranges. For each CQA, the level of importance and risk must be understood to understand and rank its impact. After identifying the CQA, acceptable ranges and risk, steps must be taken towards monitoring and controlling using various forms of analytics and controlling with appropriate operating conditions.

Critical quality attributes can be product or process related. Product related impurities are molecular variants of the product such as aggregates, fragments, incorrectly glycosylated antibody or charge variants. Whereas, process related impurities are an inherent part of the process, such as the host cells' DNA or host cell proteins (HCPs) and leachables (such as protein A) and viruses. The presence of these impurities in the final drug product can affect product purity, product efficacy and stability, and

can cause adverse immune responses in patients such as anaphylaxis (FDA, 2014). To ensure patient safety, impurities need to be reduced to acceptably low levels to meet the defined acceptance criteria. For mAbs, the final product should typically have <5% high molecular weight aggregates, <100 ppm HCPs and <10 ng/dose DNA (Chon and Zarbis-Papastoitsis, 2011, Champion et al., 2005), although in reality aggregation and HCP limits are case-by-case dependent and are defined from (pre-) clinical studies and manufacturing consistency lots (ICH, 1999).

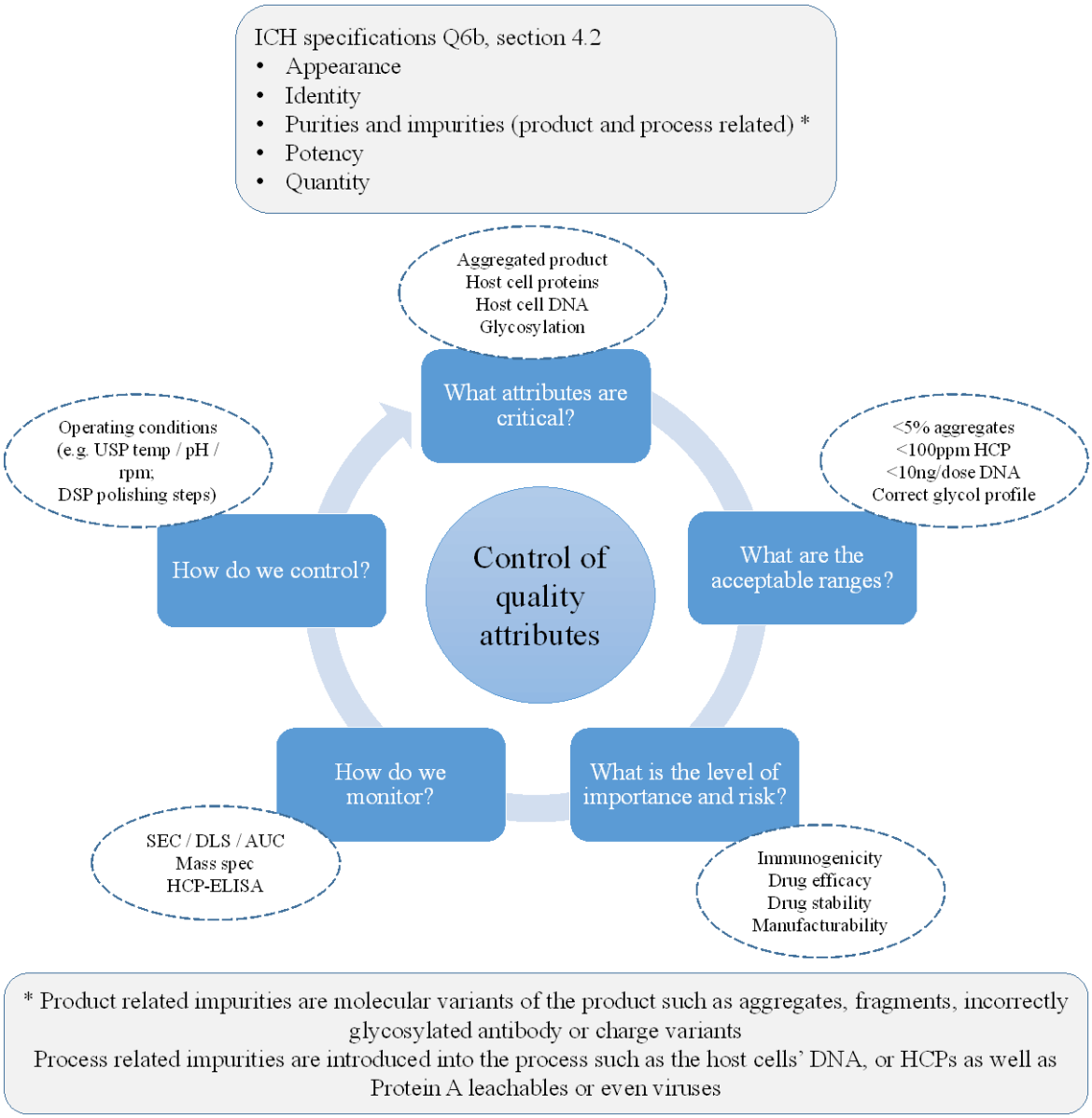

Figure 1-3: Steps to controlling quality attributes.
Schematic of the necessary steps/questions that need to be asked in order to ensure control quality attributes in a process. (ICH, 1999).

1.5. Aggregation

One CQA in particular, product aggregation, can influence production, activity and safety (Yamniuk et al., 2013). Furthermore, it can also increase the cost of goods (CoG) and the cost of development (CoD). Aggregation is the self-association of protein molecules and can differ in morphology, solubility, structure, reversibility and intermolecular bonding. Moussa et al. (2016) reviewed the issues of aggregated therapeutic proteins causing adverse immune responses in patients. The adverse immune response can cause problems for both patient safety and product efficacy (FDA, 2014). However, aggregation can occur at various points in the manufacturing process which is an issue in the bioprocess industry (see Figure 1-2). Therefore, to ensure patient safety, it is important to improve our understanding of protein aggregates and use the most appropriate analytical techniques to monitor aggregate content. Hence, product aggregation will be the focus of this thesis.

A single unaggregated form of a molecule is referred to as a monomer. Dimers, trimers and tetramers consist of 2, 3 and 4 aggregated monomers, respectively. Oligomers/multimers are used to typically refer to several aggregated monomers. Aggregates can be difficult to characterise and detect due to the different mechanisms of formation and the large potential size range. Cromwell et al. (2006) identified that aggregates can be classified as soluble/insoluble, covalent/non-covalent, reversible/non-reversible and native/denatured. Soluble aggregates are not visible and may not be removed by a 0.22 μm filter, whereas insoluble aggregates are often visible to the eye and may be removed by filtration (Cromwell et al. 2006). Covalent aggregates are the result of a chemical bond between monomers. Disulphide bonds between previously unpaired free thiols are a common mechanism for covalent aggregation (Vazquez-Rey and Lang, 2011). Conversely, non-covalent aggregates are formed based on structural regions of charge or polarity (Patel et al. 2011). Reversible aggregations are held together by weak interactions such as exposed hydrophobic regions. Above 1 μm, aggregates become insoluble and are visible if they are sufficiently large and/or undergo phase separation (Figure 1-5).

Aggregation is often seen as a multi-step process and the mechanism of which aggregation occurs by usually determines the type of aggregate formed. Figure 1-4 shows a schematic of multiple aggregation pathways adapted from Roberts (2014) review on aggregation mechanisms. The onset of aggregation can occur via 3 main pathways. One is by the unfolding of a protein from its native state which exposes surfaces on the protein such as hydrophobic regions. The exposed surfaces of multiple unfolded proteins can interact with each other. A monomeric mAb can partly unfold in either the Fab or Fc region (or both) which are both reversible. Alternatively, native proteins can interact with each other via hydrophobic areas on their outer surface.

The clustering of proteins can eventually give rise to a nuclei. A nuclei is the smallest net-irreversible aggregate which eventually turns into a soluble aggregate and further into insoluble aggregates. Unfolding, misfolding or conformation changes are typically required to allow the exposure of hidden aggregation-prone amino acid sequences to form strong inter-protein interactions which ultimately leads to the creation of an aggregate. The same forces that drive folding (electrostatic attraction/repulsion, hydrogen bonding and hydrophobic interactions) also drive aggregation, and as a result, aggregation-prone amino acid sequences tend to be highly hydrophobic, lack charges and are prone to form beta sheets when paired with adjacent strands (Roberts, 2014).

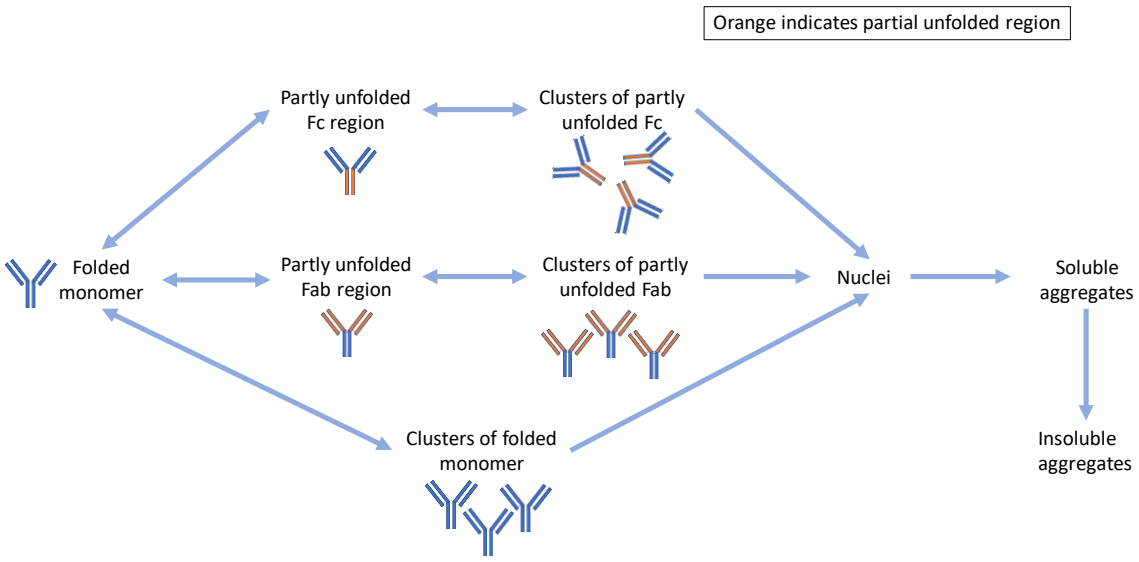

Figure 1-4: Mechanism of protein aggregation
Figure was adapted from Roberts (2014). Orange parts on mAb indicates partial folded region. Double arrows denote reversible steps, single arrows denote irreversible steps.

1.5.1. Steps in a bioprocess that cause aggregation formation

Philo and Arakawa (2009) found that aggregation of conformationally-altered monomer appeared to be the dominant mechanism for many aggregated proteins. Conformational changes can occur from the exposure of the native monomer to stresses such as temperature, shear forces, protein adsorption to bulk interfaces, chemical changes (deamidation, oxidation, etc.) or fragmentation. Throughout the manufacturing process, mAbs are subjected to these stresses which leads to the formation of aggregates.

In the bioreactor, mAbs are exposed to many different physical (e.g. temperature and pH), mechanical (agitation) and chemical stresses (e.g. oxidation, deamidation, proteases) that can cause conformational changes. Previous reports of mAb have shown aggregation levels as high as 30% (Kramarczyk et al., 2008). Protein aggregates may be formed intracellularly during protein expression or after secretion into the media. The interactions between high amounts of unfolded protein or absence

of proper folding from molecular chaperones causes intracellular aggregation (Zhang et al., 2004). MAbs are secreted into the extracellular environment, however this secretion exposes the mAbs to harsh conditions such as pH, agitation and dissolved oxygen which can lead to aggregation. The temperature of the culture also influences aggregation as the longer the proteins are kept at elevated temperatures, the higher probability of aggregation (Cromwell et al., 2006). However, higher temperature increases cell productivity, therefore there is often a trade-off between yield and product quality. Additionally, the push for higher titres to reduce the cost of manufacture has elevated the risk of aggregation in the bioreactor due to the concentration-dependent nature of aggregates. Dengl et al. (2013) showed that HMW aggregates present in the bioreactor tend to go undetected as they are removed in recovery/filtration steps and are only noticeable by increases in turbidity.

During purification, protein A chromatography which is often used for capture, exposes mAbs to low pH conditions (between pH 3 and 4) during elution, as well as the low pH hold step for viral inactivation. It is also important to mention that at large scale, proteins are exposed to metal surfaces such as stainless steel (Biddlecombe et al., 2007) and mechanical stresses through pumping and agitation in tanks. Agitation also creates a gas-liquid interface at which aggregation predominantly occurs (Vazquez-Rey and Lang, 2011). Different types of agitation have been shown to yield different types of aggregates, with stirring resulting in insoluble visible and sub-visible particles, whilst shaking causing soluble aggregates (Kiese et al., 2008). Ultrafiltration is another step at which aggregation can occur. It is typically carried out to exchange the product into the desired formulation buffer. However, buffer exchange at high concentrations can result in aggregation as the concentration of protein at the membrane surface may be higher than that of the bulk which contributes to aggregate formation. There is also a potential for aggregation of the drug product once vialed and stored in a liquid state (although this goes outside the scope of the project).

There are multiple steps within the process in which aggregation formation can occur. Therefore, it is important to understand how to remove and control the presence of

aggregates. To remove mAb aggregates, the second chromatography step in purification (e.g. ion exchange and hydrophobic chromatography) is typically utilised to decrease aggregate levels based on the interactions between the aggregates and the resin. To control the level of aggregation, optimising chromatography steps and choosing alternative materials can aid in minimising the amount of aggregates created. Examples of this includes optimising cell culture conditions to minimise thermal stress by reducing the temperature which will compromise yield, minimise mechanical stress by avoiding vortex formation and/or using surfactants. and using solvents/detergents instead of low pH for viral inactivation (Vazquez-Rey and Lang, 2011).

However, to control and remove aggregates from the process, analytical techniques are required to measure the abundance, size and type of aggregates present. Analytics plays an important and critical role in drug development and are expected to be sensitive, reproducible, robust and well controlled. However, there is a constant trade-off between sample preparation, speed, accuracy and range of detection. In addition to this, high throughput techniques that consume a small amount(s) of samples are essential to meet practical demands and restricted resources. Currently, orthogonal techniques are required to complement each other and provide confirmation and confidence in results. Molecular weight, structure and solubility are the three major features used to characterise aggregates. As there are varied sizes and different mechanisms of aggregation, aggregates can be difficult to characterise with one single technique. The next section describes different techniques used for quantification, size estimation and structural analysis of protein aggregates.

1.5.2. Quantification/Size Estimation techniques

Not one single analytical technique can provide detailed aggregation characterisation as techniques vary in throughput, detection limit, sensitivity and accuracy. Three key techniques widely used for quantification and size estimation of aggregates are size exclusion chromatography (SEC), dynamic light scattering (DLS) and analytical ultra-centrifugation (AUC). Figure 1-5 summarises the detection ranges and key

advantages of the different techniques which will be discussed in more detail in this section.

A)

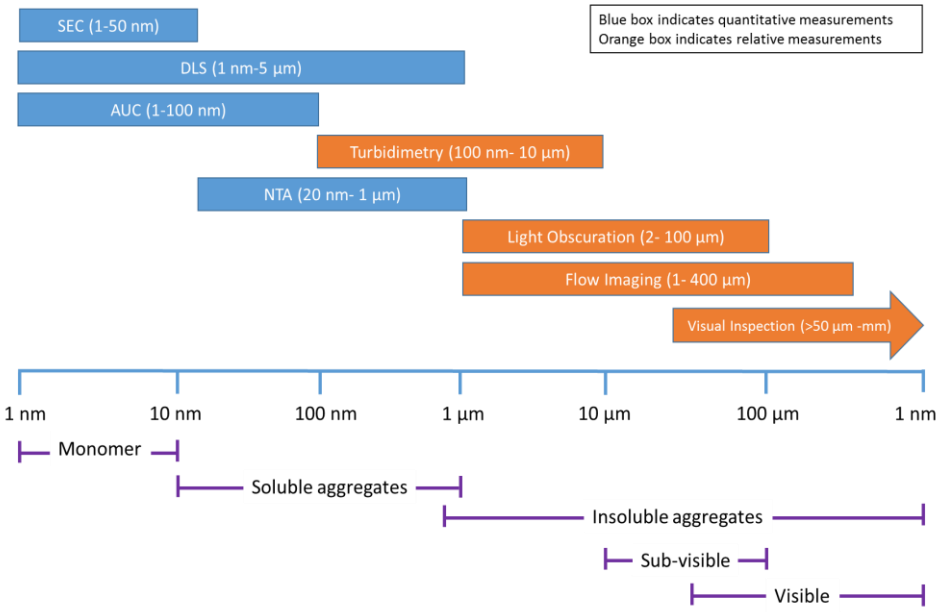

B)

	SEC	DLS	AUC
Sensitivity	Medium-High	High	High
Ease of operation	Simple to run and analyse	Simple to operate, analysis can be difficult	Requires expert skill to run and analyse
Sample Throughput	Medium	High	Low
Focus	Small aggregates (dimer/trimers)	Large aggregates	Small - intermediate aggregates
Sample	30 µL 1 mg/mL 95% purity on Protein A	100 µL 1-10 mg/mL High purity preferred	100 µL 1-10 mg/mL >95% purity

Figure 1-5: (A) Size-based detection ranges of various analytical techniques for aggregation.
Data obtained from Sharma et al. (2010) and den Engelsman et al. (2011). Size Exclusion Chromatography (SEC), Dynamic Light Scattering (DLS), Analytical Ultra centrifugation (AUC), Nanoparticle Tracking Analysis (NTA). (B) Summary of the different techniques for aggregate characterisation. Data compiled from Sharma and Kalonia (2010), den Engelsman et al. (2011) and Cole et al. (2008).

Size Exclusion Chromatography

SEC is the most common technique to quantify and size soluble aggregates less than 50 nm (Figure 1-5A). It is the most typically used technique of ensuring that the amount of mAb aggregates meet regulatory guidelines (<5%). It is a robust and well-established technique with separation on the column occurring based on size. A column is filled with silica-based micro-particles (chromatographic resin) and a running buffer (mobile phase) is pumped through the column to guide protein molecules across the column. Larger molecules which have less accessibility to the pores elute first, whereas smaller molecules which can diffuse through the micro-particles and between the micro-particles elute later in time (Figure 1-6). Accessibility to the pores is defined by the distribution coefficient (K_d) for molecule which has total exclusion (value of 0) or full access to the pores (value of 1).

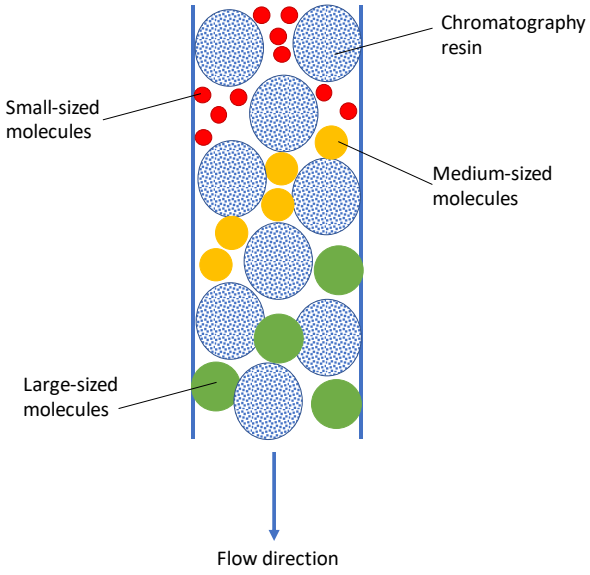

Figure 1-6: Mechanism of separation by size exclusion chromatography.
Larger molecules which have less accessibility to the pores elute first, whereas smaller molecules which can diffuse through the micro-particles and between the micro-particles elute later in time.

SEC combined with multi-angle laser light scattering (MALLS) can provide confirmation of the average molecular weight of species. However, SEC is not suited to analyse insoluble or large aggregates as they often get trapped by frits which protect the column. Additionally, the mobile phase dilutes samples from initial loading concentration, which can cause weakly associated aggregates to dissociate. Also 'sticky' aggregates which interact/adsorb onto the resin can be not only be difficult to clean but also result in a loss of protein being measured. Therefore, it is important to bear in mind when analysing results that SEC may not be a true representation of a sample. Asymmetrical Flow Field Fraction is an alternative analytical technique which can quantify larger aggregates than SEC (even insoluble aggregates). However, it is not as mature as SEC and requires in-depth method development (den Engelsman et al., 2011).

Dynamic Light Scattering

DLS is commonly used in industry to estimate the size and relative percentage of aggregate species. DLS measures Brownian motion and relates this to the size of the molecule. Brownian motion is the random movement of molecules in solvent (Figure 1-7). The larger the molecule, the slower the Brownian motion and stronger scattering of light. Conversely, small molecules move more rapidly hence have a faster Brownian motion. DLS measures the hydrodynamic radius (r_h) of a molecule, which is the diameter of a sphere that has the same diffusion coefficient (D) as the molecule. Hydrodynamic radius is calculated based on the Stoke-Einstein equation (Equation 1-1), whereby κ is Boltzmann's constant, T is temperature in Kelvin and η is the solvent viscosity.

$$r_h = \frac{\kappa T}{6\pi\eta D}$$

Equation 1-1: Stoke-Einstein equation to measure the hydrodynamic radius of molecule

The scattering of light depends on the molecular weight, concentration and shape of the molecule, as well as the light/laser wavelength and scattering angle (Sharma and Kalonia, 2010). DLS is more capable of measuring larger aggregates across a wider sample concentration range (0.1–50 mg/mL) than SEC (Krishnamurthy. R et al., 2008). As intensity of light is proportional to molecular weight, the technique is highly sensitive but often biased to large aggregates as they scatter light more strongly. The technique is poor at resolving small oligomers such as dimers and trimers as it requires a three to four fold (Krishnamurthy. R et al., 2008) difference in hydrodynamic size to resolve different species. Techniques such as nanoparticle tracking analysis (NTA) and micro-flow imaging (MFI) can characterise larger aggregates and particulates which are important to be aware of, especially when the molecule is in the final formulation. NTA is employed for sizing submicron particles (10 nm–1 µm) whereas MFI is for micro particles (1–100 µm) (Zhao et al., 2012). Both techniques enable sample visualisation, however NTA is less reproducible and requires several optimisation steps by a skilled operator. NTA is also very sensitive to the buffer which can raise the interference from the background and make it difficult for the software to track aggregates. MFI requires large amounts of sample and high shear forces and can cause particle fragmentation (Sharma et al., 2010).

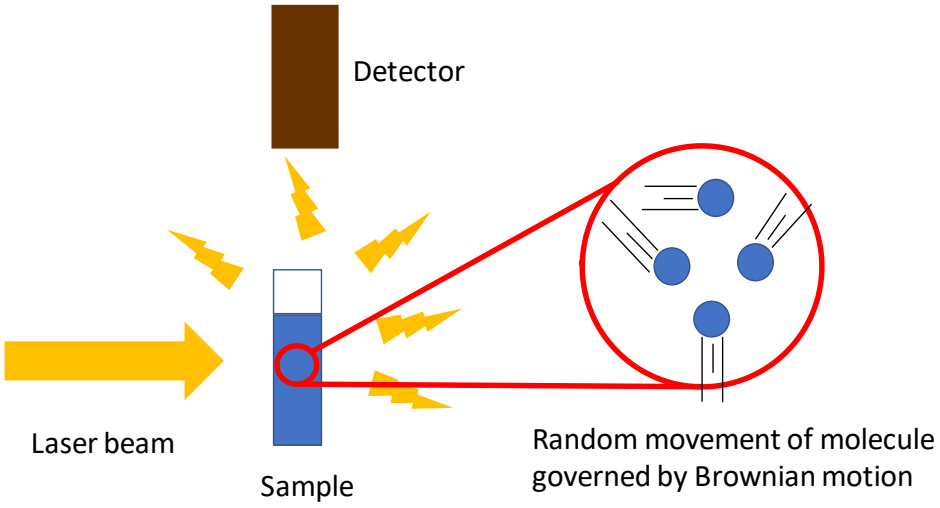

Figure 1-7: Mechanism of dynamic light scattering.

Analytical Ultracentrifugation

Sedimentation velocity analytical ultra-centrifugation (SV-AUC) uses high centrifugal speeds to study sedimentation behaviour. Radial separation causes larger species to sediment to a greater extent than smaller molecules. AUC covers the intermediate size between SEC and DLS with excellent separation and detection for low level aggregates ≤1% (Pekar and Sukumar, 2007). Berkowitz (2006) showed comparable dimer levels to SEC in samples with a range of dimer content. The major limitation with AUC is its low throughput, as it takes 12 hours to run a single sample. Samples are measured in the native state, and although it is not completely destructive, it is not recommended to use for other aggregation assays. Analysis of data is also time consuming and requires operators with expert experience. Although AUC is more expensive than SEC and DLS and requires regular calibration and intensive maintenance, it is commonly used to validate a SEC method.

1.5.3. Techniques to monitor structure analysis

Structural analysis can give insight into the mechanism of formation as well as the state of the protein (native or non-native). There are several techniques that can structurally characterise proteins (Weiss et al., 2016) which include (but are not limited to): circular dichroism (CD), hydrogen-deuterium exchange mass spectrometry (HDX-MS), cross-linked mass spectrometry, small-angle x-ray scattering (SAXS), transmission electron microscopy (TEM) and electron cryo-microscopy (Cryo-EM) and fluorescence spectroscopy. Figure 1-8 summarises the detection ranges of the different techniques used for structural analysis.

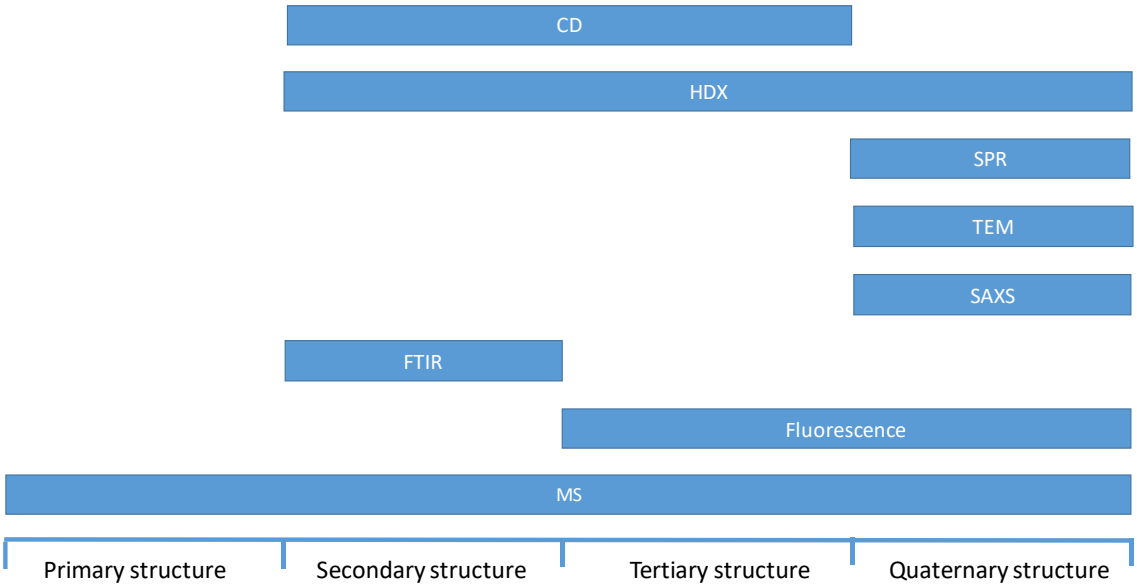

Figure 1-8: Various analytical techniques for structural analysis of aggregation. Data obtained from Wang et al. (2018) and Sharma and Kalonia (2010). Surface Plasmon Resonance (SPR), Circular Dichroism (CD), Hydrogen-Deuterium Exchange (HDX), Mass Spectrometry (MS), Small-Angle X-ray Scattering (SAXS) and Transmission Electron Microscopy (TEM).

Circular Dichroism and emerging technologies

CD has become recognised as a valuable structural technique to provide information on secondary and tertiary structure. CD measures the difference between the absorption of left and right circularly polarised light (Kelly et al., 2005). Operating in the far-UV (180-260 nm) provides quantitative estimates on the secondary structure (e.g. percentage helix, turns and sheets), whereas operating in the near-UV regions (240-340 nm) provides quantitative estimates on tertiary structure conformation (Sharma and Kalonia, 2010). CD is easy to perform and offers speed and convenience in comparison to NMR and X-ray crystallography, as it requires low sample concentration, does not require crystallised samples and samples can be recovered (Kelly and Price, 1997). However, the technique provides low resolution and sensitivity for mAbs. Historically, CD has been primarily used to investigate the secondary structure (alpha helix, beta sheets, etc.) for small molecules/proteins. The technique appears to be more sensitive to changes in alpha helices than beta sheets.

Large molecules such as mAbs are predominantly comprised of many beta sheets. Therefore, CD lacks the sensitivity and resolution to measure small and specific secondary structural changes as the CD outputs are averaged out.

For larger molecules, there are emerging complementary technologies which can provide greater resolution to understand structure related aggregation pathways. Cross-linked MS consists of covalently connecting two functional groups of the protein(s) to gain insight into the three dimensional structure of proteins in solution using MS (Sinz, 2005). MS analysis can occur with the intact protein or after enzymatic digestion. HDX-MS can pinpoint structural changes down to the primary structure (Houde and Berkowitz, 2015) as well as measuring higher order structure (Wang et al., 2018). It probes the exchange kinetics of hydrogen for deuterium and has been able to elucidate the aggregation mechanism for mAb dimers (Iacob et al., 2013). SAXS and TEM can measure quaternary structure. SAXS can provide structural information on shape and size at 1-2 nm resolution (Renaud et al., 2016) and TEM has been shown to visualise mAbs aggregated on the Fc or Fab region (Paul et al., 2012).

Fluorescence Spectroscopy

Fluorescence spectroscopy is a highly sensitive technique for both structural characterisation and aggregation detection. Fluorescence signal is sensitive to the solvent polarity, viscosity and temperature. Intrinsic fluorescence is derived from naturally fluorescent amino acids (e.g. tryptophan), whereas extrinsic fluorescence comes from the addition of fluorescent dyes. Measuring intrinsic vs. extrinsic fluorescence is often a trade-off between the intensity of fluorescence signal and invasiveness (Remtulla, 2009). The absorption and emission of light during fluorescent is illustrated by the Jablonski diagram (Figure 1-9).

Fluorescence is measured by exciting a dye with a laser/lamp light which is absorbed by the dye, and lifts the electrons of the dye to a higher excited state (Hawe et al., 2008). Once excited, energy first dissipates through vibrational relaxation which is a non-radiative process (dotted arrow in (Figure 1-9) that occurs within the same energy

level (e.g. S_2 to S_2). Energy can also dissipate by internal conversion in which an excited electron transitions to a lower vibration level in lower electronic state (e.g. S_3 to S_2). The electrons eventually relax back down to ground state by fluorescence emission. Absorbance is a very fast (10^{-15} seconds), non-radiative transition occurs in 10^{-12} seconds and fluorescence is a slower process in the order of 10^{-8} seconds (Lakowicz, 2010). Fluorescence intensity can also decrease by a dynamic process known as quenching. Quenching is when an excited fluorophore encounters a 'quencher' molecule (collisional quenching) or forms a non-fluorescent complex with the quencher (static quenching). Measuring fluorescence involved exciting a molecule at an excitation wavelength and measuring the output at an emission wavelength(s). Upon interacting with protein aggregates, an increase in fluorescence intensity is usually accompanied with a blue or red shift of the peak maximum. A blue shift indicates the dye is in a hydrophobic environment, whereas a red shift indicates the dye is in a hydrophilic environment.

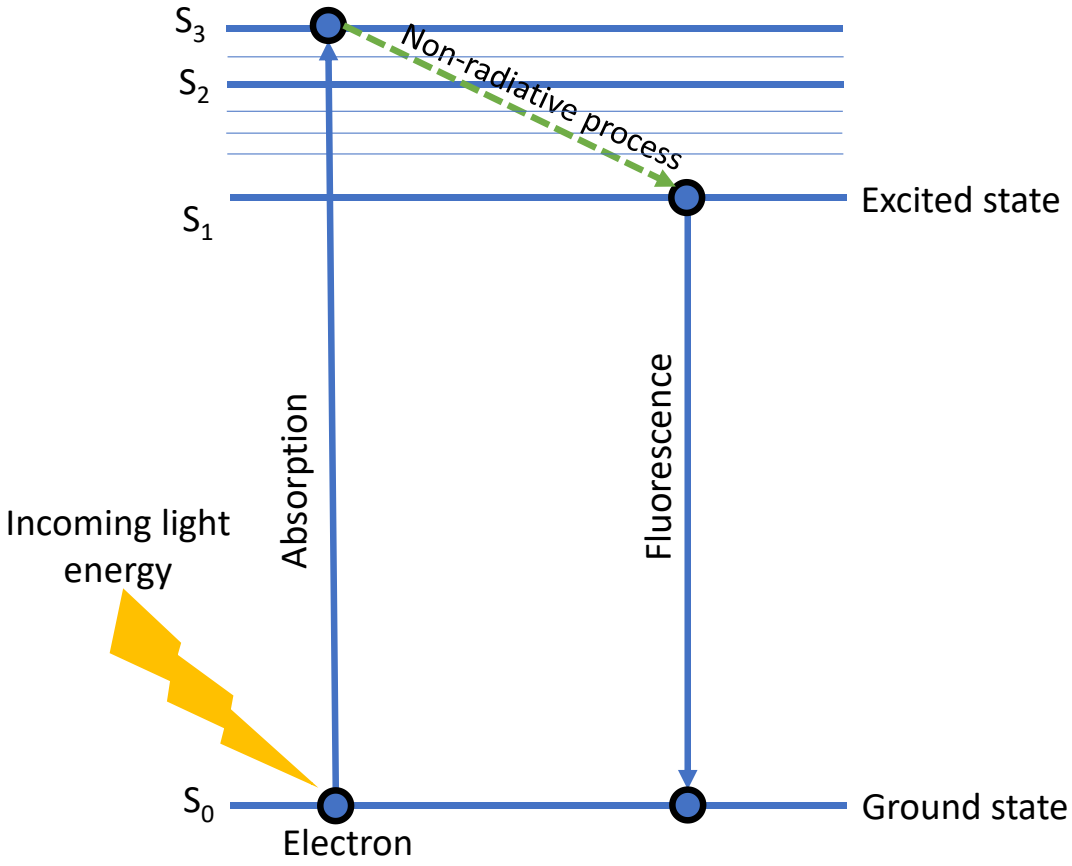

Figure 1-9: Jablonski diagram.
The first step is the absorbance of a photon from a light source which cause electrons to become excited from a lower energy to a higher energy level. S depicts energy/electronic levels. Energy dissipates by non-radiative processes such as vibrational relaxation/internal conversion. The electrons eventually relax back down to ground state by fluorescence emission.

Extrinsic fluorescence can also be used to monitor protein folding/unfolding and detect small amounts of large aggregates typically undetected by SEC (Sutter et al., 2007). This usually involves measuring onset/melting point (T_{onset}/T_{melt}) and midpoint temperatures of protein thermal unfolding transitions (Brader et al., 2015). Using fluorescent dyes, reduces the amount of mAb required. When combined with PCR or differential scanning fluorimetry, it creates a high throughput, rapid and sensitive assay that can detect molten globule intermediates and aid in identifying optimum formulation buffer conditions (Hawe et al., 2008).

Fluorescence can also be carried out in other formats including time-resolved fluorescence, anisotropy and Förster resonance energy transfer (FRET). Time-resolved fluorescence is widely used because of the increased information available from the data as compared with stationary or steady-state measurements (Lakowicz, 2010). FRET is a sensitive, distance-dependent technique that focuses on the energy transfer between two different fluorophores. The closer the fluorophores are, the more energy is transferred, which is why FRET is often referred to as a molecular ruler. The uses of FRET will be further discussed in Chapter 2 and mechanisms of FRET in Chapter 6.

1.5.4. Current efforts to measure aggregation

There has been a motivated continual effort over the last decade to improve techniques that can measure aggregation. For SEC, the development of ultra-performance liquid chromatography operating at higher pressures (Mou et al., 2014), capillary SEC (Rea et al., 2012), parallel SEC (Diederich et al., 2011) and the use of sub-2µm (Fekete et al., 2013) particle sizes has enabled higher throughputs and/or comparable performance. Other improvements include the use of longer columns, lower linear velocities and reduced sample volume. Coupling SEC and light scattering has shown to provide the ability to determine molecular weight without the need for a reference, regardless of shape and conformation (Pothecary et al., 2012). There has also been an increase in predicting and reducing aggregation using chemometric modelling/PLS. This has been used in different formats e.g. with intrinsic fluorescence (Ohadi et al., 2015), extrinsic fluorescence (Schwab and Hesse, 2017) and surface plasmon resonance (van der Kant et al., 2017).

Noticeably, most of these techniques/methods require purified samples and there is a lack of techniques that can measure aggregation in unpurified samples from cell cultures. Although there has been considerable progress to maximise titres, cell counts and viability in upstream, there is little understanding to how changes in the upstream conditions impact product aggregation in the bioreactor. Additionally, there is less flexibility in controlling aggregation in upstream as the desire for high titres and

optimised growth conditions make it difficult to change conditions. In bioreactors, the presence of HCP's, DNA, cells and other cellular impurities can interfere with measurements, hence aggregation characterisation is usually carried out on candidate molecules after purification. Although purification is possible, it results in longer timelines, increased costs/resources and key components (e.g. large aggregates) may be removed, thus ultimately providing data that may not be a true representation of the cell culture. Hence, there is a need to develop analytical assays that can measure aggregation in a complex multi-component environment, which will save time and resources and aid in screening and selecting cell lines and molecules against product quality.

1.6. Conclusion

The production of mAbs requires a versatile analytical toolbox to verify that only safe and efficacious drugs of high quality are commercialised. Analytical methods are required throughout the entire drug life cycle – from discovery and process development through to clinical trials and final market distribution – and therefore play a vital role in success. Aggregation is a major CQA that can severely affect product quality and therefore needs to be reduced to acceptably low levels. Aggregates can be difficult to characterise even after purification due to differences in size, structure, charge, solubility and mechanisms of formation. Not a single technique can provide information on size estimation and structural analysis. In terms of size quantification, even though SEC is a gold standard in the industry, both AUC and DLS serve as orthogonal techniques to SEC as they can detect aggregates not characterised by SEC, and thus increase confidence in data interpretation. In terms of structural analysis, CD, HDX-MS, SAXS, TEM and fluorescence can be used to characterise proteins which have varying levels of detection range, sensitivity, measurement speed and sample preparation required. In the next section, techniques appropriate for measuring aggregation in cell culture will be evaluated with the aims and objective of the thesis as a focus. The most feasible and appropriate technique will be selected and developed.

2 Technique evaluation/selection

2.1. Chapter Aims

In Chapter 1, current techniques to measure aggregation in purified conditions were discussed. Focusing more on the aims of the EngD, in this chapter, different techniques that are able or have the capability to measure mAb aggregates in cell culture media are evaluated.

The aims of this chapter are as follows:

1. Define the aim/objectives for the EngD and outline the characteristics of aggregates (size, type and amount) to form a criterion of characteristic that the aggregation assay should measure

2. Discuss the different techniques that could be potentially used to measure aggregation in cell culture.

3. Compare the pros and cons of each technique and select which will be the focus of the EngD

2.2. Thesis aims

The aim of this thesis was to create a quantitative high-throughput assay to measure mAb aggregation in CHO cell cultures for biopharmaceutical process development. The focus was to build an assay for use in cell line selection to measure directly into the complex cell culture supernatants. The assay was required to reliably and specifically distinguish good cell lines with less mAb aggregates, from bad cell lines with large amounts of mAb aggregates. As well as this, the assay should be capable of measuring mAb aggregates in a complex environments including other protein aggregates from host cell proteins, lipids, cell debris and DNA. In addition, there needed to be minimal sample preparation such as purification/filtration in order to measure the true representation of the aggregate species in the cell culture. In terms of aggregate characteristics, the focus was to measure soluble small-to-medium sized

aggregates (1-100 nm and mainly dimer-large aggregates) and to detect in the range 1-10%, as these are ranges typically seen within industry. The creation of this assay would impact in the following areas: faster screening of candidates, reduced timeline of product to market, better quality product, reduced immunogenicity issues, increased manufacturing consistency and lower CoG and CoD.

2.3. Choosing an approach/technique for measuring aggregation in cell culture

In the previous chapter, techniques used to measure aggregation were evaluated. However, in-line with the aims of the thesis, the focus will now be on selecting techniques that is capable of measuring aggregates in cell culture supernatants. Some of the techniques mentioned in Chapter 1 will be revisited, however, with a focus on highlighting and detailing the studies (or lack of) that have shown the techniques ability to measure aggregation in crude samples.

Figure 2-1 shows the different techniques considered for developing an assay to measure aggregates in cell culture supernatant: SEC, immunoassay, fluorescence spectroscopy and Fourier-transform infrared (FTIR) and Raman spectroscopy.

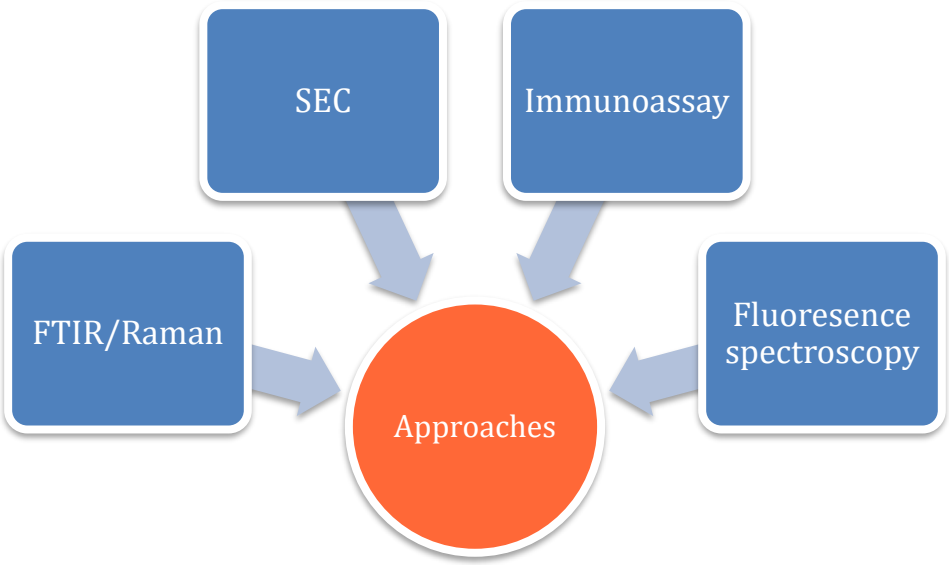

Figure 2-1: Four different approaches to consider investigating to monitor aggregation in cell culture supernatants.

2.3.1. Use of size exclusion chromatography in cell culture supernatants

Paul et al. (2014) showed the capability to use SEC to detect mAb aggregates in mammalian cell culture supernatant. Their study showed that cell culture components and HCP impurities eluted later than the purified mAb, which allowed clear separation between media/cell culture components and aggregated mAb on the SEC chromatogram. As SEC is a size-based separation technique, there are advantages and disadvantages. An advantage of the size-separation is that Paul et al. (2014) was able to separate oligomers, dimers and monomeric mAb. A disadvantage of the size-separation is that SEC would not be able to distinguish between an aggregated HCP/impurity and an aggregated mAb that are the same size.

Another concern about using SEC, is that naturally the running buffer dilutes the sample throughout the column and may cause reversible/weakly formed aggregate to dissociate. If the aggregates dissociate, then the sample would not be a true representation of the cell culture environment. As it as required to measure mAb aggregates as close to the cell culture environment as possible, this would be difficult to attain using SEC. In addition, as the assay needs to be high-throughput, typical SEC which takes roughly 30 mins per sample would be too slow. However, the advancements with ultra-performance liquid chromatography (UPLC) that use higher pressures with smaller resins have been able to shorten analysis down to 5 minutes (Chen and Ge, 2013).

Using cell culture supernatants may cause adsorption of cell culture components onto the column, which would decrease the separation efficiency of the column, thus inevitably reducing the life-time of the column. Replacing SEC columns frequently is costly. Although, adding azides to the buffer could be used to prolong the column lifetime, the azides may or may not impact the sample.

2.3.2. Use of immunoassays in cell culture supernatants

Immunoassays use ligands immobilised onto a surface that have a specific interaction with the protein of interest. There were two immunoassay techniques that showed potential in measuring aggregates in cell culture supernatants: labelled anti-mAb

assay and surface plasmon resonance (SPR). The labelled anti-mAb assay idea was proposed by Zurdo et al. (2011) and the set-up of the assay is shown in Figure 2-2.

The assay uses Fc specific anti-mAbs (which bind to other mAbs) for capture and detection. The idea was as monomeric mAbs only have one Fc region, they will only be able to bind to the immobilised anti-mAb. In comparison, as aggregated mAb are composed of multiple aggregates, there would be multiple exposed Fc regions. Thus, aggregated mAb would have the ability to bind both the immobilised-anti mAb and labelled anti-mAb for detection.

The assay would fulfil the high-throughput criteria as it would be carried out in a 96-well plate. However, the assay development would be more complex as it requires capturing and detecting anti-mAbs that do not interact with each other as this would arise to false positive. Additionally, regeneration would be difficult as it would require conditions harsh enough to remove the detection anti-mAb from the capture mAb, but not too harsh to ensure that capture anti-mAb stays immobilised to the well. The biggest limitation of this assay is that it assumes that mAb are aggregated at the Fab region leaving the Fc region free. This would mean only mAbs that are aggregated by the Fc region would not be detected. In addition, it would not be possible to distinguish between different sizes of aggregates e.g. dimer vs. HMW (high molecular weight).

An alternative to immobilising anti-mAbs could be to immobilised protein A which is also known to have a strong interaction with the mAb Fc region. The only caveat is that other proteins such as HCP are known to bind to protein A (Nogal et al., 2012), therefore the assay would not be specific to mAb aggregates.

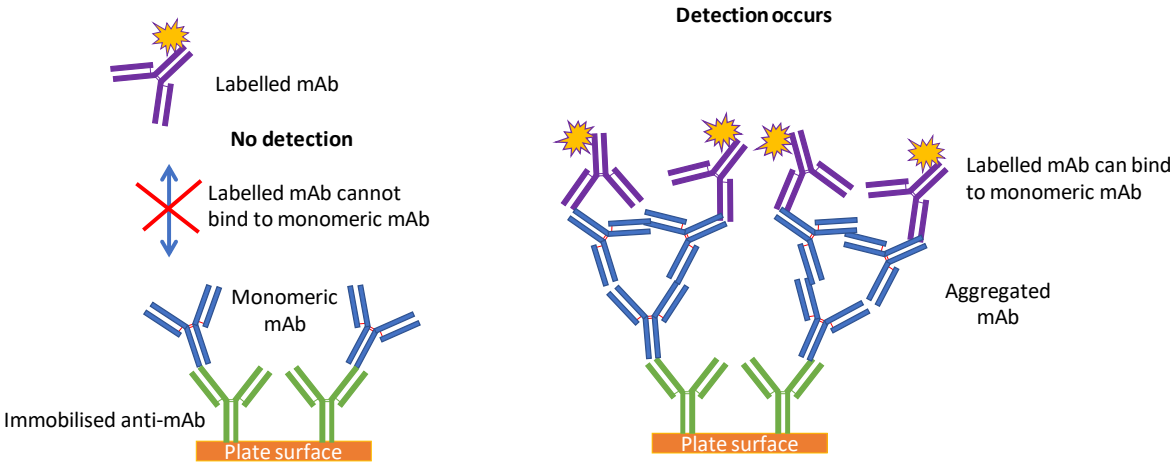

Figure 2-2: Oligomer detection assay
Figure adapted from Zurdo et al. (2011) the immunoassay monitors aggregation based on the relative abundance of secondary binding sites. Both the immobilised anti-mAb and the labelled anti-mAb only bind to Fc region of mAbs. As monomeric mAbs would only have one available Fc region, it would only be able to bind to anti-mAb. Aggregated mAb would able to bind to both immobilised and labelled, due to the availability of multiple Fc regions.

Another type of immunoassay, SPR, uses a shift in plasmon resonance (wavelength of maximum absorbance) to detect aggregation. Nanoparticles are typically used for SPR as they are sensitive to changes in inter particle separation (Yeo et al., 2015). Shorter distances between nanoparticles result in peak red shift (a shift in peak maximum to higher wavelengths), peak broadening and even a visible change in colour. The Tessier group at Rensselaer Polytechnic Institute created an assay called Affinity Capture-Self Interaction Nanoparticles Spectroscopy (AC-SINS), which involves conjugating the mAb of interest to gold nanoparticles which have a strong absorbance around 520 nm. The attractive forces between mAbs conjugated to the nanoparticles would increase or decrease the distance between nanoparticles, with shorter distances reflecting aggregation (Liu et al., 2014). Sule et al. (2013) has shown that AC-SINS can be used in the presence of cell culture media. However, rather than quantifying the amount of aggregates present, AC-SINs identifies mAbs that are likely to self-associate to be used as a predictive tool rather than direct aggregation

measurement. In addition, it can be difficult to obtain consistency in the amount of antibody immobilised per gold nanoparticle (Sule et al., 2013, Jayaraman et al., 2014). Overall, as this technique is more of predictor than measurement of aggregation, it is more suited in protein engineering studies where the protein sequence of mAbs can be altered to make them less likely to self-associate/aggregate.

2.3.3. Use of fluorescence spectroscopy in cell culture supernatants

As mentioned in section 1.5.3.2, fluorescence spectroscopy can be measured 'intrinsically' direct from the molecule of interest (aromatic amino acids) or 'extrinsically' with the introduction of fluorophores into the system. However, the use of intrinsic fluorescence as assay for cell culture supernatant would be difficult as the media and HCPs which may also contain aromatic amino acids (e.g. tryptophan) would also be measured and interfere with analysis. Therefore, in this section, extrinsic fluorescence (single dyes, FRET and labelled peptides) will be evaluated with a focus on using the technique on cell culture supernatant samples.

Extrinsic fluorescence

There is a lot of literature available on different fluorescent dyes and their mechanism of interaction with protein aggregates (Hawe et al., 2008). There have been a few recent publications that have shown the use of fluorescent dyes to distinguish monomeric and aggregated mAb in purified samples and cell culture supernatants. Paul et al. (2015a) developed a method with Bis-ANS that was able to discriminate between CHO cell culture supernatants containing different levels of mAb aggregates. Extrinsic fluorescence with partial least squares (PLS) has also been used for real-time monitoring of antibody aggregation in CHO fed-batch cultures using multi-wavelength fluorescence (Schwab and Hesse, 2017) and 2D fluorescence (Schwab and Hesse, 2013). Using fluorescent dyes, Schwab and Hesse (2017) were able to achieve high predictability with a low error using Bis-ANS and Thioflavin T. Measuring fluorescence with extrinsic dyes can be conducted in a high-throughput format using 96-well plates, which can also be eventually optimised to require lower

volumes. Depending on the range of the wavelengths being measured, a single 96-well plate can be measured in 30-40 minutes.

Despite the benefits of using fluorescent dyes, it is not possible to control what the dyes bind to in a sample. Therefore, in a complex sample such as cell culture supernatant, the fluorescent dyes may bind to other aggregated protein or other protein with exposed regions of interest (such as hydrophobic regions) that would interfere with measurement. In addition, the media would also have its own fluorescence which may or may not interfere depending on the fluorescent dyes chosen. Furthermore, most fluorescent dyes have one main form of interaction (e.g. hydrophobic interaction), meaning that only a certain type of aggregate would be detected. Similarly, to the immunoassay idea, it would not be possible to distinguish between varied sizes of aggregates. Overall, extrinsic fluorescence for application in cell culture supernatants seems more promising than intrinsic, but many controls will be required to ensure that the assay is specifically measuring mAb aggregates.

The fluorescence discussion has so far focused on the use of one fluorophore. However, there is another type of fluorescence technique widely known as fluorescence resonance energy transfer (FRET).

Fluorescence Resonance Energy Transfer

FRET is used for a wide variety of applications. The most common uses are: to visualise protein-protein interactions (Zal, 2011), to study cell membranes (Loura and Prieto, 2011). probe protein conformation changes, as a biosensor (Hochreiter et al., 2015), and to detect structural changes to nucleic acids and proteins on a single-molecule level (Roy et al., 2008).

FRET relies on the ability to transfer energy from two fluorophores (donor and acceptor) at distances between 20 to 90 Å (10 Å = 1 nm) (Lakowicz, 2010). This distance-dependent energy transfer makes FRET sensitive to measure molecular distances. Steady state and time-resolved measurement are often used to measure binding interactions and distances respectively (Lakowicz, 2010).

In terms of protein interactions, FRET is currently mostly used in the following instances: (1) to measure the precise distances between a fixed donor and acceptor on the same molecule (2) to use as a proximity indicator between a fixed donor and acceptor on multi-domain proteins to measure conformational changes, (3) to use as a proximity indicator between donor and acceptor in solution (a three-dimensional environment).

(1) provides precise distances whereas (2) relies on the absence or presence of FRET to determine if structural changes have occurred. However, the idea of using fixed donors/acceptors for a cell culture supernatant aggregation assay would require the donor and acceptor to be already attached to mAbs. This means that a donor and acceptor would have to be engineered into the DNA which may affect the folding of the mAb. In addition, the donor and acceptor would have to be removed post-measurement, as it may affect the function or stability of the mAb.

(3) suits the aggregation assay criteria by measuring FRET between a donor and acceptor that are both free in solution. This would require the donor and acceptor to have some affinity/specificity to the mAb aggregates. However, this is more complex as it would be heavily dependent on random distribution of multiple donor/acceptor in solution. In addition, compared to regular fluorescence, there is less literature available on the use of FRET for protein aggregation and most current studies focus on intracellularly formed aggregates (Kitamura et al., 2015) or analysing protein folding on a single-molecule level.

Overall, using idea (3) would require: well-planned controls and in-depth assay design to ensure specificity to mAb aggregates and that FRET is able to occur (by choosing appropriate donor and acceptor and achieving the required distances – see Chapter 5 for more details). If the FRET design works, it would be the first of its kind to measure mAb aggregates.

Labelled affinity peptides

Proteins and peptides can also be labelled with fluorescent dyes to visualise binding interaction. Labelling can occur during the synthesis of the peptide or post synthesis

by covalent bonding via reactive groups such as NHS ester groups on primary amines. For a mAb aggregation assay in cell culture supernatant, the protein/peptide would need to have specificity to mAb aggregates. Once specificity has been established, the protein/peptide can be labelled fluorescently to aid detection. Interestingly, Cheung et al. (2017) found two (out of ten) peptide sequences from a phage display peptide library that had increased affinity with aggregated mAb. Using an ELISA, they showed the "affinity peptides" had 9-fold and 7-fold better binding toward aggregated NISTmAb than control non-aggregated NISTmAb. Labelling affinity peptides with dyes was a promising idea as the peptide would be specific to mAb aggregates and the dye would give rise to a detectable signal. To make sure that the assay works, one would need to ensure that an appropriate dye/label is chosen. The conjugation of the peptide to the dye should not affect the function of the either the peptide or the dye.

2.3.4. Use of Fourier-transform infrared and Raman spectroscopy in cell culture supernatants

Fourier-transform infrared (FTIR) investigates conformational changes occurring in the secondary structure of a molecule. FTIR has mostly been coupled with chemometrics as described in Capito et al. (2013) and Telikepalli et al. (2014). Telikepalli et al. (2014) compared the second derivative FTIR spectrum of a native and heat stressed mAb. The change in the position of peak minima in the spectrum from 1637 cm^{-1} to 1690 cm^{-1} corresponded to beta sheets being altered upon stressing. Capito et al. (2013) used mid-infrared spectroscopy to quantify aggregation in cell cultures with predictability down to 1%. Changes in spectrum could be identified at certain wavenumbers such as presence of aggregates (1630-1600 cm^{-1}), change in beta sheets (1619 cm^{-1}) and change in hydrogen bonding (1622 cm^{-1}).

Like FTIR, Raman spectroscopy can investigate conformational changes occurring in the secondary and tertiary structure of a molecule. However, for quantification, both FTIR and Raman requires developing a model with real process samples and process-sample mimics (spiking mAb aggregate into cell culture supernatant of non-mAb producing cell lines to mimic real cell culture conditions). Most research with Raman

and aggregation use developed chemometrics/principal component analysis (PCA)/partial least-squares regression (PLSR) and/or heating for denaturation (Gómez de la Cuesta et al. 2014; Thiagarajan et al. 2015). With all modelling, the accuracy and reliability of the model depends on that data that was used to generate the model. Therefore, a large dataset would be needed for the model to be representative. However, a major caveat for using both FTIR and Raman is that cell culture will contain numerous amounts of proteins that may have beta sheets (or secondary/tertiary structure) that would skew results. Thus, making it hard to selectively measure increase/decrease in mAb aggregation.

2.4. Conclusion

Out of the four different approaches, FTIR and Raman were least favourable. This was because FTIR/Raman measure structural changes at wavelength/parameters that are not specific to mAbs. Hence, both techniques would not be specific to measure changes in mAb aggregation in cell culture samples. Therefore, the decision was between SEC, immunoassay and fluorescence spectroscopy. Table 2-1 highlights the main pros and cons focusing on sensitivity in cell culture supernatant, time and cost.

Using cell culture supernatant samples directly onto SEC would require a strict observation and controls in place to ensure the column is regenerated between uses. SEC would also not be able to distinguish between an aggregated HCP/impurity and an aggregated mAb that are the same size. Samples that are purified, or that have undergone a form of sample preparation such as filtration, may remove aggregated species of interest and bias the results. Additionally, the sample throughput was also lower compared to the other plate-based assay.

Although the labelled immunoassay could be high-throughput due to being plate based, developing the assay had two key steps (selecting materials and regeneration) that would be difficult/time-consuming. The assay would require capture and detection anti-mAbs that do not interact with each other (to prevent false positives measurements), and regeneration conditions that would remove only the detection anti-mAbs, whilst leaving the capture anti-mAbs immobilised. Selecting the right

anti-mAbs would take time due to the vast amount of options in the market e.g. different animals, isotypes etc. Identifying regeneration conditions which are reproducible would be vital to reduce the cost of the assay. However, because both components are mAbs it would be tricky to find buffers that would only remove the detection mAb. The biggest flaw is that based on the assay design, only mAbs aggregated at the Fab region would be detected and the assay would not be able to distinguish the size of aggregates.

SPR was only suitable as a predictor of aggregation rather than actual measurement of aggregation.

Overall, it was decided to investigate extrinsic fluorescence spectroscopy as an assay to measure mAb aggregates in cell culture supernatant. Intrinsic fluorescence may not be sensitive enough to detect low-level mAb aggregation. Extrinsic fluorescence, and in particular, the fluorescence with the single dye seemed the most promising to start with, as there was already a considerable amount of work and information available in the literature. In addition, the assay set-up was simpler and cheaper than the SEC and immunoassay approaches. A plate-based fluorescence assay would be easy to implement as most companies have plate readers. Although the sample would not be retrievable (cannot use it for other assays), reducing the volume required for measurement down to 10 µL with 384 well plates can minimise the impact of sample loss. Since there is a lack of control in binding with the use of dyes, it is important to ensure that the dye assay was created with specificity towards mAb aggregates. To start, with the fluorescent dye assay was investigated as it is the simplest. To add more specificity to the assay, the affinity peptide assay would be investigated first followed by the FRET assay. The affinity peptide assay is a simpler approach at redesigning the fluorescence assay compared to the FRET assay which is more complicated due to the number of components and biophysical understanding required to develop the assay.

Table 2-1: Pros and cons for SEC, immunoassay and fluorescence used with measuring aggregation of cell culture samples

Technique	Pro	Cons	Cost	Time
SEC	- Size based separation - Work horse for aggregation measurement	- Column regeneration - Sample dilution through buffer - Expensive columns	£££	20-30 mins per sample (5-8 min UPLC method)
Immunoassay	- Larger aggregated structure can bind to detection markers	- Predominantly measures Fab based aggregates - Difficult to choose compatible assay material and regeneration conditions	££	3-4 hours: 96 well plate
Fluorescence **-Intrinsic**	- Easy to use and set-up	- Will pick up tryptophan present in other host cell proteins - May not be sensitive to small changes to product conformation	£	30 mins: 96-well plate
-Extrinsic	- Binds to specific regions e.g. exposed hydrophobic patches - Easy to use and set-up	- Lack of control in binding to mAb aggregates - Only detects one type of interaction (e.g. hydrophobic)		

2.5. Thesis objectives

The aim of the thesis is to develop an assay which can measure mAb aggregates in cell culture supernatant samples with minimal sample preparation. Reviewing the literature found fluorescence spectroscopy to be the most promising technique currently available for detailed investigation. Three different fluorescence techniques: single extrinsic dye, FRET and labelled affinity peptide was taken forward for experimental evaluation. The objectives for the three different assays as followed:

Initial dye (single extrinsic dye) assay Objectives A

1. Measure mAb aggregates spiked into purified system (buffer)
2. Measure mAb aggregates spiked into cell culture supernatants of a non-mAb producing cell line
3. Measure mAb aggregates spiked directly in cell culture supernatants of a mAb producing cell line
4. Identify the size of aggregates the fluorescent dyes bind to using SEC with fluorescence detectors

Labelled affinity peptide assay Objectives B

1. Assess the biotinylated affinity peptide's ability to measure aggregates using Octet and Biacore
2. Measure mAb aggregates spiked into a purified system (buffer) with fluorescent affinity peptide with different buffers
3. Identify the size of aggregates the fluorescent affinity peptide bind to using SEC with fluorescence detectors
4. Calculate the K_d of the fluorescent affinity peptide and identify binding site using HDX.

FRET assay Objectives C

1. Design FRET assay by choosing the right donor and acceptor dyes and ensure specificity to mAb aggregates
2. Measure mAb aggregates spiked into purified system (buffer)

3. Conduct controls to troubleshoot (e.g. measure spectral overlap, Förster's radius)
4. Assess the use of the FRET assay with smaller proteins

3 Materials and Methods

3.1. Monoclonal antibody and null cell culture

3.1.1. Monoclonal antibody

IgG1 monoclonal antibody (mAb A and mAb B) produced in CHO cells were used in this study. The mAbs were cultured in proprietary chemically defined serum free media with mAb A produced in shake flasks and mAb B produced in a bioreactor. The culture was harvested at day 14 with viabilities and cell densities of 95% and $18x10^6$ cells/mL and 76% and $4x10^6$ cells/mL for mAb A and mAb B, respectively. The isoelectric point (pI) of IgG mAb A and B were 8.4 and 9.5, respectively. MAb A was used for experiments with purified mAb and mAb B was used for experiments with mAb in clarified cell culture supernatant. MAb A was protein A purified using MabSelect SuRe^{TM} (GE Healthcare Life Sciences, Uppsala, Sweden) with a 185 mL column (23 x 3.2 cm) using an AKTA Avant system. After purification, mAb A was neutralised to pH 7.5±0.1 and filtered using a 500 mL 0.22 µm filter system (Corning, Corning, New York). The purified mAb A was then dialysed into 50 mM sodium acetate pH 5.5 for storage at 4^0C. The CHO cell culture producing mAb B was sampled on day 1, 3, 7, 10 and 14. The mAb B samples were then spun down at 4,000 rpm for 10 mins, followed by 0.22 µm filtration (Millipore, Cork, Ireland) to remove cell debris remnants prior to assay measurements.

3.1.2. Null cell culture

The null cell line (CHO-K1A) was used to obtain time-course cell culture supernatant samples in the absence of mAb. CHO-K1A was cultured in proprietary chemically defined serum free media in three 600 mL shake flasks. For the dye assay study, shakes flasks were sampled on days 0, 3, 7, 10, 14 and harvested at day 14 with viabilities and cell densities ranging from 53%-85% and 11-$18x10^6$ cells/mL respectively. Cells were also spun down at 4,000 rpm for 10 mins followed by 0.22 µm filtration (Millipore, Cork, Ireland).

3.2. Creation of aggregates

To generate aggregates to test the assay, mAb A was subjected to thermal stress. MAb A (11 mg/mL) was stressed at 60°C for 72 hours (acetate buffer) or 7 hours (phosphate buffer) in an incubator and then 0.22 µm filtered (Millipore, Cork, Ireland). The stressed protein was used to assess the sensitivity of the dyes by spiking different amounts of stressed mAb into wells of a 96 well clear flat-bottom micro plate (Corning, Kennebunk, Maine) containing unstressed protein. Domain antibody (dAb) A (25 kDa, 5.0 mg/mL, 50 mM sodium acetate pH 5) was stressed at 45°C for 24 hrs. RNase A (0.6 mg/mL) supplied by Sigma Aldrich (Steinheim, Germany) was prepared in 50 mM sodium acetate pH 5.5 and stressed at 60°C for 5 days. Wheat germ agglutinin Alexa Fluor 350 conjugate was obtained from Thermo Scientific (Rockford, Illinois) was prepared in PBS pH 7.2.

3.3. Size Exclusion Chromatography

Samples were analysed using SEC (injection volume 10 µL) with Agilent 1100 and a TSKgel G3000SWXI (7.8 x 300 mm) column (TOSOH Bioscience). The running buffer composed of 100 mM sodium phosphate (monobasic), 400 mM sodium chloride, pH 6.8. The flow rate was 1.0 mL/min and protein were detected using UV detectors at 214 nm and 280 nm. For smaller molecules such as dAbs and RNase A, TSKgel G2000SWXI (7.8 x 300 mm) column (TOSOH Bioscience) was used with 100 mM sodium phosphate (monobasic), 200 mM sodium chloride, 5% n-propanol pH 6.8 as the running buffer with a flow rate was 0.5 mL/min.

For SEC combined with fluorescence detection (Agilent 1100) with the dyes, injection of samples was increased to 50 µL (or 100 µL) to strengthen the signal. The same ratio/amount of dye used in the plate assay was added to the samples prior to injection into the column. The following excitation/emission wavelengths were used: SYPRO Orange (495/500 nm), ProteoStat (530/605 nm), CCVJ (435/500 nm), Thioflavin T (430/495 nm), Tide Fluor 2 (440/535 nm) and Fluorescein (440/530 nm).

3.4. Dynamic Light Scattering

DLS (Wyatt DynaPro™ Plate) was used to measure the size of aggregates. Samples were run at 100 µL at approximately 10 mg/mL (where possible) using a 96 well clear flat-bottom micro plate (Corning, Kennebunk, Maine). The method programmed consisted of a 15-minute wait time before collecting acquisitions. Temperature was set to maintain at 25°C and 10 acquisitions were collected per well. Laser power was set to auto-adjust.

3.5. Plate based dye aggregation assay

50 µM Bis-ANS, 5X SYPRO Orange, 3 µM ProteoStat and 50 µM ThT was the final concentration in each well. ThT (Sigma Aldrich, Bangalore, India) and Bis-ANS (Sigma Aldrich, Steinheim, Germany) were solubilised into MilliQ water. SYPRO Orange (Life Technologies, Eugene, Oregon) was diluted using MilliQ water and ProteoStat (Enzo Life Sciences, Farmingdale, New York) was prepared based on the manufacturer's protocol. Concentration of mAb A was kept to 1 mg/mL when using stressed mAb (mAb in cell culture supernatants had varying titres) with a final volume of 200 µL in each well (n=3). The excitation/emission wavelengths for each dye were as follows: Bis-ANS 390/450-600 nm, SYPRO Orange 495/550-700nm, ProteoStat 530/560-700 nm and Thioflavin 430/460-600 nm. The assay was measured using a 96 well clear flat-bottom micro plate (Corning, Kennebunk, Maine) with Infinite M200 plate reader (TECAN). The following parameters were used for fluorescence measurement: bottom reading, integration time 20 µs and 25 flashes. The data was analysed using OriginPro and smoothed using Savitzky-Golay filter with a second-degree polynomial (Gaussian shape) and smoothing factor of 15 (number of points used to smooth the data). Wu et al. (2015) demonstrated that Savitzky-Golay was the best filter in theory and practice for fluorescence spectrum data processing. The smoothing factor of 15 was found to give a good balance between smoothing the data and not over-smoothing.

3.6. 2D fluorescence scan of media

2D fluorescence measurements of the media were carried out on Cary Eclipse fluorescence spectrophotometer (Agilent). The following conditions were under 3D scan were used: excitation at 250-700 nm, emission at 250-700 nm, 10 nm increments, medium speed, photomultipliers (PMT) 550. Measurements were carried out using 10 mm semi-micro fluorimeter quartz cuvettes (Lightpath Optical UK, Devon, England) with 1 mL of sample.

3.7. Protein and HCP concentration

Pierce Coomassie Plus (Thermo Scientific, Rockford, Illinois) was used to measure the total protein concentration in cell culture supernatant samples. Samples acquired on and before day 3 of culture were measured according to supplier's "Micro-Micro-plate" protocol due to lower concentrations of protein. Samples acquired after day 3 of culture were measured with the micro-plate protocol. A GlaxoSmithKline in-house sandwich ELISA was used to measure the concentration of HCP in the cell culture supernatants. The standard used for this assay contains thousands of HCP's based on a null cell culture supernatant that is representative for the process.

3.8. Preparative SEC to isolate monomer and aggregates

24% aggregated mAb A (10 mg/mL, 3.6 mL) was used for preparative SEC. AKTA Avant system was used with a 320 mL Superdex 200 pgXK2 600 column (GE Life Sciences). Running flowrate was 2.5 mL/min, protein was detected using UV detectors at 214 nm and 280 nm and PBS pH 7.2 was used as the running buffer. After equilibration, the stressed mAb A was applied onto the column using the sample inlet line. Isocratic elution occurred over 1.5 CV and eluted samples were collected in 2 mL fractions in a 96 deep well plates in the fraction collector. Fractionation was initiated after the absorbance was greater than 10 mAU. Samples were concentrated using Amicon Ultra-15 PLBC centrifugal filter 3 kDa MWCO (Millipore, Cork, Ireland).

3.9. Octet to measure binding interactions

The OctetRED 384 (Forte Bio) was used to measure the binding interactions between protein A and mAb monomer and mAb aggregates. 100% mAb monomer (1.90 mg/mL) and 100% mAb aggregate (1.68 mg/mL) in PBS pH 7.2 and BSA from ThermoFisher in 0.9% sodium chloride with sodium azide (Thermo Scientific, Illinois, USA). Octet was also used to check dAbs (dAb A) binding to protein A. Samples were diluted to 1 mg/mL and 80 µL of samples and buffer were aliquoted into black flat bottom 384-well plates. Dip and Read protein A biosensors (Forte Bio, Shanghai, China) were incubated in black flat bottom 96-well plates (Greiner Bio-One Ltd, Gloucestershire, UK) with 1X Kinetics Buffer or 10 mM PBS pH 7.4 (Forte Bio, California, USA) for 10 mins prior to run for pre-conditioning. 1X Kinetics Buffer was prepared by 1-in-10 dilution of 10X Kinetic buffer (Forte Bio, California, USA) into using 10 mM PBS pH 7.4. Temperature was maintained at 30^0C and the advanced quantitation method used for the experiment was as follows: regeneration, baseline, loading of sample, baseline, and buffer. For the regeneration step, 10 mM glycine pH 1.5 was used as the regeneration buffer along with either 1X KB buffer or 10 mM PBS pH 7.4 as neutralisation buffer. 10X KB buffer is comprised of PBS+ 0.02% Tween-20, 0.1% BSA and 0.05% sodium azide. During regeneration, the protein A biosensors were dipped into regeneration buffer for 5 seconds followed by neutralising buffer for 5 seconds for a total of 3 times. Sample plate shaking speed during regeneration step was maintained at 1000 rpm. During the sample loading step, the protein A sensors were dipped into the shaking sample plate (400 rpm) for 120 seconds. Following loading the sample, the biosensors were dipped into buffer (1X Kinetics Buffer or 10 mM PBS pH 7.4) for 30 seconds with sample plate shaking speed of 400 rpm.

3.10. Affinity peptide

3.10.1. Peptide Information

Affinity peptide (RDYHPRDHTATWGGG) used was from the work published by Cheung et al. (2017). The 15-amino acid peptide (unlabelled) is 1.72 kDa with a

hydropathicity of 1.73. Biotinylated affinity peptide (biotin-AP) was labelled with biotin on the C-terminal of the AP which had a total molecular weight of 2458 Da. Fluorescent affinity peptides were manufactured to have either CCVJ, ThT, Fluorescein or Tide Fluor 2 labelled on to the N terminal end of the protein. The labelled and unlabelled AP were prepared by Bachem AG (Bubendorf, Switzerland) with >90% purity and had the following molecular weights: AP-CCVJ (1976 Da), AP-ThT (2090 Da), AP-Fluorescein (2083 Da) and AP-Tide Fluor 2 (2195 Da). The AP-dyes were reconstituted with MilliQ water from a lyophilised powder.

3.10.2. Biotinylated affinity peptide assay

For Octet experiments, OctetRED 384 (Forte Bio) and Octet HTX (Forte Bio) were used with streptavidin (SA) biosensors to conjugate the biotin-labelled affinity peptide. Sensors were placed in black flat bottom 96-well plates and prior to run, sensors were hydrated in plates using buffer for 10 mins. Prior to measurement, plates were incubated at room temperature in the dark for 30 mins. Sample measurements were conducted using a 384-well black flat-bottom micro plate with 80 µL in each well. 1 mg/mL of native and aggregated lysozyme standards resolubilised in MilliQ were obtained from Enzo Life Sciences ProteoStat kit. Three assay different buffers were assessed: 10 mM PBS pH 7.4, 1X KB and PBS+0.5% Tween-20. SA sensors were dipped into wells of 20 µg/mL of the biotinylated affinity peptide to conjugate the peptide to the sensor (Forte Bio, 2018). The octet quantitation protocol used was based of the Forte Bio Technical Note 40 (Forte Bio, 2018) which followed these steps: baseline, loading biotinylated AP, baseline, loading sample, baseline. Baseline step dipped the SA biosensors into buffer for 30 secs at 1000 rpm. To load biotinylated AP, SA biosensors were dipped into biotinylated affinity peptide for 10 mins, 1000 rpm. To load sample, the SA biosensors coated with biotinylated AP were dipped into sample/control for 30 mins at 1000 rpm.

For Biacore experiments, Biacore T200 was used with streptavidin chip Series S (GE Healthcare Life Sciences, Uppsala, Sweden) to measure affinity. PBS with 0.05% Tween (PBST) and 10 mM glycine pH 1.5 was used as the running buffer and

regeneration buffer respectively. The chip was loaded with 20 µg/mL of the biotinylated affinity peptide at 10 µL/min for 5 mins. After loading the biotinylated affinity peptide, the chip was washed with twice with running buffer at 50 µL/min for 30 sec. Different concentrations of the sample (1-1000 µg/mL) and flowrates (10 or 30 µL/min) were measured to find the optimal conditions. Monomeric mAb (1.90 mg/mL, r_h=5.8 nm) and aggregated mAb (1.68 mg/mL, r_h=17 nm) in PBS were diluted as necessary. The Biacore method was as follows: sample injected into the chip for 60 seconds, chip washed with running buffer for 30 secs and then the chip regenerated with regeneration buffer for 30 secs.

3.10.3. Fluorescent affinity peptide assay

Proteins were used at specific concentrations to keep the AP-dye to protein molar ratio constant across proteins. MAb A, BSA and lysozyme were used at 1 mg/mL, 0.1 mg/mL and BSA at 0.45 mg/mL respectively. BSA was obtained from ThermoFisher in 0.9% sodium chloride with sodium azide (Thermo Scientific, Illinois, USA) and lysozyme from Sigma Aldrich (Steinheim, Germany) and was prepared in PBS. 0.1 mg/mL of native and aggregated lysozyme standard resolubilised in MilliQ were obtained from Enzo Life Sciences ProteoStat kit was used in initial experiment but was difficult to characterise. Subsequent uses of lysozyme were prepared in PBS buffer from Sigma Aldrich. The AP-dye were used at 7 µM (for 1:1 ratio) and 50 µM (7:1) ratio for equimolar and excess of dye to protein respectively for comparison. The following excitation/emission conditions were used: AP-CCVJ (435/465-600 nm), AP-ThT (430/460-600 nm), AP-Tide Fluor 2 (440/490-650 nm) and AP-Fluorescein (440/490-650 nm). Measurements were conducted using a 96 well clear flat-bottom micro plate with TECAN Infinite M200 plate reader with 200 µL in each well. Prior to measurement, samples were incubated in the plates at room temperature in the dark for 30 mins. The following parameters were used for fluorescence measurement: bottom reading, integration time 20 µs and 25 flashes. The data was analysed using OriginPro.

3.10.4. Measuring affinity with dissociation constant (K_d)

The lowest detectable concentration of AP-ThT for robust measurement was measured in 96-well plates at concentrations between 3.2 nM to 50 µM of AP-ThT in phosphate pH 7 buffer. To minimise volume of AP-ThT required, the K_d of AP-ThT and unstressed mAb A/30% aggregated mAb A was measured in 384 well clear flat-bottom micro plate (Greiner Bio One Ltd, Gloucestershire, UK) using 50 µL in each well. The mAb concentrations were measured from 0.1 mg/mL (667 nM) to 10.2 mg/mL (68 µM).

3.10.5. Buffers

50 mM potassium phosphate at pH 3.3, 6.0, 7.1, 7.92 and 9.1 were prepared to investigate the impact of pH on fluorescence with the AP-dyes. To reduce the non-specific interactions with AP-CCVJ, Tween-20 (Sigma Aldrich, Steinheim, Germany) and 0.4 M and 0.8 M sodium chloride was utilised. For the SEC experiment with dyes only, CCVJ (Sigma Aldrich, Steinheim, Germany) and ThT (Sigma Aldrich, Steinheim, Germany) were applied onto the column at the same concentration as the AP-dyes.

3.11. FRET

3.11.1. Conjugation of protein to Alexa Fluor 350

Protein was conjugated to Alexa Fluor 350 using the Alexa Fluor 350 protein labelling kit azide (Thermo Fisher Scientific, Oregon, USA). The labelling occurred between the NHS ester on Alexa Fluor 350 and a primary amine on the protein of interest to label. Recombinant protein A from *E. coli* (Thermo Scientific, Illinois, USA) was prepared with PBS pH 7.2 at 3 mg/mL for conjugation. Protein A-Alexa Fluor 350 was used in most FRET experiments. MAb A was prepared in 50 mM sodium acetate pH 5.5 at 2 mg/mL for use in the FRET positive control studies.

Following the Alexa Fluor 350 conjugation kit instructions, 50 µL of sodium bicarbonate was added to 0.5 mL of protein to increase the pH as succinimidyl esters react efficiently at pH 7.5-8.5. This protein was then added to the dye and incubated

for 1 hour at room temperature. A size exclusion column provided in the kit was set up to separate the unbound dye. 0.5 mL fractions were collected after adding the protein-dye mixture to the column. After 8 or 9 fractions were collected, absorbance at 350 nm using a TECAN Infinite M200 plate reader was measured to indicate which fraction the dye was located. This conjugation was further verified using mass spectrometry and SEC to check for size and amount dye conjugated. Conjugation resulted in mixture of components with the most abundance being 1 or 2 dyes per protein. As excess protein was used, there was also a small amount of unlabelled protein as well.

To calculate the concentration, Equation 3-1 provided in the labelling protocol was used. The measurement was automated using the TECAN Infinite M200 plate reader which measured absorbance at 280 nm and 346 nm (as well as 900 nm and 1000 nm to correct for path length). Absorbance at 280 nm and 346 nm represented the absorbance of the aromatic rings of peptides and the absorbance of the dye respectively. 0.19 was a correction factor to account for absorption of the dye at 280 nm and 73590 $M^{-1}cm^{-1}$ refers to the molar extinction coefficient for protein A. The molar extinction coefficient for protein A was calculated based on a molecular weight of 44600 Da and 0.1% at 280 nm = 0.165 (Mazzer, 2015).

$$Protein\ concentration\ (M) = \frac{[A_{280} - (A_{346} \times 0.19)]}{73590}$$

Equation 3-1: Calculation for concentration of labelled proteins

3.11.2. Plate based FRET assay

The FRET assay was conducted using a 96 well clear flat-bottom micro plate (Corning, Kennebunk, Maine) with TECAN Infinite M200 plate reader. 1 µM protein A-Alexa350, 1 µM mAb A-Alexa350, 5X SYPRO Orange and 3 µM ProteoStat were the final concentration in each well. SYPRO Orange (Life Technologies, Eugene, Oregon) was diluted using MilliQ water and ProteoStat (Enzo Life Sciences, Farmingdale, New York) were prepared based on the manual protocol. The following

parameters were used for fluorescence measurement: bottom reading, integration time 20 µs and 25 flashes. For samples with Alexa Fluor 350 with SYPRO Orange/ProteoStat, excitation was at 330 nm and the emission from 400-700 nm. Concentration of mAb was kept to 1 mg/mL in well, dAb was measured at 1, 0.18 and 0.05 mg/ml.

3.11.3. Spectral overlaps

Excitation/emission conditions for the spectral overlaps for the FRET pairs were: Alexa Fluor 350 excitation scan (300-430/460 nm) and emission scan (330/380-650 nm), SYPRO Orange excitation scan (350-570/600 nm) and emission scan (495/530-770 nm), ProteoStat excitation scan (300-590/620 nm) and emission scan (490/520-750 nm).

The dyes for the known FRET pairs were obtained from: Alexa Fluor 350 (Thermo Fisher Scientific, Oregon, USA), Alexa Fluor 488 (Thermo Fisher Scientific, Oregon, USA), Alexa Fluor 555 (Thermo Fisher Scientific, Oregon, USA), Cyanine3 (Lumiprobe, Maryland, USA) and Cyanine5 (Lumiprobe, Maryland, USA). All known FRET pairs were prepared in water. The spectral overlaps were measured using the following conditions: Alexa Fluor 350 excitation scan (300-430/460 nm) and emission scan (330/380-650 nm), Alexa Fluor 488 excitation scan (300-550/580 nm) and emission scan (430/460-700 nm), Alexa Fluor 555 excitation scan (300-590/620 nm) and emission scan (500/530-800 nm), Cy3 excitation scan 400-550/590 nm and emission scan (480/510-800 nm) and Cy5 excitation scan (500-590/720 nm) and emission scan (580/610-800 nm).

3.11.4. Cuvette based FRET assay

The Fluoromax-4 spectrofluorometer (HORIBA) was used to measure FRET using a 500 µL cuvette. The volume of sample prepared in the cuvette was 300 µL. The maximum fluorescence intensity was 2×10^6 RFU, therefore all measurements were kept below this value. For measuring FRET, the following conditions were used: excitation 330 nm, emission 400-650 nm, excitation slit 2 nm bandpass, and emission slit 1 nm bandpass.

3.12. Method to measure quantum yield and extinction coefficient

3.12.1. Quantum yield of Alexa Fluor 350

Quinine sulphate dihydrate (ACROS Organics, Geel, Belgium) was freshly prepared to approximately 0.2 mM in 0.1 M H_2SO_4. 4.08 mM Alexa Fluor 350 was prepared in PBS pH 7.2. For absorption and fluorescence measurement 10 mm x 10 mm cuvettes were used. 10 mm semi-micro fluorimeter quartz cuvettes were used for fluorescence measurements. Absorption spectra was recorded on Ultrospec 4300 Pro and fluorescence measurements were recorded on Cary Eclipse. Absorbance was measured at 346 nm. Fluorescence was measured using the following conditions: excitation 346 nm, emission 360-660 nm, excitation/emission slits width 5 nm, medium speed and PMT 500.

For the single point method, the following stocks of Alexa Fluor 350 and quinine sulphate with similar OD values were used: Alexa Fluor 350 sample 1 (OD=0.026) and Quinine Sulphate sample 2 (OD=0.030), Alexa Fluor 350 sample 6 (OD=0.054) and Quinine Sulphate sample 8 (OD=0.053), Alexa Fluor 350 sample 9 (OD=0.100) and Quinine Sulphate sample 6 (OD=0.094).

Single point method:

1. Prepared a sample of Alexa Fluor 350 (in PBS) and Quinine Sulphate (in 0.1 M H_2SO_4) with absorbance between 0.01 and 0.1.
2. Measured the emission (360 – 660 nm) of samples by excitation at 346 nm (22^0C).
3. Calculated the integrate fluorescence intensities from the spectrum.
4. Used
5. Equation 3-2 to calculate the QY.

For the comparative method, Quinine Sulphate and Alexa Fluor 350 were diluted to create five stocks with different ODs (at 346 nm). Quinine sulphate in 0.1 M H_2SO_4 was diluted to create stocks with the following OD_R at 346 nm: 0.030, 0.037, 0.053,

0.062 and 0.094. Alexa Fluor 350 was diluted using PBS to create stocks with the following OD at 346 nm: 0.026, 0.050, 0.054, 0.086 and 0.100.

Comparative point method (Wurth et al., 2013):

1. Prepared 4 samples of Alexa Fluor (in PBS) and Quinine Sulphate (in 0.1 M H_2SO_4) with different absorbance between 0.01 and 0.1
2. Measured the emission (360 – 660 nm) of samples by excitation at 346 nm (22^0C).
3. Calculated the integrate fluorescence intensities from the spectrum.
4. Plotted the magnitude of the integrated fluorescence intensity against the absorbance of the solution absorbance. Slope is equal to the quantum yield (See Equation 3-3).

$$Q = Q_R \left(\frac{I}{I_R}\right)\left(\frac{OD_R}{OD}\right)\left(\frac{n^2}{{n^2}_R}\right)$$

Equation 3-2: Quantum Yield Single point method

$$Q = Q_R \left(\frac{m}{m_R}\right)\left(\frac{n^2}{{n^2}_R}\right)$$

Equation 3-3: Quantum Yield Comparative method

The quantum yield using the single point method is calculated using Equation 3-2. Where *Q* is the quantum yield, *I* is the integrated intensity, *OD* is the optical density and *n* is the refractive index. (The subscript *R* refers to the reference fluorophore of known quantum yield). In this expression, it is assumed that the sample and reference are excited at the same wavelength, so that it is not necessary to correct for the different excitation intensities of different wavelengths. Equation 3-3 is used for the comparative method, whereby the quantum yield is obtained from the plot of

absorbance against integrated fluorescence intensities. Here, *m* is the slope of the line obtained from the plot of the integrated fluorescence intensity vs. absorbance.

3.12.2. Extinction coefficient of acceptors

The concentration of the ProteoStat provided in the kit was 3 mM. The protocol was followed to prepare a working stock with a concentration of 150 µM. The working stock was diluted using MilliQ to prepare a 30 µM stock used to create 100 µL standards between 1 µM and 10 µM. Absorbance of the standard was measured at 495 nm which is the peak absorbance of ProteoStat when an excitation scan was measured. Samples were measured in 1.5 mL semi micro UV-cuvette with a 1 cm path length (Brand UV-cuvette, Wertheim, Germany) with Ultrospec 4300 Pro spectrometer (Amersham Biosciences).

To measure the extinction coefficient, the absorbance of SYPRO Orange standards (1X – 60X) were measured at 490 nm. 490 nm is the peak absorbance of SYPRO Orange when an excitation scan was measured. Ultrospec 4300 Pro spectrometer was used to measure absorption with 1.5 mL semi micro UV-cuvette cuvettes. To convert the concentration from X to molar concentration.

3.13. 3D structure of dAbs and mAbs with hydrophobic patches

A homology model was built for dAb A by the Computational Sciences group at GSK, using CCG (Chemical Computing Group) MOE (Molecular Operating Environment) 2018.0101 Antibody Modeler. The structures were analysed for surface exposed hydrophobic patches with the MOE Patch Analyzer using the default settings. The percentage molecular surface coverage was calculated for the hydrophobic patches by comparing the reported Patch Analyzer output to a total surface area calculated by adding a molecular surface to the whole molecule, and calculating the area using a CCG svl script GObject_Area.svl.

4 Evaluation of fluorescent dyes to measure protein aggregates

4.1. Chapter Aims

This chapter describes the dye assay work which was published in a peer-reviewed journal (Oshinbolu et al., 2018a). The first assay investigates the use of fluorescent dyes to measure mAbs aggregates as well as understanding impact of cell culture components on fluorescence. The first step in developing the assay was to show its capability in purified systems. After such the assay was applied to cell culture supernatants containing CHO media/host cell protein. The assay was tested in two stages as it was crucial to understand how the assay worked in the absence of other proteins, as well as understand the assay's detection limits.

The chapter will cover the following areas:

1. The criteria for selecting fluorescent dyes for the dye assay

2. Investigating the aggregation detection with fluorescent dyes using purified mAb aggregates

3. Understanding the fluorescence that occurs naturally in the media and comparing how that overlaps with the excitation/emission spectrums of the fluorescent dyes.

4. Applying the dye assay to mAb and null cell culture supernatants to compare the background fluorescence intensities of host cell protein to mAb over the duration of a cell culture.

5. Characterising the size of aggregates the fluorescent dyes are interacting with using SEC with UV and fluorescent detectors

4.2. Fluorescence dyes selected for investigation

The main selection criteria for choosing which fluorescent dyes to use were the dye should be able to solubilise in water (to minimise skewness in data from solvents), have a strong fluorescence, and there must be previous literature available on the dye's ability to bind to antibody aggregates. In addition to this, dyes were selected that had different binding mechanism (e.g. hydrophobic, electrostatic). The four dyes selected are listed in Table 4-1.

Table 4-1: Fluorescent dyes selected to use for the dye aggregation assay

Dye	Fluorescence colour	Excitation (nm)	Emission (nm)	Reference
Bis-ANS	Blue	385 (max)	450-600	(Paul et al., 2015b, Hawe et al., 2010)
Thioflavin T	Yellow	430	450-600	(Paul et al., 2015b, Groenning, 2010)
SYPRO - Orange	Orange	495	550-650	(He et al., 2010, Zheng et al., 2011)
ProteoStat	Red	550	600	(Enzo Life Sciences)

1-anilinonaphthalene-8-sulfonate (ANS) and 4,4'-bis-1-anilinonaphthalene-8-sulfonate (Bis-ANS), Nile red and SYPRO Orange are the most frequently used extrinsic dyes for aggregate characterisation (Demeule et al., 2009). ANS and its dimeric form Bis-ANS (673 Da), have been used since the 1950s for protein characterisation. Bis-ANS and ANS hardly fluoresce in aqueous environments but strongly fluoresce when interacting with hydrophobic sites. Hydrophobic interactions and electrostatic interactions have both been discussed as the binding mechanism of ANS to proteins (Matulis and Lovrien, 1998). For Bis-ANS, hydrophobic interactions are seen as the most dominant (Bothra et al., 1998). However, due to the larger size of Bis-ANS, fluorescence can be inhibited by steric hindrance.

Fluorescence can also be used for visualisation of protein aggregates with microscopy (Demeule et al., 2007a, Demeule et al., 2007b) and to monitor protein folding/unfolding (Goldberg et al., 2011). The main application of SYPRO Orange is for staining SDS PAGE gels and Western blots. It is now known to display high

sensitivity to structurally altered/aggregated IgG structures compared to the native form (He et al., 2010). This sensitivity results in an increased fluorescence with the increasing availability/presence of hydrophobic areas of unfolded proteins.

Thioflavin T (ThT) is in a specific class of dyes called molecular rotors, which have a significant increase in fluorescence due to a decrease in torsional relaxation of molecules (Stsiapura et al., 2008). In solution, molecular rotors rotate freely, however changes to the micro-environment constrict the dye's movement, resulting in fluorescence. ThT (319 Da) fluorescence is affected more by changes in the solvent, viscosity and rigidity of the microenvironment than by polarity (Hawe et al., 2008). It is widely used to quantify amyloid fibrils which are filamentous protein aggregates about 10 nm width, 0.1 to 10 µm length and predominantly beta sheet secondary structure (LeVine, 1999). Vetri et al. (2007) showed selectivity of ThT to fibrils and ANS to amorphous aggregates with hydrophobic regions.

A novel protein aggregation dye, ProteoStat by Enzo Life Science, is also a molecular rotor. ProteoStat works in a way such that in the absence of protein aggregates or at low viscosities, the dye spins in solution with no fluorescence. In the presence of aggregates, the dye inserts itself into the exposed cavities of aggregated protein, thereby causing the dye's rotation to be constrained, resulting in fluorescence. It is currently the only commercial dye marketed for protein aggregate detection for visible to sub-visible aggregates.

Even though there is a considerable amount of work in the literature using extrinsic dyes to measure aggregation, the focus has mostly been on the use of dyes on purified samples with the exception of Paul and Hesse (2013). They suggested that Bis-ANS is a suitable dye for measuring aggregates in cell cultures supernatants upon measuring aggregated mAb after 120 hours of culture. Paul and Hesse (2013) measured samples with >65% mAb aggregates, however those working in bioprocess development will often aim to measure below 5% aggregates post purification as most mAbs tend to fall within this range to comply with regulatory guidelines. This will require the dye assay to be sensitive enough to detect aggregates in a sample

containing largely monomeric mAb. In addition, as cell cultures were only run up to 300 hours (12 days), it would be interesting to see the impact of later harvest time points (>12 days) and elevated HCP levels, on dye fluorescence.

In this chapter, the suitability of extrinsic dyes to detect less than 10% mAb aggregates in Chinese hamster ovary (CHO) cell culture supernatants at varying culture time points up to day 14 was investigated. Four dyes, Bis-ANS, SYPRO Orange, ThT and ProteoStat, were evaluated to see which was the most sensitive. To assess the potential of the four dyes for mAb aggregate detection in CHO cell cultures, firstly the dyes were evaluated in buffer with thermally stressed mAb aggregates. Two of the dyes were then applied to CHO cell culture supernatants of mAb producing and non-mAb producing cell lines to see the impact of HCPs and other process related impurities levels on fluorescence. The size of aggregates the dyes may be binding to was also characterised using size exclusion chromatography (SEC) with fluorescence detectors. In addition, 2D fluorescence spectroscopy was used to investigate the fluorescence background of the media, to see how much it would contribute in the regions where the dyes fluoresce.

4.3. Detection of varying levels of purified mAb aggregates using fluorescent dyes

The four chosen dyes interact differently with protein aggregates (Figure 4-1). To assess the potential of the four dyes for mAb aggregate detection in CHO cell cultures, firstly the dyes were evaluated in a purified system with thermally stressed mAb aggregates. The dyes were then used to measure mAb aggregate levels in CHO cell culture supernatants of mAb producing and non-mAb producing cell lines to see the implications of this complex background on fluorescence.

In the literature, different conditions have been used to stress mAbs that produced different amounts and types of aggregates. Kayser et al. (2011) stressed mAbs at 65ºC at 150 mg/mL and He et al. (2010) used 50ºC for 8 hours at 70 mg/mL prior to SEC fractionation. Paul and Hesse (2013) described how heating at 65ºC formed larger aggregates greater than 1 µm. As the unfolding temperature for mAbs is above 65ºC (Joubert M K et al., 2011), it was decided to stress below this temperature to minimise

fragmentation and formation of large aggregates. Additionally, at higher concentrations >30 mg/mL, mAbs precipitated heavily when stressed. Therefore, for simplicity mAb A was stressed at the concentration achieved post purification (11 mg/mL).

To evaluate whether the dyes (Bis-ANS, SYPRO Orange, ProteoStat and ThT) were capable of measuring aggregates in CHO cell culture supernatants, the dyes were first applied to a purified system. To measure the capability of the dye to distinguish different levels of aggregates, thermally stressed mAb A aggregates were spiked into a 96-well plate (Figure 4-1). The stressed mAb A was measured to have 20% aggregates (by SEC) with a hydrodynamic radius of 22 nm (by DLS). The aggregates were spiked into acetate buffer with unstressed monomeric mAb at varying amounts to provide samples with a 5-20% range of aggregation (Figure 4-2 and Figure 4-3). The assumption here was that the mAb aggregates generated remain aggregated even after diluted.

A)

Dye	Fluorescence colour	Excitation Emission (nm)	Method of aggregate interaction
Bis-ANS	Blue	390 450-600	Hydrophobic (dominant) and electrostatic areas.
SYPRO Orange	Orange	495 550-700	Hydrophobic areas.
ProteoStat	Red	530 560-700	Molecular rotor –inserts into the cavities of aggregated protein, constrained rotation causes fluorescence.
Thioflavin T	Yellow	430 460-600	Molecular rotor – interacts based on the hydrophobicity, viscosity, and rigidity of the microenvironment.

B)

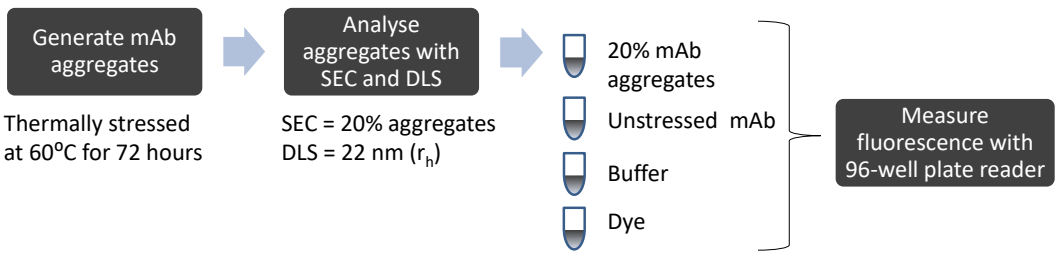

Figure 4-1: Selected dyes and spiking experiment method.
(A) Aggregation detection mechanism of each dye. Table shows the conditions excitation and emission conditions used in this study and the method by which each dye interacts with aggregates. (B) Spiking experiment method to generate aggregates for the spiking experiment. The aggregates were then measured by SEC and DLS and shown to have 20% aggregates with a hydrodynamic radius of 22 nm. To measure aggregation, the aggregate stock diluted to 1 mg/mL combined with the dye in a 96-well plate. The aggregate stock was spiked into unstressed IgG1 mAb A to generate different percentages of aggregates.

Figure 4-2 shows the fluorescence associated with each dye's emission with varying percentages of aggregates up to 20% mAb aggregates. As expected all four dyes had strong fluorescence intensities and clearly distinguished the different percentage of spiked aggregates, even as little as 5% aggregates. There was very little fluorescence in the buffer blanks (containing dye and buffer only) and good repeatability between replicates in terms of shape and peak fluorescence intensity.

Figure 4-3 shows the change in peak intensity wavelengths and the increase in fluorescence intensity with increasing amounts of aggregates. Notably, all four dyes experienced a blue shift (a shift towards lower wavelengths) with increasing level of

spiked aggregate. The highest spiked aggregate level (20%) had the greatest blue shift in all four dyes. A blue shift typically occurs due to an increase in the hydrophobicity around the dye (Themistou et al., 2009). This can be a result of the increased exposure of hydrophobic residues to the solvent upon aggregation. Bis-ANS and ProteoStat had similar degrees of blue shifts (6-8 nm) whereas SYPRO Orange and ThT had blue shifts greater than 10 nm. In these purified conditions, the fluorescence assay worked well.

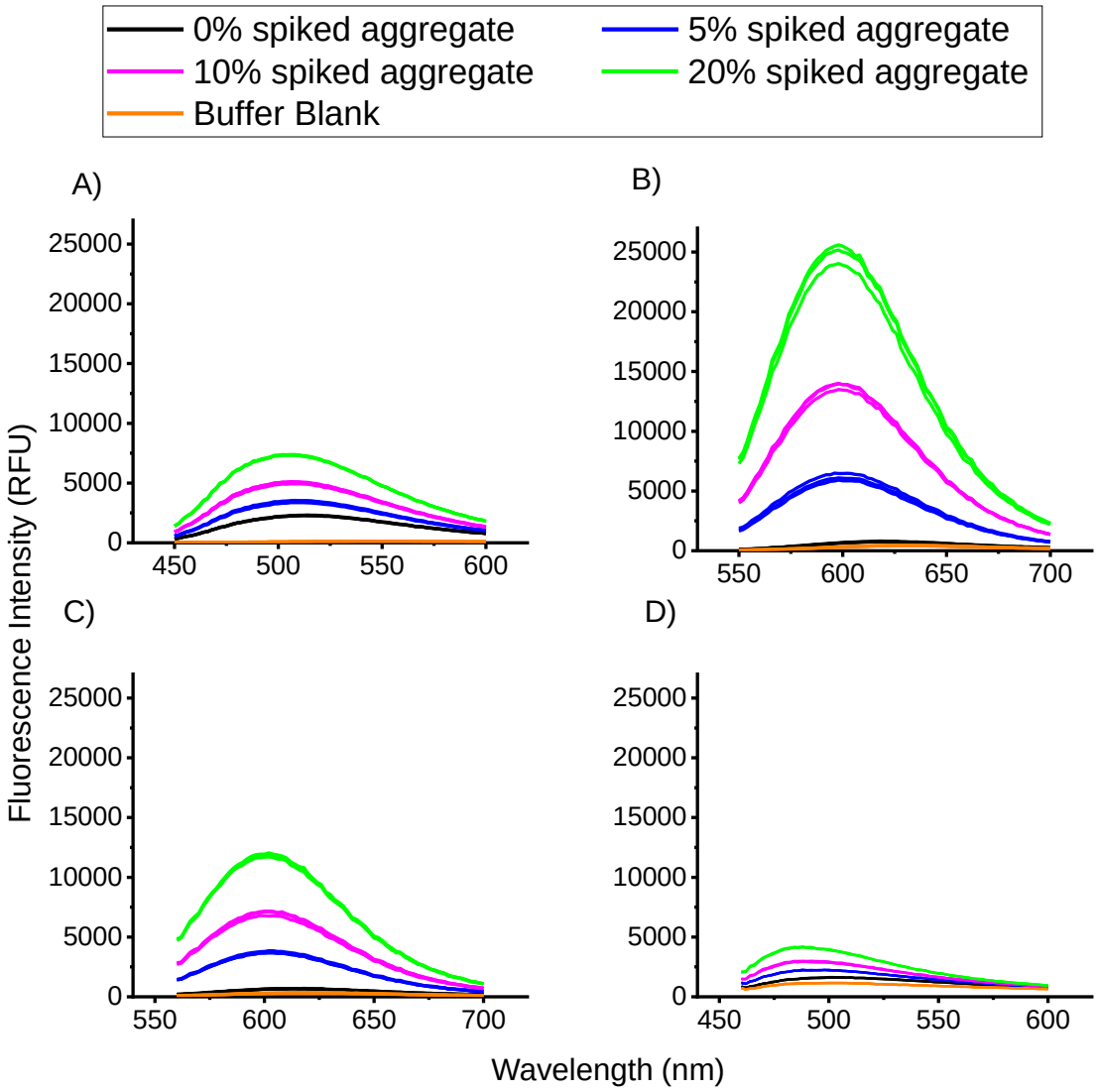

Figure 4-2: Fluorescence spectrum of dyes with mAb aggregates spiked into buffer. Thermally stressed IgG1 mAb A spiked into non-aggregated mAb. Concentration of antibody in each well was 1 mg/mL. This was performed in triplicates and all are plotted. (A) 50 µM Bis-ANS, excitation/emission- 390/450-600 nm, gain 70; (B) 5X SYPRO Orange, excitation/emission- 495/550-700 nm, gain 100; (C) 3 µM ProteoStat, excitation/emission- 530/560-700 nm gain 110; (D) 50 µM Thioflavin T, excitation/emission- 430/460-600 nm, gain 110.

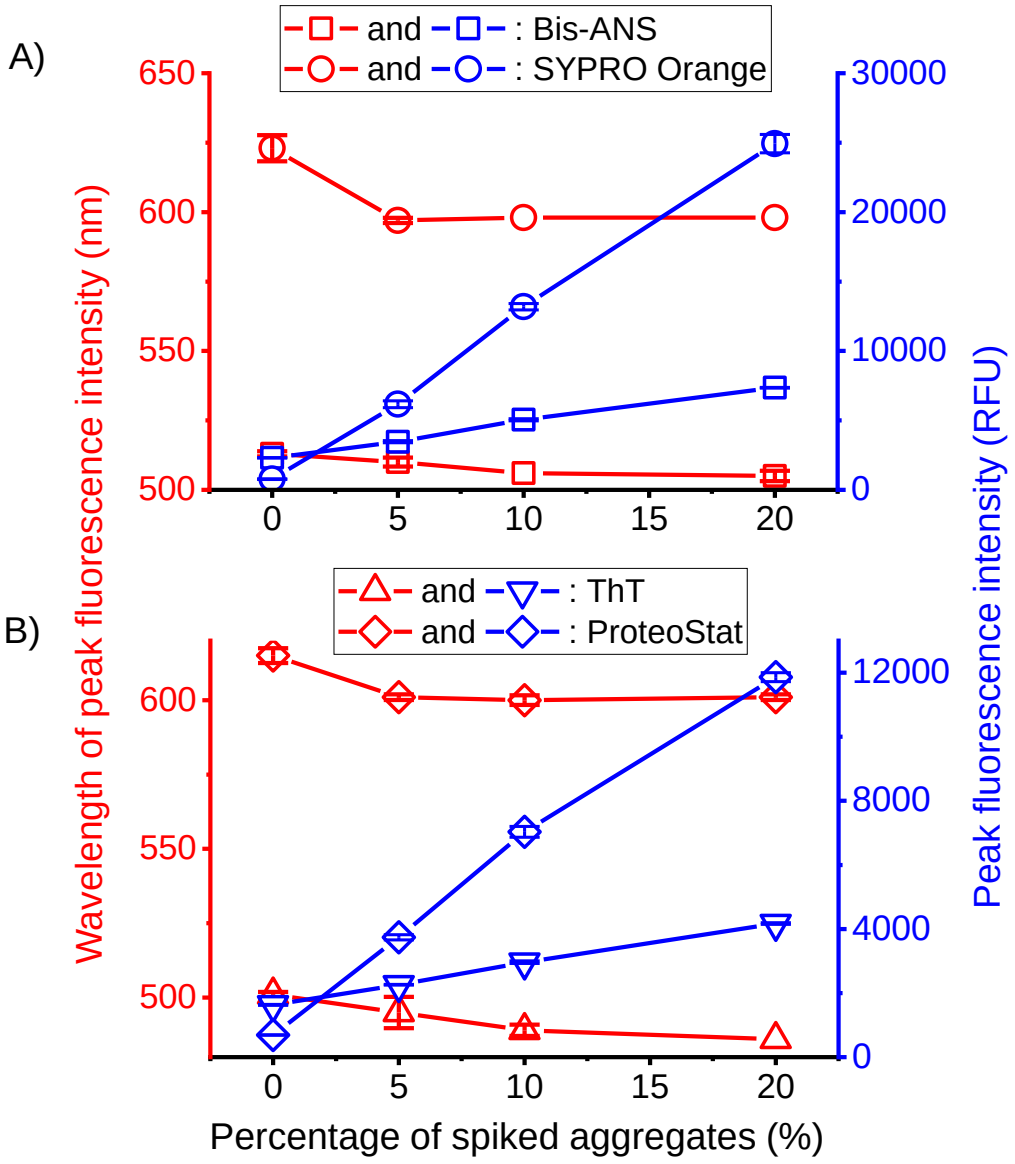

Figure 4-3: Peak height and peak wavelength against mAb A aggregates spiked into buffer.

Thermally stressed IgG1 mAb A spiked into non-aggregated mAb. Comparison of decrease in wavelength at which highest fluorescence occurs (degree of blue shift) against increasing fluorescence intensity with increasing amount aggregates. Concentration of antibody in each well was 1 mg/mL. This was performed in triplicate: (A) 50 µM Bis-ANS, excitation/emission- 390/450-600 nm, gain 70 (wavelength SD=1.63 nm, peak intensity SD= 78.4 RFU); 5X SYPRO Orange, excitation/emission- 495/550-700 nm, gain 100 (wavelength SD=4.71 nm, peak intensity SD= 657 RFU); (B) 3 µM ProteoStat, excitation/emission- 530/560-700 nm (wavelength SD=2.50 nm, peak intensity SD=168 RFU); 50 µM Thioflavin T, excitation/emission- 430/460-600 nm, gain 110 (wavelength SD=5.25 nm, peak intensity SD=37.3 RFU).

4.3.1. Key Findings

All four dyes had strong fluorescence intensities and clearly distinguished the different percentage of spiked aggregates with good repeatability. The four dyes also experienced a blue shift with increasing level of spiked aggregate indicating increased hydrophobicity. Before applying the dyes to cell culture supernatants, it was important to develop a better understanding of the background fluorescence present in media by comparing the wavelengths from which fluorescence occurs from the media to the wavelengths where the dyes fluoresce.

4.4. Fluorescence in the CHO media/cell culture supernatants

Figure 4-4 shows the fluorescence of fresh media and media kept in the fridge for two weeks. The green/red diagonal diamonds are a result of Rayleigh and Raman scattering. Rayleigh and Raman scattering occurs when a molecule has been excited to a virtual energy state by a photon with insufficient energy to completely excite the molecules (Larsson et al., 2007). The emitted light from Rayleigh scatter is of the same energy as the excitation light. Rayleigh scatter is also of higher intensity than Raman scattering. Scattering is a multi-order process with the emission of first and second order occurring at the same and double the excitation wavelength respectively (Figure 4-5).

The highest region of fluorescence in the medium (Figure 4-4A) was in the emission range of 300-450 nm which was seen in (Paul et al., 2015b) to correspond to amino acids. The weaker regions of fluorescence emission was between 450-600 nm which worked well as it was the emission region for the fluorescent dyes. The medium sample was also measured two weeks later (to compare as a cell culture is usually run for two weeks) (Figure 4-4B) with a visible reduction in fluorescence intensity. Although the amount of amino acids would be similar between the two samples, the decrease in fluorescence is might be due to other amino acids (glutamic acid, aspartic acid, serine, threonine, methionine and arginine) quenching the tryptophan fluorescence (Chen and Barkley, 1998). It could also be due to slow rate chemical reactions (such as degradation) that cause a change in the media composition over

time due to storage of the media at 4°C (Ryan et al., 2010). Calvet and Ryder (2014) showed that significant chemical changes in media stored at low temperature in the dark can occur, particularly with regards to cysteine/cystine concentration.

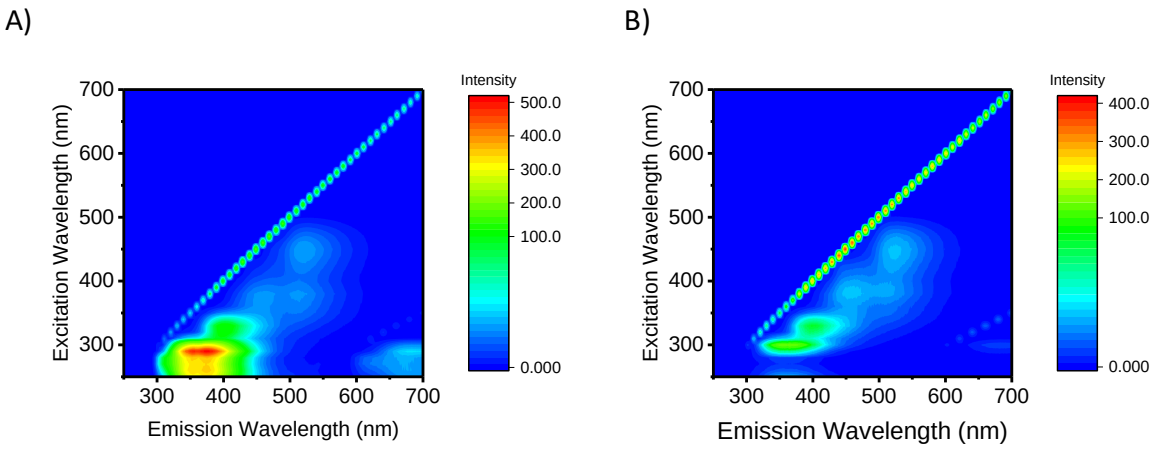

Figure 4-4: 2D fluorescence scan of CHO cell culture media.
(A) Media measured on day of preparation, (B) Media measured two weeks after initial fluorescence measurement. Measured on Cary Eclipse with excitation and emission range of 250-700 nm, PMT 550 and medium speed with 1 ml of sample.

Paul et al. (2015b) showed that the media has its own fluorescence after comparing media spiked with and without fluorescent dye (Bis-ANS and ThT). They noticed similar fluorescence intensities in the media both with and without dyes. Cyclic and conjugated components present in the media can interfere with fluorescence measurements. This includes: phenol red (a pH indicator and can cause significant quenching of fluorescence (Johnson, 2006)) and riboflavin (excitation 450-490 nm and emission 500-650 nm) which overlaps with most of the dyes used in this study (Johnson, 2006, Paul et al., 2015b, Büntemeyer and Lehmann, 2001). In addition, some serum components, vitamins, amino acids, tryptophan groups and folic acid can be fluorescent (Johnson and Straight, 2013, Waters, 2009). However, in this study, phenol red, riboflavin and serum were not added into the media. Therefore, the fluorescence in the media was most likely caused by fluorescent amino acids and/or the dyes interacting with other protein e.g. host cell proteins (HCPs).

In relation to the fluorescence spectrum of the dyes, Figure 4-6 shows the overlap with the fresh medium fluorescence and the fluorescent dyes. SYPRO Orange and ProteoStat had excitation and emission ranges in the weaker regions of media fluorescence. ThT's excitation and emission range was closer to the amino acid region of fluorescence which meant that measured fluorescence emission would not only come from the ThT but also inherently from the cell culture. However, for the dye assay, the excitation/emission conditions of 430/460-600 nm (See Figure 4-2) were chosen for experiments, which avoids the amino acid fluorescence region. This could minimise the impact of the background fluorescence on mAb aggregate measurement.

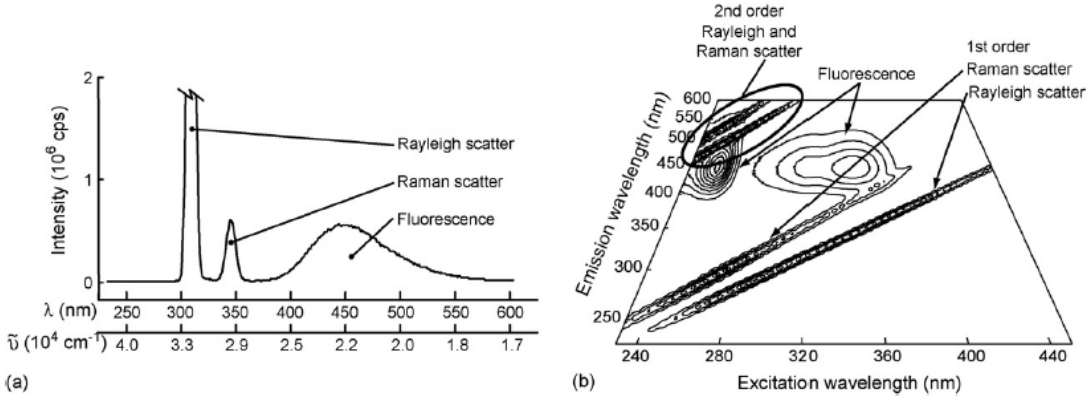

Figure 4-5: Raman and Rayleigh scattering.
Typical fluorescence emission spectrum with the different peaks marked. The upper abscissa scale is wavelength in nm and the lower scale is frequency in cm^{-1}. (b) Contour plot of an excitation/emission with the different structures marked. Obtained from (Larsson et al., 2007) with permission from Elsevier.

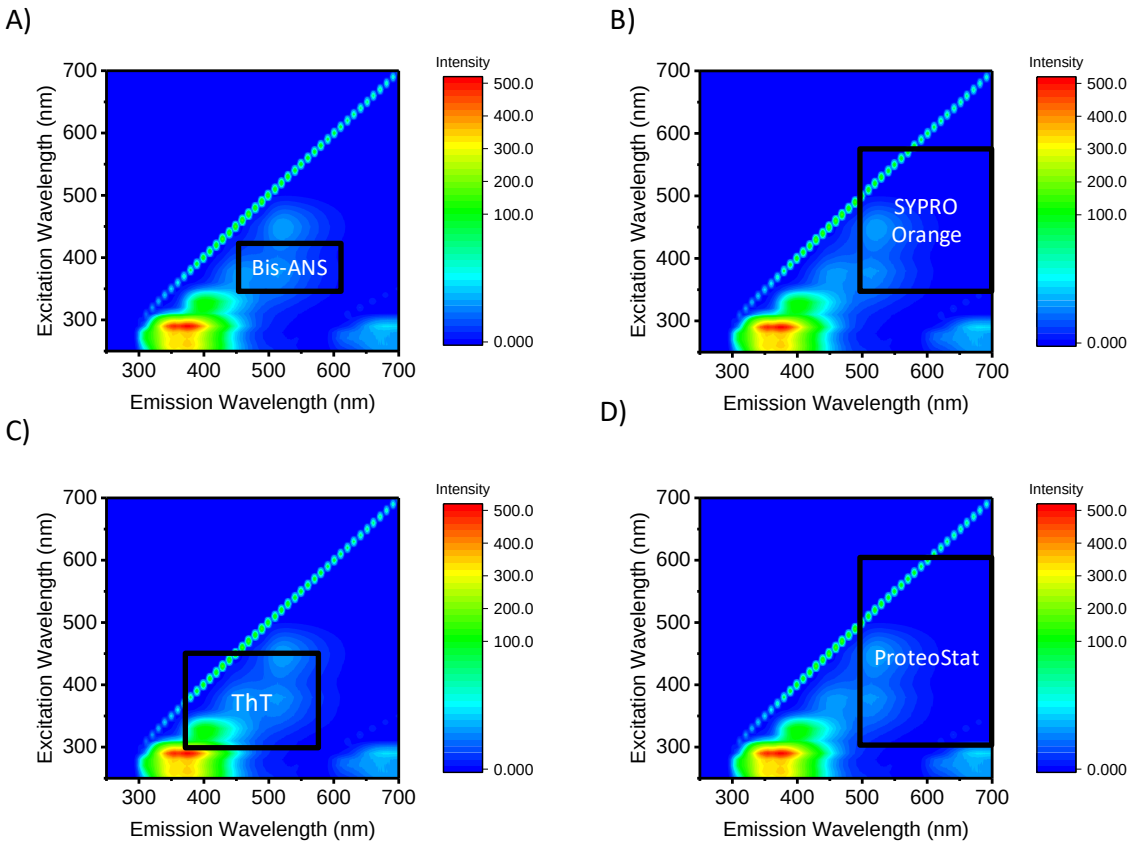

Figure 4-6: Overlaying the excitation/emission regions of dyes with 2D contour of fresh media.
(A) Bis-ANS, (B) SYPRO Orange, (C) ThT, (D) ProteoStat. 2D Media fluorescence scan (same scan as Figure 4-4A) was measured on Cary Eclipse with excitation and emission range of 250-700 nm, PMT 550 and medium speed with 1 mL of sample. Boxes indicate the approximate fluorescence region of the dyes which was either measured or obtained from online data (ThermoFisher SpectraViewer and AAT Bioquest).

4.4.1. Key Findings

In this section, the media used in this study was confirmed to have natural fluorescence, which was similar to previous reports (Paul et al., 2015a) in mammalian cell line media. The region of strongest fluorescence occurred in the emission range of 300-450 nm which corresponded to amino acids. SYPRO Orange and ProteoStat had excitation and emission ranges in the weaker regions of media fluorescence which

would make them ideal candidates for the dyes assay. ThT's excitation and emission range overlapped with the amino acid fluorescence region. However, the impact of the background on the results could be potentially minimised by using excitation/emission conditions furthest away from the amino acid fluorescence region. With this understanding of the impact of background fluorescence from the media, the next step was to get a better understanding of how the assay would perform in a more complex environment by applying dyes to the mAb B and null cell line supernatants.

4.5. Application in CHO cell culture supernatants

When the fluorescent dyes were used in purified environments, they clearly distinguished different levels of aggregates with little fluorescence in the negative controls of buffer and unstressed mAb. However, there is the potential to have background fluorescence from the media when dealing with cell cultures which may come from the dyes interacting with other protein i.e. host cell proteins (HCPs) or other components of the cell culture supernatant. To better understand the contribution that these components may add to fluorescence, interaction of the dyes in a cell culture environment in the absence of the mAb (referred to as null cell culture) was investigated. To do this, clarified null culture supernatant was used to evaluate the impact of HCP on fluorescence throughout the culture duration. The fluorescence of the dyes on different culture days of three null cell line shake flasks were compared to that of IgG mAb B (Figure 4-7 and Figure 4-8). Each sample from the different days and shake flasks had the same concentration of dye added in each well.

4.5.1. Null culture

In Figure 4-7, all four dyes showed an increase in fluorescence intensity in the null culture supernatant samples over the duration of the cell culture. A trend seen amongst all four dyes was a steady and consistent rise in fluorescence intensity between day 3 and day 10. However, on day 14, to differing extents, a rapid increase in fluorescence intensity was observed. Bis-ANS and ThT with the null culture supernatants showed

an average increase in fluorescence intensity from day 10 to day 14 of 21% and 48% respectively. ProteoStat and SYPRO Orange both showed an average increase in fluorescence intensity from day 10 to day 14 of 60%. The trend with fluorescence intensity amongst the three shake flasks on day 14 also correlated with loss of viability seen in Figure 4-9A. Shake flask 1 had the highest fluorescence intensity with the lowest viability out of the three shake flasks. Whereas, shake flask 2 had the lowest fluorescence intensity yet the highest viability on day 14. Amongst all four dyes, on average, fluorescence intensity of shake flask 1 sample was 22% higher than shake flask 2 on day 14.

It is well known that viability is a measurement of the number of cells that are alive (at the time of measurement). When cells die, the cell membrane becomes compromised, resulting in the exposure of intracellular components into the supernatant. As HCPs, can be hydrophobic, theoretically, HCPs can aggregate too with other HCPs, mAbs as well as other cellular components. This could possibly be being measured by the dye assay. Looking at the HCP concentration over the 14-day culture (Figure 4-9B), there was a decrease from day 10 to day 14 in HCP concentration for shake flask 1 and 3. For shake flask 2 there was more of a plateau. However, looking at the total protein concentration (Figure 4-9C), the null shake flask 1 had 40% higher total protein concentration than that of shake flask 2 and 3. There was also a blue shift in lambda max seen from all four dyes which refers to the dye being in a more hydrophobic environment, also seen in Figure 4-3. Between day 3 and day 14 of the null culture samples, for Bis-ANS, SYPRO Orange and ProteoStat there was a 2-3% decrease in peak wavelength. For ThT there was a greater decrease in peak wavelength of the null culture samples between day 3 and day 14 of 7%.

4.5.2. MAb B CHO culture

In Figure 4-8, all four dyes also showed a linear increase in fluorescence intensity in the IgG mAb B culture supernatant samples over the duration of the cell culture. Comparing the fluorescence intensities between the mAb and null culture supernatants, the mAb had similar intensities to null shake flask 3 with all four dyes.

This also correlated with viability as both null shake flask 3 and the mAb culture supernatant on day 14 shared similar viabilities. HCP concentration (Figure 4-9B) and total protein concentration (Figure 4-9C) of null culture shake flask 3 was also similar to IgG mAb B. This could indicate that both samples had similar levels of aggregation. Based on this trend with fluorescence intensity, viability and total protein, it explains the difference between null culture shake flask 1 (Figure 4-7) and IgG mAb B (Figure 4-8) on day 14. Null culture shake flask 1 had a lower viability (Figure 4-9A) and higher total protein concentration (Figure 4-9C) than the IgG mAb B on day 14. Hence, null culture shake flask 1 had a higher fluorescence intensity which may suggest a higher presence of aggregates.

With all four dyes, a blue shift with the IgG mAb B culture supernatants were also seen. Between day 3 and day 14 of the null culture samples, Bis-ANS, SYPRO Orange and ProteoStat had a 1-2% decrease in peak wavelength. For ThT, there was a greater decrease in peak wavelength of IgG mAb B culture samples between day 3 and day 14 of 8%. However, the strong fluorescence intensities seen in the null cultures supernatants in the presence of dyes and the absence of mAb, shows that HCP must strongly influence fluorescence of these extrinsic dyes. One possible reason could be that the dyes are interacting with secreted endogenous produced proteins as well as intracellular proteins exposed to the supernatant following apoptosis at low viabilities.

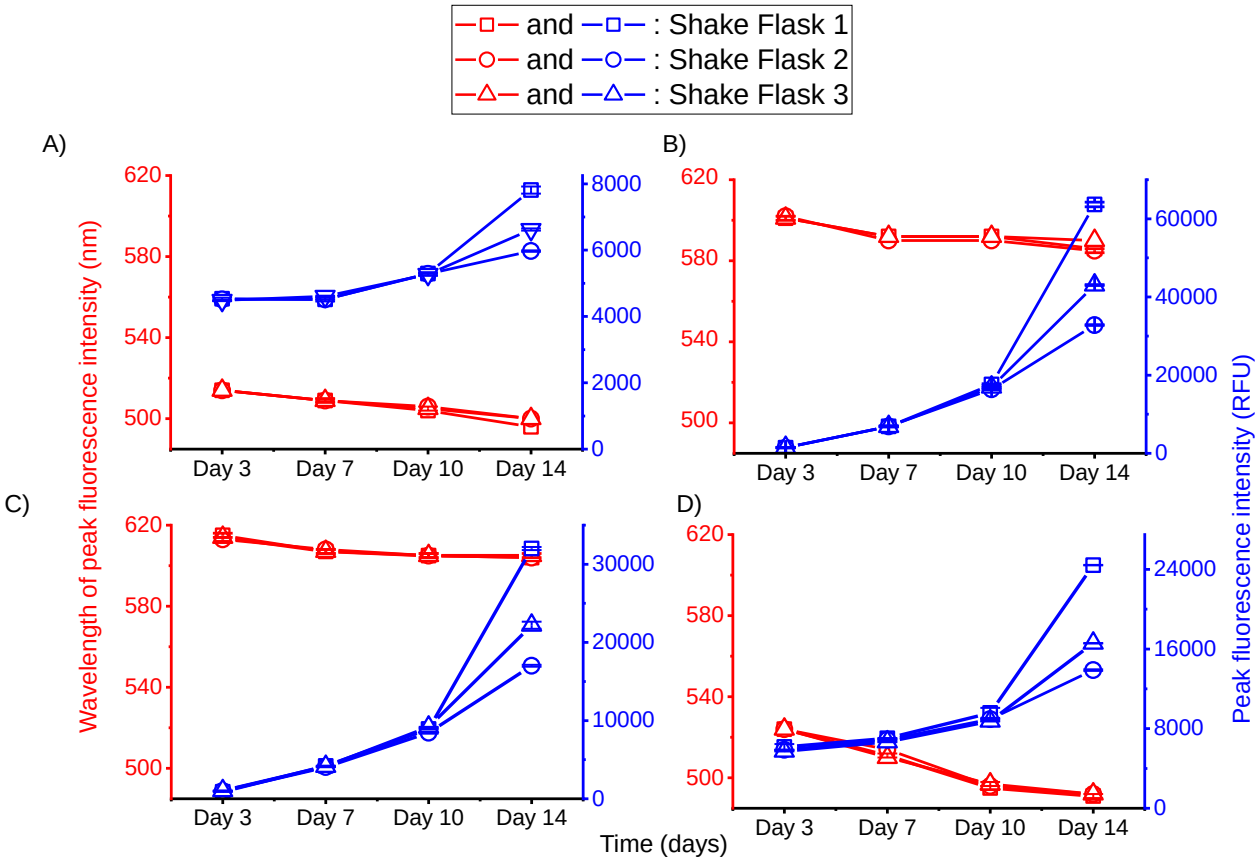

Figure 4-7: Comparison of change in peak fluorescence intensity and peak wavelength in three clarified null cell cultures shake flasks.
Supernatants were separated by centrifugation and filtration before measuring adding dye and measuring fluorescence. Comparison of decrease in wavelength at which highest fluorescence occurs (degree of blue shift) against increasing fluorescence intensity with increasing amount aggregates. Concentration of antibody in each well was 1 mg/mL. This was performed in duplicate. (A) 50 µM Bis-ANS, excitation/emission- 390/450-600 nm, gain 70 (wavelength SD=1 nm, peak intensity SD=108 RFU); (B) 5X SYPRO Orange, excitation/emission- 495/550-700 nm, gain 100 (wavelength SD=1 nm, peak intensity SD=603 RFU); (C) 3 µM ProteoStat, excitation/emission- 530/560-700 nm (wavelength SD=1 nm, peak intensity SD=449 RFU); (D) 50 µM Thioflavin T, excitation/emission- 430/460-600 nm, gain 110 (wavelength SD=1 nm, peak intensity SD=505 RFU).

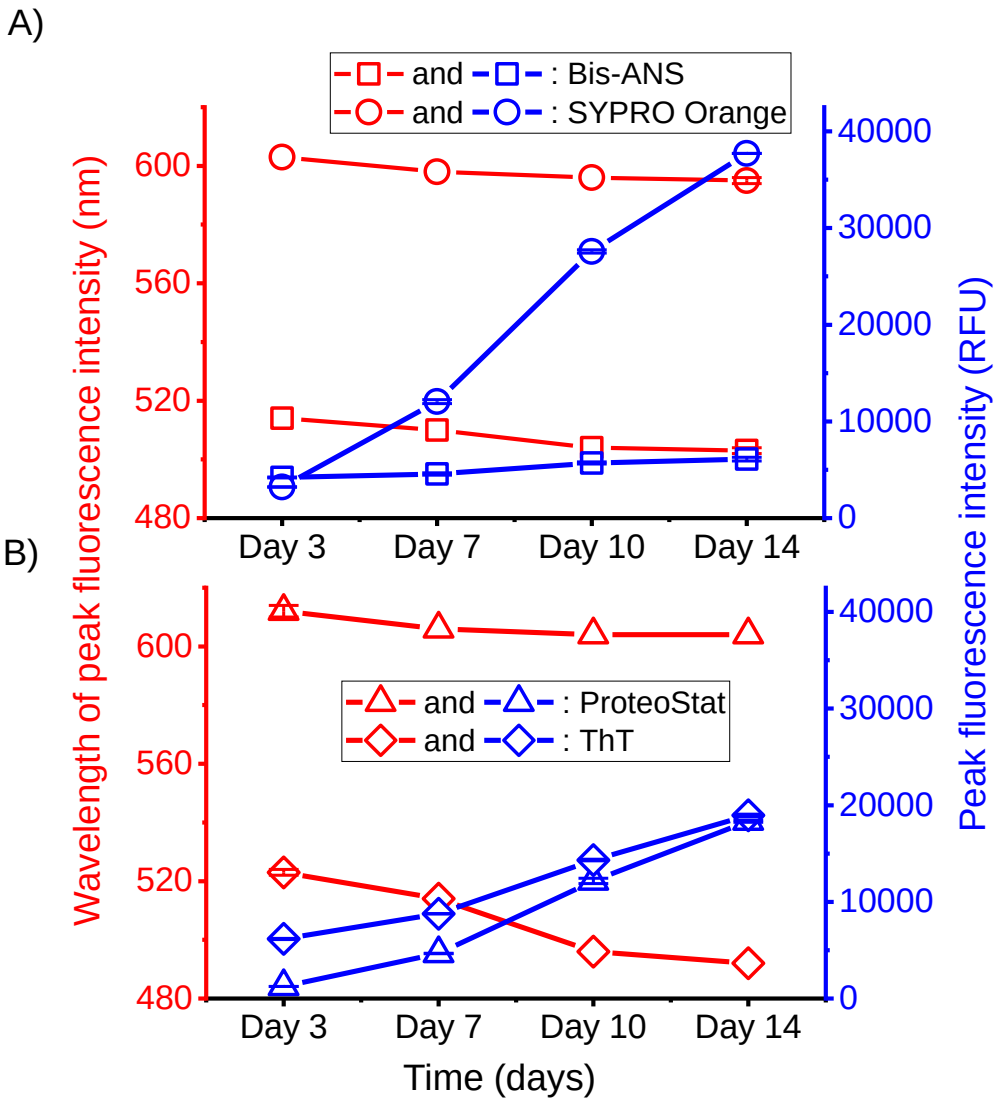

Figure 4-8: Peak height and peak wavelength against mAb clarified cell cultures. The dyes were spiked into wells containing clarified IgG1 mAb B from different time points. Supernatants were separated by centrifugation and filtration before measuring adding dye and measuring fluorescence. Comparison of decrease in wavelength at which highest fluorescence occurs (degree of blue shift) against increasing fluorescence intensity with increasing amount aggregates. Concentration of antibody in each well was 1 mg/mL. (A) 50 µM Bis-ANS, excitation/emission- 390/450-600 nm, gain 70 (wavelength SD=1 nm, peak intensity SD=200 RFU); 5X SYPRO Orange, excitation/emission- 495/550-700 nm, gain 100 (wavelength SD=1 nm, peak intensity SD=207 RFU); (B) 3 µM ProteoStat, excitation/emission- 530/560-700 nm (wavelength SD=2 nm, peak intensity SD=278 RFU); 50 µM Thioflavin T, excitation/emission- 430/460-600 nm, gain 110 (wavelength SD=1 nm, peak intensity SD=122 RFU).

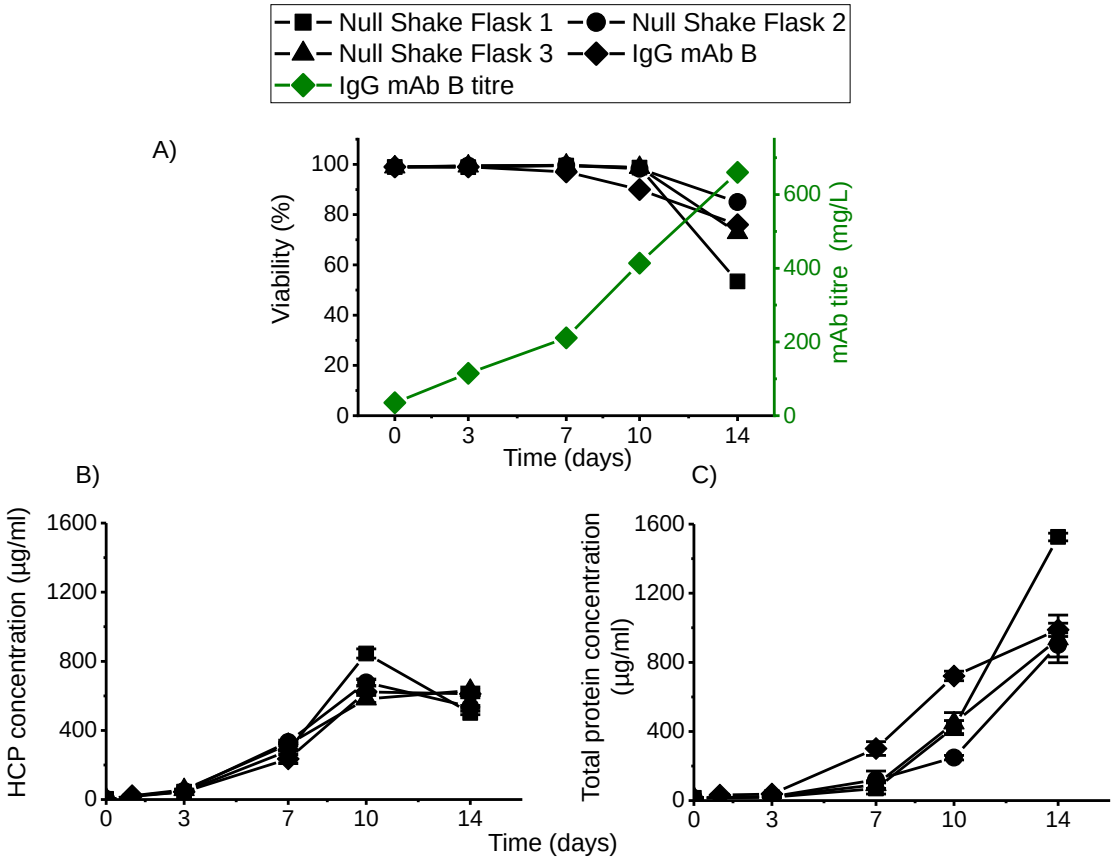

Figure 4-9: Protein concentration and viability measured in cell culture supernatants for null cell line and IgG mAb B.
(A) Viability and mAb titre as measured by ViCell and Nephelometer respectively; (B) Host cell protein (HCP) concentration over the 14-day cell culture period as measured by in-house HCP ELISA (samples were serial diluted as necessary to fit into detection, SD=26 µg/mL). The CHO HCP concentration was determined using a standard curve of known concentrations from a proprietary CHO HCP antigen standard; (C) Total protein concentration as measured by Bradford assay (measured in triplicate. SD=138 µg/mL).

4.5.3. Key Findings

All four dyes showed an increase in fluorescence intensity in the null and mAb culture supernatant samples over the duration of the cell culture. The trend with fluorescence intensity amongst the three shake flasks on day 14 also correlated with loss of viability. Overall, this emphasised that even in the absence of mAb and irrespective of culture age, that extrinsic dyes are not a specific indicator of mAb aggregation. However, they may rather be an indicator of overall protein aggregation or high molecular weight species.

4.6. Characterisation of the size of aggregates the fluorescent dyes are interacting with

Aggregates differ by size and shape depending on the mechanism of aggregation. Although the fluorescent dyes were not a specific indicator of mAb aggregation, we wanted to gain insight into what size and type of proteins the dyes may be interacting with. Focusing on SYPRO Orange and ProteoStat, null cell culture and IgG mAb B supernatants were investigated to see whether the dyes interacted more with high molecular weight (HMW) or low molecular weight (LMW) proteins or both. SYPRO Orange and ProteoStat were focused on as they were less protein concentration dependent and had two different mechanisms of interaction with the aggregates (hydrophobicity and molecular rotor respectively).

SEC was used to assess the profile of LMW to HMW species at 214 nm using clarified supernatants of the null culture (shake flask 1) and IgG mAb B (Figure 4-10). Based on the column specifications, species eluting before 5 mins would be greater than 500 kDa and after 11 mins were smaller than 10 kDa. Figure 4-10 shows an increase in peak area from day 0 to day 14 for both the null and mAb culture supernatants, indicating an increase in the concentration of HMW and LMW species over time. For the null culture, there was a sharp peak after the void volume showing a high amount of HMW species. This peak is also seen in the mAb B supernatants, though is not as intense.

To get an indication of the size of protein species that the dyes were binding to, null culture shake flask 1 and IgG mAb B were mixed with SYPRO Orange or ProteoStat prior to injecting onto the SEC column with fluorescence detectors. The IgG mAb B and null culture with SYPRO Orange in Figure 4-11A and Figure 4-11B had strong HMW peaks at around 5.5 mins. This indicated the presence of aggregates which was also shown present from the UV traces in Figure 4-10A and 4-7B at 5 mins. The IgG mAb B culture with SYPRO Orange (B) also notably detected the monomer mAb species at around 8 mins.

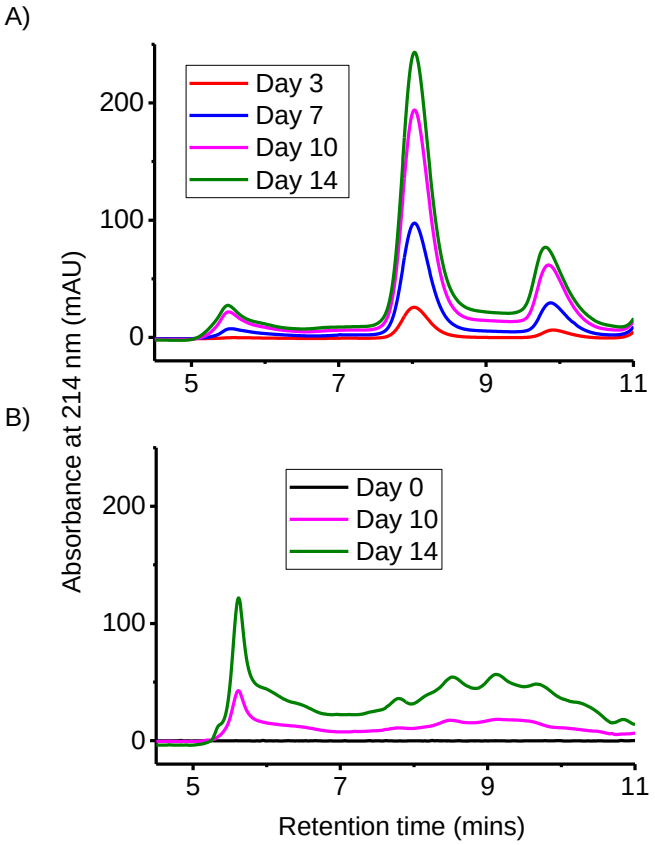

Figure 4-10: SEC of IgG1 mAb B and null cell line culture supernatants.
(A) IgG mAb B and (B) Null cell line shake flask 1 were analysed using size exclusion chromatography to understand the aggregation profile directly in culture. The samples 0.22 µm filtered before running on TSKgel2000SWI column (7.8x300mm) with a flow rate of 0.5 mL/min. The detector measured absorbance at 214 nm. Running buffer composed of 100 mM sodium phosphate (monobasic), 400 mM sodium chloride, pH 6.8.

For the null culture with ProteoStat in Figure 4-11C, there was a strong HMW peak at around 5.5 mins. The null culture with ProteoStat (Figure 4-11C) showed a stronger increase in fluorescence signal of LMW species at 9 mins compared to the null culture with SYPRO Orange (Figure 4-11A). There was also a more defined LMW species peak seen with IgG mAb B (Figure 4-11D) with ProteoStat at 10 mins than with SYPRO Orange (Figure 4-11B). The IgG mAb B culture with ProteoStat (Figure 4-11D) had a surprisingly strong monomeric mAb signal at around 8 mins, which was stronger than both the HMW and LMW. The peak at 8 mins corresponds to the mAb monomer it has consistently eluted at this time-frame. However, this has not been seen in previous literature or disclosed by the manufacturer. A strong fluorescence signal would mean that there were more hydrophobic cavities present that would constrain ProteoStat's rotation. This should normally happen in the presence of an aggregate, however as it is occurring with the monomer it may suggest that dye is sensitive at constraining itself into the tertiary structure of the mAb. As ProteoStat is a commercial dye advertised to measure mAb aggregation, detailed information on structure and binding it not publicly available at the manufacturer's discretion.

ProteoStat also detected the HMW in the null culture on day 14 (Figure 4-11C) with higher intensities than the IgG mAb B on day 14 (Figure 4-11D). This correlated to the plate dye assay which saw that the null culture shake flask 1 had higher fluorescence on day 14 than the IgG mAb B.

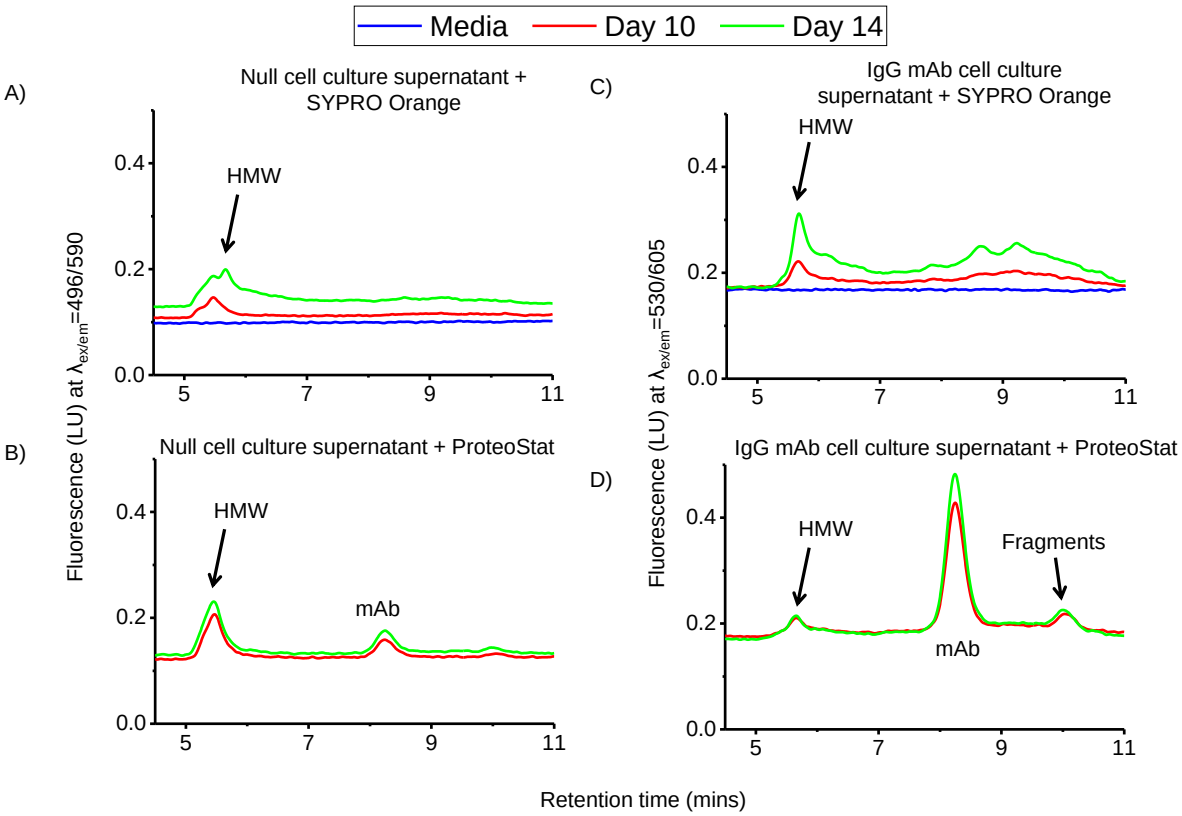

Figure 4-11 SEC of mAb and null clarified cell cultures with SYPRO Orange and ProteoStat.
(A) Null cell line shake flask 1 with 5X SYPRO Orange; (B) IgG mAb B with 5X SYPRO Orange; (C) Null cell line shake flask 1 with 3 µM ProteoStat; (D) IgG mAb B with 3 µM ProteoStat. Clarified cell culture samples were combined with dye prior to loading onto the column. A TSKgel2000SWI column (7.8x300mm) with a flow rate of 0.5 mL/min with a fluorescence detector was used. SYPRO Orange samples excitation/emission- 495/590 nm, ProteoStat samples excitation/emission- 530/605 nm. Running buffer composed of 100 mM sodium phosphate (monobasic), 400 mM sodium chloride, pH 6.8. Injection volume of 50 µL.

4.6.1. Key Findings

In this section, SEC with fluorescence detection was used to see what size aggregates SYPRO Orange and ProteoStat were binding to. The results showed that SYPRO Orange was more sensitive at detecting large molecular weight species. ProteoStat on the other hand, was not as effective as SYPRO Orange at measuring large aggregates and is perhaps better suited to smaller aggregates. Additionally, ProteoStat binds to monomeric mAb which may skew fluorescence results compared to SYPRO Orange.

4.7. Conclusion

A current challenge in bioprocessing is the ability to measure critical quality attributes without prior purification. Fluorescent dyes are known for their sensitivity and ability to measure aggregates based on different types of interactions. With the dyes used in this chapter, the main interactions with aggregates were due to interacting with exposed hydrophobic regions on proteins (Bis-ANS and SYPRO Orange), and constrained dye rotation resulting in fluorescence (ThT and ProteoStat). All four dyes used in this study worked well in purified conditions, however, there has been limited application of fluorescent dyes in cell culture. The only previous study showed Bis-ANS to be suitable to analyse mAb aggregate from cell cultures. However, from this study, an increase in fluorescence in both null and mAb clarified cultures in the presence of dyes from inoculation up to day 14 occurred. The fluorescence in the null clarified supernatant had similar (and in one case higher) fluorescence intensities when compared to mAb clarified supernatant. This showed that fluorescent dyes solely are not a specific indicator of mAb aggregation. However, the fluorescent dyes used in this study revealed their potential for use as an indicator of viability by measuring the release of cellular components as cells die. This study also provided interesting insight into the type of aggregates the dyes are interacting with. It seemed that SYPRO Orange is more sensitive for measuring large aggregates whereas ProteoStat can detect aggregates, monomeric mAb and fragments to similar extents. One potential application of SYPRO Orange may be to highlight cell lines which may produce large aggregates during the cell culture which may cause issues during harvest. It could be used to aid cell line selection in maximising viabilities and minimising the amount of protein aggregates.

5 An affinity peptide-based assay to measure monoclonal antibody aggregates

5.1. Chapter Aim

The fluorescent dye assay described in the previous chapter evaluated the capabilities of the fluorescent dyes to measure mAb aggregates in cell culture supernatants. However, findings showed that fluorescent dyes with known affinity to aggregates, on their own, were not specific indicators of mAb aggregation in cell culture medium. The fluorescent assay had to be redesigned to be more specific to mAb aggregates.

This chapter reviews the use of fluorescent/biotinylated affinity peptides to measure mAb aggregates. The chapter will cover the following areas:

1. Designing the biotinylated and fluorescent affinity peptide

2. Assessing the biotinylated affinity peptide with biosensor instruments
    a. Octet – dip and read biosensor
    b. Biacore – chip-based flow-through biosensor

3. Investigating the binding of the fluorescent affinity peptide to mAb and non-mAb proteins using various techniques:
    a. Plate readers: to measure fluorescence
    b. Size exclusion chromatography: to correlate specific protein species (UV signal) and binding of fluorescent molecules (fluorescence signal)
    c. Determining the affinity by measuring the equilibrium dissociation constant and using hydrogen deuterium exchange

5.2. Introduction

The initial dye assay was not specific at measuring mAb aggregates in cell culture supernatants (Chapter 4). Therefore, the dye assay needed to be adapted to increase the specificity of fluorescent dyes. One idea was to use the peptide sequences identified by Cheung et al. (2017) that showed specific affinity to aggregated mAb. Cheung et al. (2017) screened a phage display peptide library and identified a sequence that showed 9-fold better binding toward aggregated NISTmAb than control non-aggregated NISTmAb. The peptide sequence also showed little affinity to non-mAb proteins (BSA and lysozyme). Therefore, the idea was to use the affinity peptide to "capture" aggregated mAb, whilst using another component attached to the peptide to provide signal for detection.

Two detection methods options were fluorescence or biotinylation as shown in Figure 5-1. The biotinylation method would measure the binding affinity between the biotinylated affinity peptide (biotin-AP) and mAb aggregate using biosensor instruments such as Octet and Biacore. As streptavidin has a strong non-covalent interaction with biotin, streptavidin coated biosensors/chips were be appropriate to load the biotin-AP onto the Octet biosensors/Biacore chip.

Four fluorescent dyes (Thioflavin T (ThT), CCVJ, Tide Fluor 2 (TF2) and Fluorescein (FL)) were identified as viable options for conjugation as they all had reactive forms to use for conjugation. Two molecular rotors were chosen (ThT and CCVJ) and two non-aggregation related dyes (Tide Fluor 2 and Fluorescein) were chosen for comparison.

Theoretically, molecular rotors were a better choice than "hydrophobic-binding dyes" such as SYPRO Orange. This was because molecular rotor dyes only fluoresce when constrained by an aggregate. If the dye is placed next to the antibody binding site of the AP, then there should be an increase in fluorescence as the molecular rotor dyes become more constrained. Hence, the molecular rotor dyes were thought to be suitable in this format at measuring mAb aggregates. In Chapter 4, ThT was shown to be able to measure mAb aggregates and Hawe et al. (2010) showed that CCVJ has been used

to characterise thermally stressed IgG aggregates. As the AP should specifically draw aggregated mAbs to the conjugated dyes, these two dye conjugates should work in a dip and read format without the need of a wash step.

Tide Fluor 2 and Fluorescein are bright dyes that had no specificity towards aggregated proteins. As these dyes on their own do not interact solely with aggregated proteins, it was a good control to show whether the affinity peptide works at binding aggregates from a proof-of-concept point of view. To ensure detection of only bound conjugates, a wash step would need to be incorporated to remove excess unbound AP-dye. As such, the use of these two dyes would be more suited to an ELISA type format. Overall, both the ideas were suitable in 96-well plates format for high-throughput measurement.

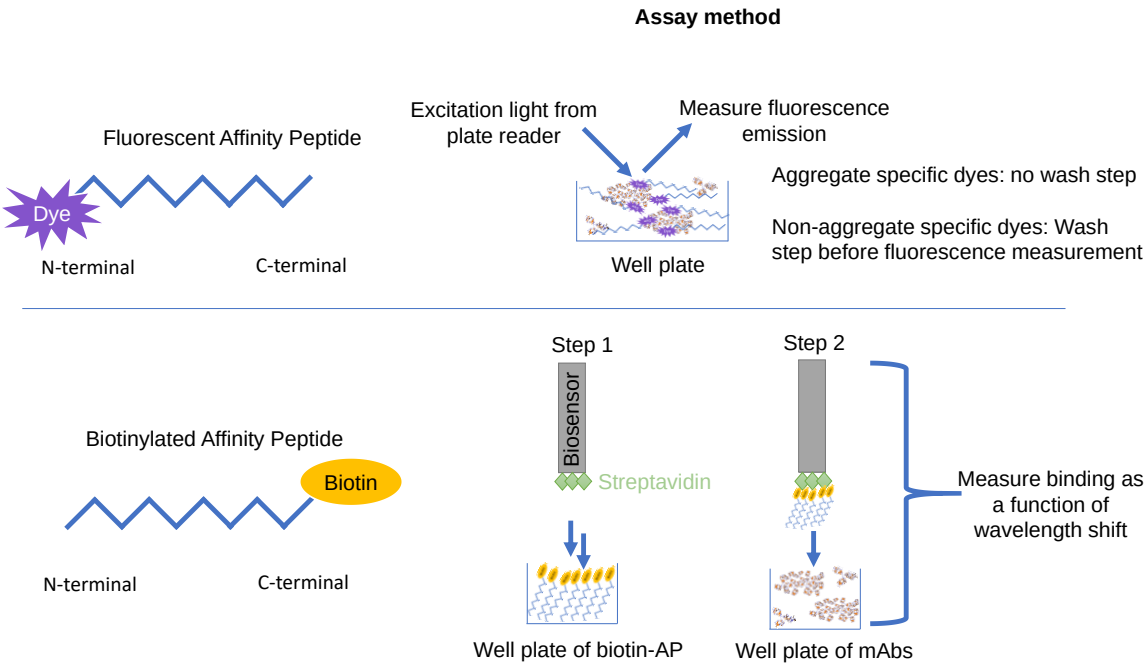

Figure 5-1: Description of the affinity peptide assay using fluorescent dyes and biotin. (Top) The fluorescent-AP assay with both the fluorescent-AP and mAbs placed in a well for measurement of fluorescence intensity by a plate reader. Higher fluorescence intensity indicates larger amount of aggregate present. A wash step would be added before fluorescence measurement for dyes that do not measure aggregation specifically. This would be further facilitated by immobilising the peptide-dye conjugate onto the surface of a well plate. (Bottom) The biotin-AP assay with a streptavidin biosensor (using Octet). Upon binding the biotin-AP to the streptavidin biosensor, the biosensor is dipped into the mAb aggregate sample to measure the binding interaction. Larger wavelength shift indicates the binding of the biotin-AP to aggregates.

5.3. Affinity peptide structure

The peptide sequence (RDYHPRDHTATWGGG) contains three glycines at the C-terminus that acted as a linked between the peptide and the pIII protein on the bacteriophage during screening. It was not certain whether the glycines played a role in binding, therefore it was kept in the sequence. As the AP was bound to the bacteriophage at the C-terminus, it was assumed the mAb aggregates interacted/bound via to the N terminus. Hence, the fluorescent-AP were designed with the dyes bound at the N-terminus, such that the dyes would be in a close proximity to

bound mAb aggregates. This was important especially for the molecule rotor dyes (ThT and CCVJ) which need to be constrained in order to fluoresce.

On the other hand, biotin was placed on the C-terminus for the biotinylated-AP to leave the N-terminus free for binding. In addition, as the peptide sequence was quite short, it was advised by Forte Bio to add a spacer (LYS) between the biotin and the peptide, to prevent the peptide from lying flat on the biosensor surface.

5.4. Plate based biosensor measurement of mAb aggregates with affinity peptide

5.4.1. Initial biosensor results using mAb aggregates

The biotin-AP was assessed using the Octet which monitors the binding between a ligand immobilised on the biosensor tip surface, and proteins/analyte in solution. An increase in optical thickness (binding) at the biosensor tip, results in an increased wavelength shift. The more molecules that bind to the biosensor tip surface, the greater the affinity between the immobilised ligand and analyte.

The first step was to bind the biotinylated-AP to the streptavidin (SA) sensor (Figure 5-2). The binding of biotin to streptavidin is one of the strongest non-covalent interaction with a K_d of 10^{-15} M, and streptavidin can bind up to four biotin molecules. In Figure 5-2, the binding was very strong as the sensors saturated (plateau) within 10 seconds. In the last 30 seconds, the sensors were washed to remove any excess biotinylated affinity peptide which saw a slight decrease in shifts. The binding of the biotinylated-AP to the SA sensor (after washing the excess) had average wavelength shifts between 1.40-1.58 nm.

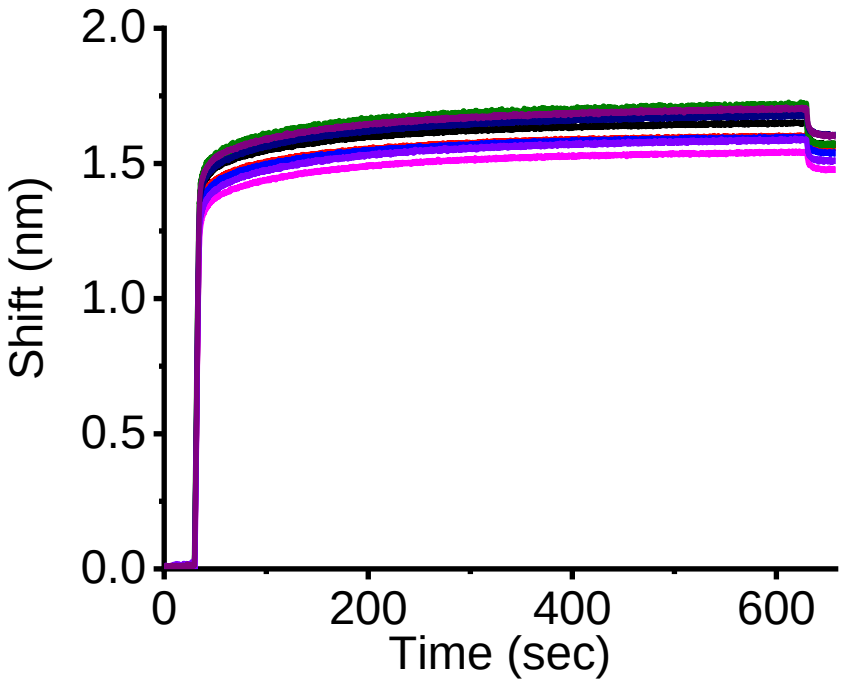

Figure 5-2: Octet measurement of biotin-AP binding to streptavidin-coated (SA) biosensors.
Eight SA biosensors dipped into 10 mM PBS for 30 secs, then into 20 µg/ml of biotin-AP for 10 mins. Sensors were dipped into buffer for 30 secs to remove excess biotin-AP. Assay was run in duplicates (one run used eight sensors for the eight different samples run in Figure 5-3). however as the results were similar only one run is shown.

After the biotin-AP was bound to the SA sensor, the sensors were inserted into the sample plate (Figure 5-3). The results of sensor set 1 and 2 followed similar trends. Compared to the interactions between biotin and streptavidin, the interactions between the biotin-AP and mAbs were slower and weaker. Figure 5-3A shows the interactions after 30 mins, whereas Figure 5-3B shows the initial slope which is important as the affinity is usually determined from the initial slope of the binding curve. In the initial slope (Figure 5-3B), 100% monomer mAb did not have a steep curve as the aggregated mAbs samples, and this was still visible after 30 minutes (Figure 5-3A). BSA had a steeper initial slope than the other mAb samples, however after 30 mins BSA and 100% monomer mAb had similar shifts of 0.80 nm and 0.81 nm respectively. As BSA had an initial steeper curve than 100% monomer mAb, this

indicated a stronger but non-specific interaction as Cheung et al. (2017) showed that the AP did not have affinity to BSA. 100% and 7% mAb aggregate followed a similar slope profile, where as 50% mAb aggregate was similar to BSA for the first few seconds, but then diverged away showing weaker affinity.

After 30 mins of incubation (Figure 5-3A), 100%, 50% and 7% mAb aggregate had a wavelength shifts of 1.31 nm, 1.05 nm and 1.09 nm. The shifts and curves of 50% and 7% mAb aggregate were close. Surprisingly, lysozyme had negative shifts indicating that the thickness at the biosensor tip was reduced by the presence of lysozyme. This would mean that lysozyme was somehow pulling off the AP bound onto the SA sensor. The lysozyme used could not be quantified using SEC, so it was thought that there may be some stability issues with this protein provided from ProteoStat. However, as there was another non-mAb protein used as a control for the assay (BSA), it was decided to omit lysozyme from future experiments.

The major problems with the Octet assay was the high interaction between biotin-AP and BSA, as well as the lack of differentiation between 50%/7% mAb aggregate and 100% monomer/BSA. Therefore, to improve the specificity and reduce non-specific interactions, the assay was repeated using more stringent buffers. Small amounts of non-ionic detergent e.g. Tween-20 can reduce non-specific binding interactions (Hakami et al., 2015). As the initial assay just used PBS, we decided to investigate with KB buffer (0.02% Tween-20) and PBS+0.5% Tween-20. 0.5% Tween-20 was chosen as it decreased non-specific interactions with the fluorescent affinity peptides in Chapter 5.6.2.

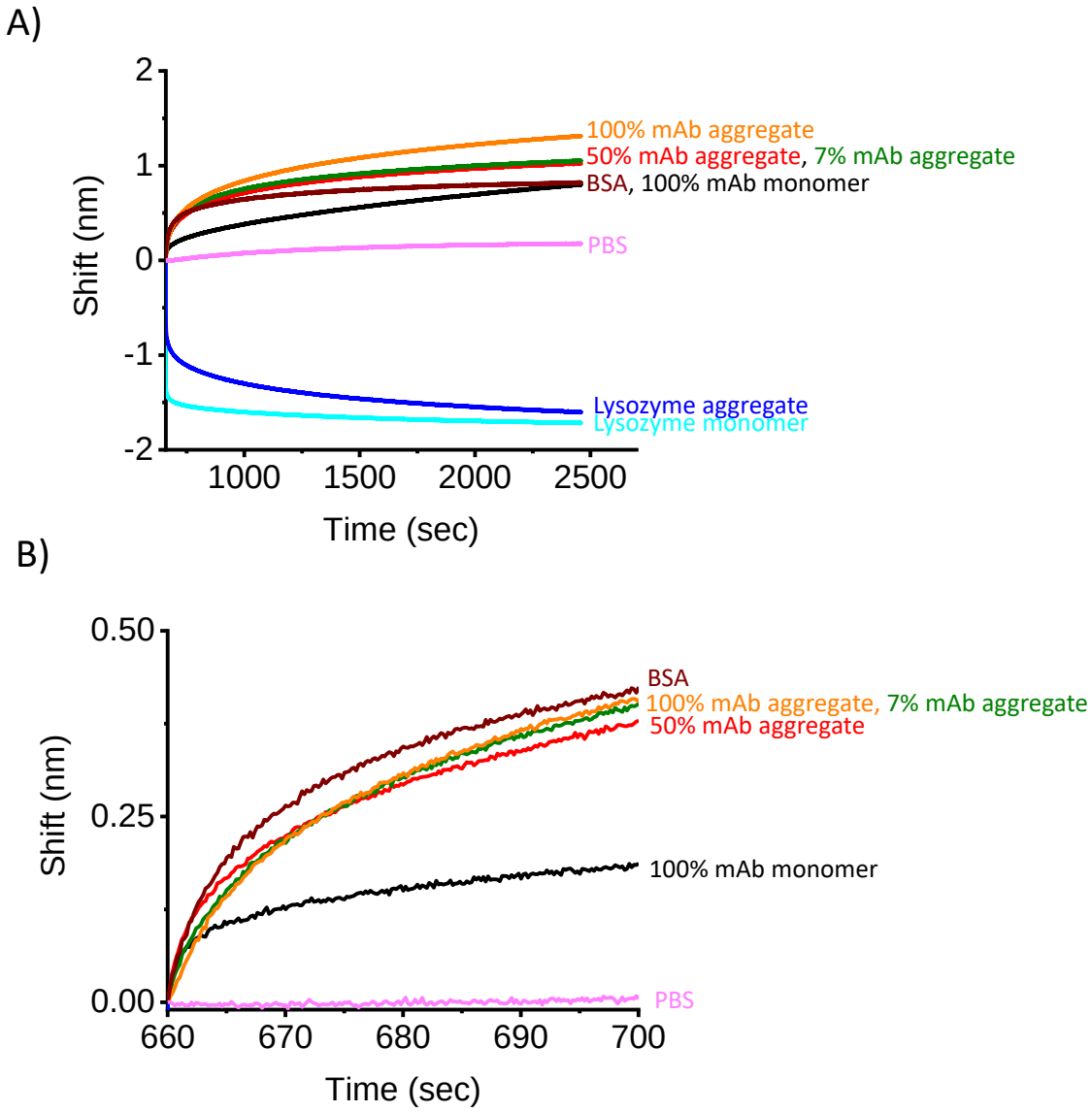

Figure 5-3: Octet measurement of the interactions between mAb, BSA, lysozyme and biotinylated affinity peptide.
(A) Octet shifts monitored for 30 mins to mimic the incubation time used in the Cheung et al. (2017) paper. (B) Zoom into the initial slope. Prior to measurement, biotinylated-AP was bound to streptavidin biosensors. Samples were prepared at 1 mg/mL in 10 mM PBS pH 7.4. Biosensor was dipped into the sample for 30 mins (to mimic the 30 minute incubation time used with the peptide in Cheung et al. (2017)). 100% mAb monomer and aggregate were obtained from isolating peaks using preparative SEC as detailed in the Materials & Methods. 100% monomeric and aggregated mAb had a r_h of 5.8 nm and 17 nm respectively. 50% and 7% mAb aggregate had a r_h of 34 nm and 7.6 nm respectively. Lysozyme was obtained from ProteoStat aggregation kit controls; however, the size of the molecule could not be accurately measured by DLS. Assay was run in duplicates using two sensor sets however as the results were similar only one set is shown.

5.4.2. Using different buffers to reduce non-specific binding

The Octet assay was repeated using kinetic buffer (KB) (Figure 5-4A) which is produced by Forte Bio who also manufactures the Octet. The KB buffer (full details in the Materials and Methods Section 3.9) contains PBS with Tween-20 (which is a surfactant known to reduce non-specific binding), BSA (acts as a blocking agent- to prevent non-specific binding (Xiao and Isaacs, 2012)) and sodium azide (a preservative). The binding of biotin-AP to SA sensor was slightly lower (1.24-1.29 nm) than previously with PBS (Figure 5-2). However, more noticeably were the small shifts (<0.2 nm) upon the biotin-AP interacting with the mAb and BSA samples (Figure 5-4B). The shifts were a tenth smaller using KB buffer compared to using PBS buffer in Figure 5-2. BSA had higher interactions than aggregated mAb. Overall, it seemed that the KB buffer inhibited almost all binding between the sample and the biotin-AP.

Another buffer investigated was PBS+0.05% Tween-20 buffer, which was chosen as it had a slightly higher percentage of Tween-20 than the KB buffer. The binding of biotin-AP to the SA sensor with PBS+0.05% Tween-20 buffer (Figure 5-5A) had a similar degree of wavelength shift (1.28-1.34 nm) to the KB buffer. The binding of the mAb and BSA samples to the biotin-AP using PBS with 0.5% Tween-20 buffer also had the same weak results as with the KB buffer. Therefore, in this instance, the use of even a higher percentage Tween-20 did not reduce the non-specificity between biotin-AP and the mAb samples.

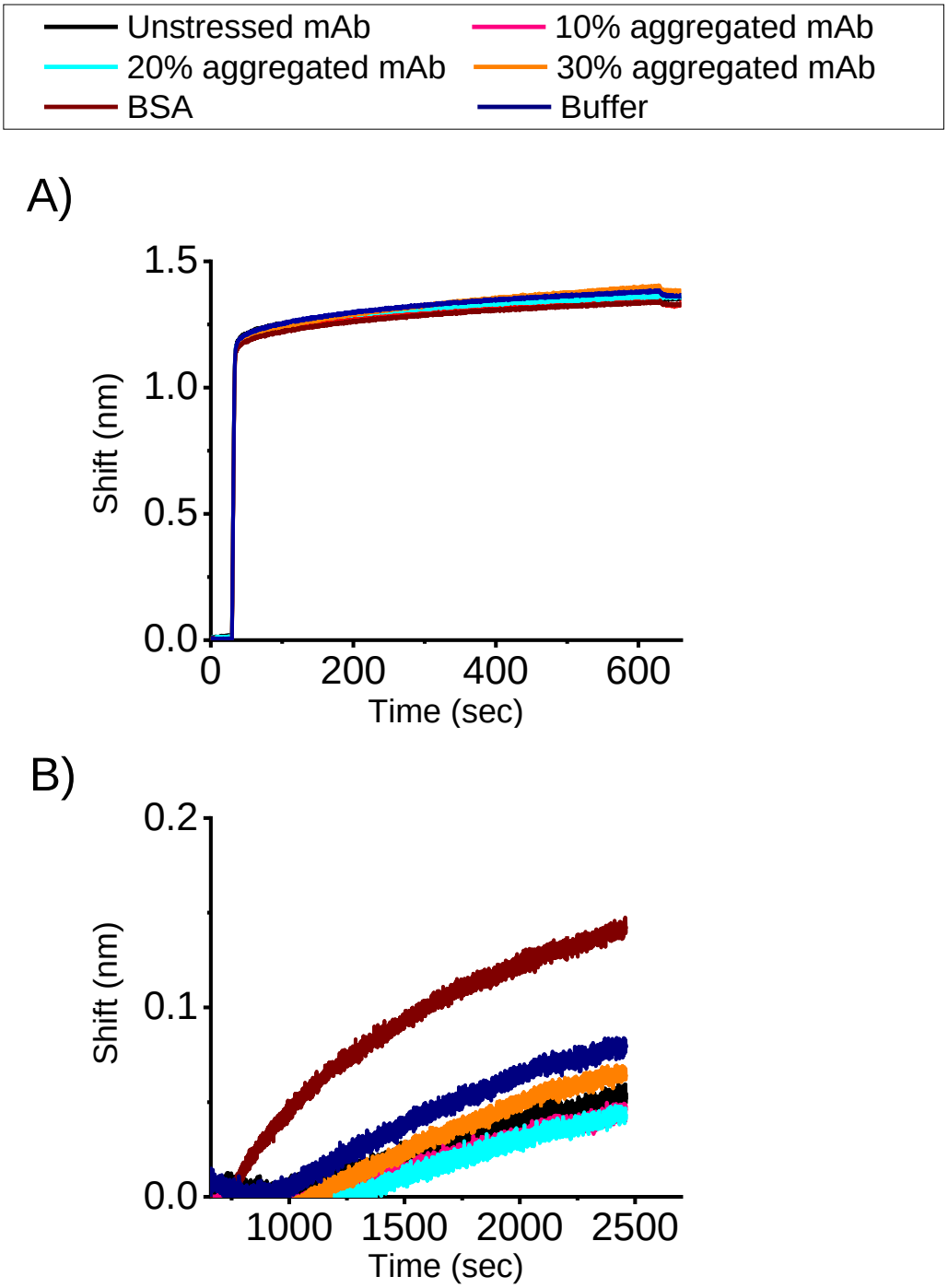

Figure 5-4: Octet assay with biotin-AP using KB buffer.
(A) Biotin-AP binding to the SA sensor, (B) biotin-AP interaction with mAb and BSA. Each biosensor was dipped into 1 mg/mL of protein sample for 30 mins. Assay was run in duplicates using two sensor sets however as the results were similar only one set is shown.

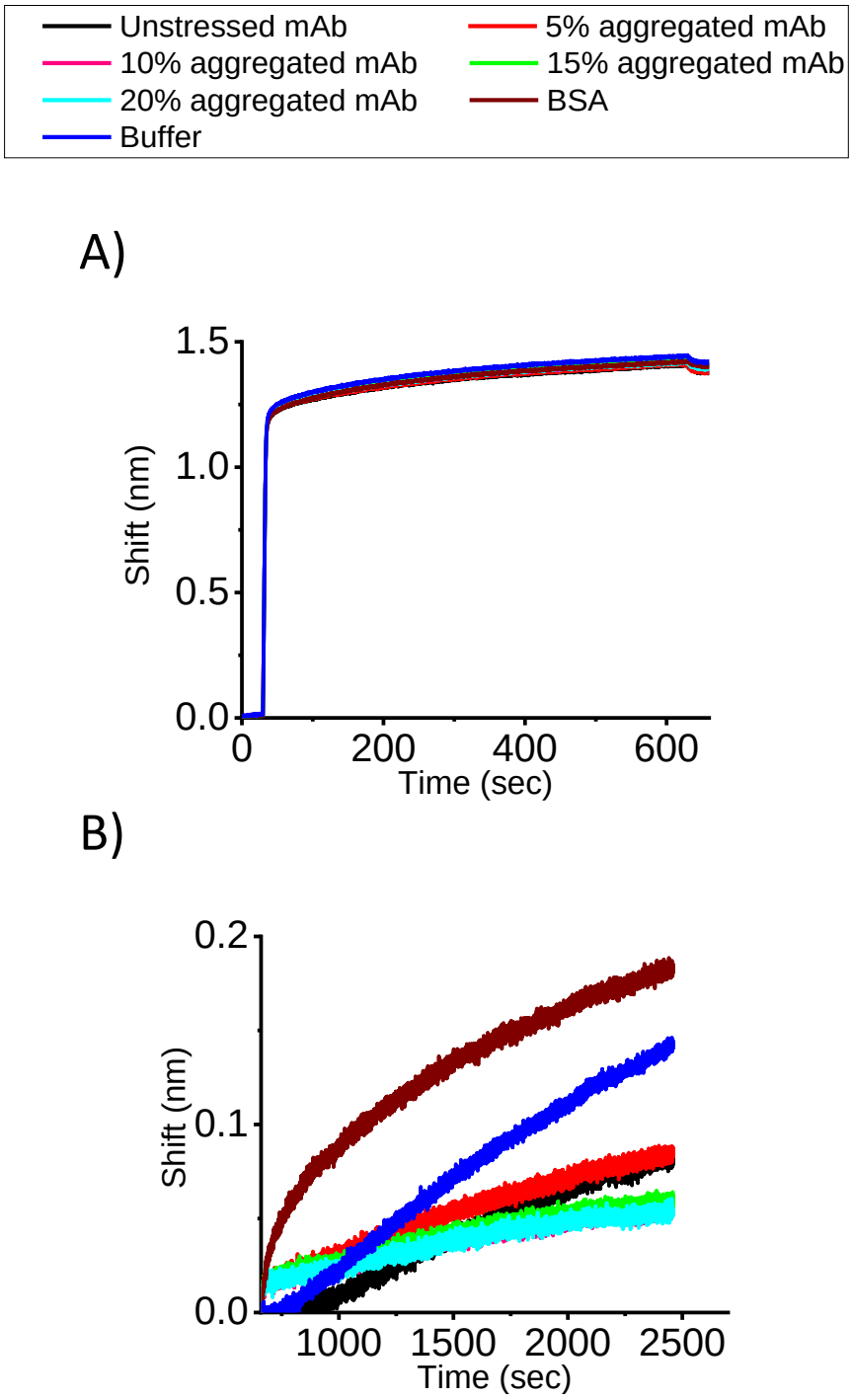

Figure 5-5: Octet assay with biotin-AP using 10 mM PBS pH 7.4+ 0.5% Tween-20 buffer.
(A) Biotin-AP binding to the SA sensor, (B) Biotin interaction with mAb and BSA sample. Each biosensor was dipped into 1 mg/mL of protein sample for 30 mins. Assay was run in duplicates using two sensor sets however as the results were similar only one set is shown.

5.5. Flow cell biosensor measurement of mAb aggregates with the affinity peptide

The Biacore system is a more well-established method to investigate binding interactions. It operates differently to Octet as the target molecules flow across the surface of a molecules immobilised on a chip over time rather than dip-and-read. In the Biacore chip, a sample is injected through a series of four flow cells (Figure 5-6). Each flow cell has their own inlet and the flow cells are typically operated in pairs to allow for buffer subtraction. Polarised light is directed toward the sensor surface and the angle of minimum intensity reflected light is detected. The angle changes as molecules bind and dissociate over time, which generates a sensorgram.

The set-up was as follows: flow cell 1 (FC1) was used as reference cell, whereby buffer and sample were passed through, however biotin-AP was not immobilised onto the flow cell surface. Flow cell 2 (FC2) was the active flow cell which had biotin-AP was immobilised on the surface and sample was flowed across. To account for buffer interactions, FC2 was subtracted from FC1.

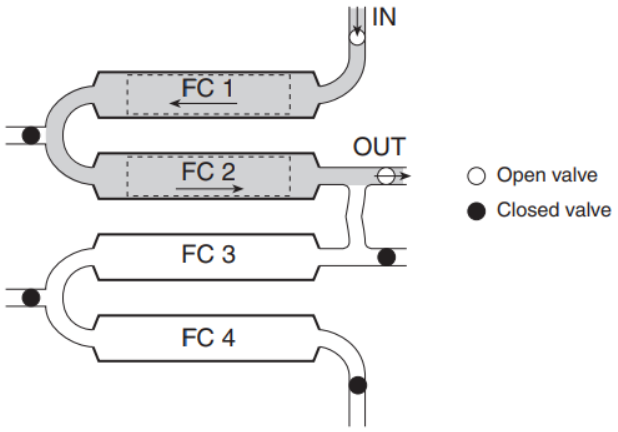

Figure 5-6: Biacore flow cell mechanism.
There are four flow cells (FC) which have their own inlets. Flow cells are used in pairs to allow for blank subtraction. Image obtained from GE Healthcare Life Sciences (2013).

The binding of biotin-AP to the streptavidin surface of FC2 (Figure 5-7) was rapid (<1 min). The curve continued to rise after 1 min due to excess binding. The wash step removed the excess bound biotin-AP producing a stable signal. After binding the

biotin-AP to the FC2 surface, 100% aggregated mAb at three different concentrations (1, 10 and 100 µg/ml) were run across both FC1 and FC2. The reference subtracted sensorgram in Figure 5-8 had a low signal (<10 RU) across all three concentrations (although there was an increase in response value with increasing concentration). Therefore, to improve the intensity of the signal, the Biacore assay was run at 1000 µg/ml mAb, with different flowrates (10 µL/min or 30 µL/min) and temperatures (25°C or 37°C) to see if better kinetics could be obtained. The reference subtracted results with 1000 µg/ml mAb (Figure 5-9) had higher response values compared to Figure 5-8 due to the increased mAb concentration. However, the only distinguishing factor between the curves was the type of sample – monomeric or aggregated mAb. Aggregated mAb binding to the biotin-AP was roughly 3X higher in response value than the monomeric mAb. Temperature and flowrate did not make an impact on the response values. Even still, as Biacore response values are typically in the 1000's (e.g. the binding of biotin-AP to sensor in Figure 5-7), the response values obtained even at 1000 µg/mL was still quite low.

There were two potential reasons for the weak binding using the Biacore. The first reason was due to the non-specific interaction between the mAb and the streptavidin. There was a high amount of mAb interacting with the streptavidin surface of the reference flow cell (FC1). This resulted in negative sensorgram when the curves were blank subtracted as the reference flow cell had higher or similar signal than the active flow cell. This occurred particularly with monomeric mAb at concentrations < 1000 µg/mL of mAb. As the mAbs interacted with the chip directly, this also meant that it was not possible to accurately use Biacore to quantify the affinity (in terms of K_d) between the peptide and mAb aggregate. The second reason for the weak interactions was maybe due to steric hindrance. The AP and the mAb aggregates both need to be in an appropriate conformation for binding to occur. As the AP was short and small, it may have been in a conformation where its binding site was hidden. This could have occurred by either the AP lying flat on the surface of the chip, or the binding site may have been blocked by having too many AP immobilised too close to each other on the

chip. The peptide/assay may have benefited from having longer linkers and/or reducing the amount of AP bound to the chip.

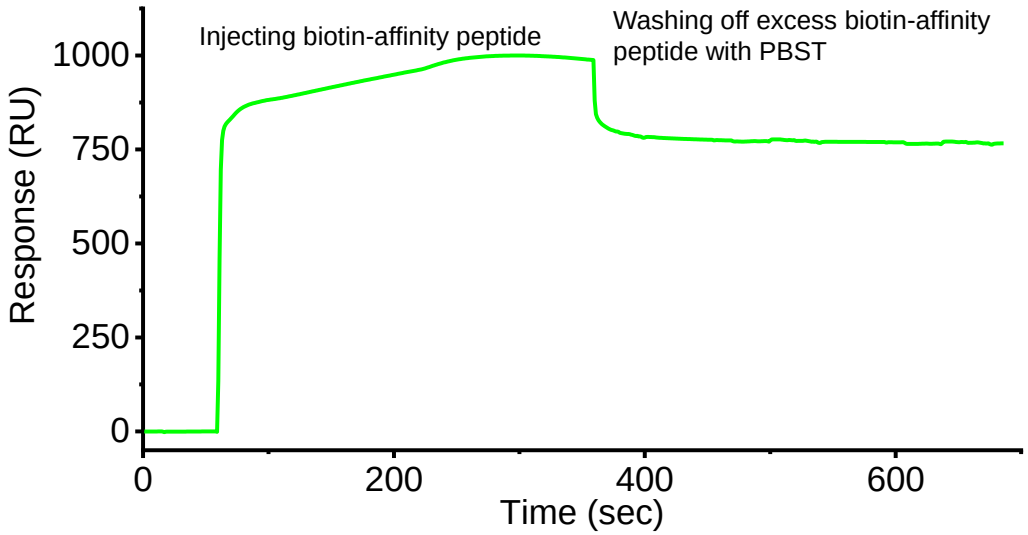

Figure 5-7: Binding biotin-AP to Biacore streptavidin chip.
20 µg/ml biotin-AP was injected onto FC2 at 10 µL/min for 5 mins. The chip was then washed twice with buffer at 50 µl/min for 30 secs twice to remove the excess unbound biotin-AP.

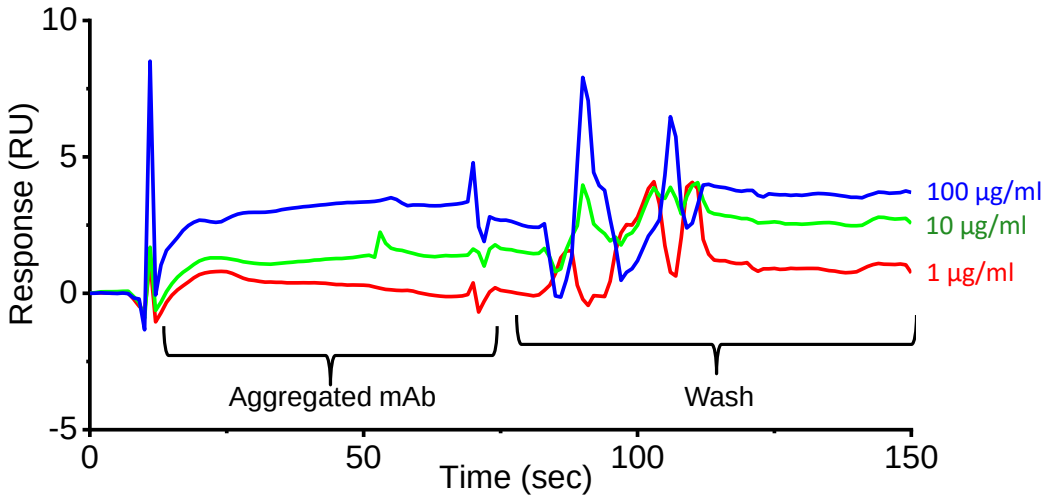

Figure 5-8: Binding of 100% aggregated mAb at different concentrations to biotin-AP.
The sensorgram is corrected for the blank by subtracting the two flow cells (FC2-FC1). Blue, green and red curves correspond to 100 µg/ml, 10 µg/ml and 1 µg/ml respectively. Aggregated mAb was loaded for the first 60 seconds, then the chip was washed (for 30 seconds) to remove excess bound molecules.

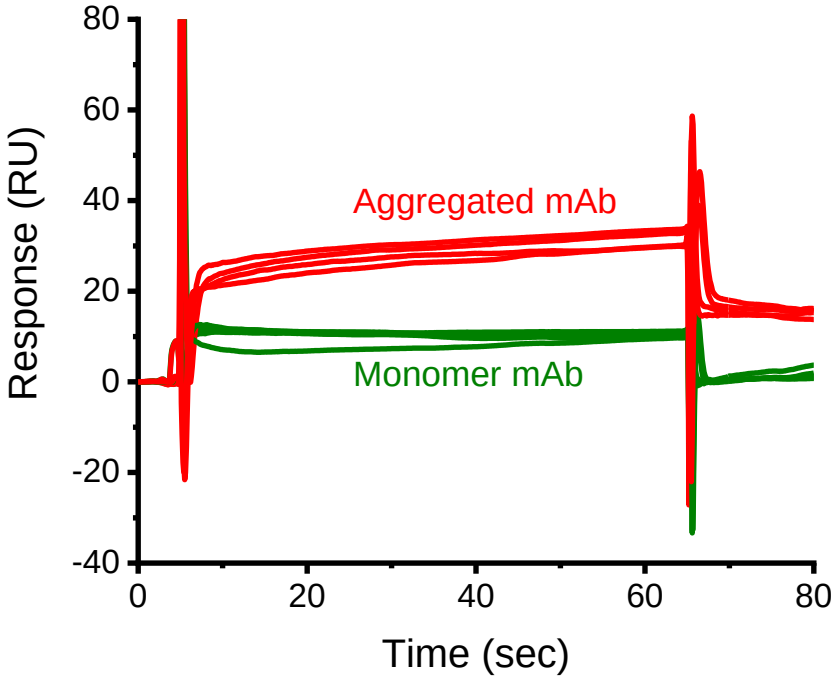

Figure 5-9: Binding of 100% aggregated and monomeric mAb to biotin-AP.
Prior to measurement biotin-AP was immobilised onto streptavidin surfaces. Data shows the blank subtracted sensorgram (FC2- FC1). Mab samples were run at 1000 µg/ml, at two different temperatures (25°C and 37°C) and two different flowrates (10 and 30 ml/min). Despite the different conditions, the sensorgram were only distinguished by being either monomeric or aggregated mAb.

5.6. Fluorescently tagged affinity peptides as tools for mAb aggregate measurement

The second affinity peptide assay idea was to conjugate the affinity peptide (AP) to a fluorescent dye at the AP N-terminus. Two molecular rotors were chosen (Thioflavin (ThT) and CCVJ) and two bright dyes (Tide Fluor 2 (TF2) and Fluorescein (FL)) were chosen for investigation. The peptides were conjugated to the dyes using amine reactive chemical groups, resulting in an amide bond at the N-terminus of the peptide.

For the initial assessment, the four AP-dyes were measured with monomeric and aggregated mAb and lysozyme (Figure 5-10-Figure 5-13). Lysozyme was included to see whether the AP-dyes had any non-specific interactions with other proteins. The AP-dyes were also measured at equimolar dye:protein (1:1) and excess (7:1 – ratio used for initial dye assay) concentrations to see whether interactions were concentration dependent.

In Figure 5-10, the fluorescence spectra of AP-ThT with lysozyme and mAb overlapped. There was a lot of variability between the replicates at both 50 µM and 7 µM AP-ThT concentration. In contrary, the AP-CCVJ fluorescence spectrums (Figure 5-11) had consistent trends at both 50 µM and 7 µM AP-CCVJ. In addition, there was a 125% increase in the AP-CCVJ fluorescence intensity with 50% aggregated mAb compared to monomeric mAb. There was also a 6 nm blue shift (shift of peak max to lower wavelengths) with AP-CCVJ fluorescence with the aggregated mAb sample (compared to monomeric mAb), indicating that the dye was in a hydrophobic environment. Furthermore, the peak intensity of AP-CCVJ with lysozyme (aggregated and monomeric forms) was very close to the MilliQ blank, indicating little non-specific interactions from other non mAb proteins.

For AP-TF2 (Figure 5-12), the trend of results varied at 50 µM and 7 µM AP-TF2 concentrations. At 50 µM AP-TF2 (Figure 5-12A), the fluorescence of AP-TF2 with the blank was higher than the fluorescence of AP-TF2 with both aggregated and monomeric mAb. Whereas, the fluorescence of AP-TF2 with the blank at 7µM (Figure 5-12B) was higher than AP-TF2 with monomeric mAb. At both

concentrations, AP-TF2 had higher fluorescence with aggregated mAb than with monomer mAb. However, the fluorescence of AP-TF2 with lysozyme (monomer and aggregate) was higher than with mAb samples. Conversely, AP-FL (Figure 5-13) had an opposite trend to AP-ThT. The fluorescence intensity of AP-FL with mAb monomer was stronger than AP-FL with aggregated mAb. AP-FL with lysozyme had a low fluorescence intensity that overlapped with the fluorescence intensity of AP-FL with the blanks. In addition, the fluorescence intensity of AP-FL with the blanks also had less symmetrical spectral curves. This trend was seen at both 50 µM and 7 µM AP-FL concentrations. AP-FL seemed more specific to monomer mAb and the presence of mAb aggregates decreased the fluorescence intensity.

From these initial results, AP-CCVJ distinguished aggregated mAb from monomeric mAb with little fluorescence from the blank and lysozyme. These results were achieved with minimal assay optimisation. It was surprising that AP-ThT did not work as well as AP-CCVJ as they are both molecular rotors. One reason for the poor performance may have been pH as certain dyes are known to be pH sensitive which can cause stronger or weaker fluorescence depending on the pH. Molecular rotor dyes (CCVJ) are sensitive to changes to their microenvironment. Therefore, it would be interesting to see how pH affects fluorescence, and if there was an optimal pH for maximum fluorescence intensity for these dyes. It is also widely known that the fluorescence intensity of fluorescein is highly susceptible to changes in pH and other environmental factors (Chen et al., 2008). Hence, a pH sensitivity experiment was conducted to understand how pH will impact results.

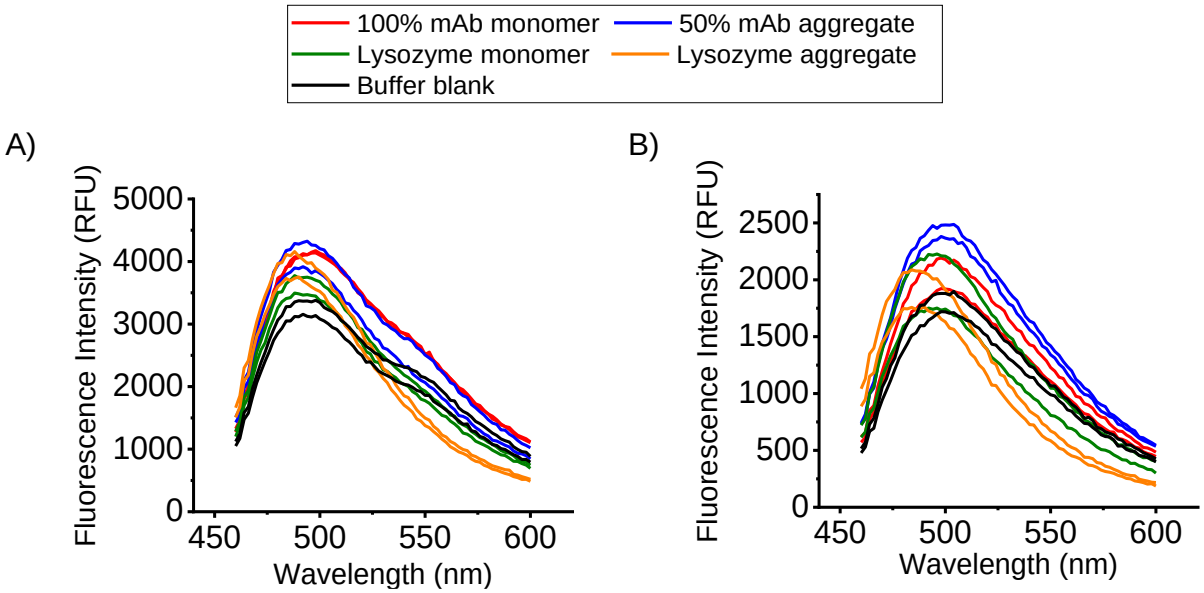

Figure 5-10: Fluorescence spectrum of affinity peptide-Thioflavin T (AP-ThT) with mAb and lysozyme.
(A) 50 µM AP-ThT and (B) 7 µM AP-ThT. Monomeric mAb (PBS pH 7.4) was obtained by isolating the monomer peak from a preparative size exclusion chromatography. 50% mAb aggregates (sodium acetate buffer pH 5.5) was obtained via thermal stressing mAb (See Materials and Methods). Lysozyme standards were obtained from ProteoStat aggregation detection kit. Concentration of antibody in each well was 1 mg/mL. Fluorescence measurement was performed in duplicates. Excitation/Emission - 430/460-600 nm.

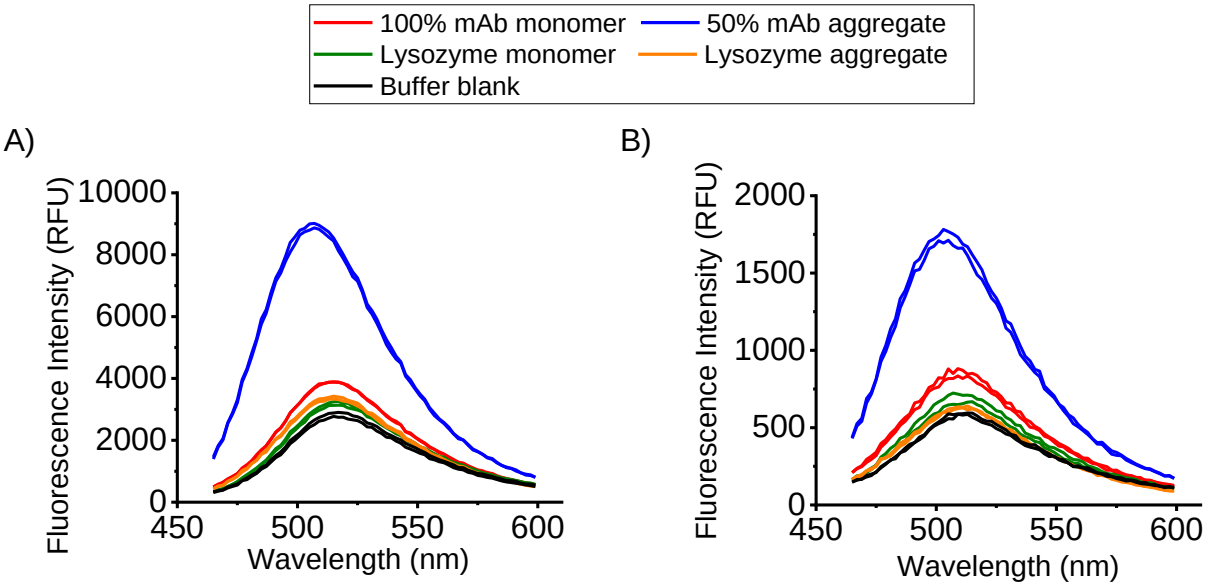

Figure 5-11: Fluorescence spectrum of affinity peptide-CCVJ (AP-CCVJ) with mAb and lysozyme.
(A) 50 µM AP-CCVJ and (B) 7 µM AP-CCVJ. Monomeric mAb was obtained by isolating the monomer peak from a preparative size exclusion chromatography which eluted the mAb in PBS. Monomeric mAb (PBS pH 7.4) was obtained by isolating the monomer peak from a preparative size exclusion chromatography. 50% mAb aggregates (sodium acetate buffer pH 5.5) was obtained via thermal stressing mAb (See Materials and Methods). Lysozyme standards were obtained from ProteoStat aggregation detection kit. Concentration of antibody in each well was 1 mg/mL. Fluorescence measurement was performed in duplicates. Excitation/Emission – 435/465-600 nm.

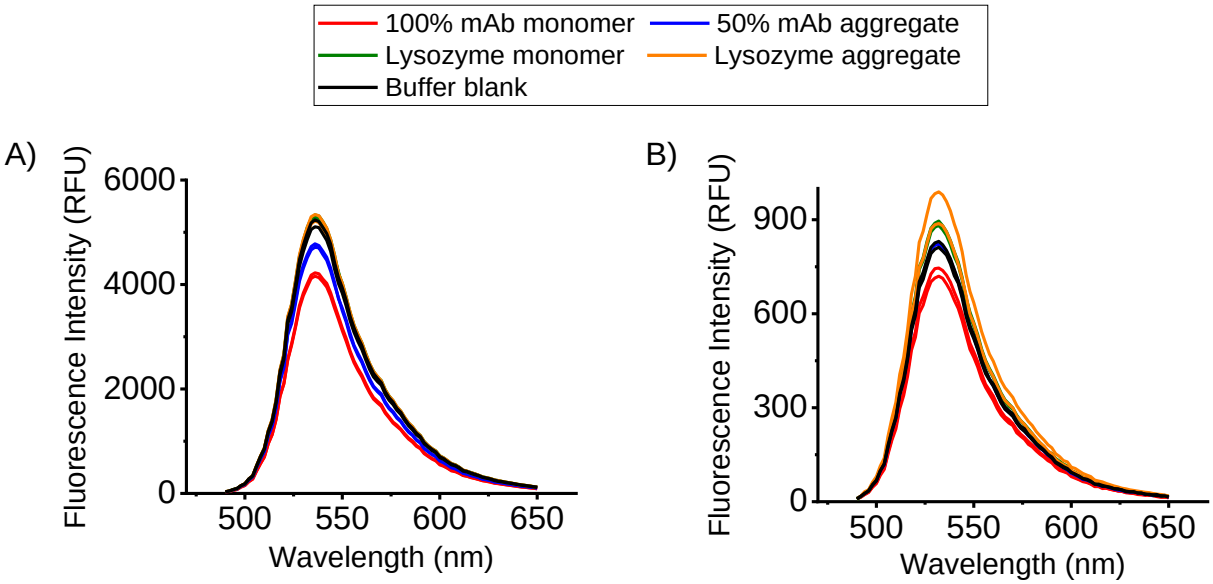

Figure 5-12: Fluorescence spectrum of affinity peptide-Tide Fluor 2 (AP-Tide Fluor 2) with mAb and lysozyme.
(A) 50 µM AP-Tide Fluor 2 and (B) 7 µM AP-Tide Fluor 2. Monomeric mAb was obtained by isolating the monomer peak from a preparative size exclusion chromatography which eluted the mAb in PBS. Monomeric mAb (PBS pH 7.4) was obtained by isolating the monomer peak from a preparative size exclusion chromatography. 50% mAb aggregates (sodium acetate buffer pH 5.5) was obtained via thermal stressing mAb (See Materials and Methods). Lysozyme standards were obtained from ProteoStat aggregation detection kit. Concentration of antibody in each well was 1 mg/mL. Fluorescence measurement was performed in duplicates. Excitation/Emission – 440/490-650 nm.

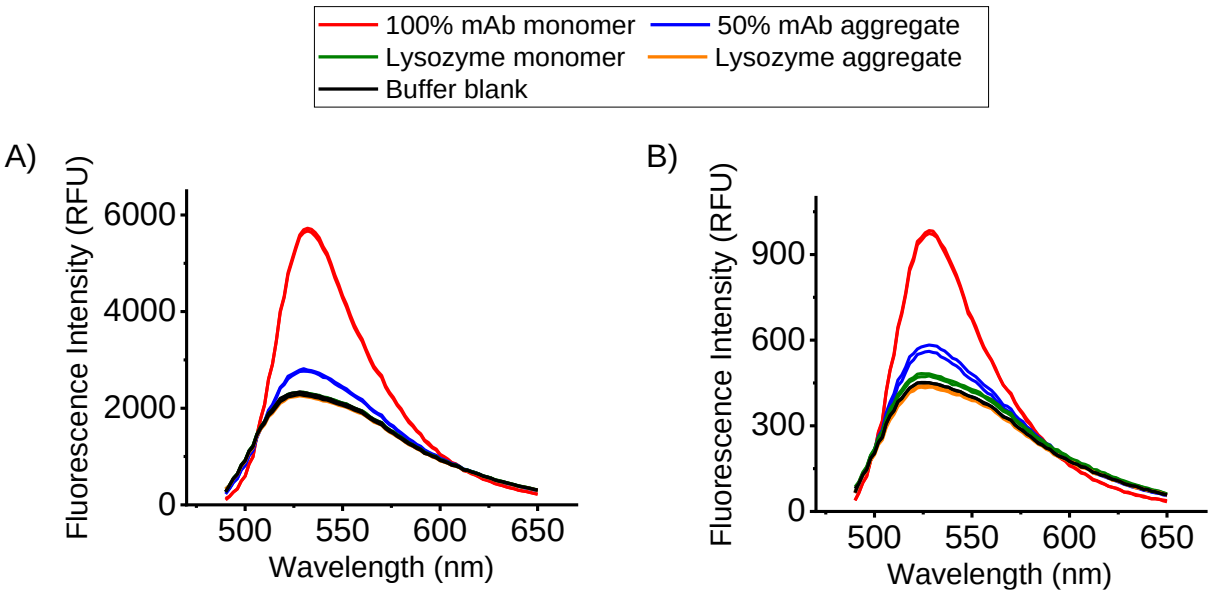

Figure 5-13: Fluorescence spectrum of affinity peptide-Fluorescein (AP) with mAb and lysozyme.
(A) 50 µM AP-Fluorescein and (B) 7 µM AP-Fluorescein. Monomeric mAb was obtained by isolating the monomer peak from a preparative size exclusion chromatography which eluted the mAb in PBS. Monomeric mAb (PBS pH 7.4) was obtained by isolating the monomer peak from a preparative size exclusion chromatography. 50% mAb aggregates (sodium acetate buffer pH 5.5) was obtained via thermal stressing mAb (See Materials and Methods). Lysozyme standards were obtained from ProteoStat aggregation detection kit. Concentration of antibody in each well was 1 mg/mL. Fluorescence measurement was performed in duplicates. Excitation/Emission 440 nm/490-650 nm.

5.6.1. pH sensitivity experiment of affinity peptide with molecular rotor dyes

It was important to investigate the impact of pH on fluorescence as dyes can be sensitive to the pH of the environment. The fluorescence of AP-CCVJ and AP-ThT were measured in 50 mM phosphate buffer at pH 3.30, 6.00, 7.08, 7.92 and 9.09 as shown in Figure 5-14 and

Figure 5-15 respectively. There were minor differences in the fluorescence intensities of AP-CCVJ with stressed and unstressed mAb pH 3.30. Notably, there was a higher AP-CCVJ fluorescence with BSA than the mAb samples. Upon increasing the pH (pH 6.00-7.92), the AP-CCVJ fluorescence with aggregated mAb was higher than with unstressed mAb. From pH 3.30 - pH 6.00 and pH 6.00 - pH 7.08, there was a 130% and 28% peak increase in AP-CCVJ fluorescence intensity with aggregated mAb respectively. Figure 5-14B showed that the optimal pH for the highest fluorescence intensity of AP-CCVJ with mAb aggregate was pH 7. However, between pH 6.00-7.92, the fluorescence intensity of AP-CCVJ with BSA was equivalent to the fluorescence of AP-CCVJ with stressed mAb. This non-specific interaction with a non-mAb protein such as BSA would cause interference when measuring mAb aggregates in multi-component environments such as cell cultures.

At pH 3, there was no difference in fluorescence intensities of AP-ThT with BSA, unstressed and stressed mAb (Figure 5-15A). However, there was higher AP-ThT fluorescence with aggregated mAb that increased with pH. From pH 3.03 – 6.00, pH 6.00 – 7.08 and pH 7.08 – 7.92, there was a 45%, 55% and 13% peak increase in AP-ThT fluorescence intensity with stressed mAb respectively.

Figure 5-15B showed that the optimal pH for the highest fluorescence for AP-ThT with mAb aggregate was close to pH 8. Compared to AP-CCVJ, AP-ThT saw lower fluorescence with BSA, almost in line with the fluorescence of AP-ThT with unstressed mAb. Previous AP-ThT results (Figure 5-10) were conducted at pH 5.5. However, the pH sensitivity study showed that the AP-ThT worked better at pH's above 6. Hackl et al. (2015) showed that Thioflavin T in both acidic and basic pH induced a significant decrease in absorbance (at 413 nm) and fluorescence. But there

was less of this effect (decrease in absorbance/fluorescence) in the presence of protein aggregates. The pH effects mentioned by Hackl et al. (2015) were not seen in the results, most likely due to the presence of aggregates.

In summary, the pH sensitivity experiment showed that the optimal pH for the affinity peptide for the highest fluorescence for both AP-CCVJ and AP-ThT were around pH 7. However, unlike lysozyme, AP-CCVJ showed to non-specifically interact with BSA. At pHs above pH 6, AP-ThT performed better than the initial experiment, and did not show non-specific interactions. Thus, AP-ThT started to become more promising than AP-CCVJ. However, to see if the non-specific interactions with AP-CCVJ and BSA could be reduced, the addition of salt and Tween-20 to the buffer was measured and is outlined in the next section.

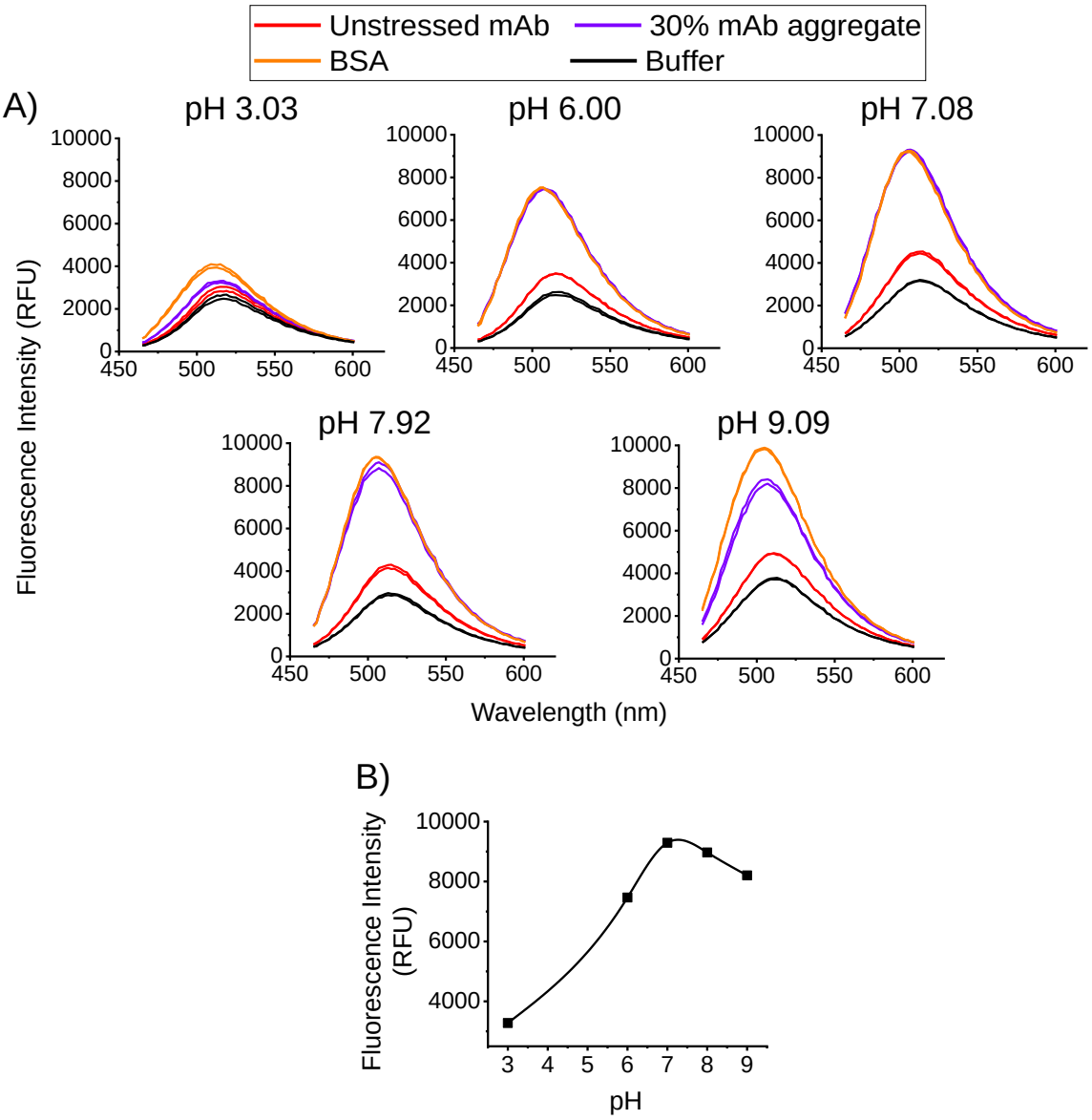

Figure 5-14: Identifying optimal fluorescence for max fluorescence intensity between affinity peptide-CCVJ (AP-CCVJ) and mAb.
(A) mAb and BSA in 50 mM phosphate buffer at five different pHs (pH 3.30, 6.00, 7.08, 7.92 and 9.09) and 50 µM AP-CCVJ. (B) Max fluorescence intensity plotted against pH. Unstressed mAb in sodium acetate pH 5.5 buffer and BSA was in a sodium chloride and sodium azide buffer. 30% mAb aggregates was obtained via thermal stressing mAb in sodium acetate buffer pH 5.5 (See Materials and Methods). Concentration of antibody and BSA in each well were 1 mg/mL and 0.45 mg/mL respectively. This was performed in duplicates. Excitation/Emission - 435/465-600 nm.

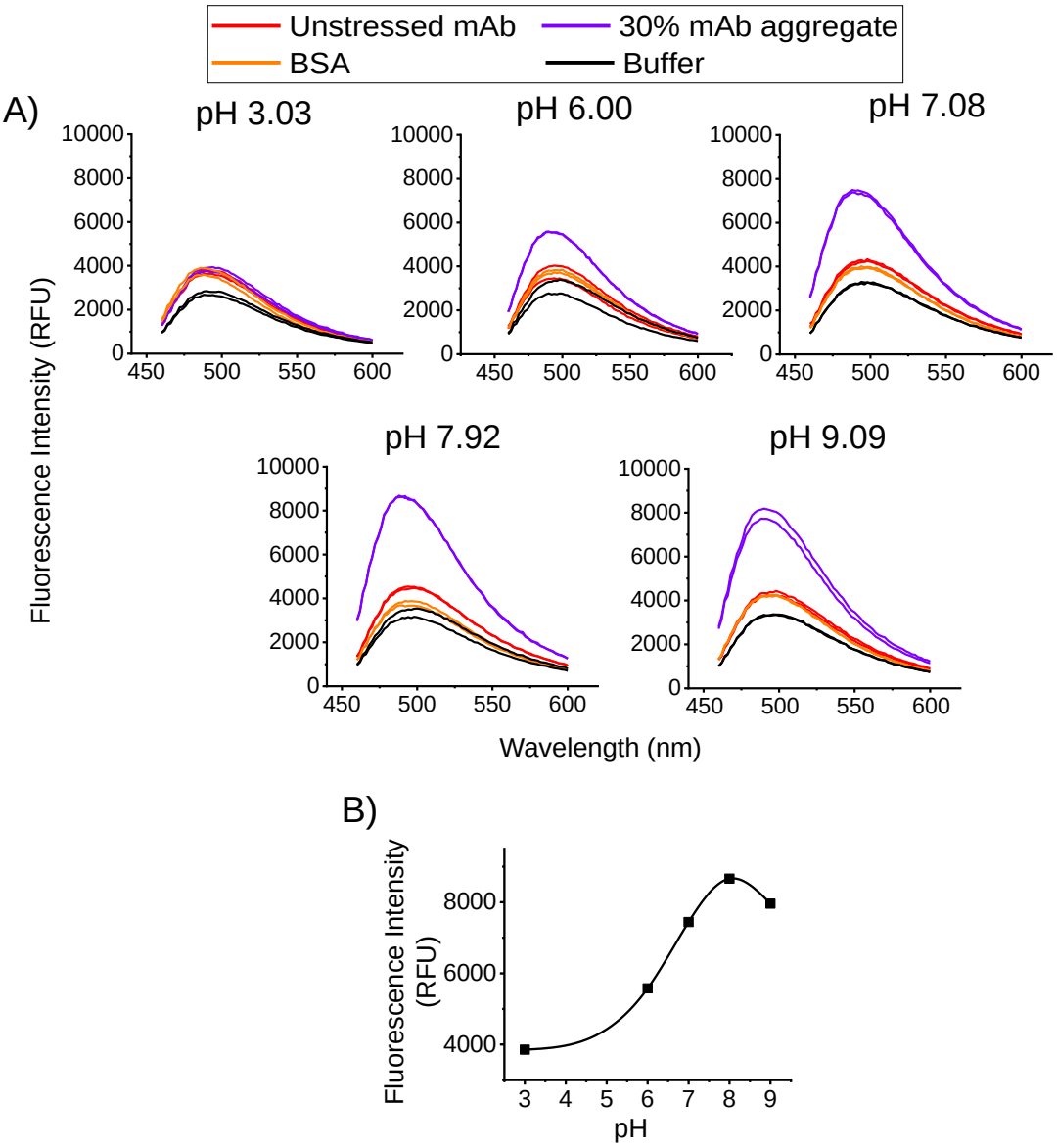

Figure 5-15: Identifying optimal fluorescence for max fluorescence intensity between affinity peptide-Thioflavin T (AP-ThT) and mAb.
(A) mAb and BSA in 50 mM phosphate buffer at five different pHs (pH 3.30, 6.00, 7.08, 7.92 and 9.09) and 50 µM AP-ThT. (B) Max fluorescence intensity plotted against pH. Unstressed mAb in sodium acetate pH 5.5 buffer and BSA was in a sodium chloride and sodium azide buffer. 30% mAb aggregates was obtained via thermal stressing mAb in sodium acetate buffer pH 5.5 (See Materials and Methods). Concentration of antibody and BSA in each well were 1 mg/mL and 0.45 mg/mL respectively. This was performed in duplicates. This was performed in duplicates. Excitation/Emission– 430/460-600 nm.

5.6.2. Reducing the non-specific interactions of affinity peptides tagged with molecular rotor dyes

From the pH sensitivity experiment in the previous section, AP-CCVJ showed non-specific interactions with BSA. As the assay needed to be specific in measuring mAb aggregates in the presence of other proteins, a more stringent buffer was investigated to reduce non-specific interactions. Although it is unlikely that BSA specifically would be present in the cell culture, other molecules with similar properties to BSA present in the media could cause complications. Mild detergents can disrupt hydrophobic interactions between molecules and high salt concentrations can also reduce non-specific binding due to charge interactions (Nicoya Life Sciences, 2015). Therefore, PBS with Tween-20 (a non-ionic detergent, 1228 Da) and salt (sodium chloride) were investigated to see their effect on minimising non-specific interactions (Brogan et al., 2004).

In 0.05% Tween-20 PBS buffer (Figure 5-16A), AP-CCVJ with BSA still had a higher fluorescence intensity than AP-CCVJ with unstressed mAb. With 0.1% Tween-20 PBS buffer (Figure 5-16B), the fluorescence intensity of AP-CCVJ with BSA reduced by almost 20%. However, in 1% Tween-20 PBS buffer, the fluorescence intensity of AP-CCVJ with lysozyme, unstressed mAb, and buffer blank increased to the intensity of AP-CCVJ with BSA.

Figure 5-16D and Figure 5-16E, show the fluorescence of AP-CCVJ in 0.5% and 1% Tween-20 PBS with 50% mAb aggregates respectively. There was a clear separation in the fluorescence intensity of AP-CCVJ with mAb aggregate and the other samples. The fluorescence intensity of AP-CCVJ with BSA was also 40% less than the fluorescence of AP-CCVJ with mAb aggregate.

Although 1% Tween-20 PBS buffer was able to distinguish the fluorescence intensities of AP-CCVJ with mAb aggregates from the other samples, this concentration of Tween-20 raised the fluorescence intensity of AP-CCVJ with the buffer as well as other samples. The fluorescence intensity of AP-CCVJ with lysozyme, BSA and the buffer blank were at a higher intensity at 1% Tween-20 than

0.5% Tween-20. In addition, the fluorescence intensities of AP-CCVJ with lysozyme, BSA and the buffer blank were also closer to the fluorescence of AP-CCVJ with mAb aggregate. It was not clear why there was an increased AP-CCVJ fluorescence at 1% Tween-20 PBS. Although Tween-20 has its own fluorescence, this was outside of the range measured in this experiment (Könemann et al., 2018). Therefore, 0.5% Tween-20 PBS was more suitable in reducing the non-specific interactions as it achieved a lower BSA fluorescence intensity than mAb.

In Figure 5-17, both 0.4 M and 0.8 M salt did not have an impact on the fluorescence. As Tween-20 had more of an effect on the fluorescence intensity more than salt, this suggested that the interactions between the affinity peptide and proteins may be hydrophobic based rather than ionic based. Moving forward, it was decided to use 0.5% Tween-20 PBS as a more stringent buffer for reducing non-specific interactions with AP-CCVJ.

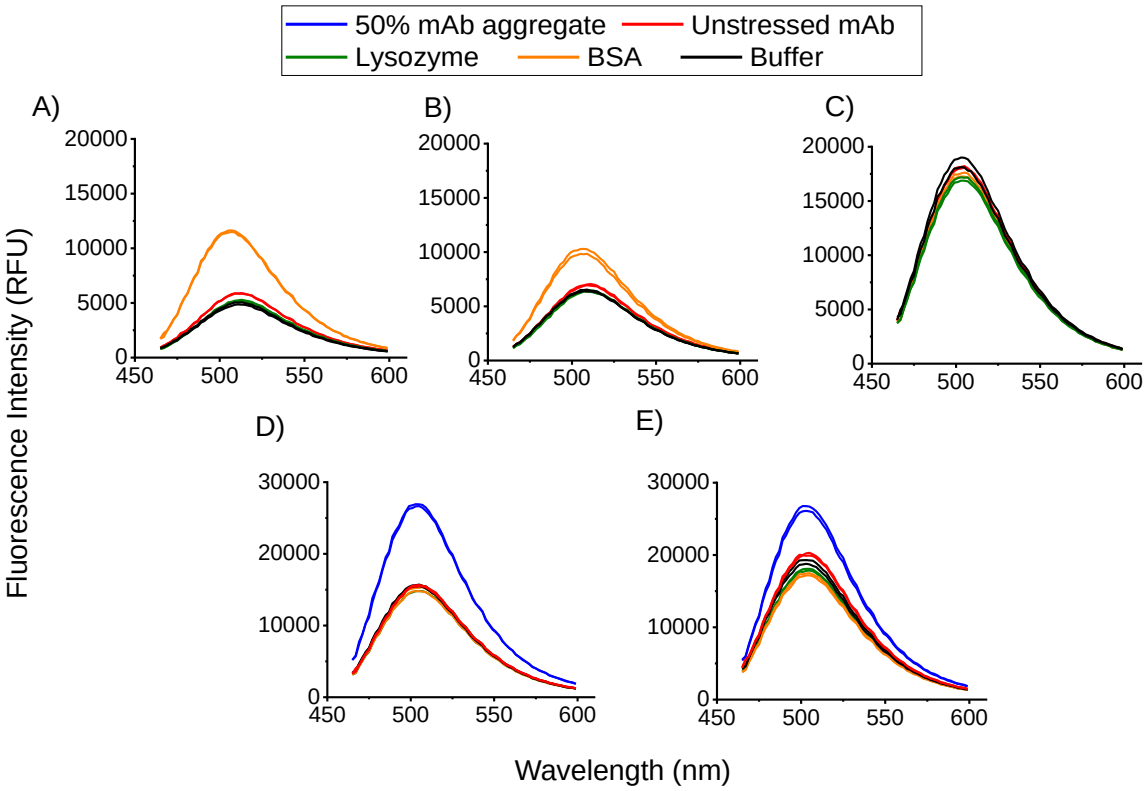

Figure 5-16: Fluorescence spectrum of affinity peptide-CCVJ (AP-CCVJ) with mAb and lysozyme with different percentages of Tween-20 in buffers.
50 µM AP-CCVJ was measured with unstressed mAb (r_h= 5.5 nm), BSA (r_h=3.8 nm) and lysozyme (unable to determine size accurately) with: (A) 0.05% Tween-20 PBS, (B) 0.1% Tween-20 PBS and (C) 1% Tween-20 PBS. 50 µM AP-CCVJ was measured with mAb aggregates with: (D) 0.5% Tween-20 PBS and (E) 1% Tween-20 PBS. Unstressed mAb (sodium acetate pH 5.5) buffer was thermally stressed (see Materials and Methods) to generate 7% (r_h= 7.5 nm) and 50% (r_h= 34 nm) mAb aggregate. MAb, lysozyme (PBS pH 7.4 buffer) and BSA (sodium chloride and sodium azide buffer) were measured at 1 mg/mL, 0.1 mg/mL and 0.45 mg/mL respectively. This was performed in duplicates. Excitation/Emission – 435/465-600 nm.

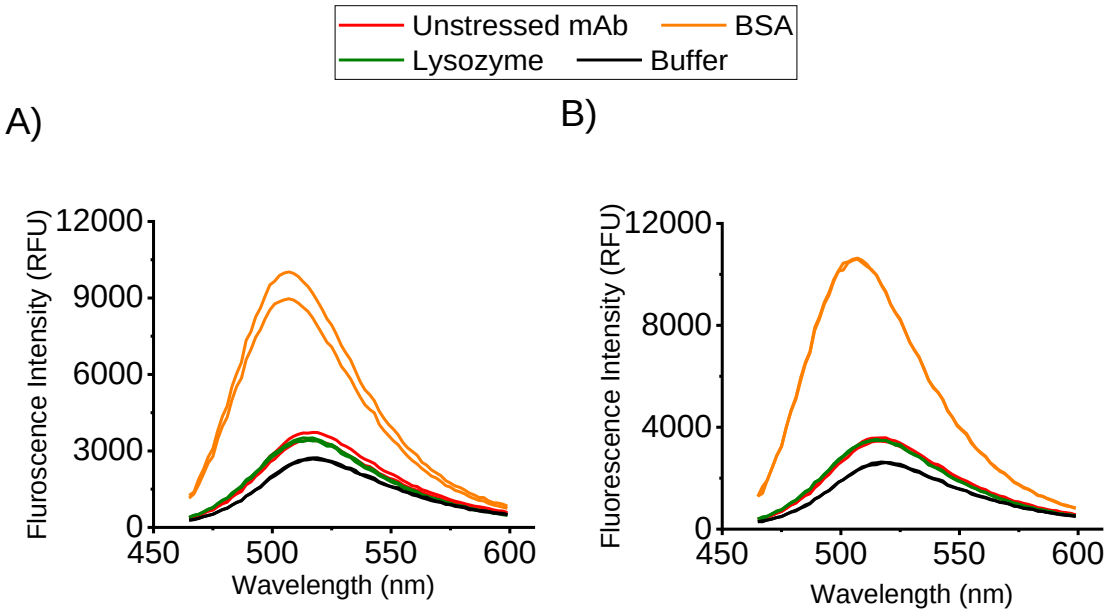

Figure 5-17: Fluorescence spectrum of affinity peptide-CCVJ (AP-CCVJ) with mAb, BSA and lysozyme.
(A) 0.4 M NaCl and (B) 0.8 M NaCl buffer. Unstressed mAb (sodium acetate pH 5.5 buffer), lysozyme (PBS pH 7.4 buffer) and BSA (sodium chloride and sodium azide buffer) were measured at 1 mg/mL, 0.1 mg/mL and 0.45 mg/mL respectively. This was performed in duplicates. Excitation/Emission – 435/465-600 nm.

5.6.3. pH sensitivity experiment of affinity peptide tagged with bright dyes

AP-TF2 and AP-FL were measured in 50 mM phosphate buffer at pH 3.30, 6.00 and 7.92 as shown in Figure 5-18 and Figure 5-19 respectively. In Figure 5-18, AP-FL showed an increase in fluorescence intensity with increasing pH. Between pH 3.30 - 6.00 and pH 6.00 - 7.92, there was a 73% and 71% increase in max peak fluorescence intensity. This made sense as fluorescein is pH sensitive, and at higher pH's when the molecule is in its deprotonated form, it is more fluorescent (Invitrogen, 2010). However, AP-FL could not distinguish between the stressed mAb, unstressed mAb and BSA across different pHs. This differed slightly from the trends in Figure 5-13 which may be due to the samples being in different buffer in Figure 5-13. AP-TF2 also could not distinguish between the stressed mAb, unstressed mAb and BSA across different pHs. Although, Tide Fluor 2 is advertised to be pH independent from pH 3-11 (AAT Bioquest, 2017), there was a slight decrease in the peak max intensities with increasing pH. From pH 3.30 - 6.00 and pH 6.00 - 7.92, there was a 7% and 17% decrease increase in the peak max respectively.

AP-TF2 and AP-FL did not distinguish between unstressed and stressed mAb at different pHs. The intensity of the fluorescence change depended on pH. From the initial experiment and the pH sensitivity, the AP-TF2 and AP-FL had not shown they could detect mAb aggregates, and the initial trend in results differed from the pH sensitivity experiment. However, the results may be due to the presence of excess unbound AP-dye skewing the results. As a wash step would be needed for these dyes based on their design, AP-TF2 and AP-FL needed to be tested in a way to confirm whether the AP-dye was binding to mAb aggregates specifically once excess unbound mAb/dye is removed.

To investigate this, SEC with UV and fluorescence detection was utilised to visualise which species/peaks the AP-dye was binding to. As SEC uses a running buffer, this could act as a "wash-step" to remove the unbound AP-dye/mAb whilst still allowing for fluorescence detection.

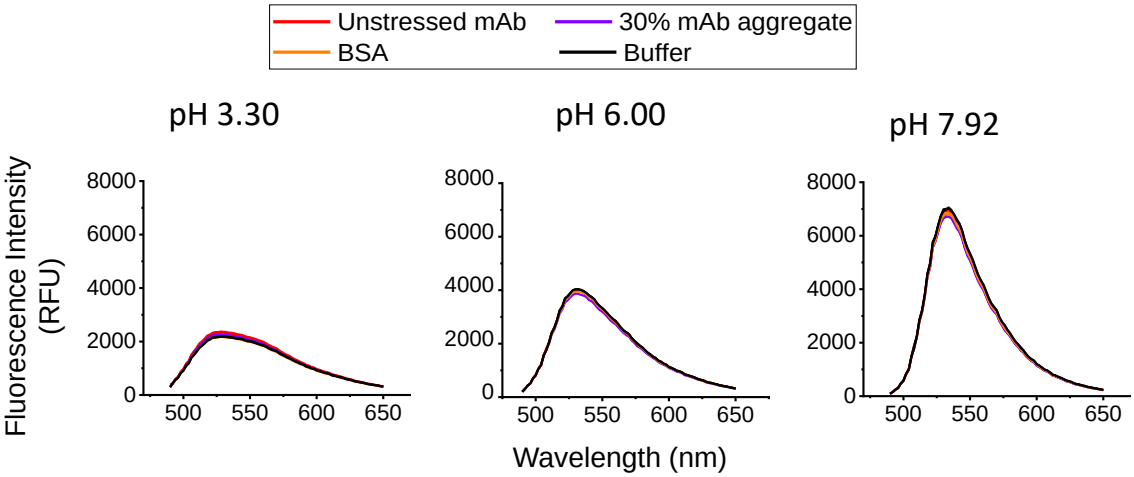

Figure 5-18: Fluorescence of affinity peptide-Fluorescein (AP-Fluorescein) with mAb and BSA at different pHs.
Measured with 50 µM AP-Fluorescein and 50 mM phosphate buffer at pH 3.30, 6.00 and 7.92. Unstressed mAb in sodium acetate pH 5.5 buffer and BSA in sodium chloride and sodium azide buffer. 30% mAb aggregates was obtained via thermal stressing mAb in sodium acetate buffer pH 5.5 (See Materials and Methods). Concentration of mAb and BSA in each well was 1 mg/mL and 0.45 mg/mL respectively. This was performed in duplicates. Excitation/Emission – 440/490-650 nm.

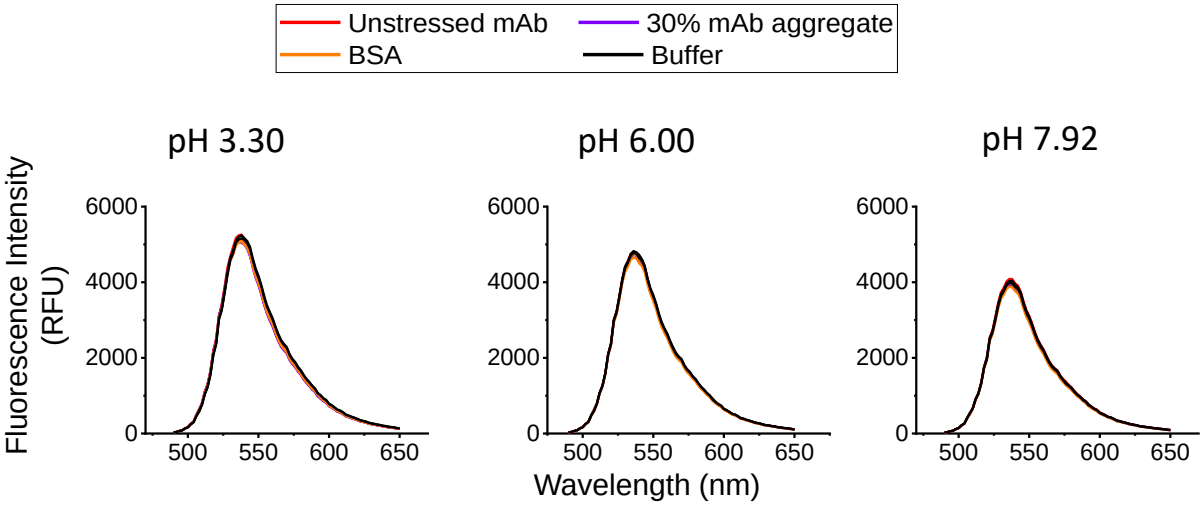

Figure 5-19: Fluorescence spectrum of affinity peptide-Tide Fluor 2 (AP-Tide Fluor 2) with mAb and BSA
Measured with 50 µM AP-Tide Fluor 2 and 50 mM phosphate buffer at pH 3.30, 6.00 and 7.92. Unstressed mAb in sodium acetate pH 5.5 buffer and BSA in sodium chloride and sodium azide buffer. 30% mAb aggregates was obtained via thermal stressing mAb in sodium acetate buffer pH 5.5 (See Materials and Methods). Concentration of mAb and BSA in each well was 1 mg/mL and 0.45 mg/mL respectively. This was performed in duplicates. Excitation/Emission - 440/490-650 nm.

5.6.4. Using SEC to understand the specificity of affinity peptides tagged to molecular rotor

The results so far showed that AP-CCVJ and AP-ThT were able to distinguish stressed mAbs from unstressed mAbs. However, AP-FL and AP-TF2 had not shown the ability to bind mAb aggregates specifically. To confirm whether AP-FL and AP-TF2 were able to bind and detect mAb aggregates, SEC with UV and fluorescence detection was utilised to visualise the binding by comparing the overlaps UV and fluorescence peaks similar to Chapter 4.6. An overlapping UV and fluorescence aggregate peak would confirm that a particular species was bound to the AP-dye. In addition, the SEC could give an idea of what type (large/small) of aggregate species that AP-dye binds to. From the pH sensitivity experiment (Section 5.6.1 and 5.6.3), most AP-dyes showed high fluorescence intensities between pH 6-8. Therefore, the

SEC buffer at pH 6.8 (which was used in previous SEC experiments) was used for this experiment.

The SEC chromatogram (Figure 5-20) showed that AP-CCVJ and AP-ThT bound to mAb aggregates stronger than the monomer. The fluorescence signal of the aggregate peak (at 5.5 min) was 29% and 55% higher than the monomer for AP-ThT and AP CCVJ respectively. The chromatograms did not distinguish what type of aggregates (large/small) that the AP-dyes bound to as there was only one fluorescence peak in both the aggregate and monomeric mAb range. Unbound and/or degraded forms of AP-CCVJ (Bachem confirmed that the conjugate had stability issues) eluted in the inclusion volume as shown by the peak between 11-15 mins. AP-ThT did not have this peak present in the SEC chromatogram.

Both AP-CCVJ and AP-ThT had low fluorescence intensity with BSA. The fluorescence of AP-ThT with BSA on SEC method compared to the plate reader experiments (Figure 5-15) correlated, since in both instances the fluorescence intensity of AP-ThT with BSA was low. In contrast, AP-CCVJ had higher fluorescence intensity with BSA in the plate reader experiments, but lower fluorescence with BSA using SEC. This implied that AP-CCVJ had higher interactions with BSA in the plate reader than SEC. One potential reason for this could be because in a plate reader, all the components are measured in the exact same concentrations as added to the system. Whereas on SEC, the components are diluted through the running buffer.

Overall, AP-ThT looked more promising than AP-CCVJ as the plate reader and SEC experiments correlated with each other. In addition, AP-CCVJ had degraded forms/unbound of the AP-dye which may reduce the yield of aggregates that could be measured and detected.

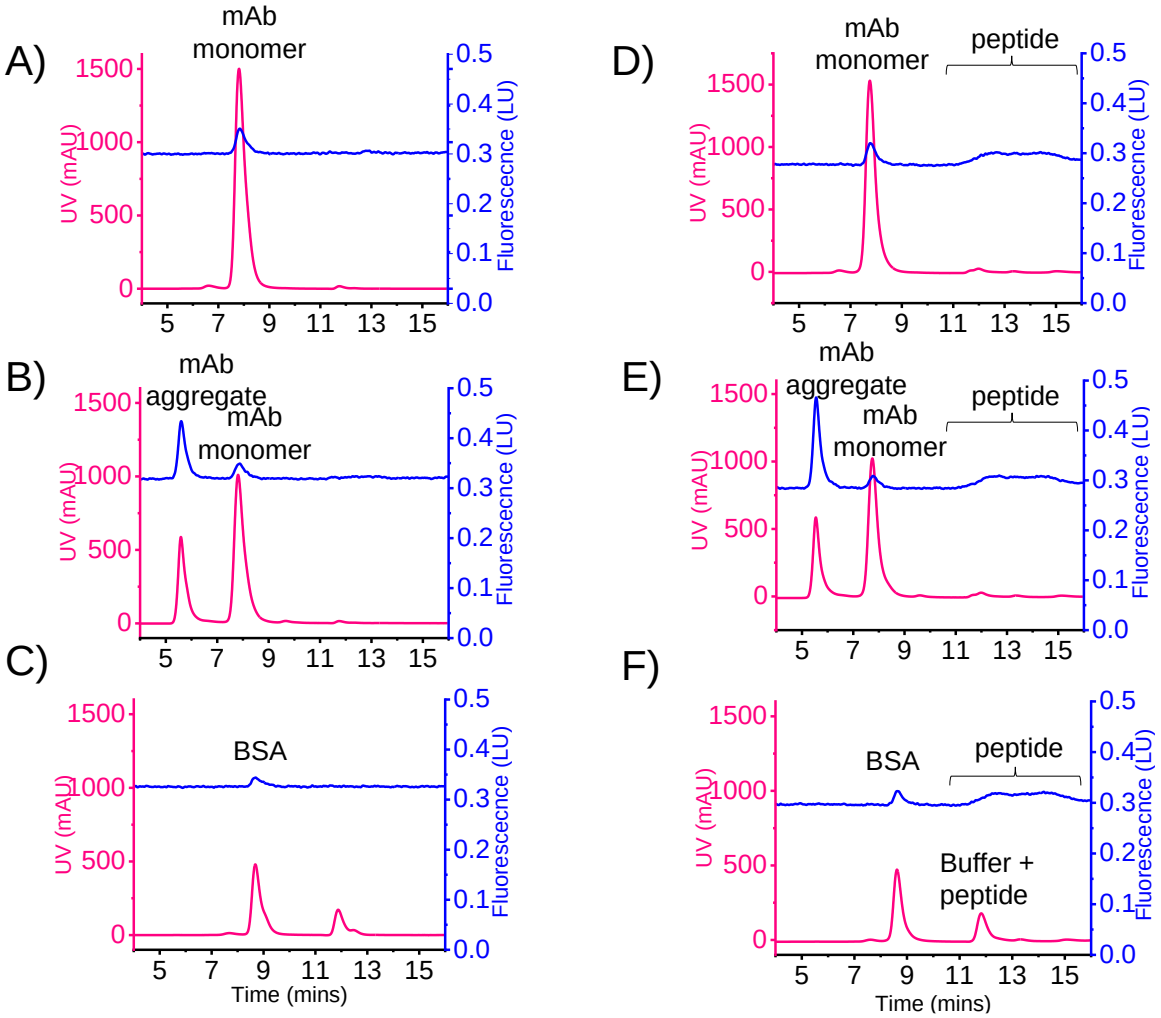

Figure 5-20: SEC with UV and fluorescence with affinity peptide-Thioflavin T (AP-ThT), AP-CCVJ, mAbs and BSA.
(A) AP-ThT with mAb monomer, (B) AP-ThT with 30% mAb aggregate, (C) AP-ThT with BSA, (D) AP-CCVJ with mAb monomer, (E) AP-CCVJ with 30% mAb aggregate and (F) AP-CCVJ with BSA. AP-ThT fluorescence measured at excitation/emission - 430/495 nm and AP-CCVJ - excitation/emission- 435/500 nm. The samples run on TSKgel2000SWI column (7.8x300mm) with a flow rate of 0.5 mL/min. The detector measured absorbance at 214 nm. Running buffer composed of 100 mM sodium phosphate (monobasic), 400 mM sodium chloride, pH 6.8.

5.6.5. Using SEC to understand the specificity of affinity peptides tagged with bright dyes

Figure 5-21 showed that both AP-FL and AP-TF2 did not bind to either monomeric mAb, aggregated mAb or BSA. The AP-dyes eluted in the inclusion volume of the column at very high fluorescence intensities (400X the intensity of AP-CCV/AP-ThT). This confirmed that the AP conjugated to Fluorescein and Tide Fluor 2 could not measure mAb aggregates.

As the non-aggregation related dyes did not work with the AP, the ability of the AP-CCVJ/AP-ThT was questioned as the results achieved so far may have been more influenced by the ThT/CCVJ dye than the AP. Therefore, it was important to identify whether the affinity of the AP-conjugate to mAb aggregates was due to the AP or the dye itself. To do this, the SEC chromatogram of the AP-dye was compared to the dye on its own as a control. Since AP-CCVJ had stability issues and required Tween-20 to reduce non-specific interactions, AP-ThT was a better conjugate to investigate with. Hence, only AP-ThT was compared to ThT in the next section.

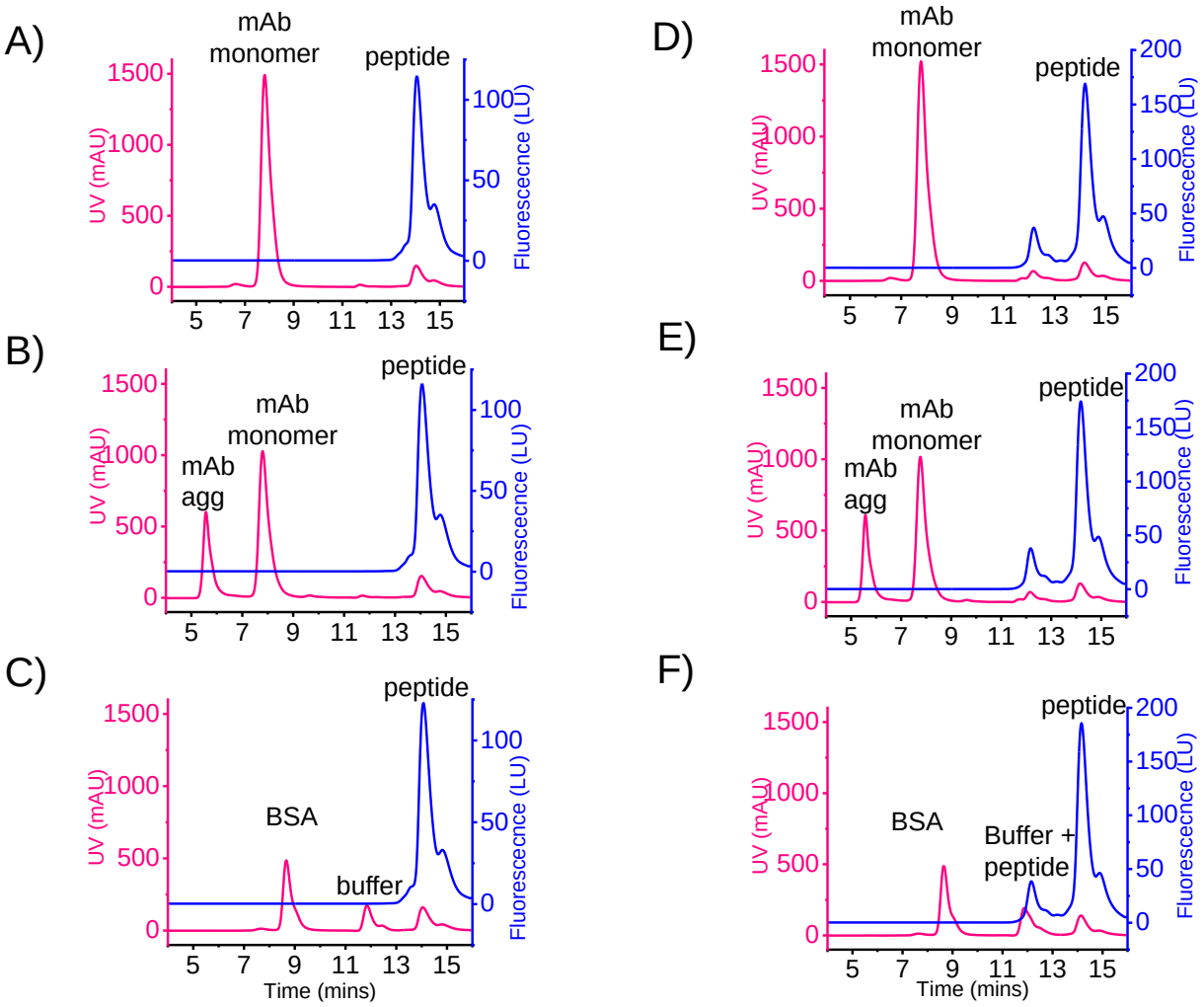

Figure 5-21: SEC with UV and fluorescence with affinity peptide-Tide Fluor 2 (AP-Tide Fluor 2), affinity peptide-Fluorescein (AP-Fluorescein), mAbs and BSA.
(A) AP-Tide Fluor 2 with mAb monomer, (B) AP-Tide Fluor 2 with 30% mAb aggregate, (C) AP-Tide Fluor 2 with BSA, (D) AP-Fluorescein with mAb monomer, (E) AP-Fluorescein with 30% mAb aggregate and (F) AP-Fluorescein with BSA. AP-Tide Fluor 2 fluorescence measured at excitation/emission- 440/535 nm and AP-Fluorescein - excitation/emission- 440/530 nm. The samples run on TSKgel2000SWI column (7.8x300mm) with a flow rate of 0.5 mL/min. The detector measured absorbance at 214 nm. Running buffer composed of 100 mM sodium phosphate (monobasic), 400 mM sodium chloride, pH 6.8.

5.6.6. Using SEC to study dye only (ThT) behaviour with mAb aggregates

In an ideal situation, the SEC chromatogram for AP-ThT would have a higher fluorescence intensity for mAb aggregate peak compared to the ThT alone chromatogram. However, comparing SEC chromatograms of AP-ThT (Figure 5-20B) and ThT alone (Figure 5-22B), there were similar fluorescence intensities for mAb monomer, mAb aggregate and BSA. Although this was not surprising as ThT even on its own can bind aggregates as shown in Chapter 4, the problem was that it was not possible to see the added specificity upon introducing the AP to the system. To see whether the affinities between AP-ThT and ThT were similar to aggregated non-mAb species, another SEC control experiment was conducted using RNase A. RNase A was chosen as it was a stable molecule to compare to BSA which is known to dimerise even without stressing. The SEC chromatogram of AP-ThT and ThT alone with monomeric and aggregated forms of RNase A (Figure 5-23) showed that neither AP-ThT nor ThT interacted with monomer or aggregated RNase A. The peak at 30 mins corresponded to the unbound AP-ThT (Figure 5-23A and Figure 5-23C) eluting the column in the void volume as it did not bind to any protein. This peak could not be seen with ThT (Figure 5-23B and Figure 5-23D) as the dye was too small.

Overall, the SEC results had not shown improved specificity of the dyes to mAb aggregates with the addition of the affinity peptide. The AP-dyes that worked well upon initial assessment was mostly due to the aggregation-based dyes (ThT and CCVJ) working on their own to detect aggregates. One reasoning as to why the AP may not have bound to mAbs could be due to the placement of the dye on the AP. The dyes may have been blocking the binding site or causing steric hindrance. Another reason could have been that the nature of the conjugation may have damaged the binding site of mAbs to AP.

To investigate into the binding affinity of the AP-dye to mAb aggregates, the equilibrium dissociation constant (K_d) was measured to quantify binding. In addition, hydrogen deuterium exchange (HDX) was conducted to provide information on binding such as location. For protein-ligand complexes, HDX measured with the protein alone is compared to that the HDX measured with both protein and ligand.

HDX measures the rate of hydrogen-to-deuterium exchange and can provide information on solvent accessibility, protein structure and conformation. This will be further discussed in the next section.

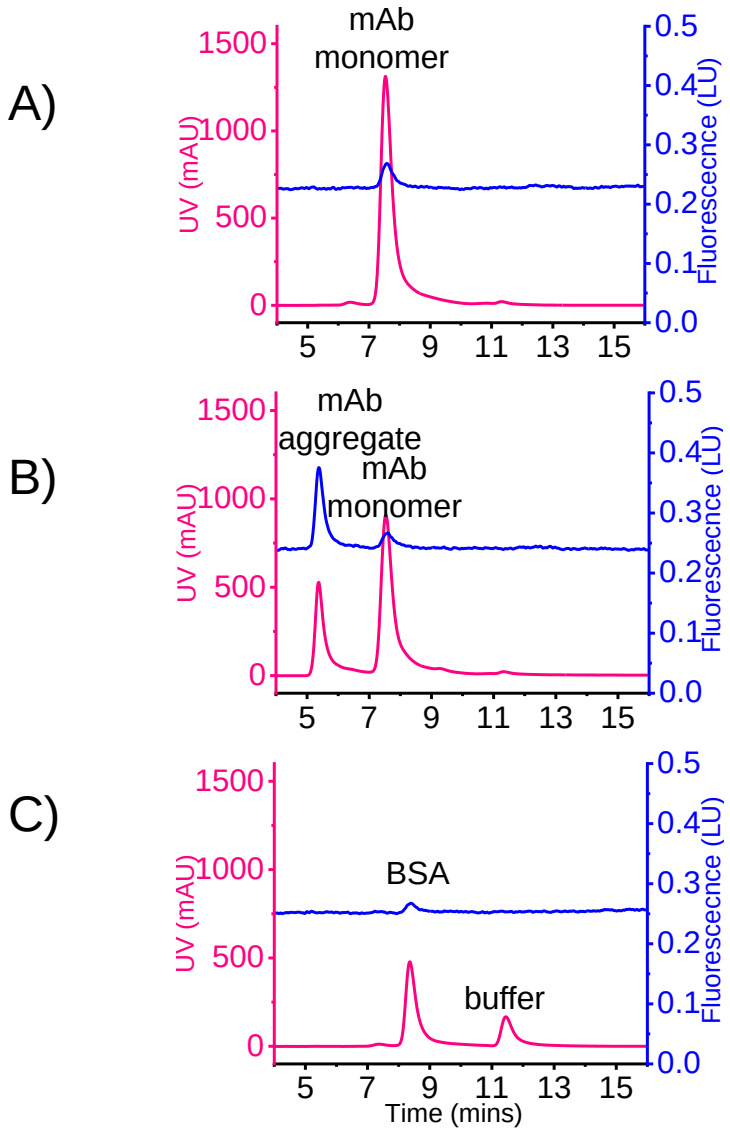

Figure 5-22: SEC with UV and fluorescence with Thioflavin T (ThT) with mAbs and BSA.
(A) ThT with mAb monomer, (B) ThT with 30% mAb aggregate, (C) ThT with BSA. ThT fluorescence was measured at excitation/emission -430/495 nm. The samples run on TSKgel2000SWI column (7.8x300mm) with a flow rate of 0.5 mL/min. The detector measured absorbance at 214 nm. Running buffer composed of 100 mM sodium phosphate (monobasic), 400 mM sodium chloride, pH 6.8.

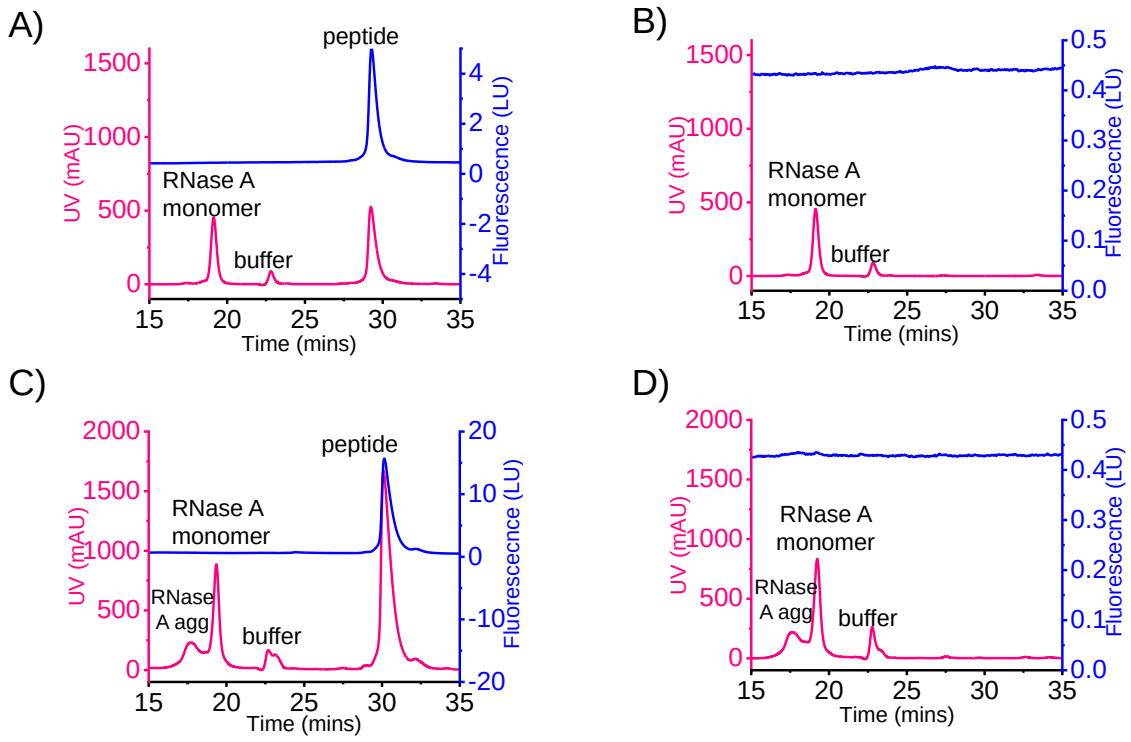

Figure 5-23: SEC with UV and fluorescence measuring affinity peptide-Thioflavin (AP-ThT), ThT and RNase A.
(A) 50 µM AP-ThT with 0.1 mg/mL RNase A monomer, (B) 200 µM AP-ThT with 0.4 mg/mL RNase A aggregate, (C) 50 µM ThT with 0.1 mg/mL RNase A monomer and (D) 200 µM ThT with 0.4 mg/mL RNase A aggregate. RNase A aggregate sample was 40% after stressing 0.6 mg/mL for 5 days at 60°C. Injection volume 100 µL. Fluorescence was measured at excitation/emission – 430/495 nm. The samples were run on TSKgel3000SWI column (7.8x300mm) with a flow rate of 0.1 mL/min. The detector measured absorbance at 214 nm. Running buffer composed of 100 mM sodium phosphate (monobasic), 400 mM sodium chloride, 0.5% n-propanol, pH 6.8. (Note: the maximum injection volume of the system was 100 µL however, with the RNase A aggregates the signal was weak therefore to improve the intensity the concentration of the dye and the RNase A was increased but the ratio (7 µM dye:1 µM RNase A) were kept the same).

5.5.7. Measurement of dissociation constant of AP-ThT

Binding affinity is typically measured and reported using the equilibrium dissociation constant (K_d), which measures the propensity for complexes to separate. The K_d (units= mol/L) describes interactions at equilibrium between the rate constant of association (k_{on}) and the rate constant of dissociation (k_{off}). The stronger the affinity/binding between complexes, the smaller the K_d. Equation 5-1 shows the equation for K_d based on a bimolecular reaction. To measure the K_d between AP-ThT and mAbs, a bimolecular interaction was assumed for simplicity.

The K_d experiment for AP-ThT was conducted in two parts. The first part was to identify the concentration of AP-ThT which would provide a robust fluorescence above the noise of the instrument, but not in excess of the molecule. This was to promote 1:1 binding between the AP-ThT and mAb and reduce the amount of background fluorescence from excess AP-ThT. After fixing the concentration of AP-ThT, monomeric and aggregated mAb were measured at increasing concentrations. This was to generate a binding curve measuring the change in fluorescence intensity with increasing concentration of mAb.

$$K_d = \frac{[A][B]}{[AB]}$$

Equation 5-1: Equilibrium dissociation constant for a bimolecular reaction, A+B ↔ AB

Figure 5-24 shows the fluorescence of AP-ThT at different concentrations without mAb. At concentrations below 0.4 µM of AP-ThT, the fluorescence intensities were almost inseparable due to being within the noise of the instrument. 0.08 µM AP-ThT had slightly higher fluorescence intensity but had a lower peak fluorescence wavelength (10 nm lower) than all the concentrations. Therefore, the lowest concentration that was most comparable to the fluorescence at 50 µM was 2 µM. For the second part of the K_d, the concentration of AP-ThT was fixed at 2 µM AP-ThT.

To measure the K_d, the fluorescence from 2 µM of AP-ThT with increasing concentrations of monomeric and 30% aggregated mAb was measured. 30%

aggregated mAb saw higher fluorescence intensities than the monomer from 1 mg/mL (7400 nM) onwards (Figure 5-25A) which was expected. The aggregate plot plateaus higher than the monomeric mAb (around 47000 nM =7.2 mg/mL).

However, despite the difference in fluorescence intensities between the monomer mAb and 30% aggregated mAb at different concentrations, the gradient/slopes of the two curves looked similar. Normalising fluorescence intensity and accounting for the buffer blank, showed that the monomer mAb and 30% aggregated mAb slopes actually overlapped in the linear region (Figure 5-25B). This overlap meant that at 2 µM of AP-ThT, both monomeric and 30% aggregated mAb had the same rate of increase in fluorescence intensity with increasing mAb concentration, despite the differences in actual fluorescence intensity units.

As the affinity between monomeric mAb and aggregated could not be distinguished at 2 µM, this suggested that the value of K_d was most likely below 2 µM. To confirm this one would need to be able to measure the affinity at AP-ThT concentrations lower than 2 µM. However, this was not possible to carry due to instrument limitations (below 2 µM would be within the noise of the instrument). As the affinity between the monomeric and aggregated mAb was similar (upon normalising) but the fluorescence intensities differed greatly, this may suggest that ThT was fluorescing irrespectively of AP capabilities of binding to mAb.

Hydrogen deuterium exchange

Hydrogen deuterium exchange (HDX) was also carried out on the AP with monomeric and aggregated mAb as an alternative way to understand the affinity. HDX measures the rate of hydrogen-to-deuterium exchange and can provide information on solvent accessibility, protein structure and conformation. The experiment was carried out by an HDX expert at GlaxoSmithKline. Certain mAb residues on the heavy chain saw deprotection higher than the random fluctuation percentage (>5%), which would indicate increased flexibility or partial denaturation in that area. This area may have indicated a potential binding region, but as the time-course results were not consistent (deuterium incorporation did not increase in line

with labelling time), the data was too unreliable. Statistical significance was also assessed using volcano plots, and the data was found to be largely random. In addition, the level of protection with the mAb aggregate+peptide sample compared to the mAb aggregate+ThT sample was similar. Overall, protection was generally too weak and widely distributed to be called an epitope, hence the mAb residues identified in heavy chain may be an artefact rather than an actual effect.

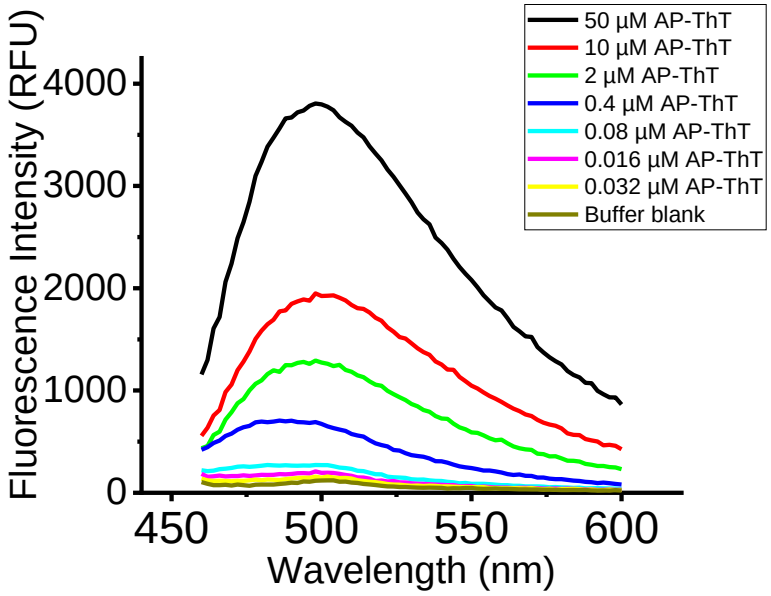

Figure 5-24: Fluorescence of affinity peptide Thioflavin T (AP-ThT) at different concentrations to determine the lowest detectable concentration of the AP-ThT to use for K_d experiments.
A range of concentrations (0.032 – 50 µM) of AP-ThT were measured in buffer in order to find the lowest concentration above the noise of the instrument to measure K_d. No mAb was present in the sample.

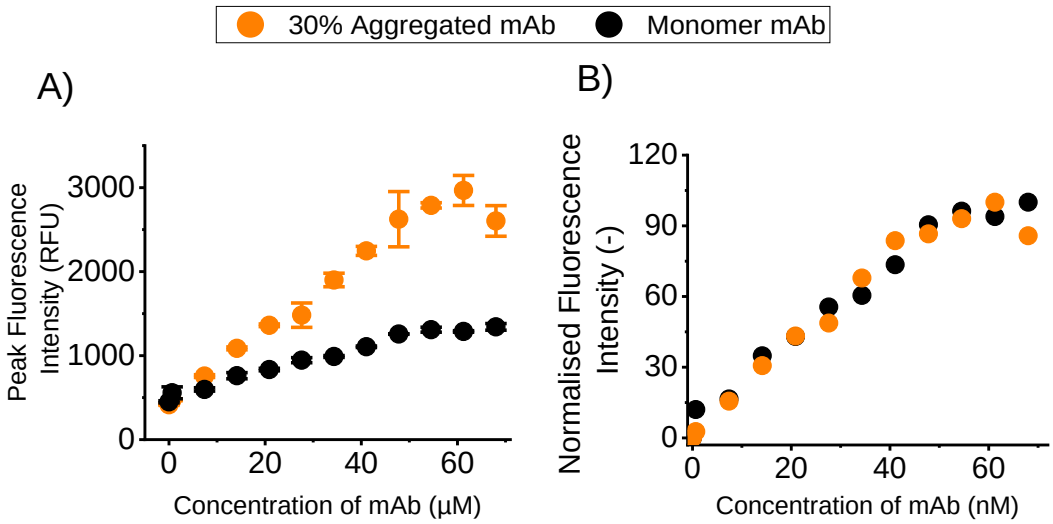

Figure 5-25: Measured and normalised fluorescence intensity of 2 µM AP-ThT with increasing mAb concentration.
(A) Raw fluorescence intensity values, (B) Normalised values (using highest fluorescence intensity and blank subtraction). Concentration of mAb was measured between 0.1 – 10.2 mg/mL with unstressed mAb and 30% aggregated mAb.

5.7. Conclusion

The biotin-AP was tested against monomeric and aggregated mAb using both Octet and Biacore systems. The Octet assay was not able to distinguish between 50% and 7% aggregated mAb. In addition, the biotin-AP had non-specific interactions with BSA that did not reduce with the addition of Tween-20 to the buffer. The Biacore assay also did not show much promise as the blank subtracted response values were weak due to the non-specific binding of mAb to the streptavidin sensor. This interaction of mAb to streptavidin chip also made it not possible to use Biacore to calculate K_d.

AP-CCVJ and AP-ThT (above pH 6) were able to distinguish aggregated mAb from monomeric mAb. However, AP-CCVJ showed non-specific interaction with BSA which was eventually resolved with the use of Tween-20. AP-FL and AP-TF2 did not show capability of binding to mAb aggregates and this was confirmed using SEC. SEC also showed that AP-ThT and ThT dye achieved the same level of binding towards mAb aggregates. Hence, there was no indicator that the addition of the

affinity peptide provided improved specificity of the dye towards mAb aggregate. It was thought that steric hindrance from the dye may be blocking the binding site of the AP towards the mAb aggregate. However, HDX was not able to identify a binding site between the peptide on its own and mAb aggregate. Therefore, more investigation would be needed into the binding kinetics and mechanism of the affinity peptide to understand how the results seen in the original study were achieved. Once, that is identified, the affinity can be redesigned appropriately to ensure the binding is not compromised by the addition of a label.

6 Fluorescence resonance energy transfer to measure protein aggregates

6.1. Chapter Aims

The fluorescent dye assay described in Chapter 4 evaluated the capabilities of fluorescent dyes to measure mAb aggregates in cell culture supernatants. The findings from that chapter were that fluorescent dyes on their own were not specific indicators of mAb aggregation in cell culture medium. Chapter 5 assessed one approach at redesigning the dye assay to increase specificity by incorporating peptides with affinity to bind mAb aggregates specifically. Despite initial promising results, there was lack of evidence to show whether the affinity peptide as designed provided additional specificity to mAb aggregates. Hence, further understanding of how the peptide worked would be required.

The second approach to redesigning the dye assay to increase specificity was to increase the complexity of the assay by introducing a second fluorophore that would be conjugated to a protein that specifically binds mAbs. The distance dependent interactions between the two fluorophores can be measured by the fluorescence technique known as Fluorescence Resonance Energy Transfer (FRET). As FRET can offer more sensitivity to the assay, it was also important to understand the assay set-up and the biophysical characteristics of FRET. This chapter will focus on the use of FRET to improve the specificity of dyes in measuring antibody aggregates in cell culture medium. The chapter will cover the following areas:

1. The design of the FRET assay to have specificity for mAb aggregates and outline reasons to choosing donors and acceptors.

2. Comparison of the FRET assay with unstressed and stressed mAb in various spectrofluorometer systems and quantifying energy transfer

3. Describe the troubleshooting methodology towards understanding reasons behind weak energy transfer in relation to the theoretical considerations required for FRET.

4. Conduct control experiments to further biophysical understanding of the FRET system and identify which theoretical aspect may be responsible for the weak energy transfer.

6.2. Designing a FRET based assay to measure antibody aggregates

6.2.1. Introduction

To adapt the fluorescent dye assay to be more specific to mAb aggregates, one approach was to use two fluorophores. The two fluorophores would work by coming together in the presence of a mAb aggregates, producing a change in a fluorescence signal. The technique that can measure the interactions between two fluorophores is Fluorescence Resonance Energy Transfer (FRET). FRET is the transfer of energy from the excited state of a fluorophore called a donor, to a second fluorophore in close proximity called an acceptor. Figure 6-1 shows the adapted Jablonski diagram to account for energy transfer from the donor to the acceptor. The donor transfers non-radiative (without the release of photons) energy to excite the acceptor. The excited acceptor eventually relaxes by fluorescing which in this case is known as a sensitised emission.

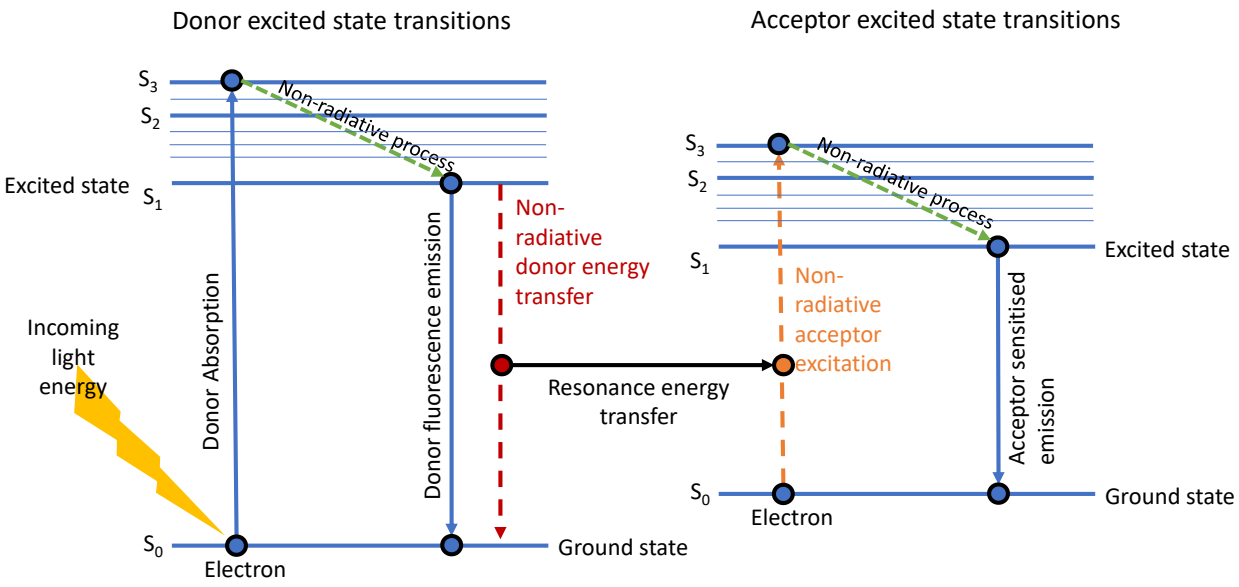

Figure 6-1: Modified Jablonski diagram for Fluorescence Resonance Energy Transfer.
The first step is the absorbance of a photon from a light source which cause electrons to become excited from a lower energy to a higher energy level. Energy first dissipates by non-radiative processes such as vibrational relaxation/internal conversion and is then released as donor fluorescence. In addition to fluorescence, non-radiative energy is transferred to the acceptor which becomes excited and eventually releases a fluorescence emission (sensitised emission). S depicts energy/electronic levels.

6.2.2. Theoretical considerations for FRET

The most common application of FRET is measuring distances between two sites on a molecule. The amount of energy transferred between the two fluorophores (donor and acceptor) on a molecule is indicative of the distance between the two sites. High energy transfer indicates a close distance between the donor-acceptor, whereas a lower energy transfer indicates the donor and acceptor are further away. It is due to this distance relationship that FRET is often referred to as a molecular or "spectroscopic ruler".

Normally, fluorescence involves a photon exciting a molecule to an excited state. However, in the case of FRET, the energy transfer relies on long range dipole-dipole interactions between the donor and the acceptor rather than a photon. The theory of

energy transfer is based on the concept of a fluorophore considered as an oscillating dipole, which can exchange energy with another dipole with a similar resonance frequency (Lakowicz, 2010).

The rate and intensity of energy transfer is governed by these four components:

1) The distance between the donor and the acceptor molecule,
2) Extent of spectral overlap between the donor's emission spectrum and the acceptor's excitation spectrum,
3) The quantum yield of the donor,
4) The relative orientation of the donor and acceptor transition dipoles.

Distance:

Distance plays a vital role in FRET as efficiency of energy transfer (E) varies inversely with the sixth power of distance between the donor and acceptor (r) (Equation 6-1). The distance can be quantified using Förster radius (R_0) (Equation 6-2), which is the distance between the donor and the acceptor at which efficiency of energy transfer is 50%. For studies of biological macromolecules, Förster distance typically ranges from 20 to 90 Å (Lakowicz, 2010) as illustrated in Figure 6-2. R_0 is a function of quantum yield of the donor chromophore (ΦD), overlap integral of the donor emission and acceptor excitation spectrum (J), orientation of the donor and acceptor transition dipoles (κ^2), and the refractive index of the medium (n). A long R_0 can cause high FRET efficiency; therefore, if the conditions used affect the donor-acceptor distance, this will affect the energy transfer rate.

$$E = \frac{1}{1 + \left(\frac{r}{R_o}\right)^6}$$

Equation 6-1: Efficiency of energy transfer

$$R_o = 0.211 \sqrt[6]{\frac{\kappa^2 \Phi D J}{n^4}}$$

Equation 6-2: Förster radius

Spectral Overlap

Another FRET requirement is that there needs to be an overlap between the donor's emission and the acceptor's excitation spectrum. A sufficient overlap (>30%) (Bajar et al., 2016, Sun et al., 2013) is critical for FRET to occur, therefore, correct selection of FRET pairs is important. Usually, fluorophores are chosen such that donors emit at shorter wavelengths and acceptors emit at longer wavelengths. However, there are two possible scenarios whereby the acceptor fluorescence emission can be contaminated by the donor. The sources of contamination are cross-talk and bleed-through. An overlap in the excitation spectra of the donor and acceptor can cause the acceptor to be excited directly by the donor's excitation light. This contamination is known as cross-talk (Ma et al., 2014). If there is an overlap of the donor and acceptor fluorescence emission, this would cause the donor fluorophore to be detected within the range of the acceptor's emission (bleed-through). Therefore, it is important to be aware of the spectral overlap, as well as the full excitation and emission spectrum when choosing a suitable donor and acceptor. Even still, though spectral overlap is important for FRET, it usually assumes 100% energy transfer which is not true in reality. Therefore, one must bear in mind other FRET parameters in conjunction when designing a FRET assay.

Quantum Yield

The quantum yield is the ratio of the number of photons emitted to the number of photons absorbed. It is a measure of the brightness of the dye, with brighter dyes observing larger quantum yields. Quantum yield is usually provided by the manufacturer, or it can be determined experimentally by comparing absorbance/fluorescence values against a reference/standard fluorophore. The donor

fluorophore must ideally have a high quantum yield to have enough energy to transfer to the acceptor.

Relative orientation

Relative orientation of the donor (κ^2) and acceptor can range from 0 to 4. The value corresponds to the following states of orientation:

- $\kappa^2 = 4$ for head-to-tail parallel transition dipoles,
- $\kappa^2 = 0$ for perpendicular dipoles (no energy transfer).

In principle, an unfavourable orientation of the donors and acceptors can prevent energy transfer between a FRET pair, but such a result is rare. Therefore, it is usually assumed that FRET will occur if the spectral properties are suitable, and the D–A distance is comparable to R_0. κ^2 is also extremely difficult to measure experimentally, therefore is generally assumed. In biological systems proteins labelled with fluorophores can adopt a variety of conformations. Thus, for most macromolecular interactions in solutions $\kappa^2=2/3$ is often assumed for randomised orientation.

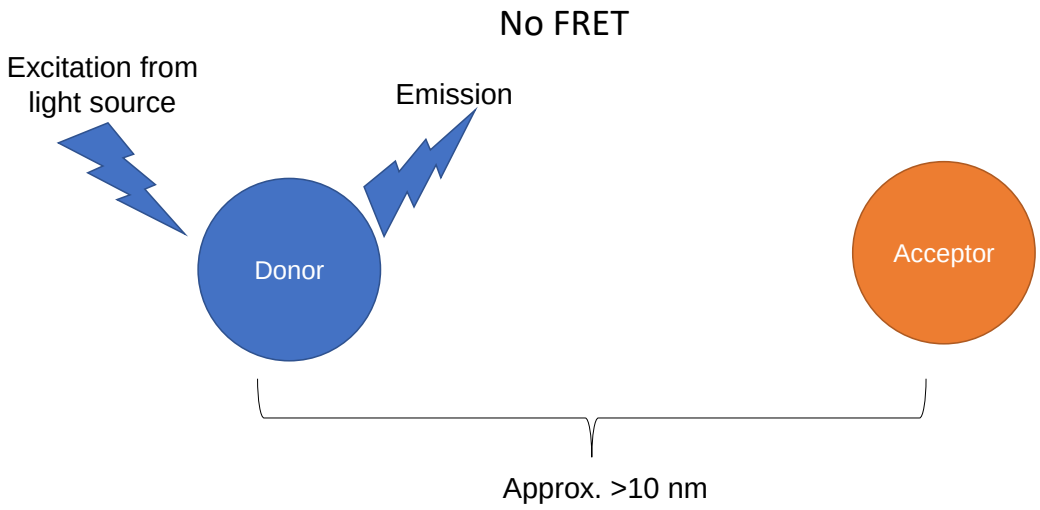

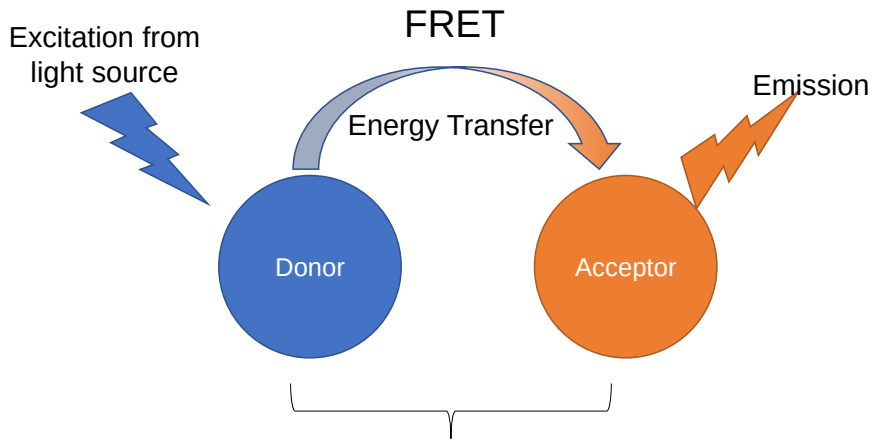

Distance can be calculated based on the Förster radius equation:

$$R_o = 0.211 \sqrt[6]{\frac{\kappa^2 \Phi D J}{n^4}}$$

Figure 6-2: Distance dependent nature of FRET.
When the donor and acceptor are at a distance shorter than 10 nm (20-90 Å), the acceptor can receive the energy emitted from the donor. At distances, greater than 10 nm, the efficiency of energy transfer decreases and becomes more difficult. R_0 is a function of quantum yield of the donor chromophore (ΦD), overlap integral of the donor emission and acceptor excitation spectrum (J), orientation of the donor and acceptor transition dipoles (κ^2), and the refractive index of the medium (n).

6.2.3. FRET based antibody aggregate assay design

Figure 6-3 illustrates the mechanism of the FRET assay design. To increase the specificity of the assay, protein A is used which can binds Fc regions of mAbs specifically via 5 IgG-binding sites. Conjugating a fluorophore (donor) to protein A will "capture" mAbs, but not distinguish between monomeric or aggregated mAbs. Therefore, the protein A-donor complex would need to transfer energy to an acceptor which only fluoresces in the presence of aggregated mAbs. This would enable the use of the fluorescent dyes used in Chapter 4 which have shown specificity to aggregated protein. Overall, the donor and acceptor would only come together in the presence of mAb aggregates, using the high specificity of protein A to mAbs and the "aggregation-fluorophores" to aggregates. The full mechanism of the FRET assay would work theoretically as follows:

1) Presence of monomeric mAb: the conjugated protein A-donor binds to monomeric mAbs by the Fc region. Due to the absence of aggregated mAb, the acceptor would be too far away to receive energy transfer from the donor. The acceptor will therefore not be excited and there would be little acceptor fluorescence emission.

2) Presence of aggregated mAb: the conjugated protein A-donor would bind to aggregated mAb by binding to the Fc region. The acceptor would be drawn closer to the mAb aggregate. As both donor and acceptor would be close together, donor would be able to transfer energy to excite the acceptor resulting in an increase in acceptor fluorescence emission.

One assumption for the FRET assay was that there would need to be free Fc on the mAb aggregate in order to bind to protein A. This may also be a limitation as the assay may not measure all the aggregates present in the sample (e.g. if there are mAbs aggregated by the Fc region).

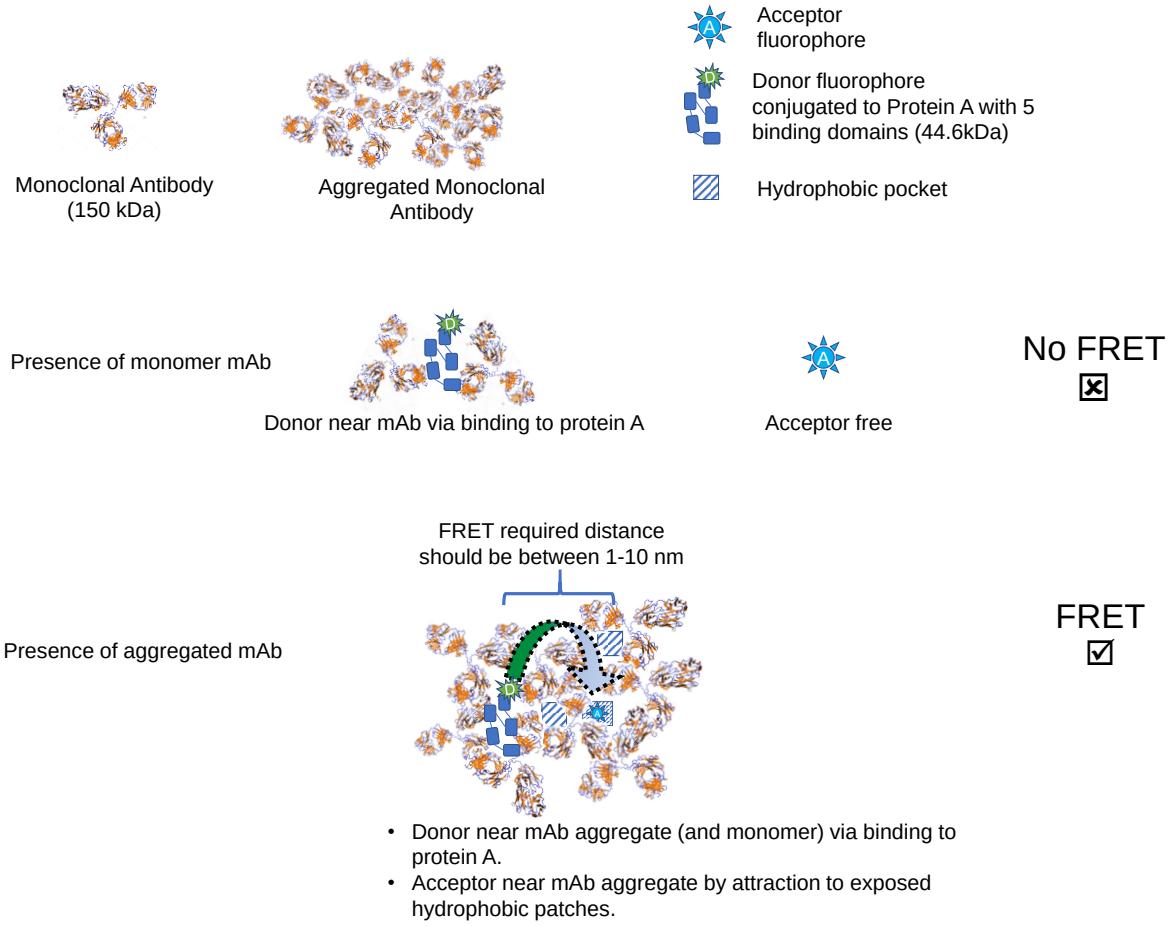

Figure 6-3: Designed FRET assay to measure mAb aggregates.
Donor is conjugated to Protein A which binds mAbs specifically. Acceptor is a dye known to measure protein aggregation. When monomeric mAb is present, the donor and acceptor should be too far away to transfer energy. Aggregated mAb draws the donor and acceptor closer together to enable energy (FRET) transfer from donor to acceptor. Protein A consists of five binding-proteins domains which is illustrated in the figure. Location of donor does not represent the actual conjugation site on to the protein A.

6.2.4. Which donor and acceptor to use for FRET assay

The donor and acceptors were chosen considering the theoretical considerations listed in Section 6.2.2. In addition, fluorophores were chosen that solubilised in water (to minimise buffer effects). The donor fluorophore also needed to be available in a reactive form to conjugate to protein A, and the acceptor fluorophore had to be capable of detecting protein aggregates.

For the acceptors, SYPRO Orange and ProteoStat were chosen as they worked well in the dye experiments in Chapter 4. SYPRO Orange and ProteoStat detect aggregates via different mechanisms (hydrophobic vs. molecular rotor), so there was an interest to see which dye mechanism worked better for FRET. Alternative acceptor dyes that measure aggregation are: Nile Red, Congo Red, ThT and DCVJ/CCVJ. Nile Red, Congo Red and DCVJ/CCVJ were only soluble in organic solvents. Although ThT was soluble in water, it has a low excitation maximum (around 350 nm), which would require a donor fluorophore to have an excitation/emission spectrum <300 nm range which was not possible.

Both SYPRO Orange and ProteoStat had excitation spectra around 400-600 nm, meaning that the donor fluorophore would need an overlapping emission spectrum in that range. Figure 6-4 shows the list of potential donors that could be used with SYPRO Orange/ProteoStat. However, other characteristics that were needed made the choice limited to Alexa Fluor 350. Alexa Fluor 350 was the only suitable donor that achieved the following criteria: had an overlapping emission spectrum from 400-600 nm, was from a family of dyes known to be very bright and was available in a reactive form (NHS ester) suitable for conjugation. Calculating the overlap using online spectral data from Thermo Fisher Scientific resulted in a 47% and 41% (see Section 5.8) for Alexa Fluor 350-SYPRO Orange and Alexa Fluor 350-ProteoStat respectively.

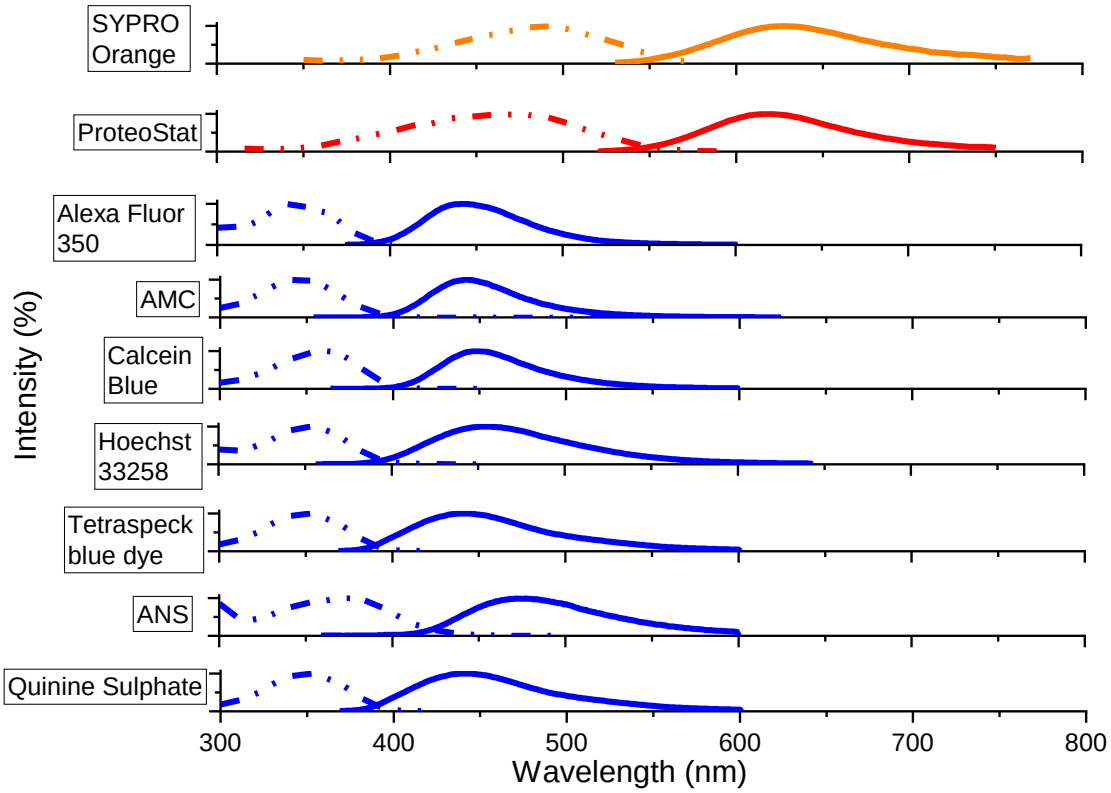

Figure 6-4: Excitation and emission spectra on list of potential donor dyes for SYPRO Orange and ProteoStat.
Dotted is excitation spectrum, bold is emission spectrum. Excitation and emission data for Alexa Fluor 350, AMC, Calcein Blue, Hoechst 33258, Tetraspeck blue dye and ANS were obtained from the ThermoFisher Spectra Viewer application. Quinine Sulphate data was obtained from UV-Vis-IR spectral analysis software (a|e) (FluorTools, 2015). Excitation and emission spectra for 5X SYPRO Orange and 3 µM ProteoStat were measured and smoothed.

6.2.5. FRET quantification techniques

There are four approaches to quantifying FRET which involve measuring the: (a) change in fluorescence emission intensity of the donor, (b) change in the sensitised fluorescence emission intensity of the acceptor, (c) decrease in the donor life-time and (d) change of fluorescence polarisation (Ma et al., 2014). (a) involves the acceptor acting as a quencher and thus decreases (presence of acceptor) or increases (absence of acceptor) in donor fluorescence can be quantified. The increase in fluorescence emission intensity (b) of the acceptor (sensitised emission) is one of the simplest ways

to measure FRET when the donor and acceptor emissions can be cleanly separated. Changes in donor fluorescence life-time (c) looks at the exponential decay of fluorescence emissions. Finally, fluorescence anisotropy (d) can be used to excite fluorophores with dipole moments similar to the plane of the polarised light (Ma et al., 2014). Of these four techniques, measuring the change in the sensitised fluorescence emission intensity of the acceptor was chosen as it looked at the impact of the decrease in the donor intensity to the increase in acceptor intensity, and it was easy to measure using a conventional plate reader.

Bajar et al. (2016) outlined three different ways to measure the change in the sensitised fluorescence: N_{FRET}, FR and ratiometric FRET. N_{FRET} and FR correct FRET signals for spectral cross talk, whereas ratiometric FRET uses the ratio between the uncorrected FRET signals. However, ratiometric FRET method had the advantage of being more sensitive to small changes in FRET. Therefore, ratiometric FRET was chosen as the quantifying method to monitor relative changes in FRET efficiency. When the FRET assay is more developed, it would be it would be better to correct for spectral cross talk for a more accurate quantification.

The "relative" FRET efficiency, also known as the proximity ratio (E_{PR}) can be determined from the measured intensities (I) of the donor (D) and the acceptor (A) as shown in Equation 6-3 (McCann et al., 2010). The value of the E_{PR} increases with efficient energy transfer ranging from 0 to 1, with larger values attributing to a donor-acceptor pair with high amounts of energy transfer. For simplicity in data analysis, the E_{PR} will be expressed as a percentage (0-100%).

$$E_{PR} = \frac{I_A}{I_A + I_D}$$

Equation 6-3: Proximity ratio

6.3. Measurement of the affinity of protein A to monomeric and aggregated mAb

Protein A is known to bind strongly to the Fc (constant region) of monomeric mAbs. However, a crucial part of the FRET design was for protein A to also bind aggregated mAb. Therefore, the affinity of protein A to monomeric and aggregated mAb was compared using the Octet. The Octet monitors the binding between a ligand immobilised on the biosensor tip surface, and proteins/analyte in solution. An increase in optical thickness (binding) at the biosensor tip, results in an increased wavelength shift. The more molecules that bind to the biosensor tip surface, the greater the affinity between the immobilised ligand and analyte.

The binding interaction between both monomeric mAb and aggregated mAb was rapid, plateauing after roughly 40 seconds. The slope for both 100% monomeric mAb and 100% aggregated mAb (Figure 6-5) were similarly steep, indicating similar levels of affinity to protein A. However, after 2 mins aggregated mAb reached higher binding shifts than the monomer. The higher affinity of protein A to aggregated mAb was most likely due to the aggregated mAb (r_h= 17 nm) being larger than the monomeric mAb (r_h= 5.8 nm). As the Octet measures differences in optical thickness, an increased wavelength shift can also be created by an increase optical thickness due to a larger structure. The interactions with monomeric and aggregated mAbs were constant even after the wash step at 350 secs. BSA was used as a negative control, which as expected, showed minimal wavelength shift upon interacting with protein A.

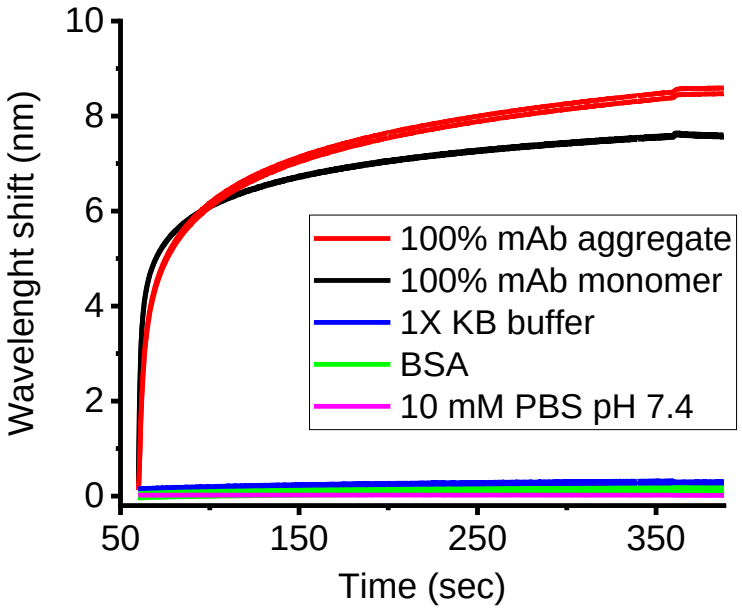

Figure 6-5: Measuring the affinity of protein A to monomeric and aggregated mAb using Octet.
100% mAb monomer (1.90 mg/mL) and 100% mAb aggregate (1.68 mg/mL) in PBS pH 7.2 and BSA (2.0 mg/mL) from ThermoFisher in 0.9% sodium chloride with sodium azide were diluted to 1 mg/ml. 80 µL of samples/buffer were aliquoted into black 384-well plates. Protein A biosensors were incubated in black 96-well plates with 10 mM PBS pH 7.4 (BSA run) or 1X KB (mAb run) for 10 mins prior to run for pre-conditioning. The run temperature was maintained at 30^0C. Conducted in duplicates.

6.3.1. Key Findings

The Octet showed that that protein A could bind to mAb aggregates. The binding interaction between both monomeric mAb and aggregated mAb was rapid, plateauing after 40 seconds. After 5 mins, aggregated mAb reached a higher plateau than monomeric mAb which was believed to be due to the large size of aggregates creating an increase in thickness on the sensor tip. With this understanding, the next step was to test the FRET assay which is discussed in the next sections.

6.4. Initial FRET results on purified mAb aggregates (plate reader)

To measure FRET using the change in acceptor sensitised fluorescence intensity method, energy transfer should cause both a decrease in donor and an increase in acceptor fluorescence intensity. Therefore, although it is important to measure both donor and acceptor spectra, the increase in relative efficiency proximity ratio (E_{PR}) would be the key indicator of the presence of aggregates. Presence of aggregated mAb was expected to have a stronger donor decrease (around 450 nm) and stronger acceptor increase (around 600 nm) in fluorescence intensity compared to monomeric mAb.

Using 96-well plates, FRET was measured with Protein A-Alexa Fluor 350 (PrA-AF350) and acceptors SYPRO Orange/ProteoStat in the presence of stressed mAb. PrA-AF350 with the acceptors in the presence of unstressed mAb was used as a negative control, and the PrA-AF350 and the acceptor in absence of protein was used as a blank.

6.4.1. Initial FRET measurement with mAb aggregates

The plate reader experiments in acetate buffer are shown in Figure 6-6 and Figure 6-7. In Figure 6-6, although there was an increase in SYPRO Orange (acceptor) fluorescence for the stressed mAb, the actual fluorescence values were very low. The E_{PR} values are summarised in Table 6-1. The E_{PR} between unstressed and stressed mAb increased by 1.7-fold at the initial conditions in Figure 6-6A/B. At lower PrA-AF350 (donor) concentration (Figure 6-6C/D) the E_{PR} between unstressed and stressed mAb increased by 2.0-fold. At higher SYPRO Orange concentration (Figure 6-6E/F), the E_{PR} between the unstressed and stressed mAb increased by 1.5-fold. The change in E_{PR} between unstressed and stressed mAb improved slightly with decreasing the PrA-AF350 (donor) concentration. However, the unstressed mAb at 600 nm consistently had a lower fluorescence than the blank in all three conditions. Theoretically, the buffer blank should have the lowest fluorescnce/ weakest energy transfer, since the donor and acceptor would only be close due to random diffusion.

For ProteoStat as an acceptor, there was a 1.3-fold increase between the unstressed mAb and stressed mAb in the initial conditions in Figure 6-7A/B. At lower PrA-AF350 (donor) concentration (Figure 6-7C/D) the E_{PR} between unstressed and stressed mAb increased by 1.4-fold. At higher ProteoStat concentration (Figure 6-7E/F), the E_{PR} between the unstressed and stressed mAb incrased by 1.3-fold. However, similarly to SYPRO Orange, ProteoStat fluorescence (600 nm) of the stressed mAb overlapped with the blank across all three conditions.

Overall, there were three main issues with the initial FRET data: weak fluorescence intensity of the acceptor, low proximity ratio (below 2% for most conditions) and the fluorecence of the acceptor in the buffer blank was slightly higher than in the acceptor in unstressed mAb. As there were many issues, to ascertain that the results were not buffer specific, the experiment was repeated using a higher pH to promote protein A-mAb binding.

Table 6-1: Summary of E_{PR} values for initial FRET experiment

	SYPRO Orange			ProteoStat		
FRET Experiment	Sample	E_{PR} (%)	Change in E_{PR}	Sample	E_{PR} (%)	Change in E_{PR}
Initial	Unstressed mAb	0.61	1.7-fold increase	Unstressed mAb	0.76	1.3-fold increase
	Stressed mAb	1.06		Stressed mAb	0.96	
Lower donor concentration	Unstressed mAb	0.55	2.0-fold increase	Unstressed mAb	0.79	1.4-fold increase
	Stressed mAb	1.18		Stressed mAb	1.14	
Higher acceptor concentration	Unstressed mAb	0.72	1.5-fold increase	Unstressed mAb	1.28	1.3-fold increase
	Stressed mAb	1.07		Stressed mAb	1.64	

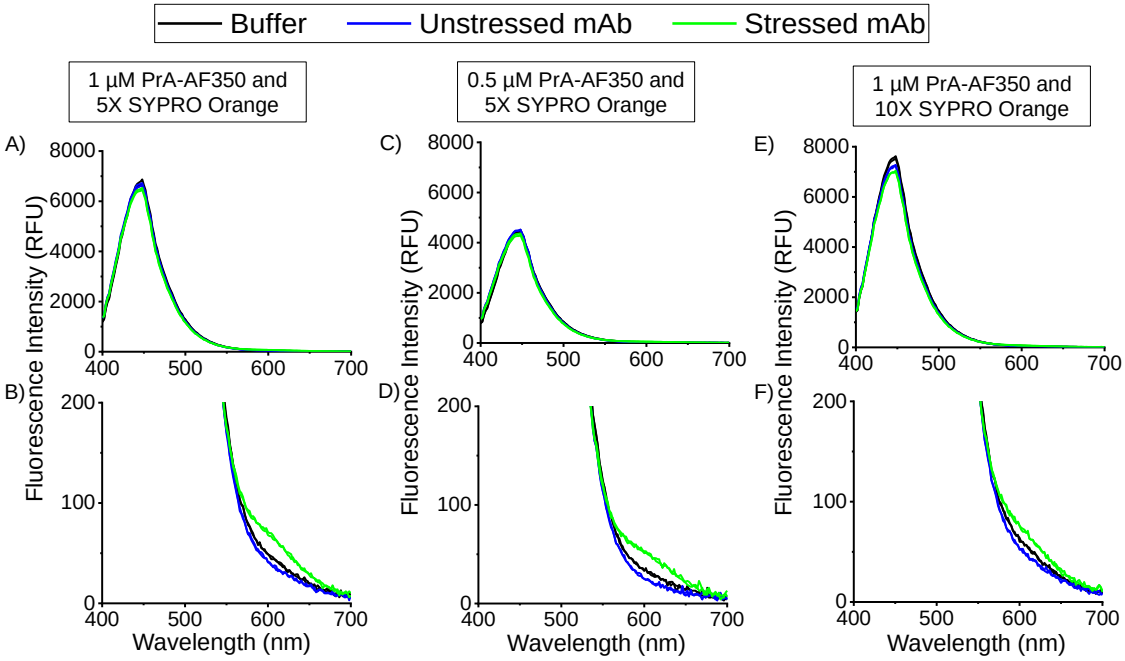

Figure 6-6: FRET with 5X SYPRO Orange (acceptor) and 1 µM Protein A-Alexa Fluor 350 (donor) at different concentrations in 50 mM sodium acetate buffer pH 5.5 using a plate reader.
(A), (C), and (E) are full scale versions and (B), (D) and (F) are zoomed into the acceptor peak regions. Donor peak fluorescence 450 nm, acceptor peak fluorescence 600 nm. The stressed mAb in (A) and (B) were 9% aggregated and for (C)-(F) 13% aggregated. Concentration of mAb in each well was 1 mg/mL. Excitation/Emission: 330/400 –700 nm, Gain 70. Conducted in duplicates.

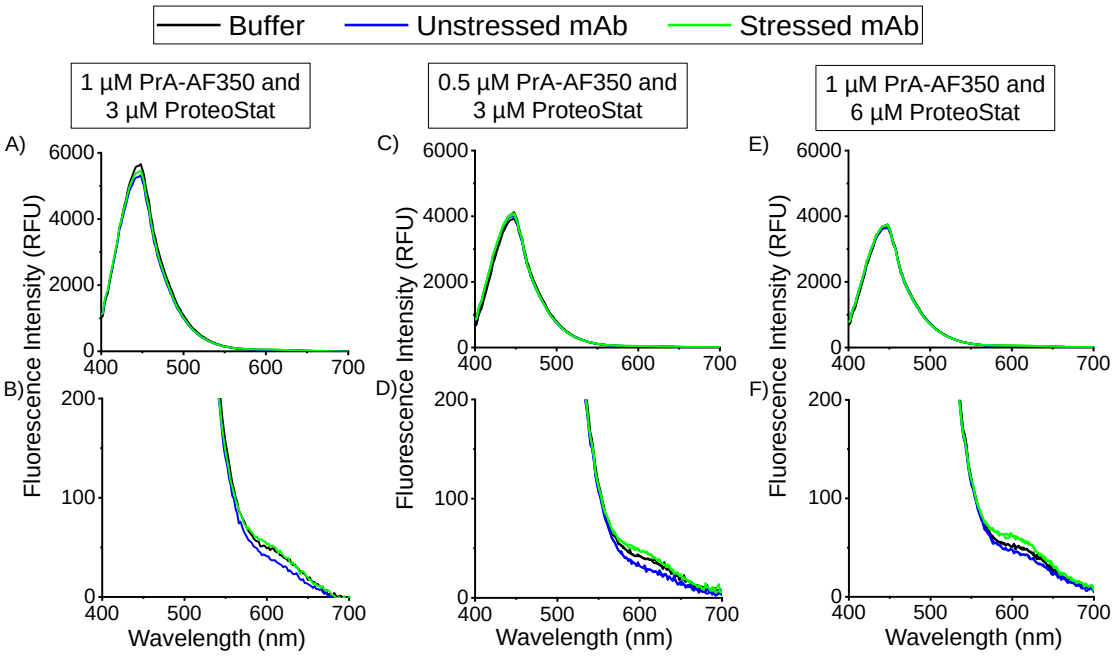

Figure 6-7: FRET with 3 µM ProteoStat (acceptor) and 1 µM Protein A-Alexa Fluor 350 (donor) at different concentrations in 50 mM sodium acetate buffer pH 5.5 using a plate reader.
(A), (C), and (E) are full scale versions and (B), (D) and (F) are zoomed into the acceptor peak regions. Donor peak fluorescence 450 nm, acceptor peak fluorescence 600 nm. The stressed mAb in (A) and (B) were 9% aggregated and for (C)-(F) 13% aggregated. Concentration of mAb in each well was 1 mg/mL. Excitation/Emission: 330/400 –700 nm, Gain 70. Conducted in duplicates.

6.4.2. Measuring FRET with mAb aggregates in a different buffer

The binding and elution of protein A to mAbs normally occurs around pH 7 and pH 4 respectively. Therefore, a buffer closer to neutral pH was used to see whether a stronger increase in energy transfer (E_{PR} >2%) would occur because of better binding between the protein A and mAb.

At pH 7 with SYPRO Orange as an acceptor (Figure 6-8), the E_{PR} between the unstressed and stressed mAb in Figure 6-8A/B increased by 1.5-fold (Table 6-2). At lower donor concentration (Figure 6-8C/D) and lower SYPRO Orange concentration (Figure 6-8E/F) the E_{PR} between the unstressed and stressed mAb increaed by 2.5-fold and 1.5-fold respectively. Similar to the acetate pH 5.5 results (Figure 6-6), the

change in E_{PR} between unstressed and stressed mAb improved slightly with decreasing the PrA-AF350 (donor) concentration.

Using ProteoStat as an acceptor (Figure 6-9), the E_{PR} between the unstressed and stressed mAb in Figure 6-9A/B increased by 1.8-fold. At lower donor concentration (Figure 6-9C/D) and lower SYPRO Orange concentration (Figure 6-9E/F) the E_{PR} between the unstressed and stressed mAb increaed by 1.1-fold and 1.3-fold respectively.

In most cases, the E_{PR} was still less than 2%. Furthermore, the acceptor fluorescence with the unstressed mAb at 600 nm consistently had a lower fluorescence than with the blank in all three conditions. As whole, compared to using a pH 5.5 buffer, the pH 7.5 buffer did not improve the energy transfer from the donor.

Table 6-2: Summary of EPR values for FRET pH 7 experiment

	SYPRO Orange			ProteoStat		
FRET Experiment	Sample	E_{PR} (%)	Change in E_{PR}	Sample	E_{PR} (%)	Change in E_{PR}
Initial	Unstressed mAb	0.51	1.5-fold increase	Unstressed mAb	0.85	1.8-fold increase
	Stressed mAb	0.79		Stressed mAb	1.55	
Lower donor concentration	Unstressed mAb	0.36	2.5-fold increase	Unstressed mAb	1.07	1.1-fold increase
	Stressed mAb	0.91		Stressed mAb	1.15	
Higher acceptor concentration	Unstressed mAb	0.60	1.5-fold increase	Unstressed mAb	1.46	1.3-fold increase
	Stressed mAb	0.92		Stressed mAb	1.89	

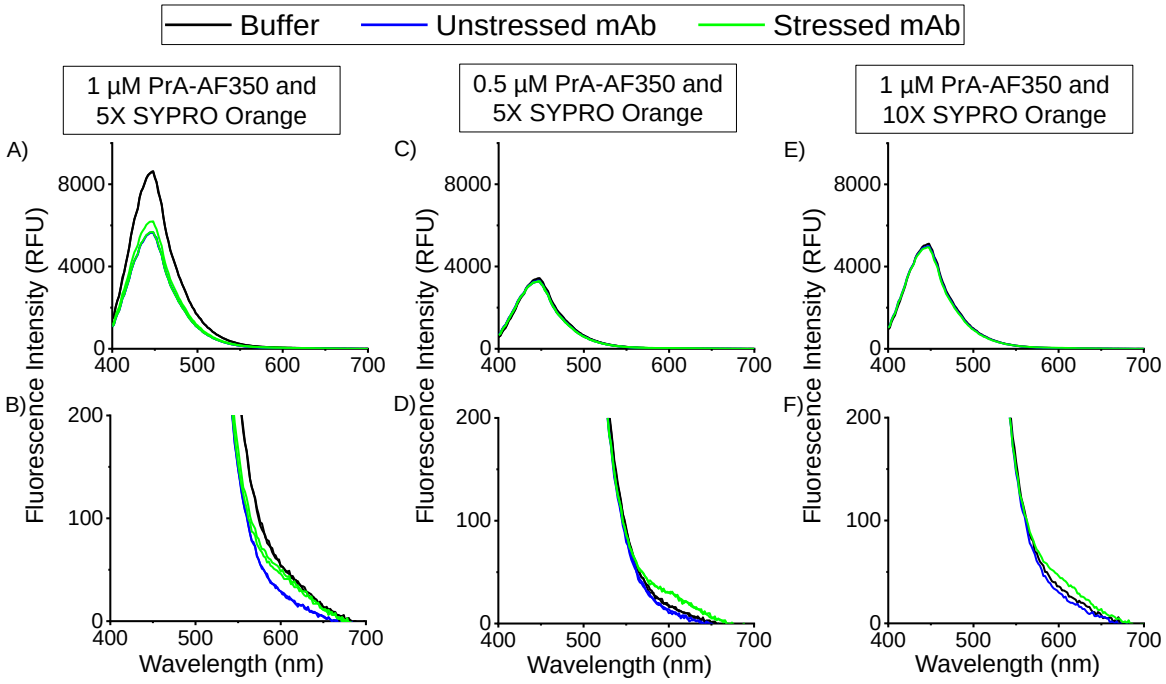

Figure 6-8: FRET with 5X SYPRO Orange (acceptor) and 1 µM Protein A-Alexa Fluor 350 (donor) at different concentrations in 50 mM potassium phosphate buffer pH 7.5 using a plate reader.
(A), (C), and (E) are full scale versions and (B), (D) and (F) are zoomed into the acceptor peak regions. Donor peak fluorescence 450 nm, acceptor peak fluorescence 600 nm. The stressed mAb was 9% aggregated (r_h= 12.5 nm). Concentration of mAb in each well was 1 mg/mL. Excitation/Emission: 330/400–700 nm, Gain 70. Conducted in duplicates.

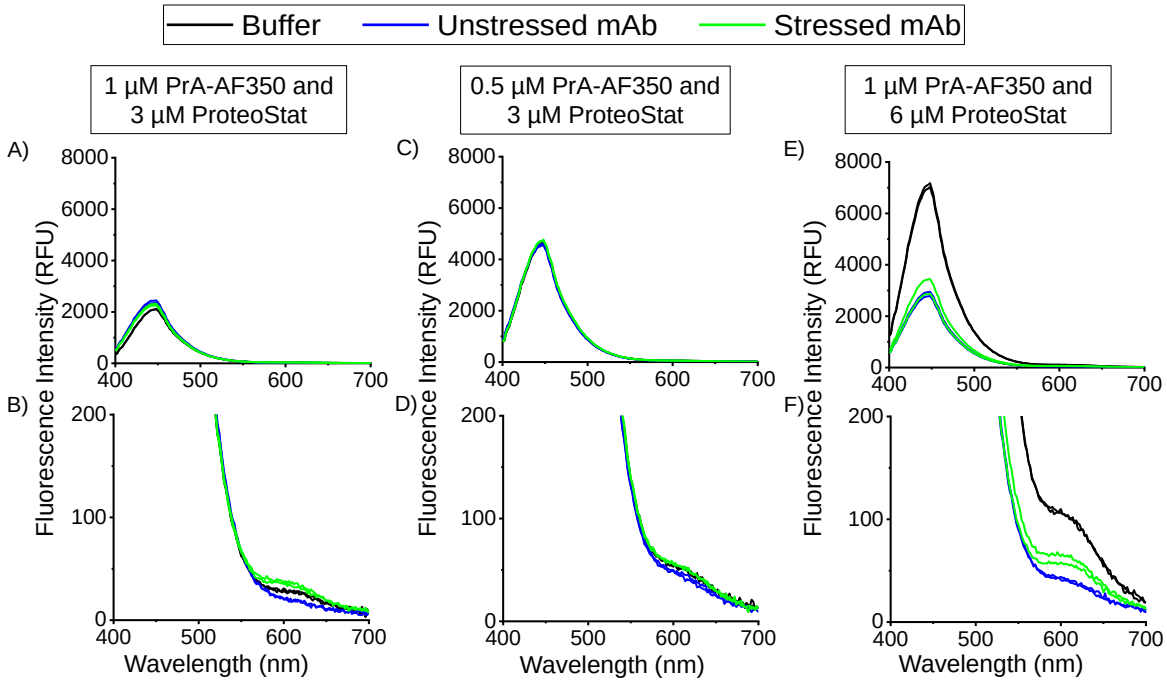

Figure 6-9: FRET with 3 µM ProteoStat (acceptor) and 1 µM Protein A-Alexa Fluor 350 (donor) at different concentrations in 50 mM potassium phosphate buffer pH 7.5 using a plate reader.
(A), (C), and (E) are full scale versions and (B), (D) and (F) are zoomed into the acceptor peak regions. Donor peak fluorescence 450 nm, acceptor peak fluorescence 600 nm. The stressed mAb was 9% aggregated (r_h= 12.5 nm). Concentration of mAb in each well was 1 mg/mL. Excitation/Emission: 330/400–700 nm, Gain 70. Conducted in duplicates.

6.4.3. Key Findings

The FRET results at pH 5.5 and pH 7.5 both showed weak energy transfer due to little decrease/increase in donor/acceptor fluorescence intensities respectively. The results did not improve with changing donor or acceptor concentrations. Additionally, the buffer blank had slightly higher acceptor fluorescence intensity than the unstressed mAb. As the initial plate reader results were not very promising, to increase the level of sensitivity and verify that the results were not instrument-specific, the experiment was repeated using a cuvette-based spectrofluorometer. Cuvette-based

spectrofluorometers use a larger volume of sample and is better set-up to collect more light from samples after excitation.

6.5. FRET results on purified mAb aggregates (cuvette spectrofluorometer)

The FRET experiment was repeated using a cuvette based spectrofluorometer to confirm whether the plate reader results were instrument-specific. In addition, to increase the chances for the acceptor to be close to the donor, higher concentrations of the acceptor were also measured.

A cuvette-based spectrofluorometer works in a similar way to plate reader with a few minor differences. The main difference is how the light is presented to the monochromator. A monochromator allows light at a specific wavelengths pass through to the sample. A plate reader uses a flash lamp which flashes light into the system towards the excitation monochromator. On the other hand, a cuvette-based spectrofluorometer uses a continuous source of light that is shone onto the monochromator. This provides a higher energy source to the sample. Cuvette-based spectrofluorometer also have greater control over parameters, diffraction grating rather than optical filters and single monochromators on the excitation and emission side (as opposed to double). However, diffraction grating can cause Rayleigh scattering, an instrumental effect caused by the scattering of the incident light at the same and double the excitation wavelength (Cao and Brinker, 2008). As such, exciting at 330 nm would result in Rayleigh scattering at 330 nm and 660 nm (second-order scattering). Therefore, it was necessary to narrow the fluorescence emission range from 400-700 nm to 400-650 nm.

The results at 1 µM PrA-AF350 and 5X SYPRO Orange (Figure 6-10A/B) were similar to the plate reader experiment. Stressed and unstressed mAb had similar PrA-AF350 (donor) intensities, which were only slightly lower than the blank. There was a 2.1-fold increase between the unstressed mAb (0.48%) and stressed mAb E_{PR} (1.03%) in Figure 6-10A/B. However, as the PrA-AF350 (donor) intensities of stressed and unstressed mAb were similar, the increase in E_{PR} here did not correspond to true FRET/energy transfer. In addition, the similar donor intensities of the stressed

and unstressed mAb were lower than the donor with the blank. The acceptor fluorescence intensity with the blank was also slightly higher than with the unstressed mAb sample. High concentrations of SYPRO Orange resulted in quenching (decreasing) of donor fluorescence intensity for all samples. At 100X and 250X SYPRO Orange, the fluorescence of the donor with the blank was lower than with the mAb samples. The SYPRO Orange intensities at 600 nm overlapped completely at 100X and 250X SYPRO Orange for the unstressed mAb, stressed mAb and buffer.

The results for 1 µM PrA-AF350 and 3 µM ProteoStat did not improve in the cuvette compared to the plate reader. Stressed and unstressed mAb with 1 µM PrA-AF350 and 3 µM ProteoStat (Figure 6-11A/B) had similar PrA-AF350 (donor) intensities, which were only slightly lower than the blank. There was no clear difference in the ProteoStat (acceptor) at 600 nm with all three samples (Figure 6-11B).

Like the SYPRO Orange results, higher concentrations of ProteoStat (10 µM and 30 µM) quenched the fluorescence of PrA-AF350. In addition, at 600 nm the higher concentrations of ProteoStat had a complete overlap in curves for the unstressed mAb, stressed mAb and buffer samples. Using higher concentrations of acceptors also made cleaning the cuvettes more difficult, which was also reflected in some of the repeats. The higher concentrations of the acceptor did not improve the energy transfer. This overall showed that the results obtained in the plate reader were due to the FRET system and was not instrument-specific.

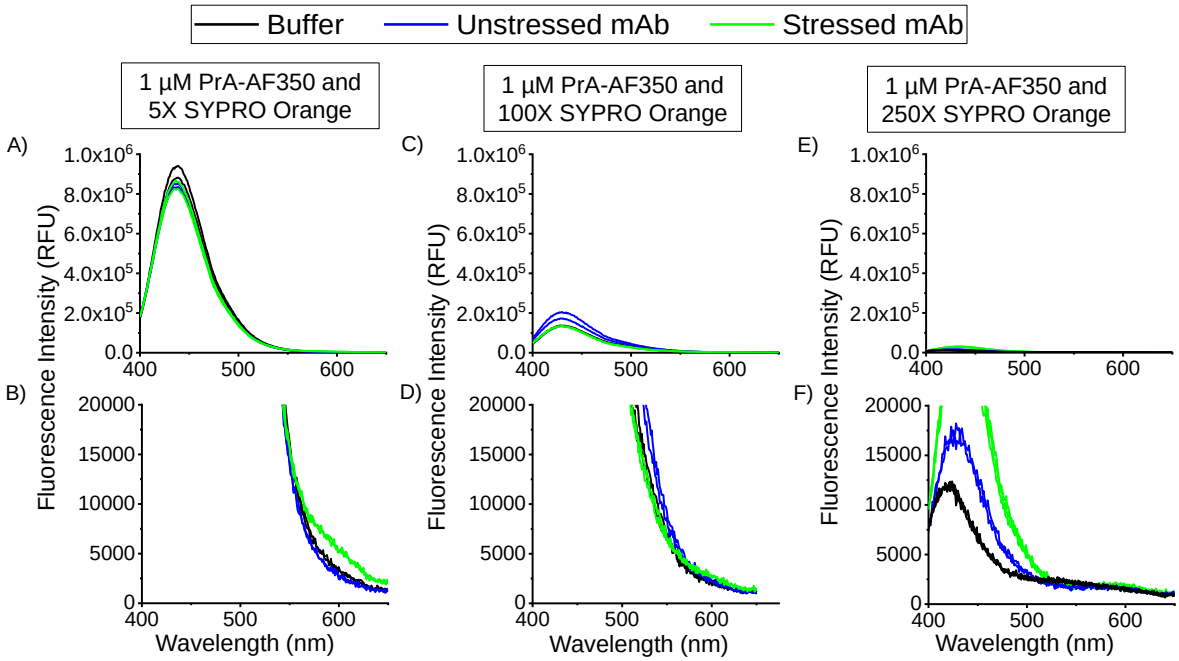

Figure 6-10: FRET with SYPRO Orange and Protein A-Alexa Fluor 350 at different concentrations in 50 mM sodium acetate buffer pH 5.5 using a cuvette spectrofluorometer.
(A), (C) and (E) are full scale versions and (B), (D) and (F) are zoomed into the acceptor peak regions. The stressed mAb was 15% aggregated (r_h= 15 nm). Concentration of mAb in each well was 1 mg/mL. Excitation/Emission: 330/400–650 nm. Excitation and emission slit bandpass was 2 nm and 1 nm respectively. Conducted in duplicates.

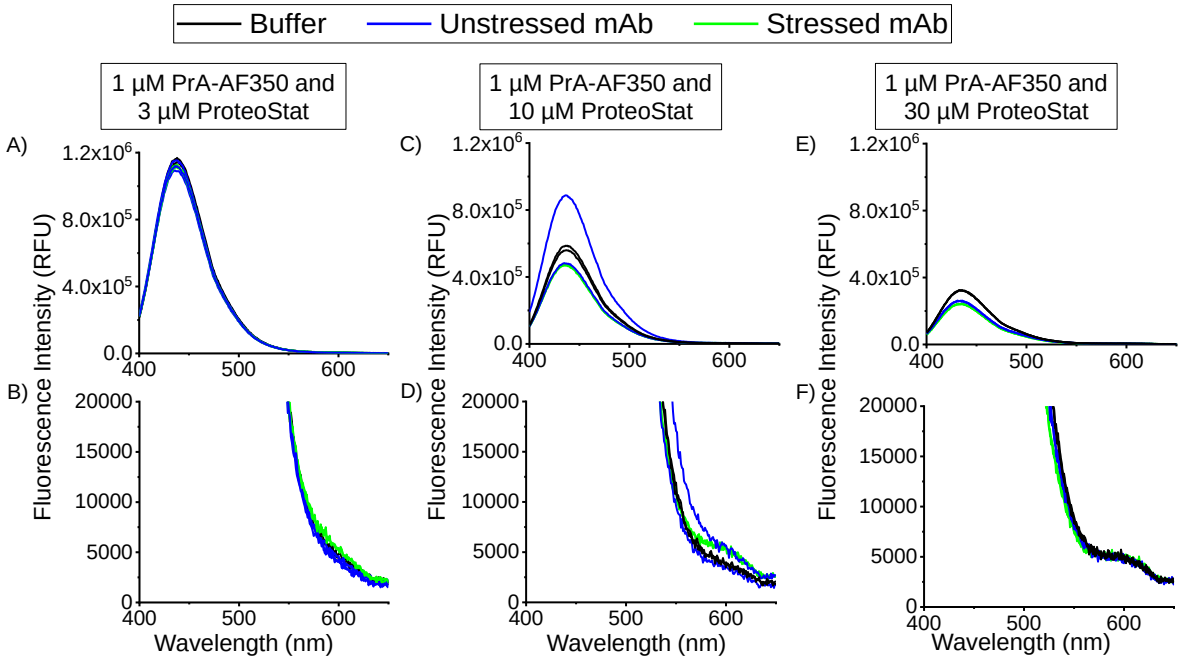

Figure 6-11: FRET with ProteoStat and Protein A-Alexa Fluor 350 at different concentrations in 50 mM sodium acetate buffer pH 5.5 using a cuvette spectrofluorometer.
(A), (C) and (E) are full scale versions and (B), (D) and (F) are zoomed into the acceptor peak regions. The stressed mAb was 15% aggregated (r_h= 15 nm). Concentration of mAb in each well was 1 mg/mL. Excitation/Emission: 330/400–650 nm. Excitation and emission slit bandpass was 2 nm and 1 nm respectively. Conducted in duplicates.

6.5.1. Key Findings

Overall, the cuvette FRET results were similar to the plate reader FRET results. Higher concentrations of acceptors (>100X SYPRO Orange and >10 µM ProteoStat) made results generally worse by quenching the fluorescence intensity of the donor even in the absence of protein. The absence of clear energy transfer from the donor to the acceptor with aggregated mAb samples was not an instrument issue, and therefore must be a problem with the design of the assay.

6.6. Analysis of weak energy transfer/FRET

The FRET assay was a complex system with many components and parameters involved that play a part in achieving energy transfer. Since the energy transfer achieved so far was weaker than intended, it was important to review the fundamentals of FRET and the set-up of the assay to aid creating troubleshooting experiments to solve the issues. A few scenarios were identified that can cause weak/lack of energy transfer.

6.6.1 Partially aggregated mAb (Control 1)

All the FRET experiments so far compared partially aggregated mAb (9-13% aggregates) to unstressed mAb. As the stressed sample contained both monomeric and aggregated mAb, weak energy transfer could occur due to the stressed sample not being homogenously aggregated. To test whether this aspect was causing weak FRET, 100% monomeric mAb and 100% aggregated mAb should be directly compared instead.

6.6.2. Transition dipole and spectral overlap (Control 2)

A second reason for weak energy transfer was related to the transition dipole (κ^2). The transition dipole is a geometric value for the dipole rotation between the donor and the acceptor and is assumed when calculating the R_0 (Equation 6-2). As it is difficult to experimentally measure κ^2, it is hard to ensure that the dipoles are in a rotation favourable for FRET; hence the assumed value of 2/3 is used for this reason. Although the parameter is important, it would be difficult to troubleshoot experimentally.

A third reason for weak energy transfer is based on spectral overlap between donor and acceptor dyes. As mentioned in Chapter 5.2, there must be spectral overlap between the donor's emission and acceptor's excitation. Although Bajar et al. (2016) highlighted a minimum 30% spectral overlap is required for FRET, a high percentage of overlap does not directly relate to high energy transfer. The intensities at which energy transfer occurs is important. A large spectral overlap that occurs at low intensities would have a low energy transfer. As well as this, the spectral overlap of

AF350-SYPRO Orange and AF350-ProteoStat were calculated based on online spectral data (except ProteoStat) which normalised the fluorescence. Normalised spectral data does not give an understanding of the intensities. To understand if the weak energy transfer were due to the spectral overlap, it was required to measure the donor and acceptor spectral overlap without normalising the fluorescence intensities.

6.6.3. Impact of buffer (Control 2)

A fourth reason for the weak energy transfer could also be due to differences in the buffer used. The buffer used in the online spectral data may not be the same buffer used in the experiment of interest. Dyes are very sensitive to solvent/chemical differences, and different buffers could result in different degrees of spectral overlap. This could make a difference between a FRET pair being suitable or not. In addition, slight differences in the buffer used between the blank and the mAb samples may explain why the blank had higher acceptor fluorescence than unstressed mAb. Overall, relying on online spectral data can lead to inaccurate assumptions of data. To understand the true spectral overlap (as well as all FRET experiment), the spectral overlap would need to be measured keeping the buffer environment the same across all samples.

6.6.4. Acceptor may not be fluorescing (Control 3 and 4)

One reason for weak acceptor emission could be due to the acceptor not fluorescing under the following circumstances:

a) A component in the assay could be preventing the donor from transferring energy to the acceptor
b) The donor is capable of transferring energy to the acceptor, but the acceptor does not receive it as it may be too far away
c) The donor is capable of transferring energy to the acceptor, but the acceptor's fluorescence is being quenched by a component

Both point a and c relate to the quenching of the fluorophore signal. Quenching can be static or dynamic, which both result from a collisional encounter between a fluorophore and quencher (Lakowicz, 2010). During static quenching, a non-

fluorescent complex is formed between the fluorophore and the quencher. Whereas, dynamic quenching occurs when a quencher diffuses to the fluorophore during excitation preventing it from being excited and fluorescing. A wide variety of substances act as quenchers of fluorescence such as oxygen, heavy atoms such as iodide and bromide, halogenated compounds, dimethylformamide, hydrogen peroxide, nitric oxide to list a few. However, none of these components were present in the current FRET assay. The only evidence of quenching seen with results was with high concentrations of the acceptor which quenched the donor's fluorescence. The distance issue (b) could be due to the use of large proteins that put the donor and acceptor at distances outside of FRET limits. As the donor and acceptor are free in solution and not bound onto the same molecule as typical FRET systems, it is generally harder to achieve the required distance for strong energy transfer. FRET would only measure the small fraction of donor and acceptors that happen to be close enough at the time of measurement.

Protein A and unstressed mAb have diameters of 9-10 nm and 10-12 nm respectively. The stressed mAb samples used in the experiments had diameters up to 30 nm. As distance is a key criterion for energy transfer, less energy would be transferred at a distance of 30 nm, which would explain the weak energy transfer. Additionally, if the acceptor interacts with the inner structure of the aggregate, there may be steric hindrance towards it interacting with the donor. Therefore, inspecting the distance issue would give better understanding of the distance required to get better energy transfer. One way the impact of distance could be investigated would be to see if shortening the distance between the donor and acceptor would improve the energy transfer. An example would be to label the mAb directly with the donor instead of protein A. In addition, calculating/measuring the R_0 would help give a quantitative understanding of the distances required for this FRET system.

6.6.5. Key Findings

There were four potential reasons for weak energy transfers: measuring partially aggregated mAb, acceptor not fluorescing, inaccurate transition dipole, inaccurate spectral overlap and differences in buffers used for samples. The following troubleshooting experiments were decided upon to give a better understanding of the FRET system against these reasons. This included: (1) comparing FRET with 100% monomeric and 100% aggregated mAb sample, (2) recalculating spectral overlap in actual buffer conditions, (3) measuring the actual R_0 for FRET pairs and (4) reducing the distance between the donor and acceptor.

6.7. Control 1: FRET with 100% mAb aggregates and 100% monomeric mAb

Most of the FRET experiments involved using a partially aggregated mAb sample. Hence, the focus of this control was to compare a fully aggregated mAb sample against a monomeric mAb sample. This was conducted by isolating aggregate peaks from stressed mAb create a "pure" aggregated sample to compare against a "pure" monomer sample.

Figure 6-12 shows the comparison between FRET with 100% aggregated and monomeric mAb (See Method and Materials Section 3.8). The E_{PR} for both acceptors with aggregated mAb was greater than in previous FRET experiments (Table 6-3). For SYPRO Orange, the E_{PR} between the unstressed and stressed mAb increased by 4.2-fold. For ProteoStat, the E_{PR} between the unstressed and stressed mAb increased by 2.6-fold. This showed that the efficiency of transfer was better by comparing more homogeneous samples. However, there was little change in the PrA-AF350 (donor) fluorescence at 450 nm between the 100% aggregated and 100% monomer mAb. Therefore, it was highly likely that the increase in E_{PR} was mostly influenced by a small amount of acceptor being excited directly due to the presence of mAb aggregate rather than true FRET. In addition, in reality the FRET assay would be measuring aggregated mAb in the presence of monomeric mAb. Overall, this control confirmed that energy transfer did not improve even with homogeneous aggregate samples.

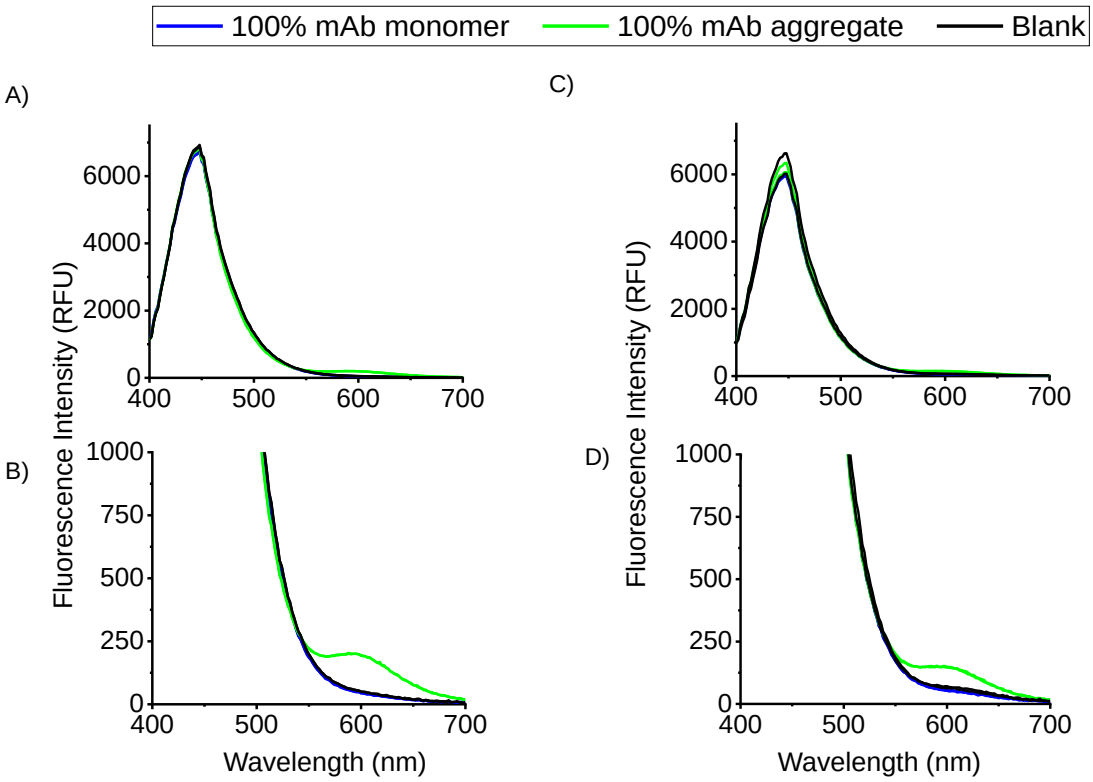

Figure 6-12: Positive FRET control 1 with 100% mAb aggregates vs. 100% monomeric mAb.
100% mAb aggregates (r_h=17 nm), 100% monomeric mAb (r_h=5.8 nm) with 1 µM Protein A-Alexa Fluor 350 with (A) 5X SYPRO Orange and (C) 3 µM ProteoStat. (B) and (D) are zoomed in plots of the acceptor spectrum for (A) and (B) respectively. Concentration of mAb in each well was 1 mg/mL.

Table 6-3: Summary of EPR values for 100% mAb monomer compared to 100% mAb aggregate

	E_{PR} (%)		Change in E_{PR}
Acceptor	100% mAb monomer	100% mAb aggregate	
SYPRO Orange	0.65	2.76	4.2-fold increase
ProteoStat	0.90	2.32	2.6-fold increase

6.8. Control 2: Calculating the donor and acceptor spectral overlap

The second control was to measure the spectral overlap of the FRET pairs without normalising the fluorescence intensities, ensuring that the samples were in the same buffer mixtures used for the FRET assay. Two different buffer mixtures were used for the different acceptors. For SYPRO Orange the buffer was: PBS, sodium acetate pH 5.5 and DMSO. For ProteoStat the mixture was: PBS, sodium acetate pH 5.5 and 1X ProteoStat buffer. The components of the buffer were as used as PrA-AF350, mAb, SYPRO Orange and ProteoStat were prepared in PBS, sodium acetate pH 5.5, DMSO and 1X ProteoStat buffer respectively. Therefore, the appropriate amounts of each buffer were used to keep the experiment consistent. AF350 without protein A conjugated was used to measure the donor's excitation/emission.

The spectral overlaps using online normalised spectral data (Figure 6-13) estimated a 47% and 41% spectral overlap for AF350-SYPRO Orange and AF350-ProteoStat respectively. In comparison, normalising the measured spectral overlap with the actual FRET buffer conditions (Figure 6-14) estimated a 48% and 51% spectral overlap for AF350-SYPRO Orange and AF350-ProteoStat respectively. Although the overlaps for SYPRO Orange were similar, there was a 10% difference between the normalised online and the normalised measured spectral data for ProteoStat. The differences in spectral overlap between online and measured was also seen with existing FRET pairs: AF350-AF488, AF488-AF555 and Cy3-Cy5 (Table 6-4). This showed the importance of measuring spectral overlap in the correct assay buffer.

The measured spectral overlaps based on intensities (Figure 6-15) showed that SYPRO Orange and ProteoStat's excitation spectra fully overlapped with Alexa Fluor 350 emission spectrum. This verified that the donor and acceptor were appropriate pairs for each other. However, the intensities of SYPRO Orange and ProteoStat were 10X and 20X lower than Alexa Fluor 350 respectively. For comparison, the acceptors of existing FRET pairs (Figure 6-16) had either 0.5X (Alexa Fluor 488 and Alexa Fluor 555) or similar (Cy5) intensities to their respective donors. Although the acceptor intensities may be higher in the presence of aggregates, the data obtained

still highlights the difference between the donor and acceptor which may (or may not) be contributing to the weak energy transfer. In addition, Cy3-Cy5 had less than the 30% minimum spectral overlap as identified by Bajar et al. (2016). As this is an already established FRET pair, this showed that the 30% minimum spectral overlap, should be seen as a guide as opposed to a requirement for FRET.

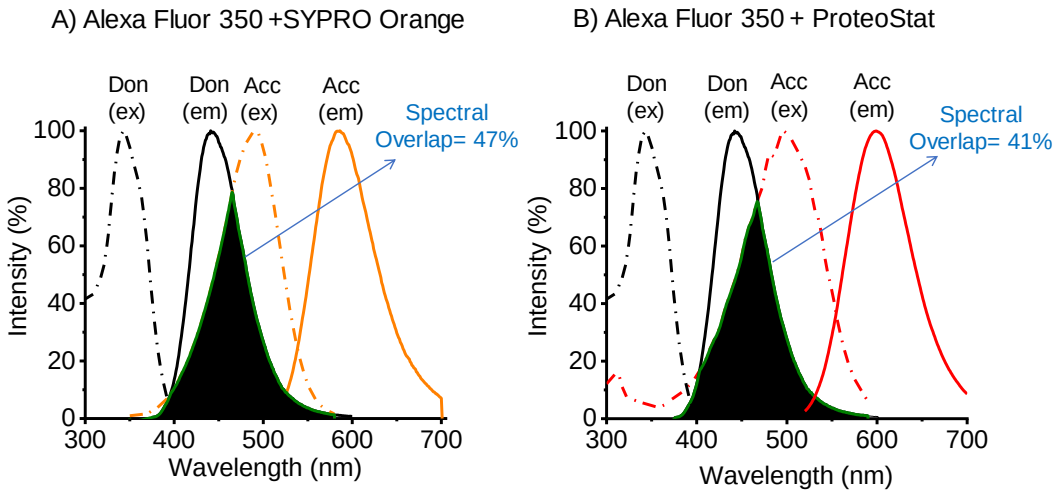

Figure 6-13: Spectral overlap of Alexa Fluor 350 (donor) with A) SYPRO Orange (acceptor) and B) ProteoStat (acceptor).
Don=donor, Acc=acceptor, ex=excitation spectrum and em=emission spectrum. Excitation and emission data obtained from ThermoFisher online Fluorescence SpectraViewer. ProteoStat excitation (ex 300-590 nm, em 620 nm, 1 nm step intervals) and and emission (ex 490 nm, em 520-750 nm, 1 nm step intervals)spectrums were measured and normalised. Spectral overlap (%) was calculated by dividing the shared overlap integral (highlighted in black) from the summed integral of the donor excitation spectrum and the acceptors emission spectrum.

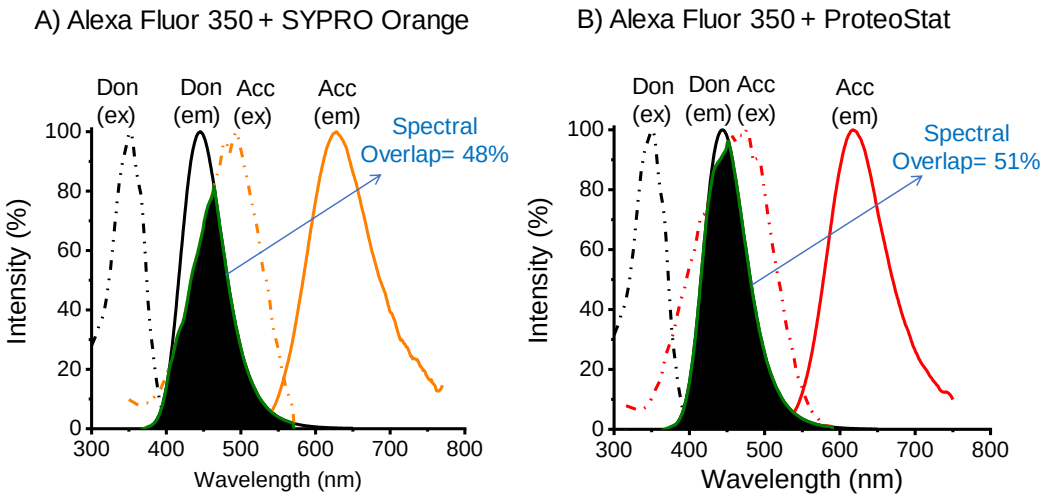

Figure 6-14: Normalised measured excitation and emission spectral overlaps of Alexa Fluor 350 (1 µM) and 5X SYPRO Orange (A) and Alexa Fluor 350 (1 µM) and 3 µM ProteoStat (B) in actual buffer conditions.
The donor dye and acceptor dyes were measured separately. The buffers used for Alexa Fluor 350 and SYPRO Orange measurement were PBS, sodium acetate and DMSO. The buffers used for Alexa Fluor 350 and ProteoStat measurement were PBS, sodium acetate and ProteoStat proprietary buffer.

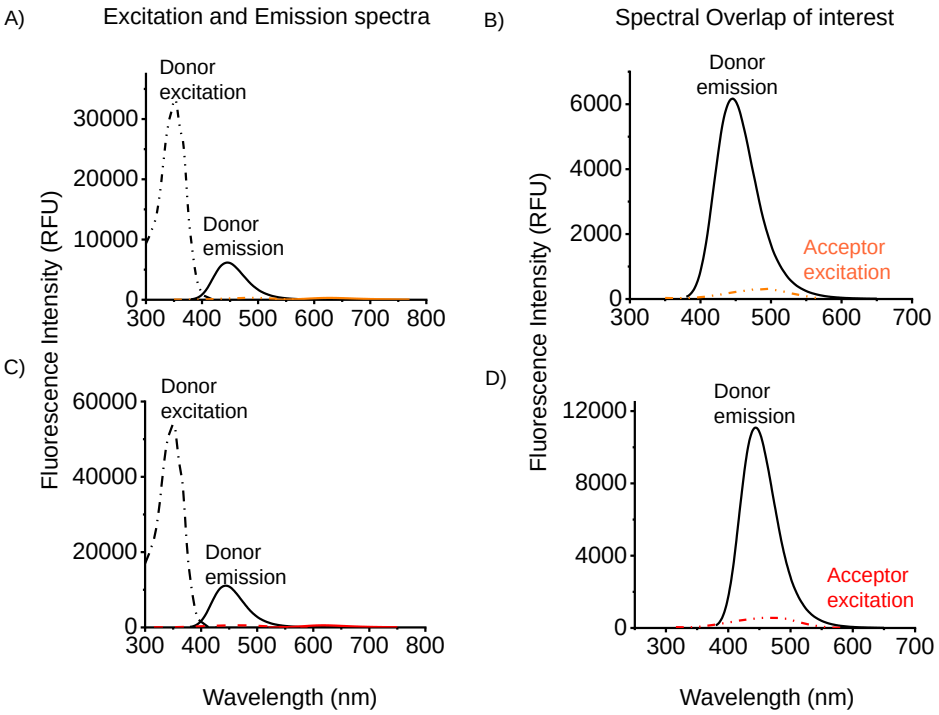

Figure 6-15: Measured excitation and emission spectral overlaps of Alexa Fluor 350 (1 µM) and 5X SYPRO Orange (A) and Alexa Fluor 350 (1 µM) and 3 µM ProteoStat (B) in actual buffer conditions.
The excitation and emission of donor and acceptors were measured separately. The buffers used for Alexa Fluor 350 and SYPRO Orange measurement were PBS, sodium acetate and DMSO. The buffers used for Alexa Fluor 350 and ProteoStat measurement were PBS, sodium acetate and ProteoStat proprietary buffer. (B) and (D) are zoomed in versions of A and B respectively.

Table 6-4: List of FRET pairs existing in the literature.
Information for spectral online data was found on (ThermoFisher, 2017). Spectral overlap was calculated by measuring the shared integral between the donor emission and acceptor excitation dividing it by the total combined integral of the donor emission and acceptor excitation. QY represents quantum yield. The QY for Alexa Fluor 350 was measured as outlined in Chapter 6.9.3.

Donor	Acceptor	R_0 (Å)	Spectral overlap based on online data (%)	Spectral overlap based on measured normalised data (%)	Spectral overlap based on measured intensities (%)
Alexa Fluor 350 (QY= 1.07*)	Alexa Fluor 488 (QY= 0.92)	50	24	28	35
Alexa Fluor 488 (QY=0.92)	Alexa Fluor 555 (QY =0.1)	70	49	58	59
Cy3 (QY= 0.1)	Cy5 (QY = 0.28)	53	26	28	18

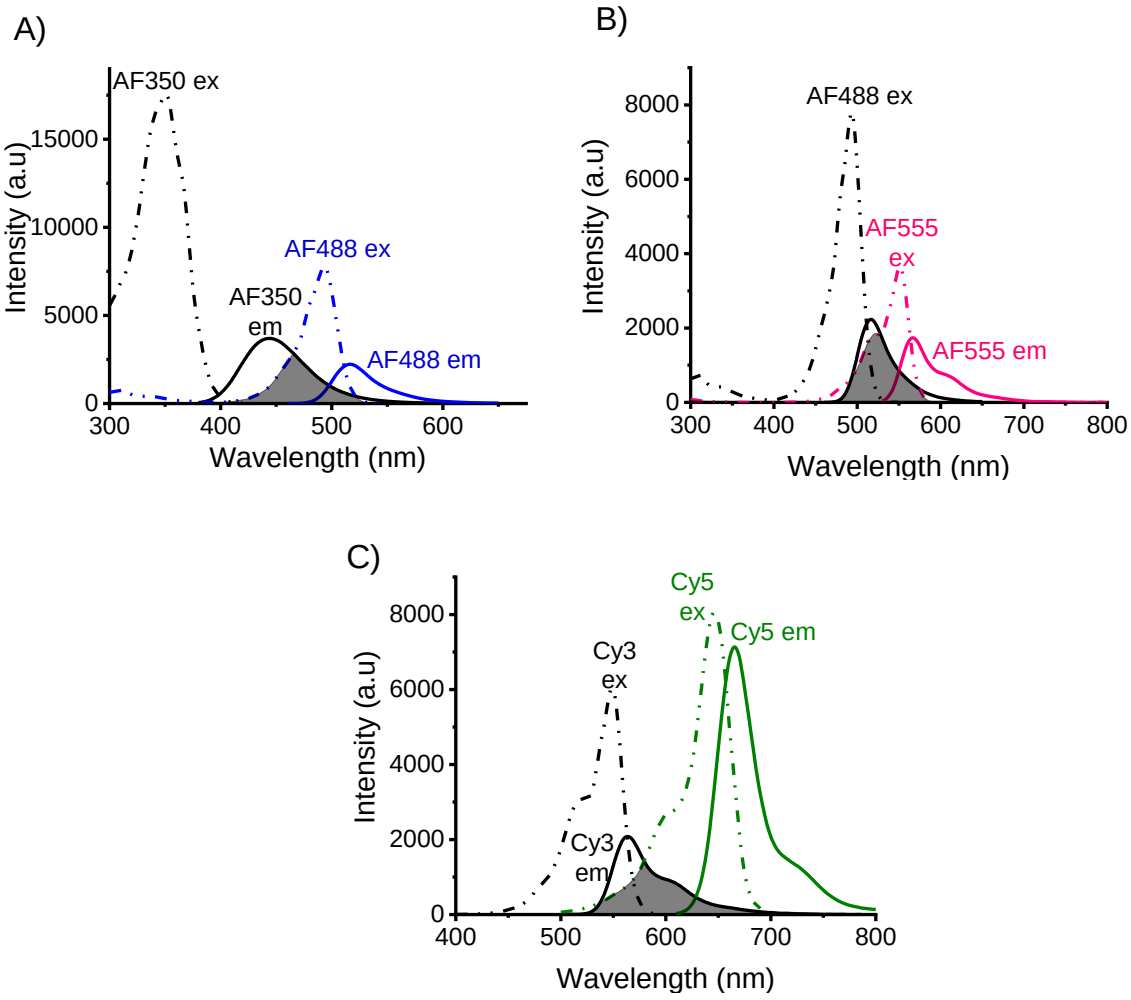

Figure 6-16: Spectral overlap of known FRET pairs based on intensities.
(A) Alexa Fluor 350 (donor) and Alexa Fluor 488 (acceptor), (B) Alexa Fluor 488 (donor) and Alexa Fluor 555 (acceptor), (C) Cy3 (donor) and Cy5 (acceptor). Dotted lines indicate excitation spectrums and solid lines indicate emission spectrums. All fluorophores were measured at 1 µM.

6.8.1. Key Findings

The donor emission and acceptor excitation spectrum of AF350-SYPRO Orange and AF350-ProteoStat completely overlapped, verifying that the FRET pairs were appropriate. The acceptor intensities of SYPRO Orange and ProteoStat were notably 10X and 20X lower than AF350 respectively. Known FRET pairs also showed their acceptors had lower intensities than the donor, albeit to a lesser extent. However, it

was not clear how much this influenced the weak FRET as the spectras of the acceptors were measured in the absence of aggregates.

This control experiment also showed that different buffers and normalising data can cause variability of the percentage spectral overlap. This emphasised the importance of measuring spectral overlaps in actual buffers with relative intensities. However, it also showed that even if there is a small spectral overlap does not mean FRET will not occur. Spectral overlaps should be used to give an idea of whether FRET is possible or not, rather than the sole determination of whether FRET will occur.

6.9. Control 3: Calculating of the Förster radius (R_0)

The R_0 requires the quantum yield of the donor and the extinction coefficient of the acceptor. The quantum yield can be calculated by comparing absorbance intensities to a standard fluorophore with a known quantum yield. The extinction coefficient was calculated using the Beer Lambert Law equation.

The quantum yield of AF350 was measured using quinine sulphate as a reference. The single point method comparative method yielded high quantum yield values. However, the single point had more variability in results. Hence, the comparative method quantum yield of 1.07 was chosen to use for R_0 calculation (See Appendix A for full detail of calculations). Theoretically the quantum yield should be 0 and 1, however since the value obtained for AF350 was slightly above 1, a reason for this may be due to human experimental error. AF350 may also be a difficult molecule to measure quantum yield which may suggest why there have not been any previous calculations for the quantum yield of AF350. Additionally, it is not uncommon for the quantum yield to be above 1 as POPOP in Appendix Table A-1 had a quantum yield 1.00±0.05.

The R_0 was calculated using the acceptor coefficient, orientation of the donor and acceptor transition dipoles (κ^2 =2/3), refractive index of the medium (n =1.34), AF350 quantum yield (ΦD =1.07) and the overlap integral of the AF350 emission and SYPRO Orange/ProteoStat excitation spectra. For AF350-SYPRO Orange, the R_0 was calculated to be 41 Å (when κ^2= 2/3). As there was a range in the extinction

coefficient for ProteoStat (51378 – 109683 $M^{-1}cm^{-1}$), the R_0 was calculated for AF350-ProteoStat to be 53 – 60 Å. Table 6-5 shows a list of known FRET pairs and most reported R_0 values above 40 Å. This means that most FRET pairs require a distance greater than 40 Å to achieve 50% energy transfer. As both the R_0 for AF350 with SYPRO Orange/ProteoStat were above 40 Å, this which gives confidence in the measured R_0 values as the values are within a reasonable distance compared to established FRET pairs. However, this also highlights the short distance required for strong FRET energy transfer.

Table 6-5: R_0 values of known FRET pairs

Donor	Acceptor	Ro (Å)
Fluorescein (FITC)	Tetramethylrhodamine (TRITC)	55
Cy3	Cy5	53
IAEDANS	Fluorescein	46
EDANS	Dabcyl (non-fluorescent)	33
Alexa Fluor 350	Alexa Fluor 488	50
Alexa Fluor 488	Alexa Fluor 546	64
Alexa Fluor 488	QSY 35 (non-fluorescent)	44
Alexa Fluor 546	Alexa Fluor 568	70
Naphthalene	Dansyl	22

6.10. Control 4: Reducing the distance by labelling mAb directly with donor

As mentioned previously, the distance between the donor and acceptor is an important factor for FRET. To investigate the distance issue and see if shortening the distance between the donor and acceptor would strengthen the energy transfer, the donor was attached directly to the mAb instead of protein A (Figure 6-17).

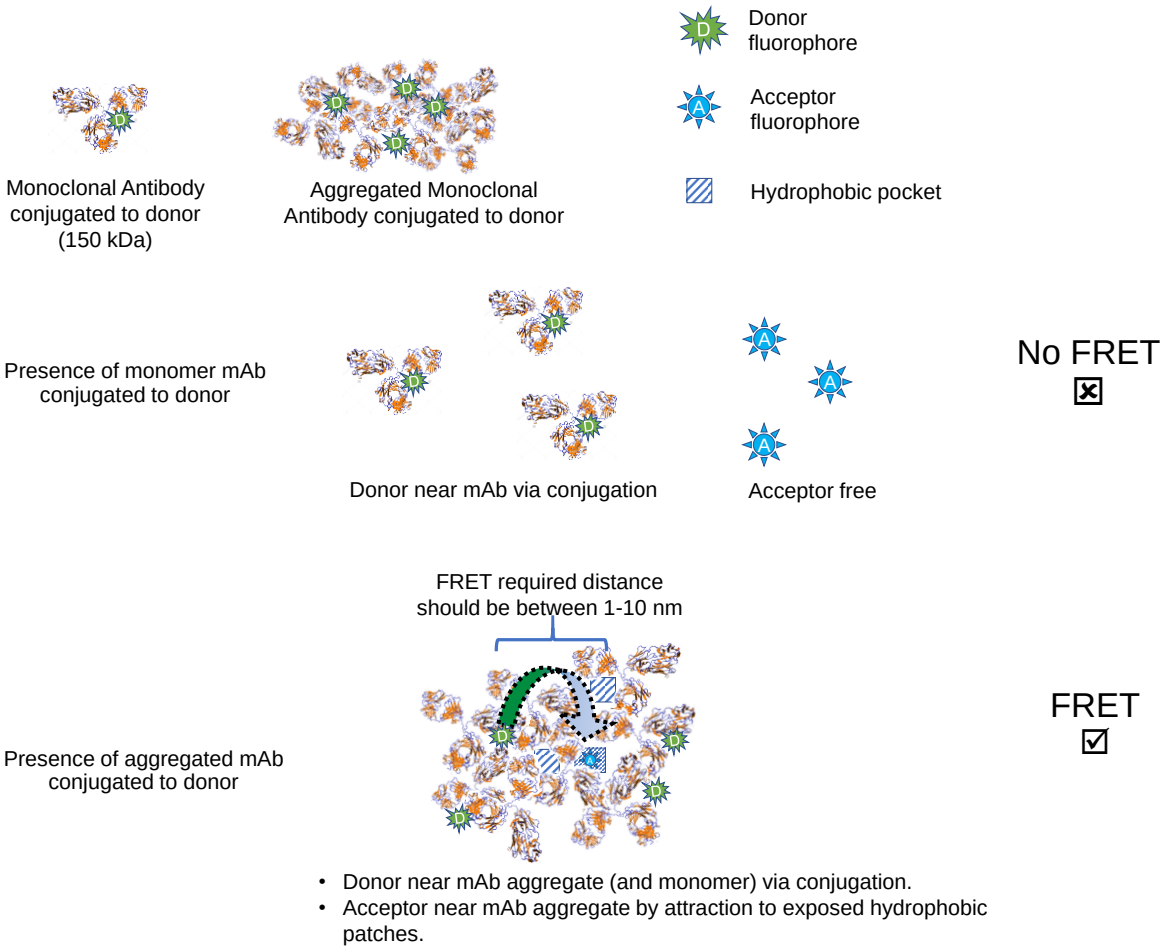

Figure 6-17: Schematic of control 4 where the mAb conjugated to donor dye to reduce the distance between the donor and acceptor.

In Figure 6-18, the change in fluorescence intensity of unstressed and stressed mAb-donor in the presence of the acceptor was compared. Upon stressing, there was an increase in fragmentation as well as aggregation, which was most likely due to various levels of dissociation of the mAb-AF350 complex upon heat stressing. It is not certain

how the fragments may interfere with FRET fluorescence. Therefore, it will be assumed that the donor fluorescence will only be from fully-conjugated mAb-AF350 molecules and that the aggregates formed are predominately aggregated mAb-AF350.

There was an increase in the acceptor fluorescence with increasing mAb-AF350 aggregate for both acceptors. The donor/acceptor fluorescence with 13.8% mAb-AF350 aggregate had the most decrease in donor intensity and highest increase in SYPRO Orange intensity compared to the control. For SYPRO Orange (Figure 6-18A/B), the E_{PR} between the unstressed mAb-AF350 and 13.8% mAb-AF350 aggregate increased by 3.0-fold (Table 6-6). This was twice as strong as the energy transfer seen in initial FRET experiment with Protein A conjugated to the donor (Figure 6-6).

For ProteoStat (Figure 6-18C/D), the E_{PR} between the unstressed mAb-AF350 and 13.8% mAb-AF350 aggregate increased by 1.7-fold (Table 6-6), which was not as great as SYPRO Orange. It was only slightly better than the initial FRET experiment with Protein A conjugated to the donor (Figure 6-7: 1.3-fold increase). All the other stressed mAb-AF350 samples showed a similar amount of decrease in donor intensity. The control, 5.3% and 7.0% mAb-AF350 aggregates had overlapping ProteoStat intensities, however 13.8% mAb-AF350 aggregate had a slightly higher intensity. This higher ProteoStat intensity did not correlate as the 13.8% mAb-AF350 aggregate had the same amount of donor intensity decrease as the other stressed samples.

Overall, even though shortening the distances by conjugating the mAb to the donor slightly improved the energy transfer, the E_{PR} were quite low. As opposed to the distance imposed by the size of protein A, the weak energy transfer may be attributed to the size of mAbs themselves. Aggregated mAbs may be too big for strong energy transfer to occur from donor to acceptor. Therefore, smaller proteins were considered for investigation as an alternative to see if they could provide stronger energy transfer.

Table 6-6: Summary of EPR values for mAb conjugated directly to Alexa Fluor 350

	E_{PR} (%)		Change in E_{PR}
Acceptor	Unstressed mAb	13.8% mAb-AF350 aggregate	
SYPRO Orange	0.48	1.42	3.0-fold increase
ProteoStat	0.78	1.32	1.7-fold increase

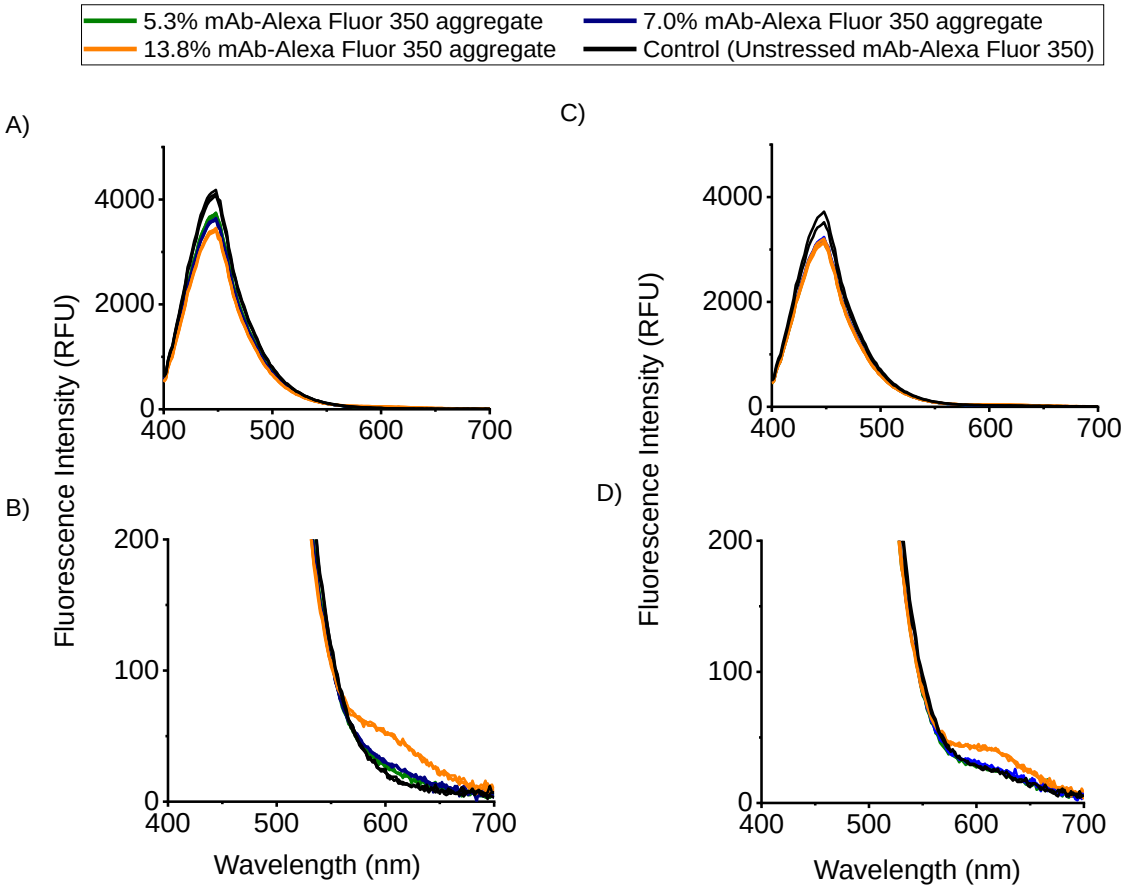

Figure 6-18: Measuring FRET by conjugating the mAb directly to the donor (1 µM mAb-AF350). (A) 5X/9 µM SYPRO Orange and (B) 3 µM ProteoStat.
(C) and (D) are zoomed in versions of acceptor region for (A) and (B) respectively. Unstressed mAb-AF350 had 0.7% aggregates with a 5.5 nm hydrodynamic radius. MAb-AF350 was stressed at the following conditions: 48 hrs at 8.6 µM (5.3% mAb-AF350 aggregate (r_h 5.3 nm)), 72 hrs at 8.6 µM (7.0% mAb-AF350 aggregate (r_h 8.5 nm)), and 72 hrs at 10.2 µM (13.8% mAb-AF350 aggregate (rh 12-13 nm). Concentration of mAb-AF350 in each well was 1 mg/mL.

6.11. Proving FRET assay works at shorter distances with smaller proteins

The main problem with using mAbs with the FRET assay was that the energy transfer was low. The proximity ratio (E_{PR}) was consistently less 2% (with the acceptor of the 100% mAb monomer compared to 100% mAb aggregate experiment). One reason for this may be due to the large size of the mAbs placing the donor and acceptor too far away. Hence, smaller proteins were investigated as an alternative to further reduce the distance between the donor and acceptor. Due to the design of the FRET assay, the alternative protein had to be able to bind to protein A. The most logical option was to use domain antibodies (dAbs), which are a single variable domain (antigen binding region) of a whole antibody (Krah et al., 2016). DAbs can be formed from either the heavy chain or light chain (Figure 6-19), and are roughly a tenth of the size of a full IgG1 molecule (Chen et al., 2009).

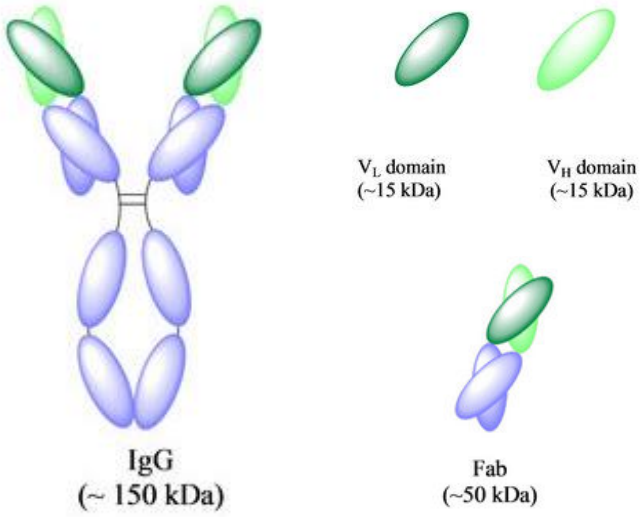

Figure 6-19: Structure of full IgG molecule, domain antibodies (dAbs) from light chain (V_L) and heavy (V_H) chain and fragment antibodies (Fab).
Obtained from Herrington-Symes et al. (2013) with permission from Advances in Bioscience and Biotechnology Journal.

6.11.1 Measurement of the affinity of protein A to dAb

Before conducting the FRET assay, the ability for the dAb to bind to protein A was measured using the Octet. The results in Figure 6-20 saw a rapid saturation (10 seconds) with a steep slope upon the protein A biosensors interacting with the dAb.

Although this confirmed that the dAb could bind to protein compared to BSA, the wavelength shift was 4 nm less compared to mAb binding to protein A (Figure 6-5). This difference is most likely due to mAbs being a bigger molecule than dAbs, and hence able to have an increase in optical thickness at the sensor tip. Additionally, the wash step (> 350 sec) showed dissociation of the dAbs from the sensor tip, meaning that the interaction between the dAb and protein A was weaker than between mAbs and protein A. However as there would not be a wash step in the assay, this was less likely to pose a problem.

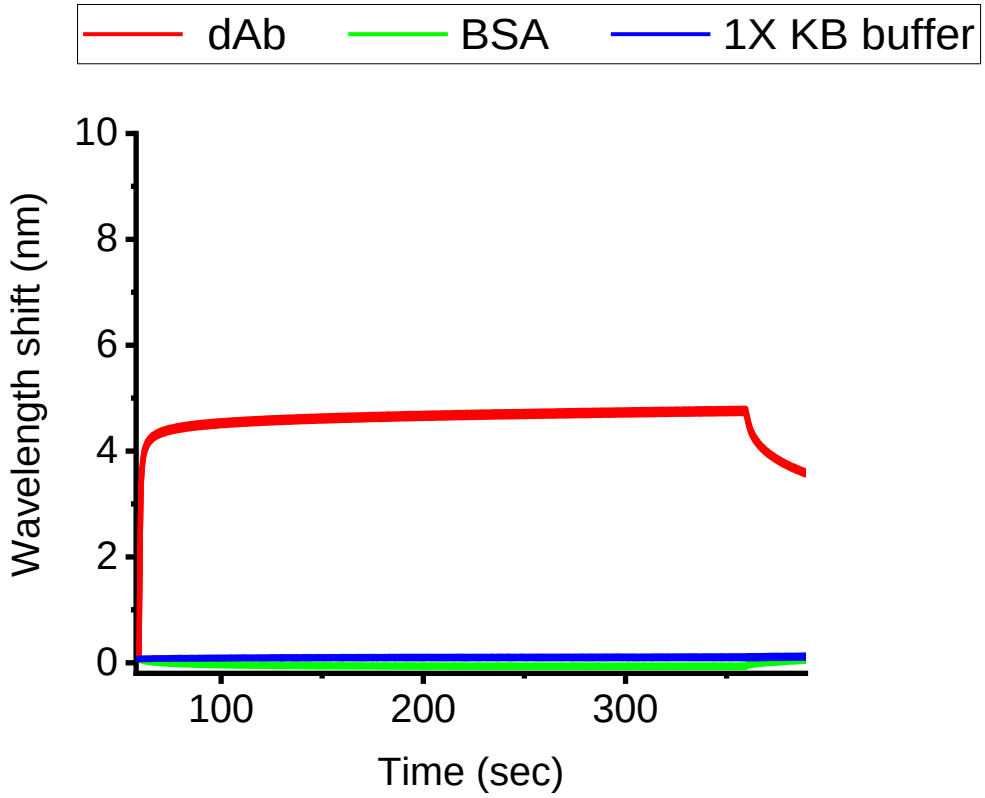

Figure 6-20: Measuring the affinity of protein A to dAb using Octet.
Samples were dAb (1.00 mg/mL, 10% aggregated) in 50 mM sodium acetate pH 5 and BSA (1.0 mg/mL) from ThermoFisher in 0.9% sodium chloride with sodium azide. 80 µL of samples/buffer were aliquoted into black flat bottom 384-well plates. Forte Bio Dip and Read Protein A biosensors were incubated in black 96-well plates with 1X KB for 10 mins prior to run for pre-conditioning. The run temperature was maintained at 30^0C. For the regeneration step, 10 mM glycine pH 1.5 and 1X KB buffer were alternated for 3 rounds.

6.11.2. Measurement of the affinity of acceptors to stressed dAbs

Before assessing FRET, dAbs were first tested to confirm that the acceptor dyes could distinguish between unstressed dAbs (10% aggregated, r_h=3.7 nm) and stressed dAbs (45% aggregated, r_h=4.5 nm). The unstressed dAb naturally had aggregates present; therefore, the comparison was made between lower vs. higher aggregates rather than monomeric vs. aggregated. Both SYPRO Orange and ProteoStat showed an increase in fluorescence intensity with the stressed dAb (45% aggregated). Comparing the fluorescence intensity between the unstressed dAb and stressed dAb, there was a 75% and 96% increase in fluorescence intensity for SYPRO Orange and ProteoStat respectively. As it was confirmed that the dAbs were capable of binding to protein A, and aggregated dAbs could be detected by the acceptor dyes, the next step was to measure FRET in this new system.

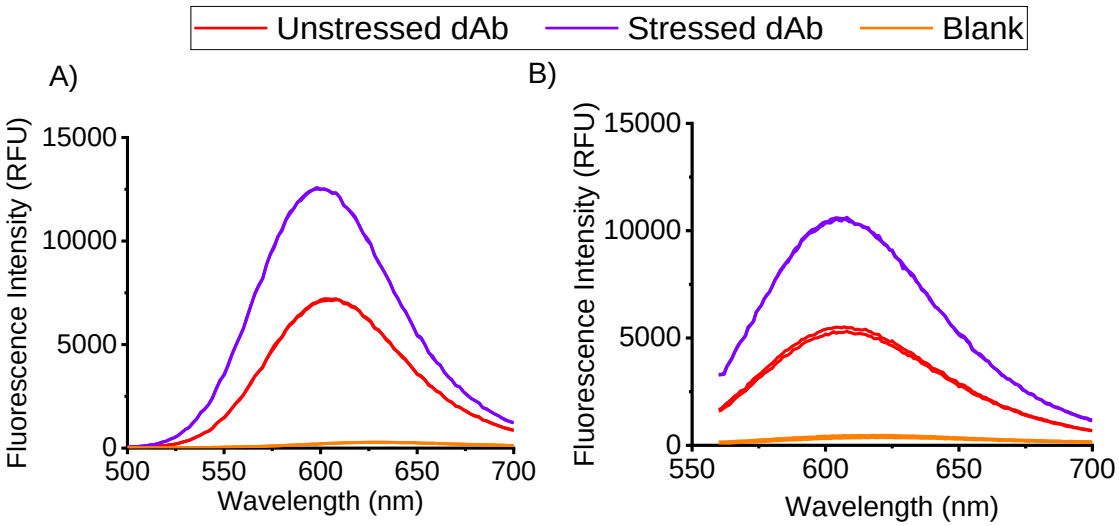

Figure 6-21: Unstressed dAb and stressed dAb in the presence of SYPRO Orange or ProteoStat.
(10% aggregated, r_h=3.7 nm) and stressed dAb (45% aggregated, r_h=4.5 nm) in presence of (A) 5X/9 µM SYPRO Orange (495/500-700 nm) and (B) 3 µM ProteoStat (530/560-700 nm). Concentration of dAb in each well was 1 mg/mL. This was performed in duplicates.

6.11.3. Initial FRET measurement with dAbs

Figure 6-22 shows the FRET results with dAbs with PrA-AF350 and SYPRO Orange/ProteoStat. Compared to the blank, the unstressed and stressed dAbs both showed a clear increase and decrease in acceptor and donor fluorescence intensity respectively. Due to the similar degree of change in the donor/acceptor intensity, the E_{PR} of the 45% aggregated dAb was similar to the 10% aggregated dAb (Table 6-7). The E_{PR} from the dAbs was 10X larger than achieved with mAbs. Showing that smaller molecules improved the energy transfer. However, the assay did not distinguish between unstressed and stressed dAb. Even measuring at lower concentrations of the dAb (7 µM and 2 µM instead of 40 µM (1 mg/mL)) and using Tween-20 in the buffer did not improve the assay's ability to distinguish the unstressed and stressed dAb (See Appendix B). Using another dAb molecule was considered. DAb B was half the size of dAb A, but when dAb B was stressed it formed insoluble aggregates which could not be used for the FRET experiments.

One potential reason why the FRET assay did not distinguish between unstressed and stressed was thought to be due to the unstressed dAb having a similar amount of exposed hydrophobic regions as the stressed dAb. Using a mAbs for comparison, mAbs are much larger than dAbs. By nature (and in some instances by design), the tertiary and quaternary structure can be stabilised by glycosylation moieties, which can cover hydrophobic regions where aggregation can occur (Courtois et al., 2016). DAbs on the other hand, are only a single variable domain of a whole antibody, and in theory may not have near the same amount of folding/protection of hydrophobic areas as mAbs. Therefore, there may be a larger proportion of hydrophobic regions exposed to the solvent even in unstressed form, than typically seen with mAbs. To validate this theory, the exposed hydrophobic regions were modelled (Appendix Figure B-4) and it was confirmed that dAb A had twice the amount of exposed hydrophobic regions than mAb A. Although, it was not certain as to what extent stressing exposed more hydrophobic regions, it could also be the case where by the net effect (in terms of amount of exposed hydrophobic regions) as a result of stressing was similar to that of the unstressed dAb.

Table 6-7: Summary of EPR values for unstressed and stressed dAb

	E_{PR} (%)		Change in E_{PR}
Acceptor	Unstressed dAb	Stressed dAb	
SYPRO Orange	14.9	15.8	1.1-fold increase
ProteoStat	11.6	10.8	0.93-fold decrease

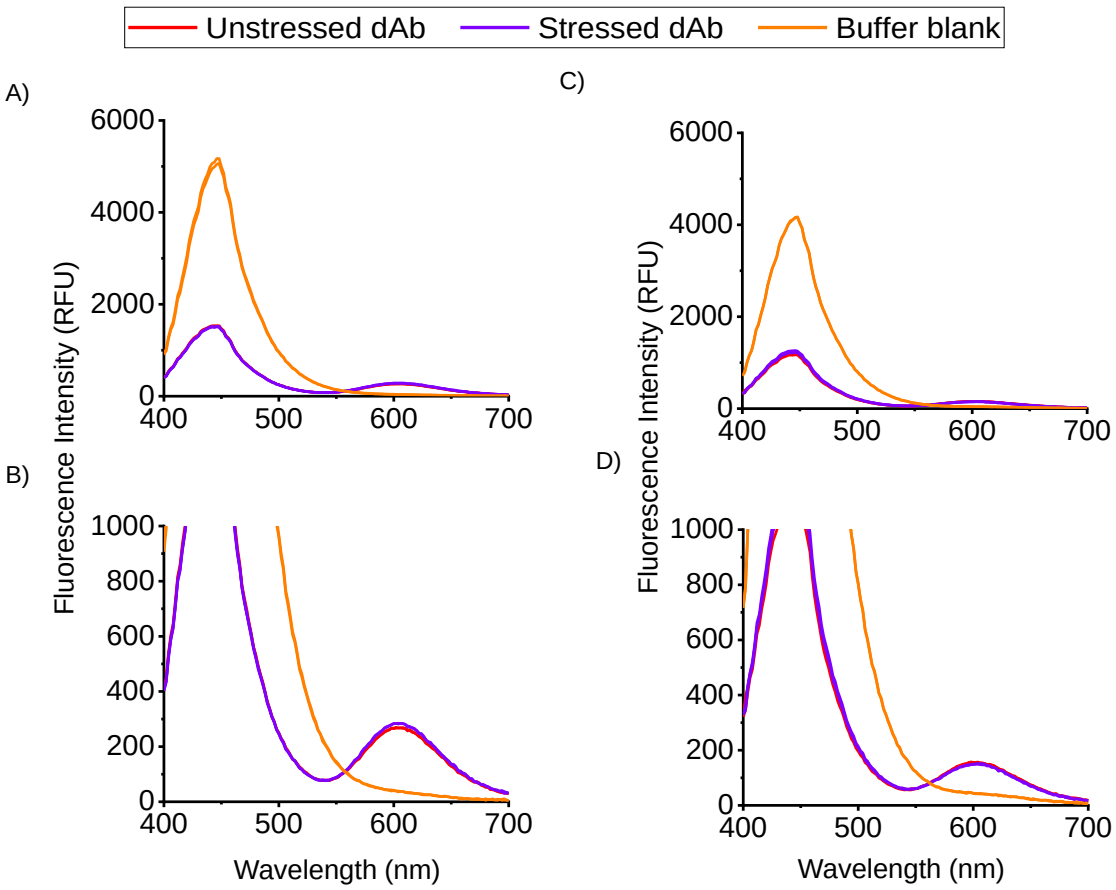

Figure 6-22: FRET with unstressed dAb and stressed dAb.
Unstressed dAb (10% aggregated, r_h=3.7 nm) and stressed dAb (45% aggregated, r_h=4.5 nm) in the presence of 1 µM PrA-AF350 and (A) 5X/9 µM SYPRO Orange, C) 3 µM ProteoStat. (B) and (D) are zoomed in versions of (A) and (C). Excitation/Emission 330 nm/400-700 nm. Concentration of dAb in each well was 1 mg/mL. This was performed in duplicates.

6.11.4. FRET with non-antibody proteins

DAbs showed energy transfer, but there was a lack of distinguishability between the unstressed and stressed forms of the molecule. As an alternative to antibodies, other non-antibody-based proteins were chosen to be investigated with the FRET assay: wheat germ agglutinin and insulin.

Wheat germ agglutinin (WGA, 38 kDa) is a plant lectin widely used in cell biology and is found to bind specifically to N-acetylglucosamine and N-acetylneuraminic acid. The dimeric lectin was readily available to purchase already conjugated to Alexa Fluor 350. As the donor is already conjugated to the protein, FRET was measured by adding the acceptor (Figure 6-23) similar to when the mAb was conjugated directly to the donor in Chapter 6.10.

Insulin (6 kDa) was also chosen as it is a widely known recombinant therapeutic, and hence it was a relevant product to the biopharmaceutical industry. However, upon stressing insulin the molecule fragmented rather than aggregating, and therefore could not be used for the FRET assay. As such the FRET assay was further investigated with only WGA-AF350.

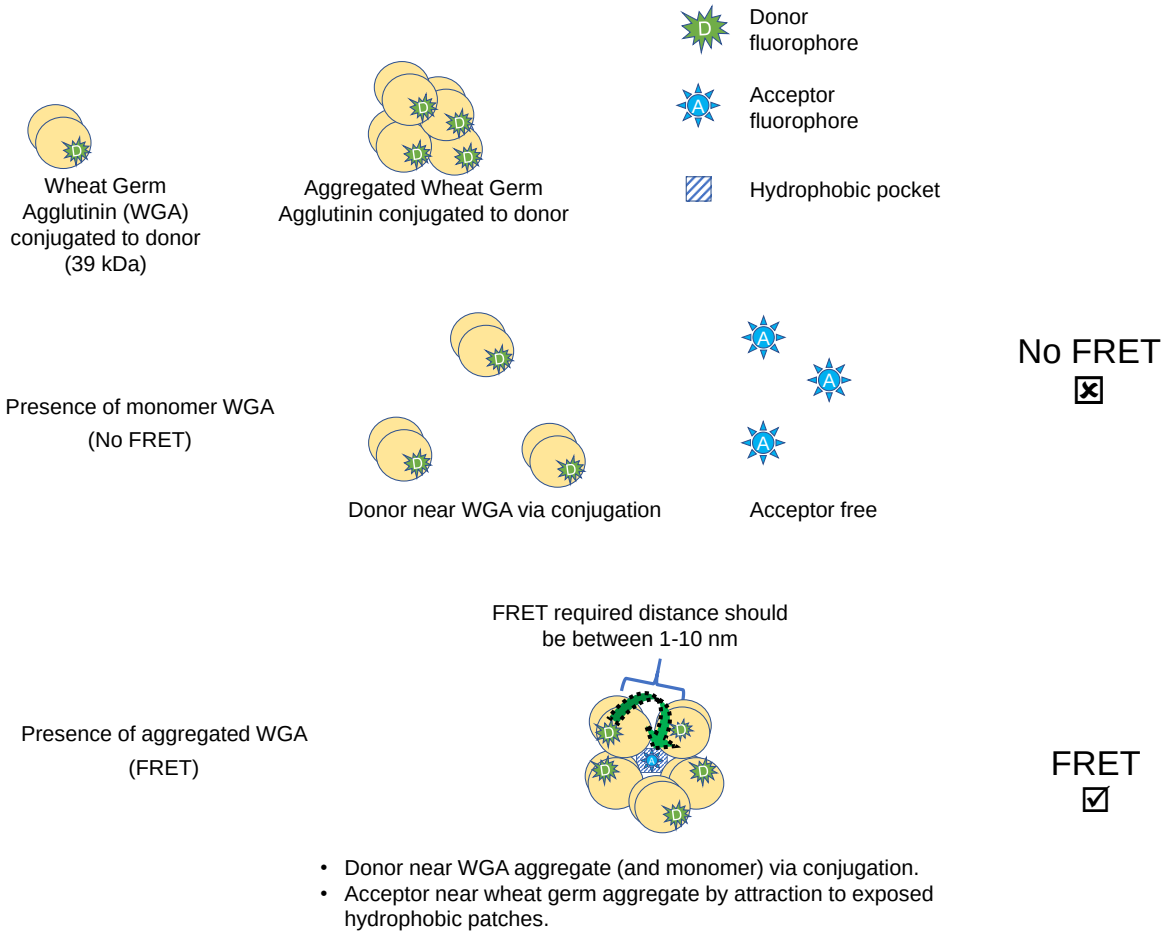

Figure 6-23: Schematic using wheat germ agglutinin-Alexa Fluor 350 (WGA-AF350) for FRET.

To assess the FRET assay with WGA-AF350, unstressed WGA-AF350 (r_h=2.5 nm) was thermally stressed at 60°C for 10 days which generated a 70% WGA-AF350 aggregate sample as measured by SEC. FRET was measured with the stressed WGA-AF350 in the presence of SYPRO Orange and ProteoStat as acceptors (Figure 6-24). There was a clear decrease in the donor fluorescence intensity at 450 nm and increase in the acceptor fluorescence intensity at 600 nm for both acceptors. The increase in the E_{PR} with WGA-AF350 was much greater than with previous molecules (Table 6-8). There was a 15-fold and 24-fold increase in the E_{PR} between the unstressed and stressed WGA-AF350 with SYPRO Orange and ProteoStat respectively.

The dAb alongside the WGA-AF350 clearly show the implication size has on energy transfer; obtaining stronger FRET with smaller molecules. Other than the molecule being the right size for FRET, another reason may be due to the amount of donor dyes on the WGA molecule. The WGA-AF350 was prepared commercially, with 6 molecules of dye per molecule of protein. Self-conjugation kits often achieved lower and varied degree of labelling despite the chemistry being the same (amine-reactive). For example, protein A usually had a range of 1-6 molecules of AF350 per protein A, with 1 molecule per protein A being the most abundant. Therefore, optimised conjugation and clean up (removal of excess dye and homogeneity of degree of labelling) may have also contributed to the improved energy transfer results.

Table 6-8: Summary of EPR values for initial WGA experiment

	E_{PR} (%)		Change in E_{PR}
Acceptor	Unstressed WGA-AF350	Stressed WGA-AF350	
SYPRO Orange	0.48	7.18	15.0-fold increase
ProteoStat	0.59	14.1	24.0-fold increase

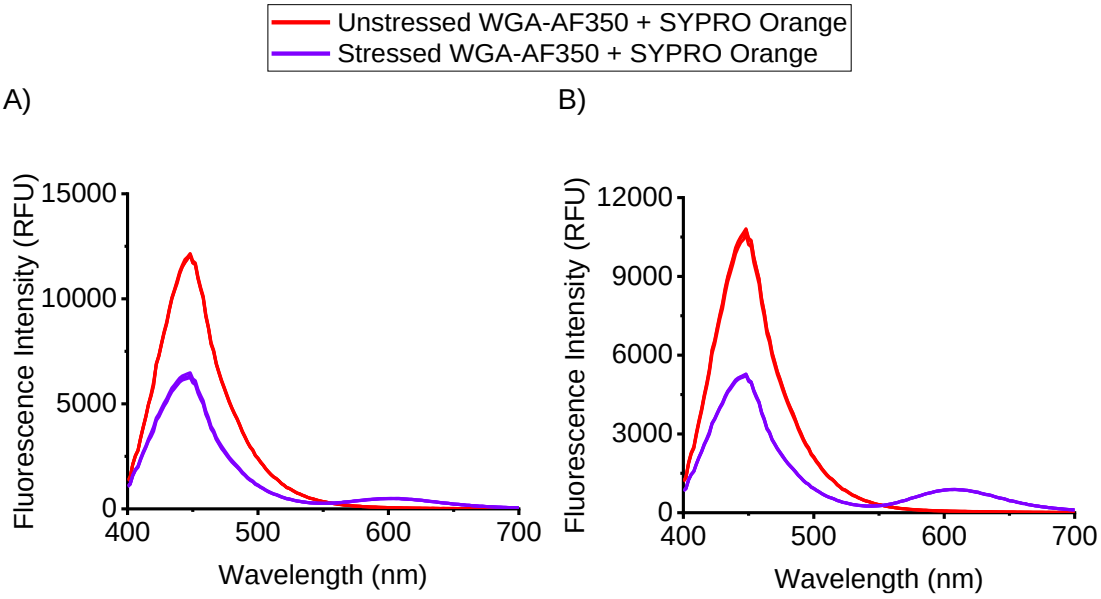

Figure 6-24: FRET with wheat germ agglutinin.
Unstressed Wheat Germ Agglutinin-Alexa Fluor 350 (WGA-AF350) and thermally stressed WGA-AF350 (70% aggregated) in the presence of (A) 5X SYPRO Orange and (B) 3 µM ProteoStat.
Concentration of WGA-AF350 in each well was kept to 1 µM in a 96-well plate and was performed in duplicates. Excitation 330 nm, emission 400-700 nm.

6.11.5. Measuring the sensitivity of FRET assay with non-antibody proteins (purified)

As WGA-AF350 was able to show better FRET, the next step was to understand the sensitivity of the assay. Sensitivity is important as it shows the smallest amount that can be measured reliably by the assay. ICH guidelines state that the detection limit is the lowest amount of analyte which can be detected but not necessarily quantitated as an exact value (ICH, 1994). There are several approaches to determining the detection limit which can be based on: visual evaluation, a signal-to-noise-ratio, the standard deviation of the response and the slope or recommended date. As the fluorescence data was plotted as a standard curve, the detection limit was calculated based on the standard deviation of the response and slope of the change in acceptor (Equation 6-4). To calculate the detection limit, the residual standard deviation was calculated using Equation 6-5. The residual standard deviation is another measure of the goodness-of-fit for data points formed around a linear function and thus describes the

spread of data from the regression line. This method of determining the detection limit for fluorescence data was also used in Kapil et al. (2009) and Mei et al. (2015).

$$\text{Detection limit} = \frac{3.3 \times SD_{res}}{\text{S}}$$

Equation 6-4: Detection Limit. SD_{res} is the residual standard deviation of a regression line. S is the slope of the calibration curve.

$$SD_{res} = \sqrt{\frac{(\Sigma(\text{Y} - Y_{est})^2}{\text{n} - 2}}$$

Equation 6-5: SD_{res} is the residual standard deviation of a regression line. Y is the observed value, Y_{est} is the estimated value from regression line and n is the number of data points.

To measure the sensitivity, a standard curve against different amounts of stressed WGA-AF350 was generated in two different backgrounds (buffer and protein A flow through). For simplicity in analysis, only the change in donor/acceptor intensity was plotted rather than the fluorescence curves.

In Figure 6-25A (purified/buffer background), the decrease in the donor intensity and increase in the SYPRO Orange intensity had a strong linearity. The R^2 for the change in SYPRO Orange intensity (R^2=0.994) was slightly higher than for the change in donor (R^2=0.915) intensity. The linearity with ProteoStat (R^2=0.981) was also slightly higher than for the change in donor (R^2=0.969) intensity, however, were both above 0.95.

The proximity ratio (Figure 6-25C and Figure 6-25D) also increased with increasing amount of WGA-AF350 aggregates, indicating an increase in energy transfer from the donor to the acceptor with increasing aggregation. For SYPRO Orange, the curve was more linear, whereas for ProteoStat the curve became more exponential shaped at higher percentages of aggregates. The detection limit in purified/buffer background

for SYPRO Orange and ProteoStat was found to be 2.92% and 5.30% WGA aggregate respectively.

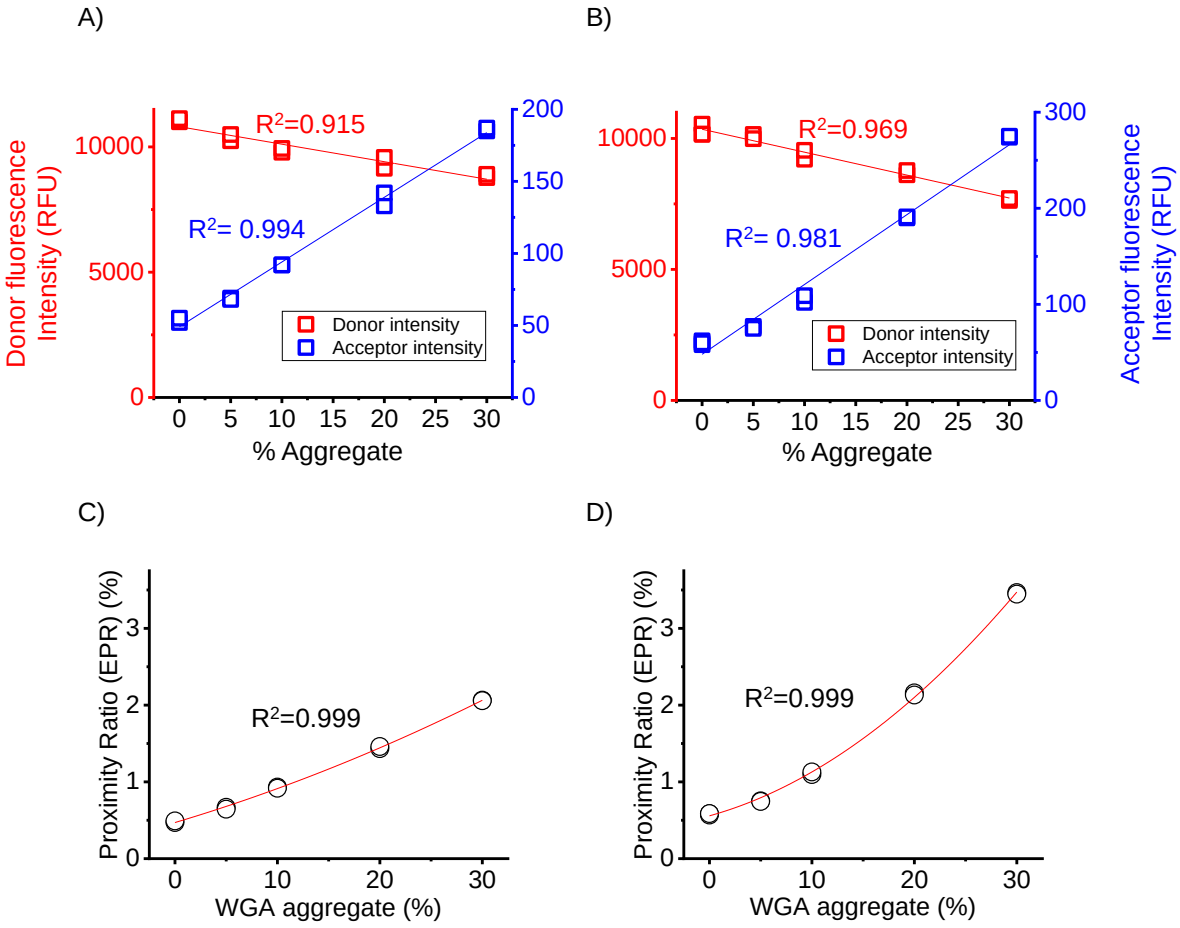

Figure 6-25: FRET with stressed Wheat Germ Agglutinin-Alexa Fluor 350 (WGA-AF350) and acceptor (5X SYPRO Orange or 3 µM ProteoStat) spiked into buffer (PBS pH 7.2).
Comparison of the change in donor fluorescence at 450 nm and acceptor fluorescence at 600 nm with (A) SYPRO Orange and (B) ProteoStat as acceptor. (A) and (B) are fitted with a linear fit. Proximity ratio (EPR) of stressed WGA with (C) SYPRO Orange and (D) ProteoStat as acceptor. (C) and (D) are fitted with a polynomial fit (order=2). Thermally stressed WGA-AF350 (70% aggregated) were spiked into unstressed WGA-AF350 to varying degrees to measure different levels of aggregate. Concentration of WGA-AF350 in each well was kept to 1 µM and was performed in duplicates in a 384-well plate.

6.11.6. Measuring the sensitivity of FRET assay with non-antibody proteins (spent media)

To understand the implication of the media on fluorescence, the FRET assay was repeated with WGA-AF350 in CHO cell culture supernatant obtained from Protein A chromatography flow-through (Figure 6-26). The flow-through had the components that would be present in the mAb CHO cell culture, however the mAbs and cells have been removed by the harvest and Protein A chromatography step. This was to mimic actual cell culture process conditions. Unstressed WGA-AF350 (r_h= 2.5 nm) and 70% aggregate WGA-AF350 (r_h= 12-13 nm) was spiked into protein A flowthrough (spent media) from 0% to 30% aggregated WGA-AF350.

One notable difference between the Figure 6-25 and Figure 6-26, was the CHO cell culture supernatant blank had lower fluorescence intensities of the donor and acceptor compared to the blank in the purified condition. Comparing the linearity of the regression values (R^2) of the buffer (Figure 6-25A and B) to spent media (Figure 6-26A and B), for both acceptors, the R^2 improved slightly in spent media, with all R^2 being above 0.95. In terms of the proximity ratio, for SYPRO Orange (Figure 6-26C), the standard curve was less linear with protein A flowthrough as background. Although there was still an increase in energy transfer from 0% to 30% mAb aggregate, the E_{PR} was slightly higher in purified conditions. The E_{PR} using protein A flowthrough conditions with ProteoStat as acceptor were also slightly less than in purified conditions. The detection limit for SYPRO Orange and ProteoStat in spent media conditions was found to be 5.92% and 4.78% WGA aggregate respectively. For SYPRO Orange, the detection limit was higher in spent media than in purified buffer whereas it was lower for ProteoStat in spent media than in purified buffer. To improve the accuracy this would need to be measured on more than one day to be able to develop an acceptance criteria. The ICH only has an acceptance criteria on detection limits using the signal-to-noise-ratio method.

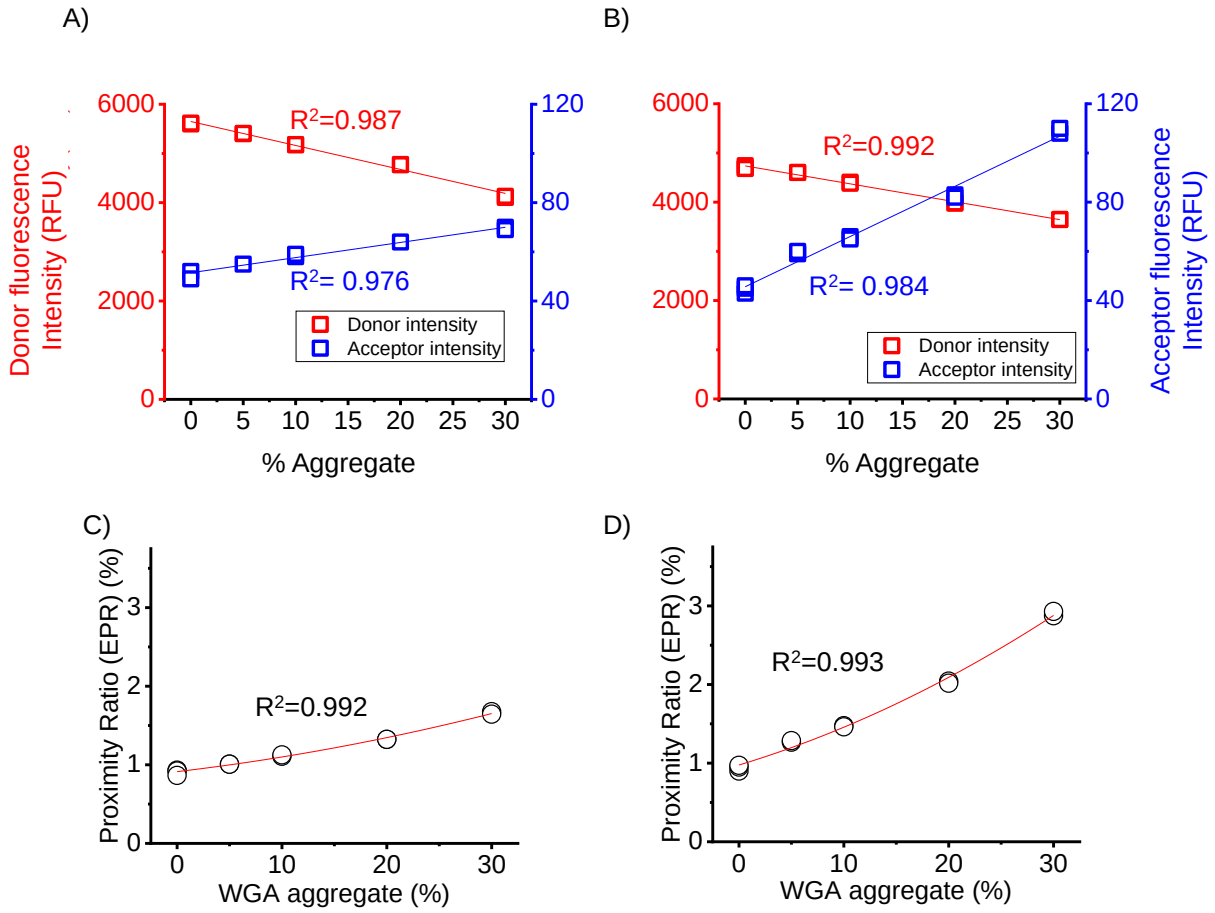

Figure 6-26: FRET with stressed Wheat Germ Agglutinin-Alexa Fluor 350 (WGA-AF350) and acceptor (5X SYPRO Orange or 3 µM ProteoStat) spiked into Protein A flowthrough.
Comparison of the change in donor fluorescence at 450 nm and acceptor fluorescence at 600 nm with (A) SYPRO Orange and (B) ProteoStat as acceptor. (A) and (B) are fitted with a linear fit. Proximity ratio (EPR) of stressed WGA with (C) SYPRO Orange and (D) ProteoStat as acceptor. (C) and (D) are fitted with a polynomial fit (order=2). Thermally stressed WGA-AF350 (70% aggregated) were spiked into unstressed WGA-AF350 to varying degrees to measure different levels of aggregate. Concentration of WGA-AF350 in each well was kept to 1 µM and was performed in duplicates in a 384-well plate.

6.11.7. Key Findings

DAbs were a viable alternative protein to test the FRET assay as they are smaller than mAbs, yet still able bind to protein A. The FRET assay showed energy transfer from the donor to the acceptor however, it was unable to distinguish between the unstressed and stressed dAbs. As dAbs are only a fraction of a full antibody, this would leave more hydrophobic areas exposed to the solvent. Therefore, the similarities in the amount exposed hydrophobic regions between the unstressed and stressed dAb was thought to be a probable reason behind their similar level of energy transfer.

Wheat germ agglutinin (WGA) already conjugated to the donor (Alexa Fluor 350) also saw quantitative energy transfer and visible changes in donor/acceptor intensity between unstressed and stressed WGA-AF350. Overall, between the unstressed and 70% aggregated WGA-AF350, there was a 15-fold and a 24-fold increase in E_{PR} for SYPRO Orange and ProteoStat respectively. 70% aggregated WGA-AF350 achieved an E_{PR} of 7.18% and 14.1% for SYPRO Orange and ProteoStat respectively. This emphasised the improvements of FRET with the use of a smaller (and stable) molecule. The improved FRET results may also be due to better conjugation done commercially rather than with conjugation-kits.

In terms of sensitivity, the FRET assay with WGA-AF350 in purified and spent media conditions provided good linearity with an R^2 above 0.9 and 0.95 respectively for change in donor/acceptor intensity respectively. The E_{PR} for ProteoStat was stronger than SYPRO Orange in both purified and spent media conditions. The detection limit for SYPRO Orange and ProteoStat in purified conditions was found to be 2.92% and 5.30% WGA aggregate respectively. The detection limit for SYPRO Orange and ProteoStat in spent media conditions was found to be 5.92% and 4.78% aggregate respectively.

Overall, the standard curves between the purified and the protein A flowthrough conditions were able to show the assay can measure as low as 5% WGA-AF350 aggregates, which was one of the key criteria for the thesis. In addition, the use of

spent media still resulted in similar trends to purified conditions, highlighting the specificity of the assay in crude conditions.

6.12. Conclusions

Table 6-9 summarises all the key experiments conducted in this FRET chapter and the corresponding proximity values. The initial results from the FRET assay (Table 6-9 Experiment 1) yielded weaker energy transfer than expected and there was a lack of clear decrease/increase in donor/acceptor fluorescence intensities. Four potential scenarios were identified as causes of weak/lack of energy transfer: 1) the use of partially aggregated mAb, 2) acceptor not fluorescing, 3) transition dipole orientation and spectral overlaps not sufficient and 4) impact of the different buffer components. The control experiments confirmed that AF350 and SYPRO Orange/ProteoStat were suitable pairs in terms of overlap wavelengths. However, there was improved energy transfer/E_{PR} when the distance between the donor and the acceptor was reduced which coincidentally occurred with smaller proteins (wheat germ agglutinin and dAbs). The design of the FRET assay with protein put a large distance between the donor and the acceptor.

Reflecting on the aims of the assay/thesis, the FRET assay did not work with mAbs as the design of the FRET assay with protein A put a large distance (>20-90Å) between the donor and the acceptor. In addition, the FRET design with protein A had limitations as it would only be able to measure aggregates that have the Fc portion of the molecule free for binding which may not always be the case depending on the nature of the aggregate.

The importance of distance was also emphasised when the R_0 for the FRET pairs were measured to be 41 Å and 53-60 Å for AF350-SYPRO Orange and AF350-ProteoStat respectively. Energy transfer was improved by reducing the distance by using smaller proteins. The FRET assay with wheat germ agglutinin-AF350 was able to show quantification down to 5% aggregate in purified and CHO host cell protein background.

However, not all small proteins were found suitable for FRET. Figure 6-27 details the key questions to use to determine whether a protein is suitable for the FRET assay. The protein of interest needs to have a soluble aggregated form. This was not the case for insulin (data not shown) and some dAbs molecules that either fragmented or formed insoluble aggregates upon stressing. The protein of interest should also only have exposed hydrophobic regions in its aggregated form, if not it would have similar results to the dAb (unable to distinguish unstressed and stressed protein). As the assay worked with wheat germ agglutinin conjugated directly to the donor, ideally the protein of interest would need to be conjugated directly to the donor dye.

Overall, the FRET assay is a long way from completion. There was a lot of troubleshooting that took longer than expected in order to and understand of the FRET assay and the results. Most of this was because the FRET design utilised FRET in an unconventional way – with large molecules and both the donor and acceptors free in solution. FRET is normally used with small proteins and nucleotides, typically with either the donor and/or acceptor immobilised onto the small proteins and nucleotides. Working in a 3D environment with both the donor and acceptors free in solution increased the difficulty of obtaining a strong FRET signal. Even still, there is a lot of room to improve and move forward with the assay which will be discussed in the next section.

Table 6-9: Summary of key progress in FRET experiments.
Increase/decrease is relative from the EPR from unstressed/monomer to aggregated mAb/dAb.

Experiment	Measurement of FRET by E_{PR}		
	SYPRO Orange (acceptor)	**ProteoStat (acceptor)**	**Key findings**
1) MAbs (MW: 150 kDa)	Unstressed mAb: 0.61% 13% aggregated mAb: 1.06% **Increase by 1.7-fold**	Unstressed mAb: 0.76% 13% aggregated mAb: 0.96% **Increase by 1.3-fold**	Weak energy transfer, lack of clear decrease/increase in donor/acceptor fluorescence intensities
2) MAbs: 100% monomer vs aggregate (MW: 150 kDa)	100% monomer mAb: 0.65% 100% aggregated mAb: 2.76% **Increase by 4.2-fold**	100% monomer mAb: 0.90% 100% aggregated mAb: 2.32% **Increase by 2.6-fold**	Improved energy transfer using a fully aggregated sample. Donor intensity remain unchanged therefore difficult to attribute the improved E_{PR} solely to improved energy transfer.
3) MAbs: Labelling mAb with donor (MW: 150 kDa)	Unstressed mAb-AF350: 0.48% 13.8% mAb-AF350 aggregate: 1.42% **Increase by 3.0-fold**	Unstressed mAb-AF350: 0.78% 13.8% mAb-AF350 aggregate: 1.32% **Increase by 1.7-fold**	Compared to Experiment 1, improved energy transfer. E_{PR} values still low.
4) DAbs (MW: 25 kDa)	Unstressed dAb (10% agg): 14.9% 45% aggregated dAb: 15.8% **Increase by 1.1-fold**	Unstressed dAb (10% agg): 11.6% 45% aggregated dAb 10.8% **Decrease by 0.93-fold**	Stronger energy transfer/E_{PR} values achieved, however lack of specificity to dAb aggregates.
5) Wheat germ agglutinin (MW: 38 kDa)	Unstressed WGA-AF350: 0.48% 70% aggregated WGA-AF350: 7.18% **Increase by 15-fold**	Unstressed WGA-AF350: 0.59% 70% aggregated WGA-AF350: 14.1% **Increase by 24-fold**	Stronger FRET achieved in both purified and CHO media containing HCP

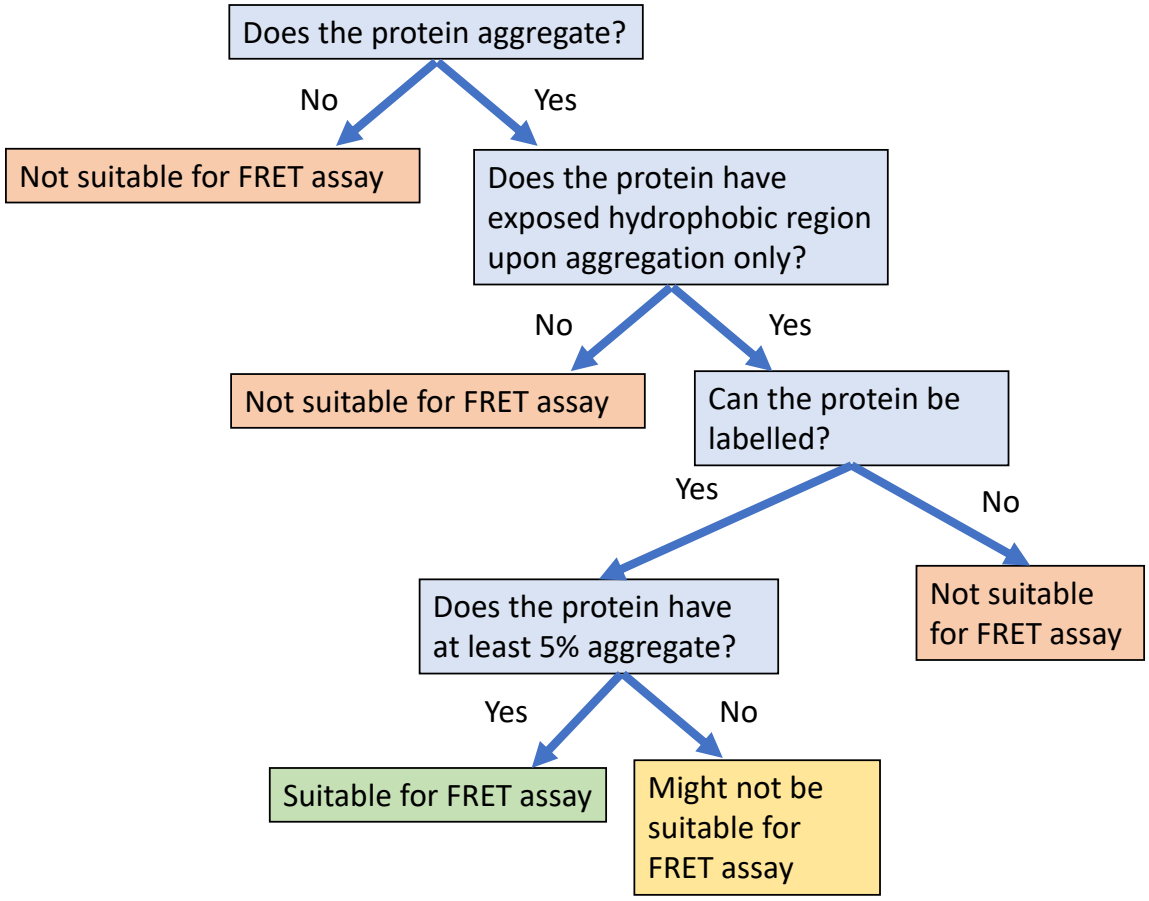

Figure 6-27: FRET decision-tree

7 Conclusion and Future work

7.1. Conclusions

The aim of this thesis was to create a quantitative high-throughput assay to measure mAb aggregation directly from CHO cell cultures for biopharmaceutical process development. The focus was to build an assay for use in cell line selection to measure directly in complex cell culture supernatants. The assay needed to be robust and accurate in distinguishing good cell lines with less mAb aggregates, from cell lines with large amounts of mAb aggregates. In addition, minimal sample preparation (e.g. purification) was essential as key components (e.g. large aggregates) may be removed, thus ultimately providing data that may not be a true representation of the cell culture. In terms of aggregate characteristics, the focus was to measure the traditional problematic ranges typically seen within industry: soluble, small-to-medium sized aggregates (<100 nm, dimer to large aggregates), and to detect in the range 1-10% of total mAb aggregate.

Thesis Objectives A focused on investigating the use of fluorescent dyes with mAbs in cell culture supernatant. Fluorescent dyes (Bis-ANS, SYPRO Orange, ThT and ProteoStat) with known to sensitivity measure aggregates, were shown on their own, not to be a specific indicator of mAb aggregation when applied to cell culture supernatants. All four dyes used were able to identify down to 5% mAb aggregates in purified conditions (Obj A1). However, the presence of host cell protein caused interference (Obj A2 and A3). Even so, SEC indicated the size of species that the fluorescent dyes were more sensitive to (SYPRO Orange – large aggregates, ProteoStat – aggregates, monomer and fragments) (Obj A4). To circumvent this problem with the initial dye assay, specificity was attempted to be introduced into the assay in two ways: by the addition of an affinity peptide that had been shown to be specific to mAb aggregates in a previous study, and by designing a FRET assay.

Assessing the biotinylated affinity peptide with the biosensor instruments (Octet and Biacore) (Obj B1), weak affinity to mAb aggregate and non-specific interactions were seen in both instruments. The biotinylated affinity peptide in the Octet (plate

biosensor) was only capable of distinguishing 100% mAb monomer and 100% mAb aggregate after a long period of incubation at weak intensities. On the Biacore (flow-cell biosensor), weak interactions were also seen, alongside non-specific interactions between the mAb and streptavidin sensor. Although the fluorescent affinity peptide seemed promising, it failed to show improved specificity compared to the fluorescent dyes on their own suggesting a lack of specificity in this application (Obj B2 and B3). To check this, hydrogen deuterium exchange was used with the unlabelled peptide and mAb aggregate, and there was no clear indicator of binding region or affinity (Obj B4). Therefore, it was concluded that there needed to be a more detailed understanding of how the binding/interaction worked to achieve the positive results seen in the original study. Subsequently, the design of the peptides would need to be altered to ensure the affinity peptide is labelled in a way that has minimal steric hindrance in binding.

The FRET assay was designed by choosing the appropriate donor and acceptors and using protein A with specificity to mAb aggregates (Obj C1). Troubleshooting the weak energy transfer and conducting controls such as approximating Forster radius for the system, showed mAb aggregates were too big to achieve distances needed for FRET (Obj C2 and C3). Smaller molecules achieved stronger energy transfer seen both quantitatively and qualitatively (Obj C4). Reflecting on the assay criteria, the assay was able to reliably distinguish wheat-germ agglutinin aggregates (selected as example of small non-antibody-based protein) down to 5% aggregates with a standard curve achieving a strong linear fit (R^2>0.9). The assay also required minimal sample preparation as it only needed the dye components to be added to the culture. The assay was also used at low volumes in 384-well plate with 50 µL (sample and FRET components combined) and tested in CHO host cell protein background to prove the assays capability to measure protein aggregation directly from CHO cell cultures.

7.2 Future work

The future work can be addressed in three sections: short-term, mid-term and long-term plans.

7.2.1. Short-term

Use of dye to identify large aggregates

From the initial dye assay, SYPRO Orange displayed sensitivity to large aggregates. A potential application is to use SYPRO Orange to highlight cell lines which may produce large aggregates during mAb cell culture which may cause issues during harvest. The harvest step usually involves the use of filtration (e.g. depth filtration). The presence of large aggregates can make filtration more difficult as pores can be blocked more easily, requiring more filter units to achieve the desired clarification. SYPRO Orange could be used in the cell culture supernatant of mAb producing cell lines to aid cell line selection in maximising viabilities and minimising the amount of protein aggregates. Using SYPRO Orange would not only help pick the best cell line that would produce the candidate mAb with the least amount of total aggregates, but also help decide which day would be better to harvest considering manufacturability, as well as productivity.

Determining the size range suitable measuring protein aggregation with FRET assay

Although the FRET assay was shown to be more suitable for aggregates of smaller proteins, it is not known what the size limit would be. As the assay was not suitable for mAbs (150 kDa) but worked with a 40 kDa lectin, it makes sense to conduct the FRET assay with a range of proteins between 40-150 kDa to find out where the cut-off point of the assay is. Proteins would either need to be purchased conjugated to the donor dye or self-conjugated using kits. Proteins which could be used are: concanavalin A (100 kDa lectin) and neutrAvidin (60 kDa).

Robustness of assay to different types of aggregates

Another short-term future work objective for the FRET assay would be to test out the assay with aggregates generated by different stresses. All the stressed proteins in this thesis were generated by thermal stressing. Using aggregates generated by different types of stresses (e.g. agitation or pH induced) would aid in validating the results of

the assay and/or may indicate the limits of the assay in terms of types of aggregates that can be detected.

7.2.2. Mid-term

Improve labelling using kits and find optimal ratios of assay components

Commercial wheat germ agglutinin had more donor dye conjugated per molecule than protein A. As mentioned in the FRET chapter, the amount of conjugated donor may have also played a role in improving the strength of energy transfer. Therefore, some ideas to improve labelling include: 1) finding the optimal number of donor dyes required on the protein of interest, 2) finding out what region of the protein the donor dye is binding to, and 3) finding a way to make labelling consistent and reproducible (by potentially using other covalent bonding techniques). Other aspects of the FRET assay that needs to be optimised are the concentration/ratio of donor, protein and acceptor.

Understanding the mechanism and location of mAb aggregates binding to affinity peptide

In order to develop an assay that would work for mAbs, the affinity peptide has the most potential as it has been technically proven to have affinity towards aggregated mAbs. In the context of the thesis, it did not work as well the published literature, due to lack of understanding of how the affinity peptide works in the absence of any labelling. Therefore, in the continued efforts to develop an assay to measure the aggregation of mAbs, further understanding into where the binding region is, how it works and quantifying how the level of affinity differs between unaggregated and aggregated mAb would be necessary.

A first step towards understanding the affinity would be to reproduce the results of the original work published that was able to distinguish mAb monomer from mAb aggregates. There are three different ways in which this could be done. The first is to conduct the same phage ELISA as in the study by using immobilised mAb aggregate to a well plate and measuring the degree of binding to phage (displaying the AP).

Detection would occur using the fluorescent anti-phage antibodies. The second way would be to "reverse" the ELISA, by immobilising the AP to a well and incubating with mAb aggregate. After washing unbound aggregate, fluorescent anti-antibody could be used for detection. The third way would be to use NMR or mass spectrometry with an isotope labelled-AP to detect binding to mAb aggregates.

Another factor to investigate is to see whether the AP binds stronger to larger or smaller aggregates. The aggregates used in the original study were cross-linked to generate stable aggregates however, it created a mixture of small (~7 nm) and large (~250 nm) aggregates. As the aggregates were not separated, there was no indication of whether the AP bound to smaller or larger aggregates. Therefore, by using the cross-linking method and purifying/separating out the different sized aggregates, it would be clearer the influence of size on the assay's ability to detect aggregates.

Once the binding site has been identified, the affinity peptide could be redesigned in various formats. These include varying the length of spacers between the peptide and the label (biotin/dye), changing the location of the biotin/dye, using alternative dyes or different types of labelling to allow nanomolar/picomolar amounts of the peptide to be used without hindering sensitivity of detection. Additionally, there was a four-amino acid residue sequence (GGGS) that was included in the sequence used to connect the peptide to the pIII protein of phage. However, it was unknown whether the sequence aided in binding ability. Therefore, it would also be worth producing the peptide with and without the sequence to see if there is an impact on the binding.

7.2.3. Long-term

From a wider perspective, there are a few future trends looking towards improving the manufacturability of therapeutic proteins. In terms of assay development, aggregation is not the only critical quality attribute of interest that can benefit from having assays capable of early detection in crude feeds. Other quality attributes of interest include measuring: glycosylation (in particular the degree of mannosylation, galactosylation, fuscosylation and sialyation) and impurities such as host cell protein which are further discussed in the published review paper (Oshinbolu et al., 2018b).

The continued shift to accelerate biologic manufacturing of mAbs, vaccines, and novel biotherapies is moving from just improving individual steps and more towards improving the upstream and downstream processes together as one unified process than separate streams. There is also a motivation to head towards continuous manufacturing as it has the potential to increase efficiency, flexibility, agility and robustness of manufacturing. It can achieve this by reducing the number of steps and holds and using smaller equipment and facilities (Dream, 2018). Analytical assays will need to be able to support this increase in productivity by being high throughput yet still robust. In addition, there is a growing use of automation in the industry. A future plan with analytical assay is to develop them in a way such that they can be automated to run on liquid handling equipment such as TECAN. If the assay could be used alongside automated bioreactors systems (e.g. GE Healthcare's ambr systems) for cell line selection, then it will reduce the amount of human error and shorten the time taken to complete the assay.

References

AAT BIOQUEST. 2017. *Tide Fluor™ 2, succinimidyl ester [TF2 SE]*Superior replacement for fluorescein** [Online]. AAT Bioquest. Available: https://www.aatbio.com/products/tide-fluor-2-succinimidyl-ester-tf2-se-superior-replacement-for-fluorescein [Accessed].

ALLEN, M. W. 2010. Measurement of Fluorescence Quantum Yields. Technical Note 52019. *ThermoFisher*.

BAJAR, B. T., WANG, E. S., ZHANG, S., LIN, M. Z. & CHU, J. 2016. A Guide to Fluorescent Protein FRET Pairs. *Sensors (Basel),* 16.

BERKOWITZ, S. A. 2006. Role of analytical ultracentrifugation in assessing the aggregation of protein biopharmaceuticals. *AAPS J,* 8**,** E590-605.

BIDDLECOMBE, J. G., CRAIG, A. V., ZHANG, H., UDDIN, S., MULOT, S., FISH, B. C. & BRACEWELL, D. G. 2007. Determining antibody stability: creation of solid-liquid interfacial effects within a high shear environment. *Biotechnol Prog,* 23**,** 1218-22.

BOTHRA, A., BHATTACHARYYA, A., MUKHOPADHYAY, C., BHATTACHARYYA, K. & ROY, S. 1998. A fluorescence spectroscopic and molecular dynamics study of bis-ANS/protein interaction. *J Biomol Struct Dyn,* 15**,** 959-66.

BRADER, M. L., ESTEY, T., BAI, S., ALSTON, R. W., LUCAS, K. K., LANTZ, S., LANDSMAN, P. & MALONEY, K. M. 2015. Examination of Thermal Unfolding and Aggregation Profiles of a Series of Developable Therapeutic Monoclonal Antibodies. *Molecular Pharmaceutics,* 12**,** 1005-1017.

BÜNTEMEYER, H. & LEHMANN, J. 2001. The Role of Vitamins in Cell Culture Media. *In:* LINDNER-OLSSON, E., CHATZISSAVIDOU, N. & LÜLLAU, E. (eds.) *Animal Cell Technology: From Target to Market: Proceedings of the 17th ESACT Meeting Tylösand, Sweden, June 10–14, 2001*. Dordrecht: Springer Netherlands.

CALVET, A. & RYDER, A. G. 2014. Monitoring cell culture media degradation using surface enhanced Raman scattering (SERS) spectroscopy. *Anal Chim Acta,* 840**,** 58-67.

CAO, G. & BRINKER, C. J. 2008. Optical and Dynamic properties of Semiconductors Nanostructure. *Annual Review of Nano Research, Volume 2.*

CAPITO, F., SKUDAS, R., KOLMAR, H. & HUNZINGER, C. 2013. Mid-infrared spectroscopy-based antibody aggregate quantification in cell culture fluids. *Biotechnol J,* 8**,** 912-7.

CHAMPION, K., MADDEN. H, DOUGHERTY. J & SHACTER E 2005. Defining Your Product Profile and Maintaining Control Over It, Part 2: Challenges of Monitoring Host Cell Protein Impurities. *BioProcess International,* 3**,** 52-27.

CHEN, A. K., CHENG, Z., BEHLKE, M. A. & TSOURKAS, A. 2008. Assessing the sensitivity of commercially available fluorophores to the intracellular environment. *Anal Chem,* 80**,** 7437-44.

CHEN, W., ZHU, Z., XIAO, X. & DIMITROV, D. S. 2009. Construction of a human antibody domain (VH) library. *Methods Mol Biol,* 525**,** 81-99, xiii.

CHEN, X. & GE, Y. 2013. Ultra-High Pressure Fast Size Exclusion Chromatography for Top-Down Proteomics. *Proteomics,* 13**,** 10.1002/pmic.201200594.

CHEN, Y. & BARKLEY, M. D. 1998. Toward Understanding Tryptophan Fluorescence in Proteins. *Biochemistry,* 37**,** 9976-9982.
CHEUNG, C. S., ANDERSON, K. W., PATEL, P. M., CADE, K. L., PHINNEY, K. W. & TURKO, I. V. 2017. A new approach to quantification of mAb aggregates using peptide affinity probes. *Sci Rep,* 7**,** 42497.
CHON, J. H. & ZARBIS-PAPASTOITSIS, G. 2011. Advances in the production and downstream processing of antibodies. *N Biotechnol,* 28**,** 458-63.
COLE, J. L., LARY, J. W., T, P. M. & LAUE, T. M. 2008. Analytical ultracentrifugation: sedimentation velocity and sedimentation equilibrium. *Methods Cell Biol,* 84**,** 143-79.
COURTOIS, F., AGRAWAL, N. J., LAUER, T. M. & TROUT, B. L. 2016. Rational design of therapeutic mAbs against aggregation through protein engineering and incorporation of glycosylation motifs applied to bevacizumab. *MAbs,* 8**,** 99-112.
CROMWELL, M. E., HILARIO, E. & JACOBSON, F. 2006. Protein aggregation and bioprocessing. *AAPS J,* 8**,** E572-9.
DEMEULE, B., GURNY, R. & ARVINTE, T. 2007a. Detection and characterization of protein aggregates by fluorescence microscopy. *Int J Pharm,* 329**,** 37-45.
DEMEULE, B., LAWRENCE, M. J., DRAKE, A. F., GURNY, R. & ARVINTE, T. 2007b. Characterization of protein aggregation: the case of a therapeutic immunoglobulin. *Biochim Biophys Acta,* 1774**,** 146-53.
DEMEULE, B., PALAIS, C., MACHAIDZE, G., GURNY, R. & ARVINTE, T. 2009. New methods allowing the detection of protein aggregates: a case study on trastuzumab. *MAbs,* 1**,** 142-50.
DEN ENGELSMAN, J., GARIDEL, P., SMULDERS, R., KOLL, H., SMITH, B., BASSARAB, S., SEIDL, A., HAINZL, O. & JISKOOT, W. 2011. Strategies for the assessment of protein aggregates in pharmaceutical biotech product development. *Pharm Res,* 28**,** 920-33.
DENGL, S., WEHMER, M., HESSE, F., LIPSMEIER, F., POPP, O. & LANG, K. 2013. Aggregation and chemical modification of monoclonal antibodies under upstream processing conditions. *Pharm Res,* 30**,** 1380-99.
DIEDERICH, P., HANSEN, S. K., OELMEIER, S. A., STOLZENBERGER, B. & HUBBUCH, J. 2011. A sub-two minutes method for monoclonal antibody-aggregate quantification using parallel interlaced size exclusion high performance liquid chromatography. *Journal of Chromatography A,* 1218**,** 9010-9018.
DREAM, R. 2018. *CQAs Challenges and Impact on End-To-End Integrated Continuous Biomanufacturing* [Online]. American Pharmaceutical Review. Available: https://www.americanpharmaceuticalreview.com/Featured-Articles/355185-CQAs-Challenges-and-Impact-on-End-To-End-Integrated-Continuous-Biomanufacturing/ [Accessed 2019].
ENZO LIFE SCIENCES. *PROTEOSTAT Protein aggregation assay: for microplates of flow cytometry: product manual* [Online]. Available: http://www.enzolifesciences.com/ENZ-51023/proteostat-protein-aggregation-assay/ [Accessed].
FDA. 2014. *Guidance for industry: immunogenicity assessment for therapeutic protein products* [Online]. Available:

http://www.fda.gov/downloads/drugs/guidancecomplianceregulatoryinformation/guidances/ucm338856.pdf. [Accessed 1 June 2017].
FEKETE, S., GANZLER, K. & GUILLARME, D. 2013. Critical evaluation of fast size exclusion chromatographic separations of protein aggregates, applying sub-2μm particles. *Journal of Pharmaceutical and Biomedical Analysis,* 78-79**,** 141-149.
FINKLER, C. & KRUMMEN, L. 2016. Introduction to the application of QbD principles for the development of monoclonal antibodies. *Biologicals,* 44**,** 282-90.
FLETCHER, A. N. 1969. Quinine Sulfate as a fluorescence quantum yield standard. *Photochemistry and Photobiology,* 9**,** 439-444.
FLUORTOOLS. 2015. *a|e - UV-Vis-IR Spectral Software 1.2* [Online]. Available: www.fluortools.com [Accessed].
FONIN, A. V., SULATSKAYA, A. I., KUZNETSOVA, I. M. & TUROVEROV, K. K. 2014. Fluorescence of dyes in solutions with high absorbance. Inner filter effect correction. *PLoS One,* 9**,** e103878.
FORTE BIO 2018. Technical Note 40: High Precision Streptavidin Biosensor (SAX) Quantitation and Kinetic Assays. *Forte Bio.*
GE HEALTHCARE LIFE SCIENCES. 2013. *GE Biacore T100 training course_basics PDF* [Online]. [Accessed].
GOLDBERG, D. S., BISHOP, S. M., SHAH, A. U. & SATHISH, H. A. 2011. Formulation development of therapeutic monoclonal antibodies using high-throughput fluorescence and static light scattering techniques: role of conformational and colloidal stability. *J Pharm Sci,* 100**,** 1306-15.
GROENNING, M. 2010. Binding mode of Thioflavin T and other molecular probes in the context of amyloid fibrils-current status. *J Chem Biol,* 3**,** 1-18.
HACKL, E. V., DARKWAH, J., SMITH, G. & ERMOLINA, I. 2015. Effect of acidic and basic pH on Thioflavin T absorbance and fluorescence. *European Biophysics Journal,* 44**,** 249-261.
HAKAMI, A. R., BALL, J. K. & TARR, A. W. 2015. Non-ionic detergents facilitate non-specific binding of M13 bacteriophage to polystyrene surfaces. *J Virol Methods,* 221**,** 1-8.
HALL. M, HILL. D & D, P. 2017. *Global Pharmaceuticals, 2016 industry statistics.* [Online]. Hardman&co. Available: http://www.hardmanandco.com/docs/default-source/sector-docs/life-sciences-documents/02.03.17-global-pharmaceutical-industry-2016-statistics.pdf [Accessed 1 August 2017].
HAUGLAND, R., SINGER, V., JONES, L. & STEINBERG, T. 1996. *Merocyanine Dye Protein Stains*. US patent application.
HAWE, A., FILIPE, V. & JISKOOT, W. 2010. Fluorescent Molecular Rotors as Dyes to Characterize Polysorbate-Containing IgG Formulations. *Pharmaceutical Research,* 27**,** 314-326.
HAWE, A., SUTTER, M. & JISKOOT, W. 2008. Extrinsic fluorescent dyes as tools for protein characterization. *Pharm Res,* 25**,** 1487-99.
HE, F., PHAN, D. H., HOGAN, S., BAILEY, R., BECKER, G. W., NARHI, L. O. & RAZINKOV, V. I. 2010. Detection of IgG aggregation by a high throughput method based on extrinsic fluorescence. *J Pharm Sci,* 99**,** 2598-608.

HERRINGTON-SYMES, A. P., FARYS, M., KHALILI, H. & BROCCHINI, S. 2013. Antibody fragments: Prolonging circulation half-life special issue-antibody research. *Advances in Bioscience and Biotechnology,* Vol.04No.05**,** 10.

HOCHREITER, B., PARDO GARCIA, A. & SCHMID, J. A. 2015. Fluorescent Proteins as Genetically Encoded FRET Biosensors in Life Sciences. *Sensors (Basel, Switzerland),* 15**,** 26281-26314.

HORIBA. 2017. *A Guide to Recording Fluorescence Quantum Yields* [Online]. Available: http://www.horiba.com/fileadmin/uploads/Scientific/Documents/Fluorescence/quantumyieldstrad.pdf [Accessed].

HOUDE, D. J. & BERKOWITZ, S. A. 2015. *Biophysical Characterization of Proteins in Developing Biopharmaceuticals*, Elsevier

IACOB, R. E., BOU-ASSAF, G. M., MAKOWSKI, L., ENGEN, J. R., BERKOWITZ, S. A. & HOUDE, D. 2013. Investigating monoclonal antibody aggregation using a combination of H/DX-MS and other biophysical measurements. *J Pharm Sci,* 102**,** 4315-29.

ICH. 1994. *ICH Harmonised Tripartite Guidelines Validation of Analytical Procedures: Text and Methodology Q2(R1)* [Online]. Available: https://www.ich.org/fileadmin/Public_Web_Site/ICH_Products/Guidelines/Quality/Q2_R1/Step4/Q2_R1__Guideline.pdf [Accessed].

ICH. 1999. *ICH Topic Q 6 B. Specifications:Test procedures and Accepttance Criteria for Biotechnological/Bioogical products* [Online]. Available: http://www.ema.europa.eu/docs/en_GB/document_library/Scientific_guideline/2009/09/WC500002824.pdf [Accessed 1 July 2017].

ICH. 2009. *ICH Harmonised Tripartite Guidelines Pharmaceutical Development Q8 (R2) Step 4 version* [Online]. Available: http://www.ich.org/products/guidelines/quality/article/quality-guidelines.html [Accessed 15 February 2015].

INVITROGEN 2010. pH Indicators. *Molecular Probes Handbook.* 11 ed.

JAYARAMAN, J., WU, J., BRUNELLE, M. C., CRUZ, A. M., GOLDBERG, D. S., LOBO, B., SHAH, A. & TESSIER, P. M. 2014. Plasmonic measurements of monoclonal antibody self-association using self-interaction nanoparticle spectroscopy. *Biotechnol Bioeng,* 111**,** 1513-20.

JOHNSON, I. D. 2006. Practical Considerations in the Selection and Application of Fluorescent Probes. *In:* PAWLEY, J. B. (ed.) *Handbook Of Biological Confocal Microscopy.* Boston, MA: Springer US.

JOHNSON, W. L. & STRAIGHT, A. F. 2013. Chapter 5 - Fluorescent Protein Applications in Microscopy. *In:* SLUDER, G. & WOLF, D. E. (eds.) *Methods in Cell Biology.* Academic Press.

JOUBERT M K, LUO, Q., NASHED-SAMUEL, Y., WYPYCH, J. & NARHI, L. O. 2011. Classification and characterization of therapeutic antibody aggregates. *Journal Biological Chemistry* 286**,** 25118-33.

KAPIL, R., DHAWAN, S. & SINGH, B. 2009. Development and validation of a spectrofluorimetric method for the estimation of rivastigmine in formulations. *Indian J Pharm Sci,* 71**,** 585-9.

KAYSER, V., CHENNAMSETTY, N., VOYNOV, V., HELK, B. & TROUT, B. L. 2011. Conformational stability and aggregation of therapeutic monoclonal antibodies studied with ANS and thioflavin T binding. *mAbs,* 3**,** 408-411.

KELLY, S. M., JESS, T. J. & PRICE, N. C. 2005. How to study proteins by circular dichroism. *Biochimica et Biophysica Acta (BBA) - Proteins and Proteomics,* 1751**,** 119-139.

KELLY, S. M. & PRICE, N. C. 1997. The application of circular dichroism to studies of protein folding and unfolding. *Biochim Biophys Acta,* 1338**,** 161-85.

KIESE, S., PAPPPENBERGER, A., FRIESS, W. & MAHLER, H. C. 2008. Shaken, not stirred: mechanical stress testing of an IgG1 antibody. *J Pharm Sci,* 97**,** 4347-66.

KITAMURA, A., NAGATA, K. & KINJO, M. 2015. Conformational Analysis of Misfolded Protein Aggregation by FRET and Live-Cell Imaging Techniques. *International Journal of Molecular Sciences,* 16.

KÖNEMANN, T., SAVAGE, N. J., HUFFMAN, J. A. & PÖHLKER, C. 2018. Characterization of steady-state fluorescence properties of polystyrene latex spheres using off- and online spectroscopic methods. *Atmos. Meas. Tech.,* 11**,** 3987-4003.

KOZLOWSKI, S. & SWANN, P. 2006. Current and future issues in the manufacturing and development of monoclonal antibodies. *Adv Drug Deliv Rev,* 58**,** 707-22.

KRAH, S., SCHROTER, C., ZIELONKA, S., EMPTING, M., VALLDORF, B. & KOLMAR, H. 2016. Single-domain antibodies for biomedical applications. *Immunopharmacol Immunotoxicol,* 38**,** 21-8.

KRAMARCZYK, J. F., KELLEY, B. D. & COFFMAN, J. L. 2008. High-throughput screening of chromatographic separations: II. Hydrophobic interaction. *Biotechnol Bioeng,* 100**,** 707-20.

KRISHNAMURTHY. R, SUKUMAR. M, DAS. T K & A, L. N. 2008. Emerging Analytical Technologies for Biotherapeutics Development. *Bioprocess International***,** 32–42.

LAKOWICZ, J. R. 2010. Principles of Fluorescence Spectroscopy. *Springer*.

LARSSON, T., WEDBORG, M. & TURNER, D. 2007. Correction of inner-filter effect in fluorescence excitation-emission matrix spectrometry using Raman scatter. *Anal Chim Acta,* 583**,** 357-63.

LAWRENCE, S. 2007. Billion dollar babies--biotech drugs as blockbusters. *Nat Biotechnol,* 25**,** 380-2.

LEVINE, H. 1999. Quantification of beta-sheet amyloid fibril structures with thioflavin T. *Methods Enzymol,* 309**,** 274-84.

LIU, Y., CAFFRY, I., WU, J., GENG, S. B., JAIN, T., SUN, T., REID, F., CAO, Y., ESTEP, P., YU, Y., VÁSQUEZ, M., TESSIER, P. M. & XU, Y. 2014. High-throughput screening for developability during early-stage antibody discovery using self-interaction nanoparticle spectroscopy. *mAbs,* 6**,** 483-492.

LOURA, L. M. S. & PRIETO, M. 2011. FRET in Membrane Biophysics: An Overview. *Frontiers in Physiology,* 2**,** 82.

MA, L., YANG, F. & ZHENG, J. 2014. Application of fluorescence resonance energy transfer in protein studies. *Journal of molecular structure,* 1077**,** 87-100.

MATULIS, D. & LOVRIEN, R. 1998. 1-Anilino-8-naphthalene sulfonate anion-protein binding depends primarily on ion pair formation. *Biophys J,* 74**,** 422-9.

MAZZER, A. 2015. *Understanding the Influence of Adsorption-Mediated Processes on Antibody Aggregation in Bioprocessing.* Doctor of Philosophy in Biochemical Engineering, UCL.

MCCANN, J. J., CHOI, U. B., ZHENG, L., WENINGER, K. & BOWEN, M. E. 2010. Optimizing methods to recover absolute FRET efficiency from immobilized single molecules. *Biophysical journal,* 99**,** 961-970.

MEI, Q., SHI, Y., HUA, Q. & TONG, B. 2015. Phosphorescent chemosensor for Hg2+ based on an iridium(iii) complex coordinated with 4-phenylquinazoline and carbazole dithiocarbamate. *RSC Advances,* 5**,** 74924-74931.

MOU, X., YANG, X., LI, H., AMBROGELLY, A. & J POLLARD, D. 2014. *A high throughput ultra performance size exclusion chromatography assay for the analysis of aggregates and fragments of monoclonal antibodies*.

MOUSSA, E. M., PANCHAL, J. P., MOORTHY, B. S., BLUM, J. S., JOUBERT, M. K., NARHI, L. O. & TOPP, E. M. 2016. Immunogenicity of Therapeutic Protein Aggregates. *J Pharm Sci,* 105**,** 417-30.

MULLARD, A. 2014. New drugs cost US$2.6 billion to develop. *Nature Reviews Drug Discovery,* 13**,** 877.

NOGAL, B., CHHIBA, K. & EMERY, J. C. 2012. Select host cell proteins coelute with monoclonal antibodies in protein A chromatography. *Biotechnol Prog,* 28**,** 454-8.

OHADI, K., LEGGE, R. L. & BUDMAN, H. M. 2015. Intrinsic fluorescence-based at situ soft sensor for monitoring monoclonal antibody aggregation. *Biotechnol Prog,* 31**,** 1423-32.

OHAGE, E., IVERSON, R., KRUMMEN, L., TATICEK, R. & VEGA, M. 2016. QbD implementation and Post Approval Lifecycle Management (PALM). *Biologicals,* 44**,** 332-40.

OSHINBOLU, S., SHAH, R., FINKA, G., MOLLOY, M., UDEN, M. & BRACEWELL, D. G. 2018a. Evaluation of fluorescent dyes to measure protein aggregation within mammalian cell culture supernatants. *J Chem Technol Biotechnol,* 93**,** 909-917.

OSHINBOLU, S., WILSON, L. J., LEWIS, W., SHAH, R. & BRACEWELL, D. G. 2018b. Measurement of impurities to support process development and manufacture of biopharmaceuticals. *TrAC Trends in Analytical Chemistry,* 101**,** 120-128.

PAN, X. 2018. *Scale-down of CHO Cell Fed-batch Cultures.* PhD Doctorate, Wageningen University.

PAUL, A. & HESSE, F. 2013. Characterization of mAb aggregates in a mammalian cell culture production process. *BMC Proceedings,* 7**,** P80.

PAUL, A. J., SCHWAB, K. & HESSE, F. 2014. Direct analysis of mAb aggregates in mammalian cell culture supernatant. *BMC Biotechnology,* 14**,** 99.

PAUL, A. J., SCHWAB, K., PROKOPH, N., HAAS, E., HANDRICK, R. & HESSE, F. 2015a. Fluorescence dye-based detection of mAb aggregates in CHO culture supernatants. *Analytical and Bioanalytical Chemistry,* 407**,** 4849-4856.

PAUL, A. J., SCHWAB, K., PROKOPH, N., HAAS, E., HANDRICK, R. & HESSE, F. 2015b. Fluorescence dye-based detection of mAb aggregates in CHO culture supernatants. *Anal Bioanal Chem,* 407**,** 4849-56.

PAUL, R., GRAFF-MEYER, A., STAHLBERG, H., LAUER, M. E., RUFER, A. C., BECK, H., BRIGUET, A., SCHNAIBLE, V., BUCKEL, T. & BOECKLE, S. 2012. Structure and Function of Purified Monoclonal Antibody Dimers Induced by Different Stress Conditions. *Pharmaceutical Research,* 29**,** 2047-2059.

PEKAR, A. & SUKUMAR, M. 2007. Quantitation of aggregates in therapeutic proteins using sedimentation velocity analytical ultracentrifugation: practical considerations that affect precision and accuracy. *Anal Biochem,* 367**,** 225-37.

PHILO, J. S. & ARAKAWA, T. 2009. Mechanisms of protein aggregation. *Curr Pharm Biotechnol,* 10**,** 348-51.

POTHECARY, M., BALL, S. & CLARKE, P. 2012. *Protein applications for advanced multi-detector size-exclusion chromatography*.

PRAHL, S. 2017. *Quinine Sulfate* [Online]. Available: http://omlc.org/spectra/PhotochemCAD/html/081.html [Accessed].

REA, J. C., LOU, Y., CUZZI, J., HU, Y., DE JONG, I., WANG, Y. J. & FARNAN, D. 2012. Development of capillary size exclusion chromatography for the analysis of monoclonal antibody fragments extracted from human vitreous humor. *Journal of Chromatography A,* 1270**,** 111-117.

REMTULLA, N. 2009. *Feasibility of microfluidic routes to monitor protein stability as a tool for bioprocessing.* UCL

RENAUD, J. P., CHUNG, C. W., DANIELSON, U. H., EGNER, U., HENNIG, M., HUBBARD, R. E. & NAR, H. 2016. Biophysics in drug discovery: impact, challenges and opportunities. *Nat Rev Drug Discov,* 15**,** 679-98.

ROBERTS, C. J. 2014. Therapeutic protein aggregation: mechanisms, design, and control. *Trends Biotechnol,* 32**,** 372-80.

ROY, R., HOHNG, S. & HA, T. 2008. A Practical Guide to Single Molecule FRET. *Nature methods,* 5**,** 507-516.

RYAN, P. W., LI, B., SHANAHAN, M., LEISTER, K. J. & RYDER, A. G. 2010. Prediction of cell culture media performance using fluorescence spectroscopy. *Anal Chem,* 82**,** 1311-7.

SCHWAB, K. & HESSE, F. 2013. 2D fluorescence spectroscopy for real-time aggregation monitoring in upstream processing. *BMC Proceedings,* 7**,** P94-P94.

SCHWAB, K. & HESSE, F. 2017. Estimating Extrinsic Dyes for Fluorometric Online Monitoring of Antibody Aggregation in CHO Fed-Batch Cultivations. *Bioengineering (Basel),* 4.

SHARMA, D. K., KING, D., OMA, P. & MERCHANT, C. 2010. Micro-flow imaging: flow microscopy applied to sub-visible particulate analysis in protein formulations. *AAPS J,* 12**,** 455-64.

SHARMA, V. K. & KALONIA, D. S. 2010. Experimental Detection and Characterization of Protein Aggregates. *Aggregation of Therapeutic Proteins.* John Wiley & Sons, Inc.

SINZ, A. 2005. Chemical cross-linking and FTICR mass spectrometry for protein structure characterization. *Anal Bioanal Chem,* 381**,** 44-7.

STSIAPURA, V. I., MASKEVICH, A. A., KUZMITSKY, V. A., UVERSKY, V. N., KUZNETSOVA, I. M. & TUROVEROV, K. K. 2008. Thioflavin T as a molecular rotor: fluorescent properties of thioflavin T in solvents with different viscosity. *J Phys Chem B,* 112**,** 15893-902.

SULE, S. V., DICKINSON, C. D., LU, J., CHOW, C. K. & TESSIER, P. M. 2013. Rapid analysis of antibody self-association in complex mixtures using immunogold conjugates. *Mol Pharm,* 10**,** 1322-31.

SUN, Y., ROMBOLA, C., JYOTHIKUMAR, V. & PERIASAMY, A. 2013. Forster resonance energy transfer microscopy and spectroscopy for localizing protein-protein interactions in living cells. *Cytometry A,* 83**,** 780-93.

SUTTER, M., OLIVEIRA, S., SANDERS, N. N., LUCAS, B., VAN HOEK, A., HINK, M. A., VISSER, A. J., DE SMEDT, S. C., HENNINK, W. E. & JISKOOT, W. 2007. Sensitive spectroscopic detection of large and denatured protein aggregates in solution by use of the fluorescent dye Nile red. *J Fluoresc,* 17**,** 181-92.

TELIKEPALLI, S. N., KUMRU, O. S., KALONIA, C., ESFANDIARY, R., JOSHI, S. B., MIDDAUGH, C. R. & VOLKIN, D. B. 2014. Structural characterization of IgG1 mAb aggregates and particles generated under various stress conditions. *J Pharm Sci,* 103**,** 796-809.

THEMISTOU, E., SINGH, I., SHANG, C., BALU-IYER, S. V., ALEXANDRIDIS, P. & NEELAMEGHAM, S. 2009. Application of fluorescence spectroscopy to quantify shear-induced protein conformation change. *Biophys J,* 97**,** 2567-76.

THERMOFISHER. 2017. *Fluorescence SpectraViewer* [Online]. ThermoFisher. Available: https://www.thermofisher.com/uk/en/home/life-science/cell-analysis/labeling-chemistry/fluorescence-spectraviewer.html?ICID=svtool&UID=11045ph8 [Accessed].

VAN DER KANT, R., KAROW-ZWICK, A. R., VAN DURME, J., BLECH, M., GALLARDO, R., SEELIGER, D., AßFALG, K., BAATSEN, P., COMPERNOLLE, G., GILS, A., STUDTS, J. M., SCHULZ, P., GARIDEL, P., SCHYMKOWITZ, J. & ROUSSEAU, F. 2017. Prediction and Reduction of the Aggregation of Monoclonal Antibodies. *Journal of Molecular Biology,* 429**,** 1244-1261.

VAZQUEZ-REY, M. & LANG, D. A. 2011. Aggregates in monoclonal antibody manufacturing processes. *Biotechnol Bioeng,* 108**,** 1494-508.

VETRI, V., CANALE, C., RELINI, A., LIBRIZZI, F., MILITELLO, V., GLIOZZI, A. & LEONE, M. 2007. Amyloid fibrils formation and amorphous aggregation in concanavalin A. *Biophys Chem,* 125**,** 184-90.

WANG, X., AN, Z., LUO, W., XIA, N. & ZHAO, Q. 2018. Molecular and functional analysis of monoclonal antibodies in support of biologics development. *Protein & Cell,* 9**,** 74-85.

WATERS, J. C. 2009. Accuracy and precision in quantitative fluorescence microscopy. *J Cell Biol,* 185**,** 1135-48.

WEISS, W. F. T., GABRIELSON, J. P., AL-AZZAM, W., CHEN, G., DAVIS, D. L., DAS, T. K., HAYES, D. B., HOUDE, D. & SINGH, S. K. 2016. Technical Decision Making With Higher Order Structure Data: Perspectives on Higher

Order Structure Characterization From the Biopharmaceutical Industry. *J Pharm Sci,* 105**,** 3465-3470.

WU, H., SUN, J. & ZHENG, L. 2015. *The analysis of the different filtering algorithm effects on the fluorescence spectrum data processing*.

WURTH, C., GRABOLLE, M., PAULI, J., SPIELES, M. & RESCH-GENGER, U. 2013. Relative and absolute determination of fluorescence quantum yields of transparent samples. *Nat Protoc,* 8**,** 1535-50.

XIAO, Y. & ISAACS, S. N. 2012. Enzyme-linked immunosorbent assay (ELISA) and blocking with bovine serum albumin (BSA)--not all BSAs are alike. *J Immunol Methods,* 384**,** 148-51.

YAMNIUK, A. P., DITTO, N., PATEL, M., DAI, J., SEJWAL, P., STETSKO, P. & DOYLE, M. L. 2013. Application of a kosmotrope-based solubility assay to multiple protein therapeutic classes indicates broad use as a high-throughput screen for protein therapeutic aggregation propensity. *J Pharm Sci,* 102**,** 2424-39.

YEO, E. L. L., CHUA, A. J. S., PARTHASARATHY, K., YEO, H. Y., NG, M. L. & KAH, J. C. Y. 2015. Understanding aggregation-based assays: nature of protein corona and number of epitopes on antigen matters. *RSC Advances,* 5**,** 14982-14993.

ZAL, T. 2011. Visualization of Protein Interactions in Living Cells. *Self Nonself,* 2**,** 98-107.

ZHANG, Y. B., HOWITT, J., MCCORKLE, S., LAWRENCE, P., SPRINGER, K. & FREIMUTH, P. 2004. Protein aggregation during overexpression limited by peptide extensions with large net negative charge. *Protein Expr Purif,* 36**,** 207-16.

ZHAO, H., DIEZ, M., KOULOV, A., BOZOVA, M., BLUEMEL, M. & KURT, F. 2012. Characterization of Aggregates and Particles Using Emerging Techniques. *In:* MAHLER, H.-C. & JISKOOT, W. (eds.) *Analysis of Aggregates and Particles in Protein Pharmaceuticals.* New Jersey: John Wiley & Sons, Inc.

ZHENG, K., BANTOG, C. & BAYER, R. 2011. The impact of glycosylation on monoclonal antibody conformation and stability. *mAbs,* 3**,** 568-576.

ZURDO, J. 2013. Developability assessment as an early de-risking tool for biopharmaceutical development. . *Pharmaceuticals Bioprocessing,* 1**,** 29-50.

ZURDO, J., MICHAEL, R., STALLWOOD, Y. & AASTRUP, T. 2011. Improving the Developability of Biopharmaceuticals. *Innovations in Pharmaceutical Technology,* 37**,** 34-40.

Appendix A: Quantum Yield

A1. How to measure quantum yield

Allen (2010) outlined two methods to calculate relative quantum yield: single-point and comparative method. The single point method uses the integrated emission intensities from an unknown sample and a reference, at single identical concentrations. Although it is fast and easy, it is not always reliable as it is based on only one value. In contrast, the comparative method utilises a reference at different concentrations. The comparative method takes more time to measure but provides higher accuracy by using the slope of the standard curve to calculate the quantum yield.

When measuring the quantum yield, there are two factors that can skew measurement. One factor is the inner filter effect. Although the quantum yield is mostly independent of excitation wavelength, fluorescence intensity can vary (non-linearly) based on the concentration (Fonin et al., 2014). This can cause reabsorption of fluorescence which can perturb quantum yield results. Therefore, to minimise these reabsorption effects, sample absorbance should be kept below 0.1 in 10 mm cuvette (HORIBA, 2017, Wurth et al., 2013).

Secondly, different instruments can have skewed (lower/higher) fluorescence intensity at certain wavelengths. Therefore, it is important to correct the spectrum for instrumental wavelength response. This can be done by measuring the fluorescence of the reference and dividing the whole spectrum against literature wavelength-corrected spectrum to generate a correction factor. This correction factor can then be applied to the correct the intensities for the fluorophore of interest. Correcting for wavelength not only makes all the intensities proportional but also gives an idea of how accurate the instrument measurement is.

Out of the most common reference molecules (Appendix Table A-1), quinine sulphate was chosen as it had similar excitation/emission properties as the Alexa Fluor 350. Quinine sulphate is widely used as a reference standard (Fletcher, 1969) and has a

quantum yield of 0.577 in 0.1 M H_2SO_4 at 22^0C. The wavelength-corrected spectrum of quinine sulphate in sulphuric acid buffer was used from Prahl (2017).

Appendix Table A-1: Quantum Yield of different standards obtained from (Lakowicz, 2010)

Compound	Solvent	Excitation wavelenght (nm)	Temperature (C)	Quantum Yield
Quinine Sulphate	0.1 M H_2SO_4	350	22	0.577
		366	-	0.53±0.023
B-Carboline	0.1 N H_2SO_4	350	25	0.60
Fluorescein	0.1 M NaOH	496	22	0.95±0.03
9,10-DPA	Cyclohexane	-	-	0.95
9,10-DPA	-	366	-	1.00±0.05
POPOP	Cyclohexane	-	-	0.97
2-Aminepyridine	0.1 N H_2SO_4	285	-	0.60±0.05
Tryptophan	Water	280	-	0.13±0.01
Tyrosine	Water	275	23	0.14±0.01
Phenylalanine	Water	260	23	0.024
Phenol	Water	275	23	0.14±0.01
Rhodamine 6G	Ethanol	488	-	0.94
Rhodamine 101	Ethanol	450-465	25	1.0
Cresyl Violet	Methanol	540-640	22	0.54

A2. Quantum Yield comparative method

The fluorescence spectra of AF350 and Quinine Sulphate are shown in Appendix Figure A-1. The integrated fluorescence intensity for each sample was calculated and plotted against its absorbance (OD/OD_R) in Appendix Figure A-2 to obtain the slope. The slope for AF350 (m) and for Quinine Sulphate (m_R) was $5.85x10^9$ RFU/a.u and $3.15x10^9$ RFU/a.u respectively. Using Equation A-1, the slopes and the refractive index (n and n_R), the quantum yield for AF350 was calculated to be 1.07. As the

quantum yield must be between 0 and 1, human error in measurement may be the reason for the high quantum yield value.

$$Q = Q_R \left(\frac{m}{m_R}\right)\left(\frac{n^2}{{n^2}_R}\right) = 0.577\left(\frac{5.85 \times 10^9}{3.15 \times 10^9}\right)\left(\frac{1.33^2}{1.33^2}\right) = 1.07$$

Equation A-1: Comparative method calculation for Quantum Yield of Alexa Fluor 350.

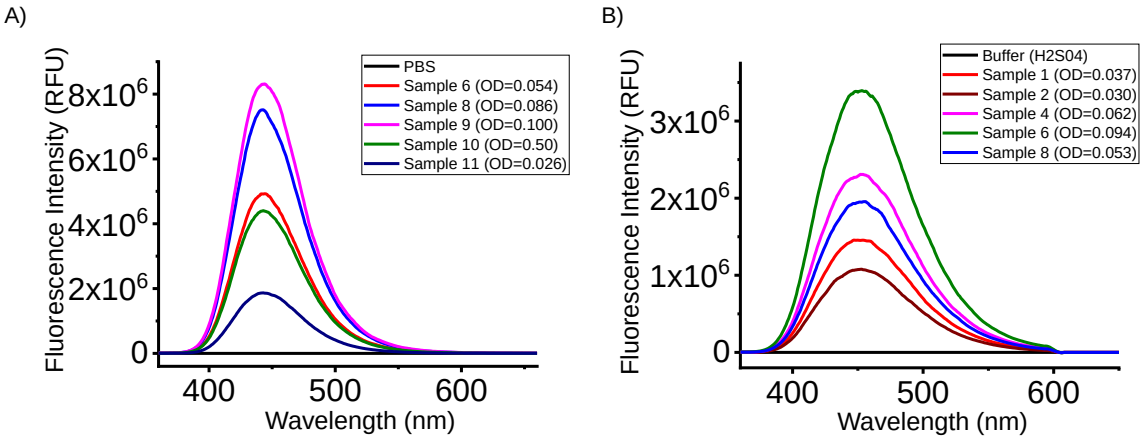

Appendix Figure A-1: Fluorescence spectra of (A) Alexa Fluor 350 and (B) Quinine Sulphate.
Measured using the following conditions: excitation 346 nm, emission 360-660 nm, excitation/ emission slits widths 5 nm, speed medium, and PMT voltage of 500. Data was analysed and smoothed using OriginPro. The spectra were blank subtracted and corrected for wavelength intensity.

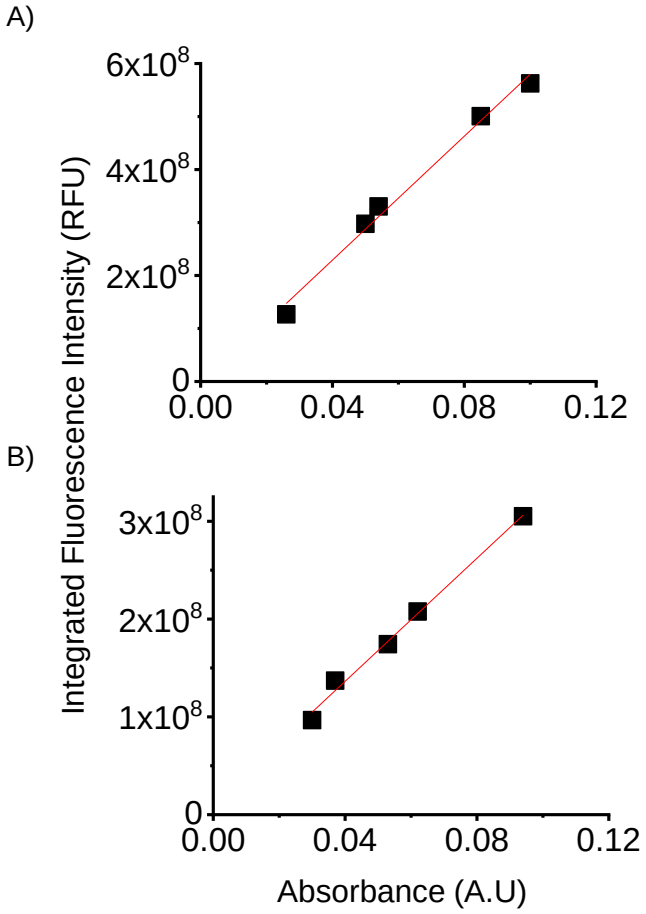

Appendix Figure A-2: Integrated fluorescence intensities against A346 absorbance for A) Alexa Fluor 350 and B) Quinine Sulphate.
Red line is linear fit. Slope and adjusted R^2 for Alexa Fluor 350 was 5.85E+09 RFU/a.u and 0.985 respectively. Slope and R^2 for Quinine Sulphate was 3.15E+09 RFU/a.u and 0.990 respectively.

A3. QY single point method

Using Alexa Fluor 350 and quinine sulphate samples with similar OD values, the quantum yield for Alexa Fluor 350 using the single point method was calculated at three different ODs to be 0.87, 1.07 and 1.00 (Equation A-2).

Both the single point and comparative method yielded high quantum yields. This correlated well as Alexa Fluor dyes are characteristically very bright. However, the quantum yield values obtained using the single point method were more variable. As the comparative method calculated based on five standards with different absorbances

as opposed to one, it was decided to use the comparative method (QY=1.07) for R_0 calculations (despite being above 1).

$$Q = 0.577\left(\frac{1.27 \times 10^8}{9.66 \times 10^7}\right)\left(\frac{0.03}{0.26}\right)\left(\frac{1.33^2}{1.33^2}\right) = \mathbf{0.87}$$

Alexa Fluor 350 sample 1 (OD=0.026 a.u) and Quinine Sulphate sample 2 (OD=0.030 a.u)

$$Q = 0.577\left(\frac{3.30 \times 10^8}{1.74 \times 10^8}\right)\left(\frac{0.053}{0.054}\right)\left(\frac{1.33^2}{1.33^2}\right) = \mathbf{1.07}$$

Alexa Fluor 350 sample 6 (OD=0.054 a.u) and Quinine Sulphate sample 8 (OD=0.053 a.u)

$$Q = 0.577\left(\frac{5.62 \times 10^8}{3.05 \times 10^8}\right)\left(\frac{0.094}{0.100}\right)\left(\frac{1.33^2}{1.33^2}\right) = \mathbf{1.00}$$

Alexa Fluor 350 sample 9 (OD=0.100 a.u) and Quinine Sulphate sample 6 (OD=0.094 a.u)

Equation A-2: Single point method calculation for Quantum Yield of Alexa Fluor 350

A4. Extinction coefficient of SYPRO Orange

To work out the extinction coefficient (EC) of SYPRO Orange, the concentration needed to be converted from X to molarity. The molecular weight was found in the Molecular Probes patent (Haugland et al., 1996) and was confirmed by mass spectrometry. 5000X SYPRO Orange was found to have concentration of approximately 9 mM. Using this concentration, stocks of SYPRO Orange at different molar concentrations were created. The EC was calculated by plotting the molar concentrations against absorbance (Appendix Figure A-3), with the gradient (11235 $M^{-1}cm^{-1}$) equal to the EC of SYPRO Orange.

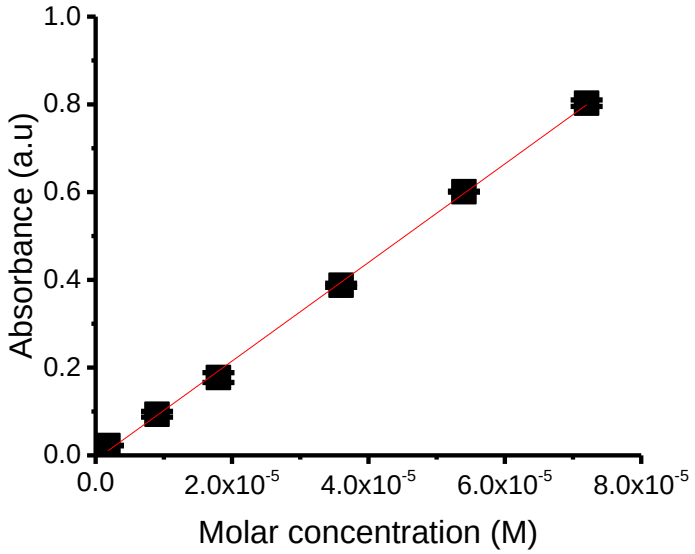

Appendix Figure A-3: SYPRO Orange molar concentration against absorbance at 490 nm.
Adjusted R^2 = 0.999, Slope = 11235 $M^{-1}cm^{-1}$ (Extinction coefficient). Error bars are based on standard deviation. Measured in triplicates

A5. Extinction coefficient of ProteoStat

As the concentration of ProteoStat was already known, the Beer Lambert Law was used to calculate the EC. However, there was a notable batch variability in repeated attempts to measure the EC (Appendix Table A-2). As it was difficult to ascertain which was correct, the highest (109683 $M^{-1}cm^{-1}$) and lowest (51378 $M^{-1}cm^{-1}$) EC were both used to calculate a R_0 range. It was not clear as to why the EC fluctuated with batches and there is not a lot known about the molecule/structure of ProteoStat.

Appendix Table A-2: ProteoStat Extinction Coefficient measured across three different batches of ProteoStat.

Attempt	Batch	Extinction coefficient ($M^{-1}cm^{-1}$)
1	1	51378
2		59343
3	2	84643
4		80667
5	3	109683

Appendix B: FRET

FRET with dAbs with Tween-20 buffer and at different dAb concentration

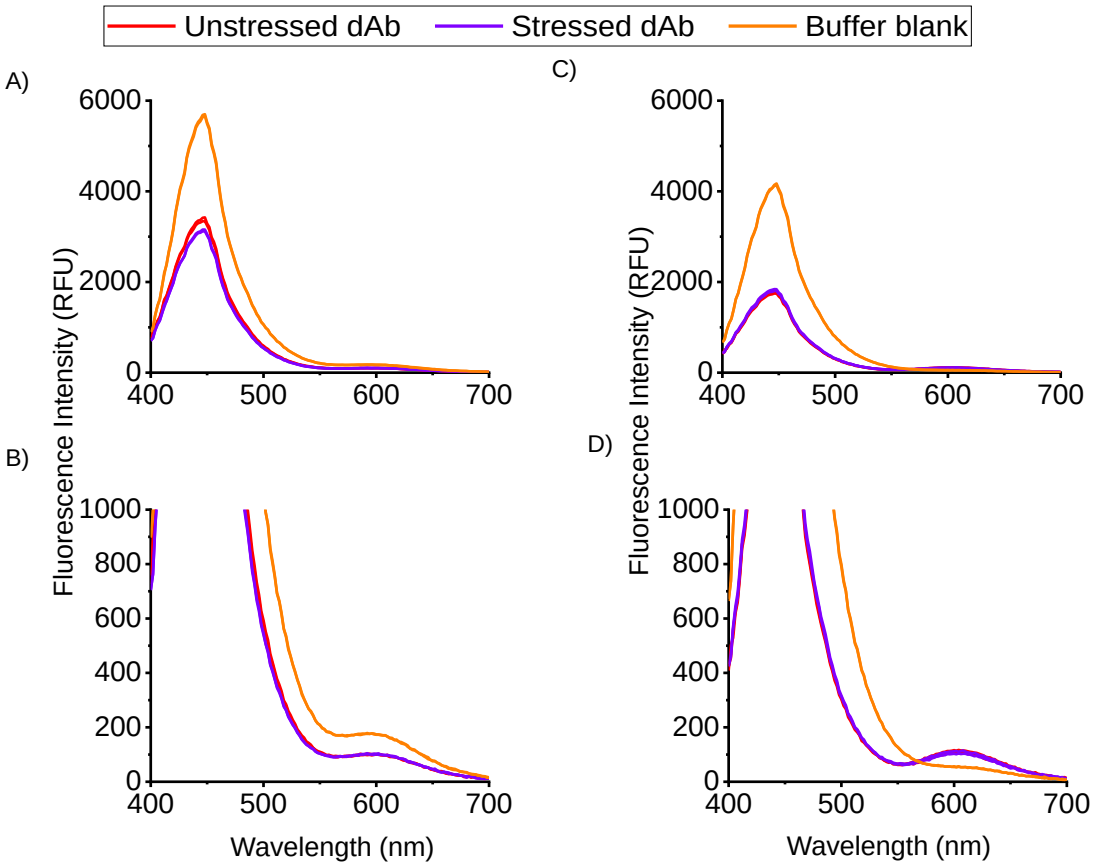

Appendix Figure B-1: FRET with dAbs in 0.5% Tween-20 buffer.
Unstressed dAb (10% aggregated, r_h=3.7 nm) and stressed dAb (45% aggregated, r_h=4.5 nm) in the presence of 1 µM PrA-AF350 and A/C) 5X/9 µM SYPRO Orange, B/D) 3 µM ProteoStat (C and D are zoomed in versions of A and B). Excitation/Emission- 330 nm/400-700 nm. Concentration of dAb in each well was 1 mg/mL. This was performed in duplicates which are both shown in the figure.

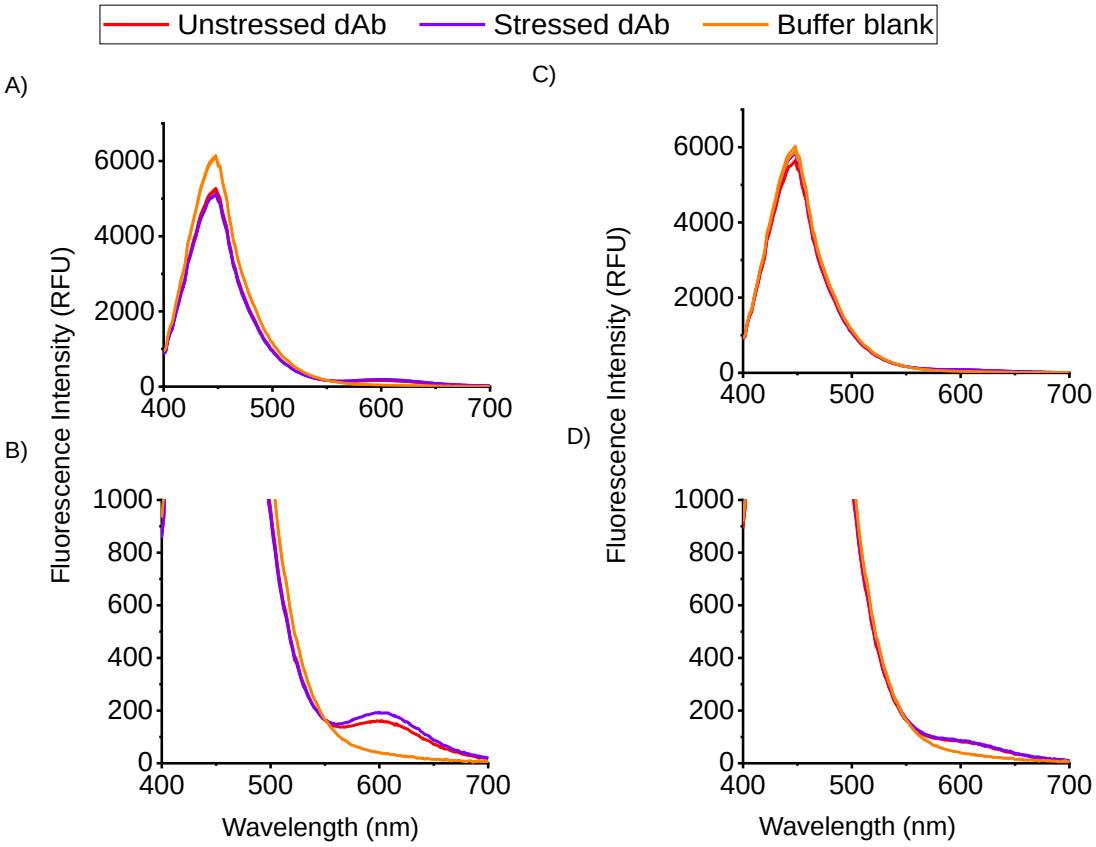

Appendix Figure B-2: FRET with lower concentrations of dAb and SYPRO Orange. 1 µM PrA-AF350 and 5X SYPRO Orange. Unstressed dAb (10% aggregated, rh=3.7 nm) and stressed dAb (45% aggregated, r_h=4.5 nm) at A and B) 0.18 mg/mL (7 µM) dAb and C and D) 0.05mg/mL (2 µM) dAb. (B and D are zoomed in versions of A and C). Excitation/Emission- 330 nm/400-700 nm. This was performed in duplicates which are both shown in the figure.

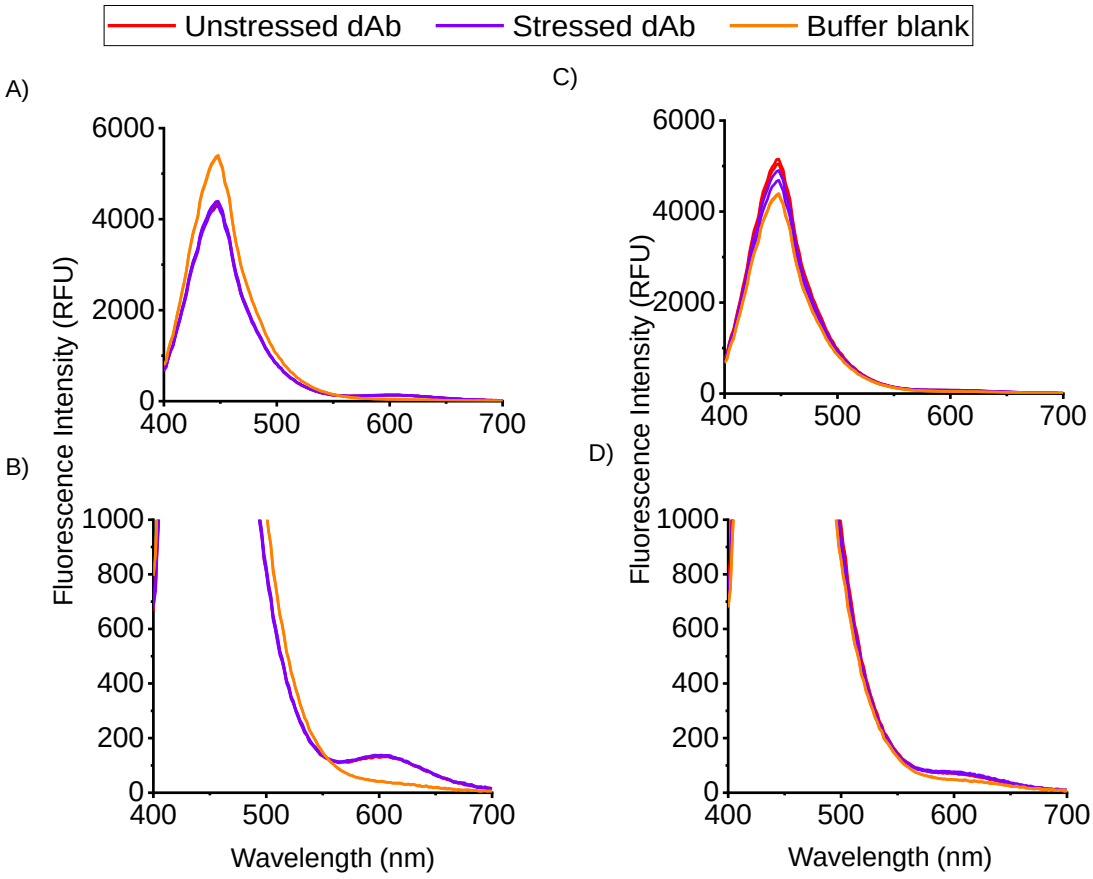

Appendix Figure B-3: FRET with lower concentration of dAb and ProteoStat. Unstressed dAb (10% aggregated, r_h=3.7 nm) and stressed dAb (45% aggregated, r_h=4.5 nm) in the presence of 1 µM PrA-AF350 and 3 µM ProteoStat at A/C) 0.18 mg/mL (7 µM) dAb and B/D) 0.05 mg/mL (2 µM) dAb. (C and D are zoomed in versions of A and B). Excitation/Emission- 330 nm/400-700 nm. This was performed in duplicates which are both shown in the figure.

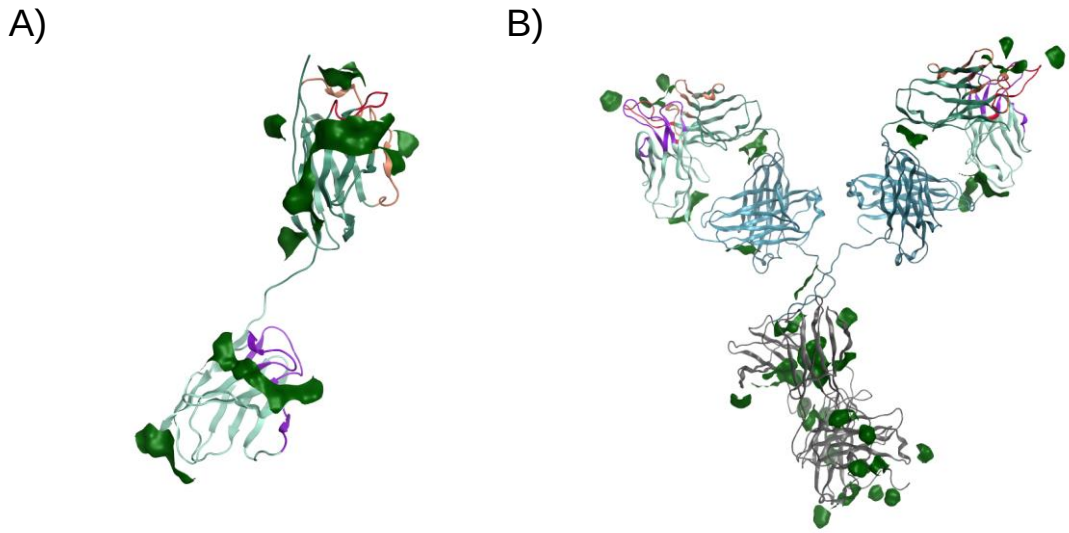

Appendix Figure B-4: DAb A and mAb A with surface exposed hydrophobic patches highlighted.
DAb A is comprised of two dAbs linked together. (A) DAb A and (B) MAb A. Structures were analysed for surface exposed hydrophobic patches with MOE Patch Analyzer using the default settings. Structures are displayed in ribbon format, orientated with CDRs annotated (purple and orange correspond to light chain and heavy chain CDRs respectively) and predicted hydrophobic patches displayed as green molecular surfaces. Percentage molecular surface coverage for hydrophobic patches was calculated to be 9.5% for dAb A and 4.3% for mAb A using the MOE Patch Analyzer based on the protein structure. Data was provided from the GSK Computational Sciences department.

Appendix C: Validation

Validation of equipment and assays in industry are made compliant to the International Council for Harmonisation of Technical Requirements for Pharmaceuticals for Human Use (ICH) guidelines Q2 (R1) (ICH 1994). These guidelines list the characteristics, which need to be considered during the validation of analytical procedures. The typical validation characteristics are accuracy, precision and repeatability, robustness, specificity, detection limit, quantitation limit, linearity and range. These characteristics demonstrate that an analytical procedure is suitable for its intended purpose, which in this case, is to accurately reflect the amount of aggregated mAb species in the presence of the monomer of the mAb.

The dye assay must be accurate and comparable to current methods of analysis, which for aggregation is typically size exclusion chromatography. Although the mechanisms by which the dye assay and SEC measure aggregates are different; and has an inability to handle large aggregates and the presence of a mobile phase which causes dilution, formation or dissociation of aggregates. Nonetheless SEC is the "gold-standard" which is routinely used and hence is suitable.

Precision is important. The dye assay will need to have a high level of repeatability (within-a-day variability) and reproducibility (day-to-day variability). Precision also extends to operator and equipment variability as one should be able to get the similar data irrespective of minor pipetting errors between operators or the use of different pipettes or spectrophotometers.

Specificity is a key factor especially when dealing with clarified supernatant. Upon validation the assay needs to prove that its response is specific enough to the aggregated mAb. This can be hindered by the presence of the monomer, which is in the majority as well as other proteins and cell culture components. This ties with also minimising the interference of other components with the assay as this can interfere with the detection/quantitation limit. For example, there is the possibility of

hydrophobic dyes not only binding to exposed hydrophobic regions on aggregated mAb, but also to other aggregated host cell proteins in the supernatant sample.

Another key validation aspect is identifying the quantitation limit. This is the lowest and highest concentration of the mAb that can be determined. The upper limit would determine the range at which the assay can be used. Ideally the assay should be able to distinguish a difference of 1-2% aggregate in samples, particularly at the lower range (<10%), as this is the problematic range typically seen in industry.

Robustness is a measure of the capacity of the assay to remain unaffected by small process changes such as incubation time, sample preparation and temperature. A known issue with using well-plate formats with analysis is the evaporation and/or loss of fluorescence with the sample during analysis. Since measurements with spectrophotometers can take 2-3 hours for one 96-well plate, by the time it takes the spectrophotometer to gets to the last sample photo-bleaching and/or evaporation (essentially concentrating) may occur. If the concentration changes, this changes the experimental conditions completely. Reducing the number of samples on a plate and/or reducing the excitation window so that the time for analysis is shortened can reduce this.

Aside from using dyes/probes immunoassays/ELISA-like protocols is an alternative to measuring aggregates. Immunoassays are based on the response from an antigen-antibody or antibody-antibody interaction. The key issue is the binding between these two components and the inter- and intra-reproducibility. With an ELISA where antibodies are bound onto a surface like a 96-well plate, there needs to be a level of certainty that the amount bound to the surface is the same in each well and each plate.